université de BORDEAUX

université de BORDEAUX

THÈSE PRÉSENTÉE

POUR OBTENIR LE GRADE DE

DOCTEUR DE

L'UNIVERSITÉ DE BORDEAUX

ECOLE DOCTORALE SCIENCES ET ENVIRONNEMENTS

SPÉCIALITÉ: PHYSIQUE DE L'ENVIRONNEMENT

Par Mohammad Traboulsi

Modélisation de l'évolution passée et future des côtes sableuses

Sous la direction de: Dr. Déborah Idier et Dr. Bruno Castelle

Soutenu le 11 Décembre 2025

Membres du jury:

M. **Julien CHAUCHAT**	Directeur de recherche, INRAE Grenoble	Rapporteur
M. **Albert FALQUÉS**	Professeur, Universitat Politècnica de Catalunya	Rapporteur
Mme. **Nadia SÉNÉCHAL**	Professeure, Université de Bordeaux	Présidente/Examinatrice
Mme. **Angélique MELET**	Chargée de recherche, Mercator Ocean Intl.	Examinatrice
Mme. **Alexandra TOIMIL**	Chercheuse, Universidad de Cantabria	Examinatrice
M. **Bruno CASTELLE**	Directeur de recherche, Université de Bordeaux	Directeur
Mme. **Déborah IDIER**	Directrice de recherche, BRGM	Directrice
M. **Arthur ROBINET**	Ingénieur-chercheur, BRGM	Invité
M. **Vincent MARIEU**	Ingénieur de recherche, Université de Bordeaux	Invité

- 2025-

All models are wrong, but some are useful.

Statistician, George E. P. Box (1919–2013)

Acknowledgments

This doctoral work represents several years of research, but it also reflects a journey shaped by the people who supported me, challenged me, and accompanied me throughout this process.

I would like to begin by thanking my supervisors, Déborah Idier and Bruno Castelle. Their complementary perspectives, high standards, and constant availability played a central role in the development of this thesis. I am especially grateful for the trust they placed in me and for the freedom they gave me to explore ideas, make mistakes, and progressively build my own approach to research, while always providing guidance when it was needed. Working under their supervision was demanding, and sometimes challenging, but it was above all deeply formative, and I sincerely thank them for that.

I am also very grateful to Arthur Robinet and Vincent Marieu, who followed my work from the very beginning. Arthur helped me maintain a broader perspective when I became absorbed in details, and was a constant reference point when I needed to step back and regain direction. Vincent was invaluable during more technical phases of the PhD, particularly when problems became blocking or frustrating. His calm and pragmatic approach helped move things forward many times. I thank them both for their support, patience, and involvement throughout these years.

I would like to warmly thank the members of my PhD jury, Nadia Sénéchal, Julien Chauchat, Albert Falqués, Angélique Melet, and Alexandra Toimil, for the time they dedicated to evaluating this work and for the quality of their questions and discussions during the defense. Their feedback and perspectives were both rigorous and constructive, and greatly contributed to placing this work in a broader scientific context.

I also thank the members of my comité de suivi de thèse, Yann Hueze (referent), Alexandra Toimil, and Jack McCarroll, for their guidance throughout the PhD. Their insights, questions, and recommendations during follow up meetings helped me refine my approach and maintain a clear direction over the course of the project.

My sincere thanks go as well to my co authors and collaborators, Rémi Thiéblemont, Jérémy Rohmer, Maurizio D'anna and Alexandre Nicolae Lerma, for their expertise, constructive feedback, and the quality of the discussions we shared, which strengthened this work considerably.

A PhD is also defined by daily life and by the people who share it. I am deeply thankful to my colleagues and friends at BRGM and EPOC for creating a supportive and stimulating environment. In particular, I would like to thank Georgios, Elsa, Marine, Emilie, Ivana, Mila, Martin, Carlos, Betty, Vania, Natan, Monique, Carla, Clément, Alex, Dominique, and many others. Thank you for the

coffee breaks, the conversations that went beyond science, the shared frustrations and small victories, and for making this experience feel collective rather than solitary.

Outside academia, I owe a great deal to friends who helped me maintain balance and perspective. My college friends Fadel, Yasser, Ali, and Bilal were a constant reference point throughout these years. In Bordeaux, I was fortunate to find a second family in Ayoub, Ayman, Georges, Zeid, Younes, Reem, Youssef, Lea, Sibelle, Riwa, and Caroline. Thank you for the shared moments, the conversations, and the simple fact of being there. You reminded me that life exists beyond research and that stepping back is sometimes just as important as pushing forward.

Finally, I would like to thank my family. To my brothers Kassem, Mahdi, Hadi, and Rida, thank you for your constant support and patience throughout this journey. Even from a distance, your presence and confidence in me were always felt. Knowing that you were there made the more difficult moments easier to face, and I am deeply grateful for that.

I also thank BRGM for welcoming me and providing an environment in which this research could be carried out. I am grateful to Cyril for his support, to Éric for his guidance during the early stages, and to Nafissato for her invaluable help with administrative matters. My thanks also extend to all the administrative and technical staff, as well as to EPOC, for providing a rich and stimulating academic setting.

This work was funded by the ANR, whose financial support made this project possible.

Modélisation de l'évolution passée et future des côtes sableuses

Résumé : Les côtes sableuses sont des environnements dynamiques qui réagissent en permanence à l'influence combinée des vagues, des marées et de l'élévation du niveau de la mer. Avec l'accélération de cette élévation et la persistance des déficits sédimentaires, ces systèmes deviennent de plus en plus vulnérables, en particulier là où l'occupation humaine limite leur ajustement naturel. Malgré les récents progrès en modélisation morphodynamique côtière, la prévision à long terme du trait de côte reste difficile. La plupart des modèles ne représentent qu'un couplage simplifié entre le transport sédimentaire longitudinal et la réponse du profil transversal, considérant encore ces composantes comme faiblement interactives, sans rétroaction explicite entre l'évolution en plan du trait de côte et les translations volumétriques du profil sous l'effet de l'élévation du niveau marin. Cette thèse s'attaque à cette limitation par le développement et l'application de LX-ST, un cadre de couplage à complexité réduite intégrant la dynamique en plan du modèle LX-Shore et la translation de profil simulée par le modèle ShoreTrans. LX-ST inclut plusieurs niveaux de couplage et, via ShoreTrans, peut représenter différents modes de translation du profil, distinguant notamment les réponses dunaires adaptatives et des réponses contraintes face à l'élévation du niveau de la mer. Ses capacités ont été testées sur des cas synthétiques et réels (Lacanau, côte aquitaine, France), montrant que LX-ST reproduit les principaux comportements des systèmes littoraux, notamment la variabilité longitudinale, les rétroactions induites et les réponses non linéaires à l'élévation du niveau marin. Les projections à l'horizon 2100, selon divers scénarios de trajectoires socio-économiques partagées, combinent deux grandes sources d'incertitude : l'élévation du niveau de la mer et le déficit sédimentaire à long terme. Des projections probabilistes du trait de côte ont été obtenues avec LX-Shore, tandis que LX-ST a permis d'affiner la représentation de l'évolution dunaire et des évolutions morphologiques à proximité du d'ouvrage. L'analyse de sensibilité a montré que le déficit sédimentaire domine l'incertitude durant les premières décennies, tandis que l'élévation du niveau marin devient la principale source d'incertitudes dans la seconde partie du siècle, selon le scénario considéré. Un résultat important est la mise en évidence de changement de trajectoire, c'est-à-dire des transitions dans le schéma spatial de l'évolution du trait de côte, résultant des rétroactions entre le transport longitudinal et la translation de l'avant-côte. Les résultats soulignent également la sensibilité des projections au mode de réponse du profil (adaptatif ou érosif), avec des implications majeures pour la persistance ou la disparition des systèmes dunaires. Ce travail contribue à améliorer la compréhension et la prévision de l'évolution à long terme des côtes sableuses dominées par les vagues face à l'élévation future du niveau de la mer.

Mots-clés : Côtes sableuses, Morphologie littorale, Modélisation, Élévation du niveau de la mer, Ouvrages côtiers

---

BRGM

DRIS/R3C, 45000 Orléans, France

EPOC

UMR CNRS 5805 EPOC, 33600 Pessac, France

Modeling past and future evolution of sandy coasts

Abstract: Sandy coasts are dynamic environments that continuously respond to the combined influence of waves, tides, and sea-level rise. With the acceleration of this rise and the persistence of sediment deficits, these systems are becoming increasingly vulnerable, particularly where human occupation constrains their natural adjustment. Despite recent advances in coastal morphodynamic modeling, long-term shoreline prediction remains challenging. Most models represent only a simplified coupling between longshore sediment transport and the cross-shore profile response, still considering these components as weakly interactive, without explicit feedback between the planform shoreline evolution and the volumetric translations of the profile under sea-level rise. This thesis addresses this limitation through the development and application of LX-ST, a reduced-complexity coupling framework that integrates the planform dynamics of the LX-Shore model with the profile translation simulated by the ShoreTrans model. LX-ST includes several levels of coupling and, through ShoreTrans, can represent different modes of profile translation, notably distinguishing between adaptive dune responses and constrained responses to sea-level rise. Its capabilities were tested on both synthetic and real cases (Lacanau, Aquitaine coast, France), showing that LX-ST reproduces key coastal behaviors, including longitudinal variability, induced feedbacks, and nonlinear responses to sea-level rise. Projections to the year 2100, based on various Shared Socioeconomic Pathway scenarios, combine two major sources of uncertainty: sea-level rise and long-term sediment deficit. Probabilistic shoreline projections were obtained using LX-Shore, while LX-ST refined the representation of dune evolution and morphological changes near the seawall. Sensitivity analysis showed that sediment deficit dominates uncertainty during the first decades, whereas sea-level rise becomes the main source of uncertainty in the second half of the century, depending on the scenario considered. An important result is the identification of trajectory changes, i.e., transitions in the spatial pattern of shoreline evolution, resulting from feedbacks between longshore transport and nearshore evolution. The results also highlight the sensitivity of projections to the mode of profile response (adaptive or erosive), with major implications for the persistence or disappearance of dune systems. This work contributes to improving the understanding and prediction of the long-term evolution of wave-dominated sandy coasts under future sea-level rise.

Keywords : Sandy coasts, beach morphology, Modeling, sea-level rise, sea-walls

---

BRGM

DRIS/R3C, 45000 Orléans, France

EPOC

UMR CNRS 5805 EPOC, 33600 Pessac, France

Contents

ACKNOWLEDGMENTS iii
RÉSUMÉ v
ABSTRACT vi
LIST OF FIGURES ix

1 Introduction **1**
1.1 Background and motivation 2
1.2 Research problem & objectives 6
1.3 Thesis structure 8

2 Literature Review **10**
2.1 Primary processes governing shoreline evolution 11
2.2 Modelling long-Term evolution of sandy coasts 21
2.3 Uncertainty in shoreline modelling 31
2.4 Synthesis and research gap 35

3 Model Development **37**
3.1 Introduction 38
3.2 Models used for long-term modelling 38
3.3 LX-ST development and tests on idealized and real cases 51

4 Lacanau Case & Projections **68**
4.1 Preamble 69
4.2 Introduction 69
4.3 Study site, models, and methodology 71
4.4 Results 82
4.5 Discussion 91
4.6 Conclusion 95

5 Conclusion & Perspectives **97**
5.1 Main Conclusion 98
5.2 Key Findings 99
5.3 Perspectives and future research direction 100

A Appendix A **103**

List of Figures

1.1 Projected global mean sea-level rise under different SSP scenarios 2
1.2 Global distribution of sandy shorelines 3
1.3 Examples of beaches for which we expect contrasting responses to future sea-level rise 4

2.1 Space–time domains of coastal processes and their relevance to shoreline evolution 12
2.2 Cross-shore beach profiles under summer and winter wave conditions 13
2.3 Schematic of longshore drift showing wave-induced current and sand transport . . 16
2.4 Alongshore sediment transport and angle effect 16
2.5 Examples of large-scale sandy shoreline features and morphodynamic patterns . . 17
2.6 Examples of complex shoreline shapes 18
2.7 Surf-zone geometry showing X_s, h_b, $H_{s,b}$, β, and MSL 19
2.8 Main factors causing sea level changes 20
2.9 Spatio-temporal scales of coastal morphodynamics and modelling approaches . . . 22
2.10 Conceptual representation of the Bruun Rule 24
2.11 Active coastal zone and closure depth 25
2.12 Shoreline change projections with the Bruun rule 32

3.1 Components of the ShoreTrans model 39
3.2 ShoreTrans Profile translation scheme 41
3.3 ShoreTrans Hard boundaries and non-erodible layers 43
3.4 Barrier translation modes 44
3.5 LX-Shore model overview 45
3.6 LX–Shore overview and architecture 46
3.7 Shoreline detection in LX–Shore 47
3.8 Bypassing regimes and implementation in LX-Shore 49

4.1 Study site at Lacanau, France 72
4.2 Historical shoreline retreat at Lacanau (1950–2014) 73
4.3 Schematic of the LX-ST framework 75
4.4 ShoreTrans dune response schematics 76
4.5 Wave forcing time series (ERA5) 78
4.6 Sea-level rise trajectories and distributions at Lacanau 79
4.7 Distribution of background erosion rates at Lacanau 79
4.8 Global sensitivity analysis at Lacanau 81
4.9 Shoreline envelopes and retreat probability distributions under three SLR scenarios 83

4.10 Onset year of accelerated downdrift erosion 84
4.11 Shoreline–dune evolution under sea-level rise 85
4.12 Shoreline evolution and Sobol indices updrift of the seawall 88
4.13 Shoreline evolution and Sobol indices downdrift of the seawall 89
4.14 Breakpoint analysis of Sobol indices at the downdrift transect 90

Chapter 1

Introduction

1.1 Background and motivation **2**
1.2 Research problem & objectives **6**
1.3 Thesis structure **8**

1.1 BACKGROUND AND MOTIVATION

Coastal zones have long been focal points of human settlement, cultural exchange, and economic activity. Today, they are home to nearly 40 % of the global population and continue to attract dense urbanization due to their accessibility, temperate climate, and provision of vital resources such as fisheries, tourism, and trade infrastructure (Poumadère et al. 2015). Yet, these same advantages have led to intense human concentration along coasts, which in turn increases their vulnerability. As climate change intensifies, the dual threats of sea-level rise (SLR) and coastal erosion place growing pressure on these densely populated zones.

Sea-level rise, a long-recognized direct consequence of global warming, has been accelerating since the late 19th century and is expected to persist throughout the 21st century and beyond (Masson-Delmotte et al. 2021). Coupled with an increasing frequency of extreme sea levels, this trend threatens to transform what were once rare flooding events into near-annual disasters for millions living in low-lying European coastal zones (Garner et al. 2021). On sandy coasts in particular, where wave action and sediment dynamics govern shoreline position, the impacts of SLR are projected to be among the most economically and ecologically damaging (Van De Wal et al. 2024). Among all

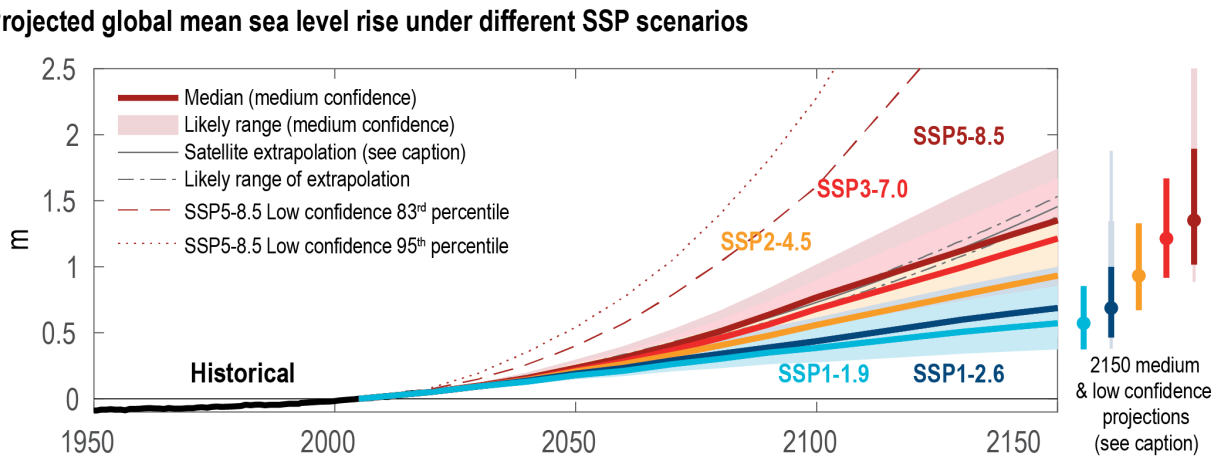

Figure 1.1: Projected global mean SLR under historical data and different Shared Socioeconomic Pathways (SSP) scenarios from 1950 to 2150, based on IPCC AR6 (2021) projections (source: Fox-Kemper et al. (2021)).

coastal environments, sandy beaches stand out for their intrinsic value and vulnerability. They form the first natural line of defense against marine hazards and offer critical ecosystem services. They also form one-third of the ice-free global shoreline (Luijendijk et al. 2018). This global significance is illustrated in Fig. 1.2, which maps the distribution of sandy shorelines worldwide. However, their morphodynamics are governed by a highly complex interplay of processes that act across spatial and temporal scales, from daily wave conditions to centennial-scale climate trends (Cowell and Thom 1995; Castelle and Masselink 2023). This complexity is further amplified by anthropogenic pressures such as urban development, coastal armoring, and sediment supply disruption, which reduce the system's adaptive capacity (Cooper and Pile 2014). As a result, open sandy beaches, which are continuously evolving under the influence of waves, tides and storm surges, are exceptionally sensitive to SLR.

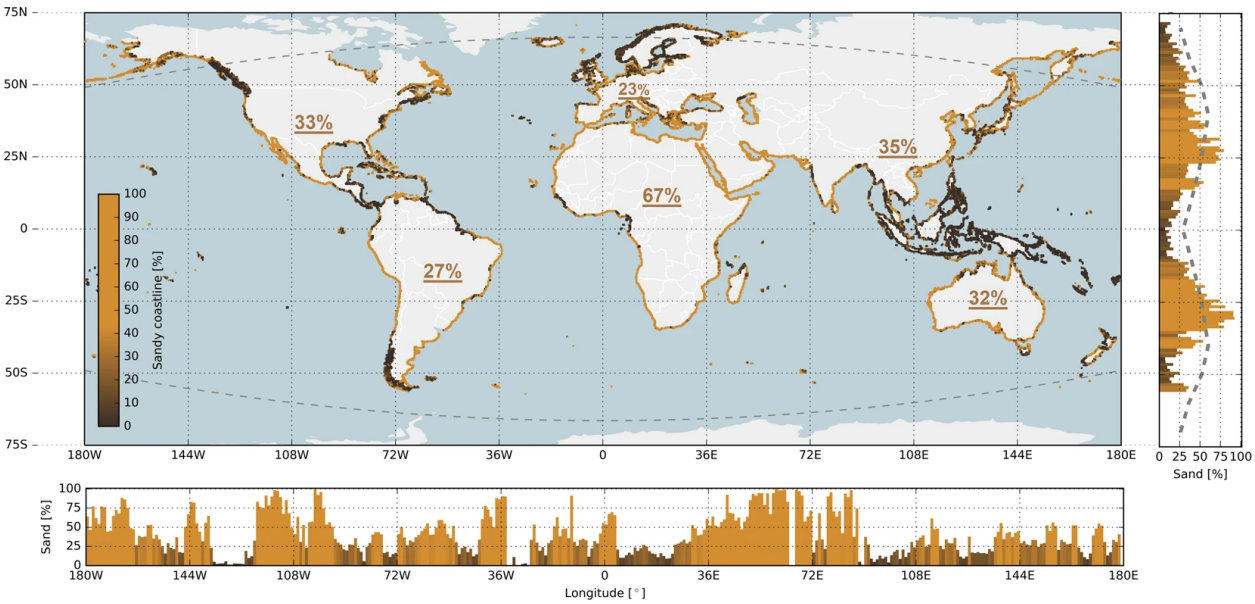

Figure 1.2: Global distribution of sandy shorelines (from: Luijendijk et al. (2018)).

Despite this complexity, global-scale studies have sought to estimate future shoreline retreat using simplified modeling approaches. A prominent example is the global study by Vousdoukas et al. (2020), which projected that nearly half of the world's sandy beaches may face near extinction by 2100 under SLR.

This projection, although widely cited and influential, was based on satellite-derived shoreline data and a modified Bruun-rule formulation to estimate landward retreat. By coupling this rule with global datasets of beach morphology, wave conditions, and satellite-derived shoreline trends, they constructed a model that could be applied consistently across scales (Vousdoukas et al. 2020).

While Vousdoukas et al. (2020) presented the first global assessment of sandy beach response to sea-level rise, an inevitable consequence of such pioneering large-scale analyses is the reliance on simplified assumptions that may amplify apparent shoreline loss. In their approach, beaches were classified as "near extinct" when modelled retreat exceeded 100 m by 2100. This uniform threshold, however, does not account for the capacity of beaches to migrate landward where space is available. Many contemporary systems, shaped during postglacial SLR, have retreated by comparable distances within a century while maintaining their geomorphic and ecological function. By translating this adaptive process into a static retreat metric and applying the Bruun rule uniformly at the global scale, the framework overlooks critical factors such as sediment supply, backshore accommodation, and geomorphological diversity. As highlighted by Cooper et al. (2020), these simplifications can lead to an exaggerated perception of coastal vulnerability. More broadly, this debate underscores a key limitation shared by many reduced-complexity shoreline models: the challenge of representing local adaptation processes and sediment feedbacks within globally applied formulations. This limitation reflects the difficulty of representing the wealth of coastal response modes within global models, which struggle to account for highly localized geomorphic and sedimentary characteristics. As illustrated in Figure 1.3, the response of sandy coasts to sea-level rise can differ drastically depending on local constraints such as coastal defenses or accommodation space. A beach backed by a seawall,



Figure 1.3: Examples of beaches for which we expect contrasting responses to future sea-level rise depending on local boundary conditions: a) a sandy beach constrained by a seawall in Hawaii (photo credit: Shellie Habel, UH Mānoa – SOEST), where landward migration is impeded, leading to progressive narrowing and potential collapse (coastal squeeze); b) severe scarping at South Kingscliff on the Tweed Coast (photo credit: Jono Kingston), where the beach responds dynamically to storm-induced erosion, with potential for recovery and landward migration if space permits.

for instance, may undergo rapid narrowing or collapse due to coastal squeeze, while a similar beach with undeveloped hinterland may simply migrate landward in response to rising seas. Such misclassifications underscore how global-scale projections can obscure local resilience mechanisms or, in some cases, give the impression of severe risk where site-specific conditions suggest otherwise (Cooper et al. 2020).

This debate reignited longstanding criticisms of the Bruun rule itself. Since its introduction in the 1960s, this concept has offered a convenient first-order tool for relating SLR to shoreline retreat. But as early as the 2000s, scholars such as Cooper and Pilkey (2004) had warned that its assumptions (uniform sediment distribution, closed sediment budgets, no change in wave climate) are "so restrictive they probably do not exist in nature". Across diverse coastal environments, observed shoreline retreat frequently departs from Bruun-type predictions, most notably in areas influenced by complex bathymetry or longshore sediment transport gradients (El-Raey 1995; Dennis et al. 1995b; Dennis et al. 1995a; Midun and Lee 1995; Volonte and Nicholls 1995).

The persistence of such oversimplified models, despite longstanding critique, reflects the broader difficulty of representing long-term coastal change in the face of highly variable drivers and limited predictive capacity. The need for reliable, long-term shoreline projections has never been greater. Forward-looking adaptation strategies, infrastructure planning, and risk mitigation efforts all hinge on understanding how coastlines will respond to changing boundary conditions over the coming decades. Yet, modelling shoreline evolution on such timescales remains deeply challenging. High-resolution process-based models offer detailed representations of nearshore hydrodynamics and sediment transport, making them indispensable for storm-scale event simulations. However, their high computational cost and sensitivity to uncertain initial conditions make them unsuitable for

centennial-scale, scenario-based analyses under deep uncertainty (Zhang et al. 2012; Seenath 2022; Hunt et al. 2023).

At the heart of this challenge lies the issue of uncertainty, not only in future climate trajectories, but also in the coastal models themselves. SLR projections, particularly beyond 2050, become increasingly sensitive to assumptions about Antarctic ice sheet instability and global emission pathways. Wave climate projections are also uncertain, influenced, among others, by the choice of global circulation model, the clustering of storm events, and the temporal sequencing of extremes (D'Anna et al. 2021b). These external ambiguities are further compounded by internal limitations: model structure, calibration requirements, assumptions about shoreface behavior, and the omission of key processes such as overwash or bar dynamics. Even seemingly technical decisions, like the method used to estimate the depth of closure, can ripple through the simulation, shaping long-term erosion outcomes (Montaño et al. 2020). For these reasons, it has become increasingly clear that future shoreline projections must explicitly account for the multiple layers of uncertainty. Recent studies have shown that the contribution of different sources of uncertainty evolves over time, with model assumptions dominating in the near term, while sea-level rise becomes the primary driver in the second half of the century (D'Anna et al. 2021b). To capture the full range of possible outcomes, large ensembles of simulations are needed, sampling across scenarios, models, and internal variability (Toimil et al. 2021). This demand underscores the importance of fast-running shoreline models, which allow thousands of realizations to be performed within feasible computational budgets.

As previously discussed, the limitations of existing shoreline modelling approaches are threefold: first, highly simplified geometric models remain inadequate for application at local or regional scales; second, fully process-based models, while physically robust, are too computationally demanding to extend confidently over decadal time horizons; and third, the increasing emphasis on uncertainty quantification requires tools capable of fast and repeated simulations. To address these constraints, reduced-complexity models have gained traction. By emphasizing the dominant coastal processes, they achieve both computational efficiency and broad spatial coverage (Vitousek et al. 2017; Antolínez et al. 2019; Robinet et al. 2018; Tran and Barthélemy 2020; Chataigner et al. 2022). Recent developments such as LX-Shore (Robinet et al. 2018) and IH-LANSloc (Álvarez-Cuesta et al. 2023) blend empirical transport formulations with morphological adaptability, enabling probabilistic scenario modelling and coastal vulnerability assessments. These advances represent an important step forward, yet key limitations remain, particularly in resolving cross-shore feedbacks between shoreline retreat and profile translation, in capturing long-term adjustments driven by sea-level rise, and in representing spatial variability in sediment size and availability.

Despite widespread criticism, legacy assumptions like those embedded in the Bruun rule continue to shape the backbone of many reduced-complexity models accounting for SLR effect. A large number of contemporary frameworks still rely on static equilibrium profile concepts that translate shorelines landward under SLR, often overlooking local bathymetric variation, sediment pathways, and feedback mechanisms (Vousdoukas et al. 2017; Robinet et al. 2018). This is particularly problematic in

morphologically complex or human-altered settings, where such assumptions become increasingly invalid. Moreover, most one-line and hybrid models represent the shoreline as a single evolving contour, an abstraction that cannot resolve the planform dynamics of features such as spits, headlands, or sediment bypassing across embayments (Hunt et al. 2023). While these simplifications may be justified in idealized domains or for some environments, their limitations become evident when applied to complex real-world coastlines requiring nuanced, site-specific adaptation strategies.

In addition, many modelling frameworks focus exclusively on shoreline position, neglecting substantial morphological changes that occur across the broader coastal profile. It is entirely possible for a shoreline to appear stable while the subaerial beach narrows or disappears, especially in front of rigid structures such as seawalls. Conversely, retreating shorelines may mask even more consequential losses, such as the erosion of protective dunes, which exposes hinterland areas to heightened flood risk (McCarroll et al. 2021a). Ignoring profile evolution leads to misrepresentations not only of sediment budgets but also of hazard exposure, as total water levels and inundation extents are closely tied to local topography (Toimil et al. 2023a). The influence of SLR extends well beyond passive shoreline encroachment: it reshapes the shoreface, alters wave transformation patterns, and modifies the interplay of cross-shore and longshore processes over decadal timescales (Toimil et al. 2023b). Accurately capturing this coupled morphodynamic response requires moving beyond assumptions of equilibrium retreat or stationary topobathymetry, toward models that resolve vertical and volumetric changes across the entire coastal compartment.

As sandy shorelines continue to adjust under the influence of natural variability and human interventions, there is a growing need to combine shoreface and shoreline modelling in order to better account for wave and SLR effects in long-term predictions of coastal evolution. The challenge lies in developing approaches that can simulate decadal to centennial morphodynamic change with sufficient physical basis, while remaining computationally efficient and flexible enough to allow uncertainty quantification.

1.2 RESEARCH PROBLEM & OBJECTIVES

Despite decades of progress in coastal morphodynamic modelling, a critical gap remains in our ability to simulate the combined effects of longshore transport and shoreface retreat under sea-level rise (SLR) at time scales relevant for adaptation planning (Hoagland et al. 2023). Existing models tend to address these processes in isolation or under assumptions limiting their capacity to support scenario-based decision-making in real-world settings (Hunt et al. 2023; Hoagland et al. 2023).

The fundamental issue lies in the lack of dynamic coupling. As sea level rises, the shoreface retreats and modifies wave transformation, which reshapes longshore sediment transport patterns (Robinet et al. 2018). Sediment gradients along the coast and cross-shore profile translations are not independent phenomena but coupled components of an integrated morphodynamic system.

Few existing models integrate these components within a computationally efficient framework suitable for scenario-based planning (Robinet et al. 2018; Álvarez-Cuesta et al. 2023; Roelvink et al. 2020). Models focused on planform change assume a fixed cross-shore profile, representing sea-level rise through highly simplified approaches such as uniform retreat rates or direct application of the Bruun rule. Conversely, profile-evolution models typically neglect the alongshore variability and planform complexity associated with headlands, engineered structures, or sediment-bypassing zones. This fragmentation limits our ability to represent how sandy coasts actually evolve under compound forcing and site-specific constraints.

The challenge, then, is not simply one of scale or speed, but of integration. Longshore sediment transport and shoreface retreat are inherently coupled processes: changes in wave climate and shoreline orientation influence sediment gradients, while shoreface retreat modifies the active profile and available accommodation space. Capturing this interdependence, especially under accelerating sea levels, requires a modelling approach that is both morphodynamically aware and computationally tractable.

The overarching objective of this thesis is twofold. First, to improve the modelling of future evolution of wave-dominated sandy coasts by more explicitly accounting for shoreface response to SLR. Second, to integrate such modelling within an uncertainty quantification framework, enabling systematic assessment of how external forcing and model assumptions shape long-term shoreline change. Together, these objectives aim to advance the capacity of reduced-complexity models to provide robust insights into the decadal to centennial evolution of sandy shorelines.

In this thesis, I address this challenge through the development and application of LX-ST, a coupling method that integrates longshore planform dynamics and rule-based shoreface response under SLR. I built the model by combining two recent advances: LX-Shore, a reduced-complexity, grid-based shoreline model grounded in empirical transport laws and capable of handling flexible morphologies (Robinet et al. 2018), and ShoreTrans, a profile-based model that simulates landward retreat and sediment redistribution in real profiles without parametrization (McCarroll et al. 2021a). While each model captures a different dimension of coastal evolution, their integration within the LX-ST forms a novel platform for resolving three-dimensional shoreline response across medium to long timescales with low to moderate computational cost. This integration required bridging technical gaps between fundamentally different model components and related codes developed independently: the 2D-grid based LX-Shore code in FORTRAN and the transect-based ShoreTrans code in MATLAB, highlighting the modularity and interoperability challenges often overlooked in coastal modelling practice

Beyond technical integration, the objective is also to advance our scientific understanding of how future shoreline trajectories unfold under combined SLR and sediment deficits. By enabling simulations across a range of scenarios, LX-ST aims at allowing exploration of the conditions under which coastlines transition between persistence, narrowing, and retreat. In particular, it aims at supporting the identification of spatial and temporal tipping points, such as thresholds in sediment

supply or sea-level trajectories, that may trigger abrupt changes in coastal behavior. The model's demonstrated capacity to account for site geometry, accommodation space, and morphodynamic feedbacks allows it to project change and to interpret how, where, and when these changes occur.

The contributions of this thesis are threefold:

1. **Coupling Framework:** development of the LX-ST framework (Chapter 3).
2. **Benchmarking and Validation:** Application of LX-ST to synthetic and real cases to evaluate consistency, numerical stability, and the capacity to reproduce known shoreline behaviors under varying SLR and sediment conditions (Chapter 3).
3. **Scenario-Based Projections and Uncertainty Assessment:** Deployment of LX-ST within an uncertainty quantification framework to explore shoreline evolution across ensembles of SLR trajectories and erosion regimes, quantify spatial uncertainty in retreat estimates, and assess coastal trajectory shifts under future forcing. The use of LX-Shore for probabilistic analyses strengthens this framework by quantifying uncertainty, while LX-ST provides the physical basis to interpret it (Chapter 4).

This doctoral research is carried out within the framework of the SHORMOSAT ANR project (2022-2026). This project aims at 'Understanding and predicting contemporary shoreline evolution in a changing climate by satellite data assimilation in hybrid models', in order to improve the prediction of shoreline change under sea-level rise and climate variability. My PhD represents one component of this broader project, focusing specifically on the development and application of the coupled LX-ST model to quantify shoreline and shoreface response under multiple sea-level rise scenarios.

1.3 THESIS STRUCTURE

The thesis is organized as follows:

Chapter 2 establishes the foundation for the research through three interconnected components. It first reviews the primary drivers of coastal change, examining how sea-level rise, wave climate variability, sediment supply, and human interventions interact across temporal and spatial scales. It then introduces shoreline evolution models: process-based, reduced-complexity, and data-driven, highlighting their respective capacities and limitations in representing coupled longshore-cross-shore dynamics. Finally, it discusses probabilistic approaches in coastal modelling, with a focus on uncertainty quantification and the ways in which uncertainties from climate forcing, model parameters, initial conditions, and structural assumptions can propagate through time and affect long-term projections.

Chapter 3 presents the first core contribution of the thesis: the development of the LX-ST coupling that integrates LX-Shore for longshore sediment transport with ShoreTrans for cross-shore profile

adjustment. The chapter details the model architecture, coupling logic, and performance validation using both synthetic test cases, but also a case inspired from a real-world site (Lacanau, France).

Chapter 4 investigates shoreline evolution trajectories under future sea-level rise (SLR) and sediment supply scenarios on the Lacanau site. The approach combines large-ensemble simulations with LX-Shore, using a probabilistic framework, and deterministic simulations with LX-ST to capture both the probabilistic range of retreat and the underlying morphodynamic mechanisms. This integration enables risk-informed projections of coastal change and supports the identification of key controls driving trajectory shifts by 2100.

Chapter 5 concludes the thesis with a synthesis of the main findings, a discussion of current limitations—both methodological and conceptual—and outlines directions for future research. Particular attention is given to enhancing model realism, integrating human interventions, and leveraging hybrid methods that combine physical modelling with data-driven inference.

Chapter 2

Literature Review

2.1 Primary processes governing shoreline evolution **11**

2.1.1 Wave-driven cross-shore transport 12

2.1.2 Longshore sediment transport 15

2.1.3 Sea-level rise effect 20

2.2 Modelling long-Term evolution of sandy coasts **21**

2.2.1 The challenge of modelling long term coastal change 22

2.2.2 Shoreface response to sea-level rise 23

2.2.3 One-Line and planform evolution models 27

2.2.4 Hybrid and coupled approaches 28

2.2.5 Data-driven and machine learning approaches 30

2.2.6 Comparative synthesis and applicability envelope 31

2.3 Uncertainty in shoreline modelling **31**

2.3.1 Computational demands and model selection 33

2.3.2 Quantifying parameter influence through global sensitivity analysis . . 33

2.3.3 Uncertainty propagation and temporal dynamics 34

2.4 Synthesis and research gap **35**

▸ OVERVIEW This chapter establishes the conceptual and methodological foundations for the work presented in this thesis. It is structured around three interlinked themes that progressively narrow from broad physical principles to specific modelling challenges. The first part examines the primary physical drivers of coastal change: sea-level rise (SLR), wave climate variability, sediment supply, and human interventions; emphasizing their relative importance, interaction mechanisms, and the temporal and spatial scales at which they operate. The second part provides a review of existing shoreline evolution models, from fully process-based to reduced-complexity and data-driven approaches, with a focus on their ability to represent coupled longshore–cross-shore dynamics under changing boundary conditions. The third part addresses probabilistic frameworks in coastal modelling, detailing how uncertainties stemming from climate forcing, model structure, parameter selection, and initial conditions can propagate and amplify over decadal to centennial horizons. It also introduces GSA methods, which help identify the dominant drivers of shoreline variability and quantify the relative influence of uncertain inputs on projected coastal change.

2.1 PRIMARY PROCESSES GOVERNING SHORELINE EVOLUTION

Shoreline change is driven by a range of physical processes, yet only a subset of these operate persistently at the spatial and temporal scales relevant to long-term coastal evolution. Among them, longshore sediment transport, cross-shore transport, and sea-level rise (SLR) constitute the primary mechanisms responsible for shaping the planform and profile of sandy coasts over decadal to centennial timescales (Bozzeda et al. 2023; Robinet et al. 2018). As illustrated in Fig. 2.1, these three processes occupy a central zone in the coastal space–time domain, linking nearshore dynamics across scales from individual storm events to multi-decadal trends, and from the beachface to the lower shoreface (Voller et al. 2020). Their interaction governs sediment pathways and shoreline position through complex feedbacks—changes in shoreline orientation affect wave breaking and longshore currents; SLR alters the active profile and sediment budgets; and cross-shore exchange modulates the supply available for alongshore redistribution (Kinsela et al. 2022; Hunt et al. 2023).

Processes such as tectonic uplift, geological subsidence, or long-term sediment supply shifts, while significant over millennial scales, are not dynamically coupled with the time horizons of shoreline response addressed in this work. These boundary conditions provide the broader geologic context but evolve too slowly to explain observable shoreline change over human planning horizons (Komar 1977). The focus here is therefore on the three dominant processes whose spatial and temporal signatures align with both the resolution of available observations and the demands of scenario-based modelling (Harley et al. 2022). The sections that follow examine each of these drivers in turn, emphasizing their mechanisms, variability, and mutual feedbacks.

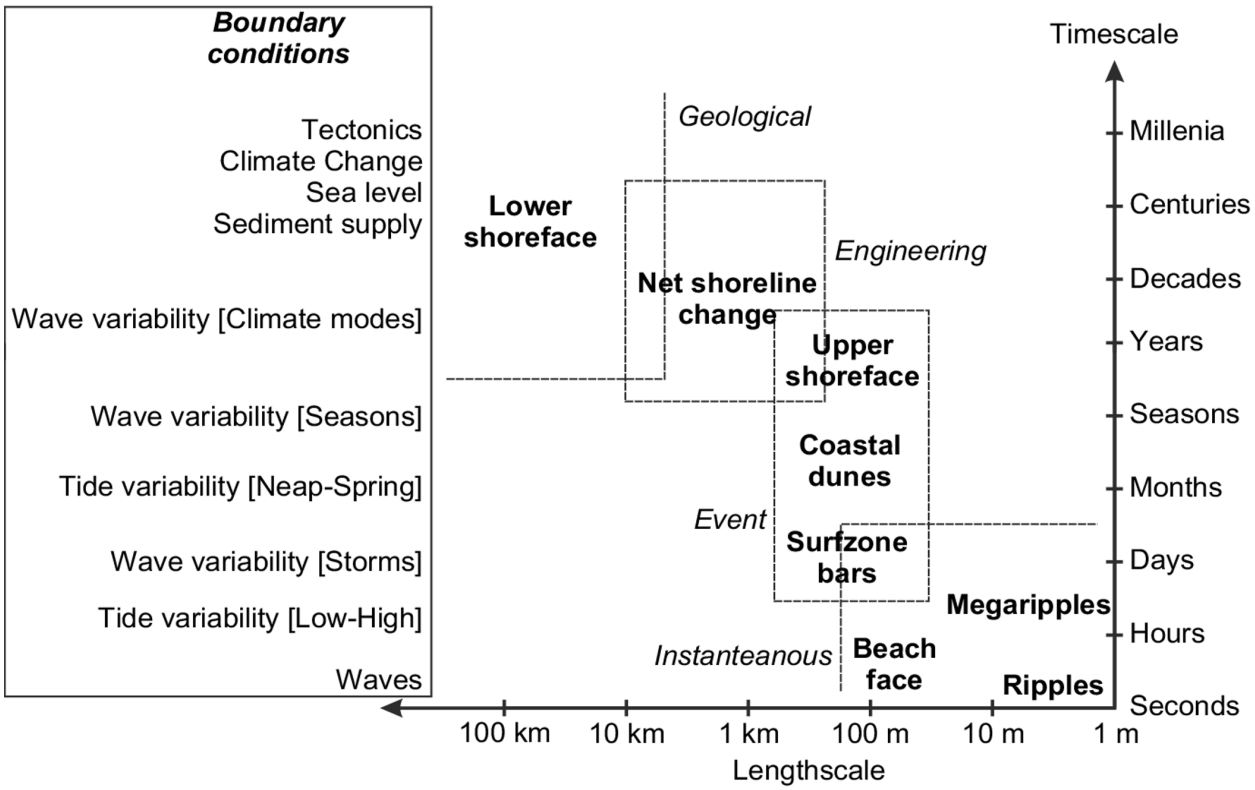

Figure 2.1: Characteristic spatial and temporal scales of key coastal processes and geomorphic units (from: Castelle and Masselink (2023)).

2.1.1 Wave-driven cross-shore transport

Among the various mechanisms that shape sandy coastlines, cross-shore sediment transport stands out for its dynamic complexity and episodic response. Unlike longshore transport (Section 2.1.2), which tends to reflect a persistent directional forcing from wave direction, cross-shore transport emerges from a subtle balance between opposing forces. It is governed by short-term, non-linear processes that respond rapidly to wave transformation, water depth, sediment characteristics, and beach slope; making it a central driver of beach profile evolution from storm-induced erosion to post-event recovery.

This transport mechanism becomes especially pronounced during high-energy events such as storms, when waves approach the shore with high intensity and more direct incidence (Dean 1995). The result is often a disequilibrium in the beach profile, with erosion of the upper foreshore and dune toe, and offshore transport of sediment that may form temporary bars or deepen the nearshore profile (Davidson et al. 2013; Yates et al. 2009).

▸ Note The following description of cross-shore transport mechanisms draws largely on the synthesis provided by Castelle and Masselink (2023).

A central process in this transport regime is the imbalance between onshore and offshore forces acting on sediment particles. Onshore-directed transport is primarily driven by wave nonlinearity,

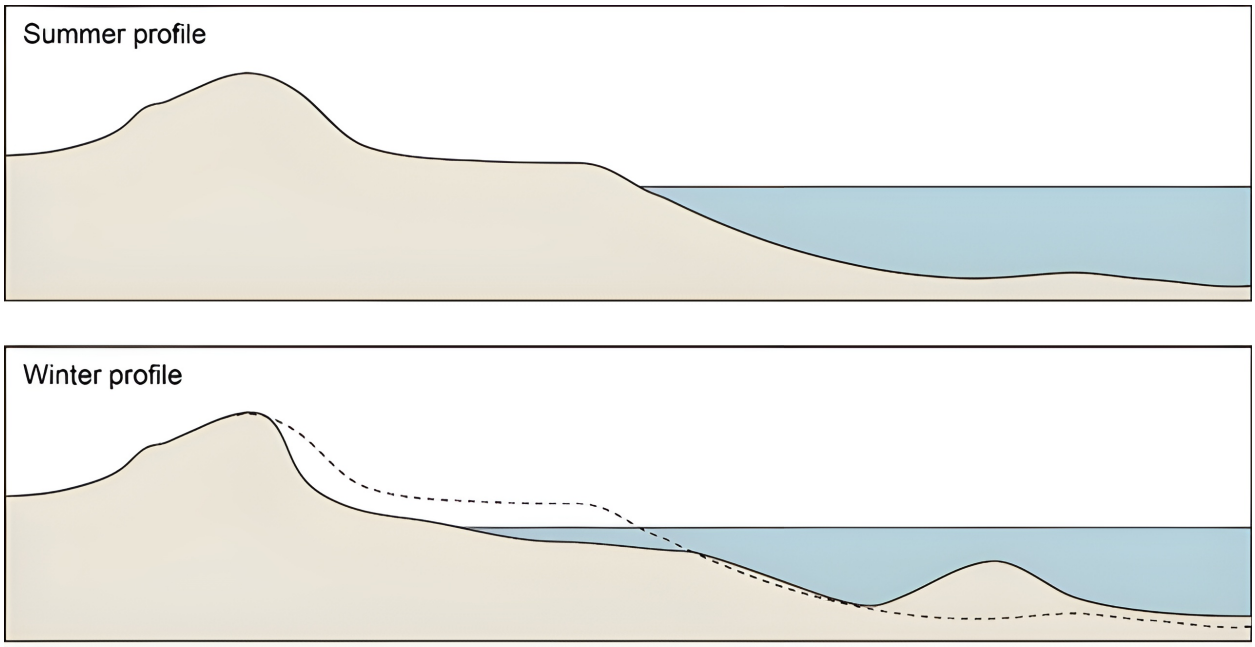

Figure 2.2: Cross-shore beach profile changes between summer and winter conditions (from: Hallin (2019))

.

notably the skewness and asymmetry of near-bed orbital velocities. As waves approach the coast and transform in shallow water, their shape changes, from symmetric sinusoidal forms to increasingly skewed and asymmetric profiles, resulting in stronger shoreward velocities under the crest and weaker velocities under the trough. These asymmetries translate into net onshore bedload transport, even in the absence of a net current (Ruessink 1998; Smith and Mocke 2002; De Bakker et al. 2016). This mechanism dominates during moderate wave conditions with weak or non-breaking waves and promotes the gradual onshore migration of bars and the rebuilding of berms, often observed during fair-weather periods (Trowbridge and Young 1989; Gallagher et al. 1998).

Conversely, offshore-directed transport is largely governed by undertow: the seaward return flow that balances the wave-induced mass transport in the upper water column. During storm conditions, intense wave breaking generates strong undertows capable of mobilizing large volumes of sediment and transporting it offshore. This mechanism underlies the formation of storm-induced erosion profiles, characterized by beach flattening and offshore bar development (Sallenger Jr et al. 1985; Roelvink and Stive 1989; Gallagher et al. 1998). In addition to undertow, infragravity waves can either enhance or oppose offshore transport. Their direction and influence depend on local wave conditions, particularly the ratio of incident to infragravity wave heights (Osborne and Greenwood 1992; De Bakker et al. 2016).

At any given location along the profile, the net cross-shore transport results from the complex superposition of these processes. When nonlinearity-driven bedload transport dominates, sediment tends to accrete landward. When undertow or infragravity-driven suspension dominates, sediment is carried offshore. The relative dominance of each depends on wave height, wave period, water depth, and sediment characteristics (Thornton et al. 1996; Hoefel and Elgar 2003).

Importantly, these processes are not uniformly distributed across the beach profile. Gradients in wave breaking, turbulence, and energy dissipation across the cross-shore axis generate spatial variability in transport rates, which in turn drive morphological change. Bars and berms form, migrate, and decay in response to these gradients and their feedback with morphology (Castelle and Masselink 2023; Dubarbier et al. 2015). For example, bar migration is typically offshore during energetic conditions, and onshore during calm periods, reflecting a dynamic response to shifting hydrodynamic forcing.

Turbulence plays a pivotal role in enhancing sediment suspension and vertical mixing during breaking. This effect is strongest near the wave breakpoint, where breaking-induced vortices can entrain sediment well above the bed and redistribute it across the water column (Svendsen 1987; Hally-Rosendahl et al. 2014). The net transport then depends on how this suspended sediment interacts with mean flows like undertow or swash backwash.

Finally, sediment characteristics exert a controlling influence on transport mode and magnitude. Fine sands are more readily suspended and advected, while coarser grains tend to remain in bedload. This grain-size dependency introduces feedbacks between transport processes and local morphology: sediment sorting, armoring, and selective mobilization can all modify the local response to hydrodynamic forcing over time (Bailard and Inman 1981; Castelle and Masselink 2023).

These processes operate on relatively short timescales, typically from days to months, and are strongly influenced by individual storm events or seasonal patterns in wave energy. For example, intense winter storms can rapidly erode sediment from the beach and dunes, while calmer post-storm periods allow for partial recovery through onshore transport (Robinet et al. 2020; McCarroll et al. 2021a). The resulting variability in the cross-shore profile is often the dominant component of short-term shoreline change, particularly on wave-exposed coasts (Hunt et al. 2023). Such fluctuations are frequently well captured by equilibrium shoreline models at seasonal to interannual scales (Yates et al. 2009; Splinter et al. 2014; Jaramillo et al. 2021).

However, the relevance of these fluctuations to long-term shoreline evolution depends critically on both the magnitude of the events and the system's ability to recover. When storm-induced erosion is followed by incomplete re-accretion or when energetic events occur in tight succession, residual changes can accumulate, creating a persistent retreat signal over time (D'Anna et al. 2021b). In such cases, cross-shore processes cease to be merely cyclical and instead exert a directional influence on shoreline position. Conversely, when sediment recovery is rapid and consistent, and no external trend (such as SLR or sediment deficit) dominates the system, these fluctuations typically revert to a mean state, contributing only stochastic variability to the shoreline record. Numerous studies and modelling frameworks have shown that, in the absence of clustered extremes or chronic recovery failure, cross-shore sediment transport acts as high-frequency noise superimposed on longer-term trajectories (Fenster et al. 2001; Yates et al. 2009; Splinter et al. 2014; Jaramillo et al. 2021; Hunt et al. 2023)

In summary, cross-shore sediment transport arises from the interplay between wave-driven asymmetries, mean currents such as undertow, turbulence, and infragravity oscillations, modulated by local morphology and sediment properties. These processes are highly dynamic, often acting in opposing directions, and can lead to either reversible fluctuations or net shoreline change depending on their intensity, frequency, and recovery potential. In this thesis, cross-shore sediment transport is recognized as a key mechanism driving short-term shoreline fluctuations, particularly in response to storms and seasonal wave conditions. In this thesis, wave-driven cross-shore transport is considered a high-frequency process whose net influence tends to average out over decadal to centennial timescales, and accordingly it is not incorporated into the long-term modelling framework developed during this PhD work.

2.1.2 Longshore sediment transport

Longhsore sediment transport (LST) refers to the net movement of sediment along the coast induced by waves approaching the shoreline at an oblique angle. As shown in Fig. 2.3, this oblique incidence generates longshore currents within the surf zone, which entrain and carry sediment parallel to the coast, a process often referred to as longshore drift (Berman 2011). On sandy, wave-dominated coastlines, LST governs the redistribution of sediment and thus exerts a primary control on shoreline evolution across event to decadal timescales and alongshore distances ranging from tens of meters to several kilometers.

The rate of LST fundamentally depends on wave height and wave approach angle at breaking. The most widely used formulation is the CERC equation, which expresses volumetric transport (Q_s) as (Coastal Engineering Research Center (U.S.) 1984):

$$Qs = KH_b^2 \sin(2\alpha_b) \tag{2.1}$$

where H_b is the breaking wave height, α_b the breaking wave angle, and K an empirical constant. This formulation highlights the quadratic dependence on wave height: doubling H_b produces roughly a fourfold increase in transport, reflecting the scaling of wave energy flux with H^2. Its simplicity makes it attractive for large-scale assessments, though it does not account for site-specific characteristics. By contrast, the Kamphuis (1991) equation introduces additional parameters; wave period, beach slope, and sediment grain size, allowing improved representation in settings where sediment properties significantly influence mobility.

A key feature of the CERC formulation (and similar LST formulations) is the angular dependence expressed as $\sin(2\alpha)$. Transport peaks when deep-water waves approach at approximately 45°, dropping to zero for shore-normal or shore-parallel incidence (Fig. 2.4). These LST characteristics, together with longshore gradients in wave energy and angles at breaking wave can fosters self-organization of the shoreline into large-scale features such as cuspate forelands, spits or alongshore

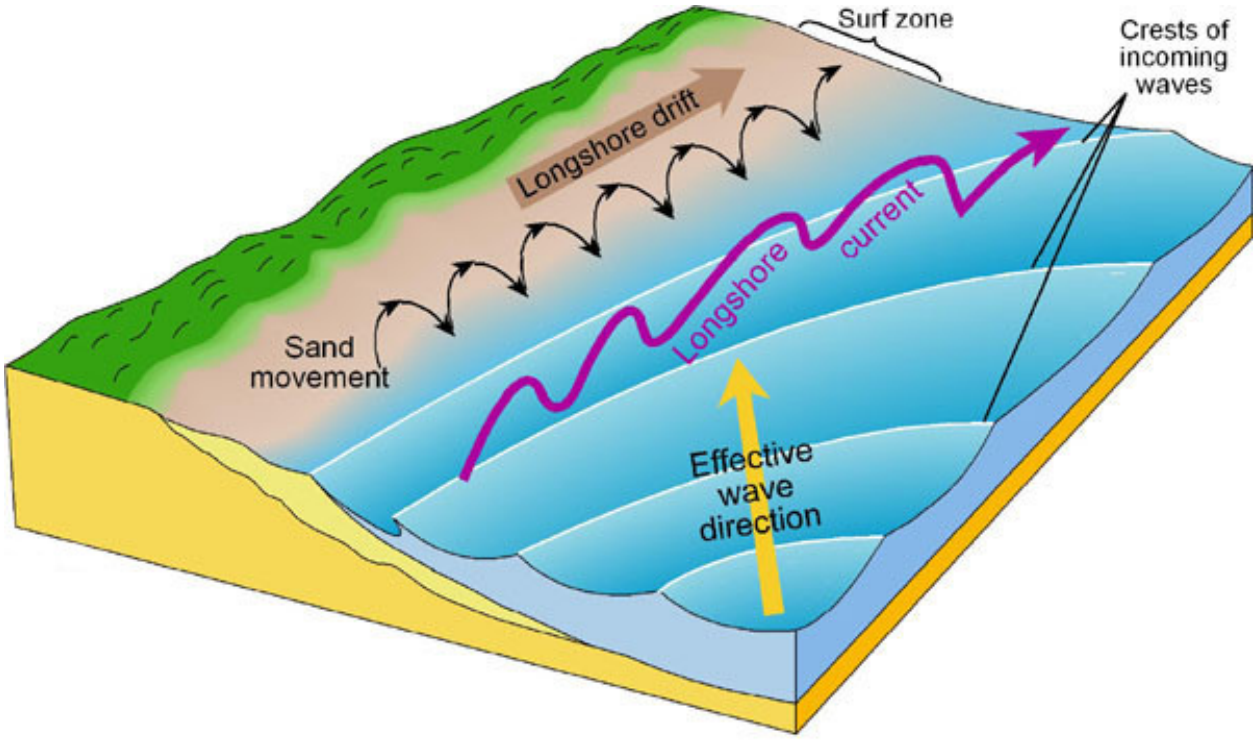

Figure 2.3: Conceptual schematic of longshore drift illustrating the effect of oblique wave incidence on shoreline processes. Waves approaching the coast at an angle generate a longshore current within the surf zone, which transports sediment parallel to the shore and produces a net littoral drift along the coastline (from: Revision World (2025)).

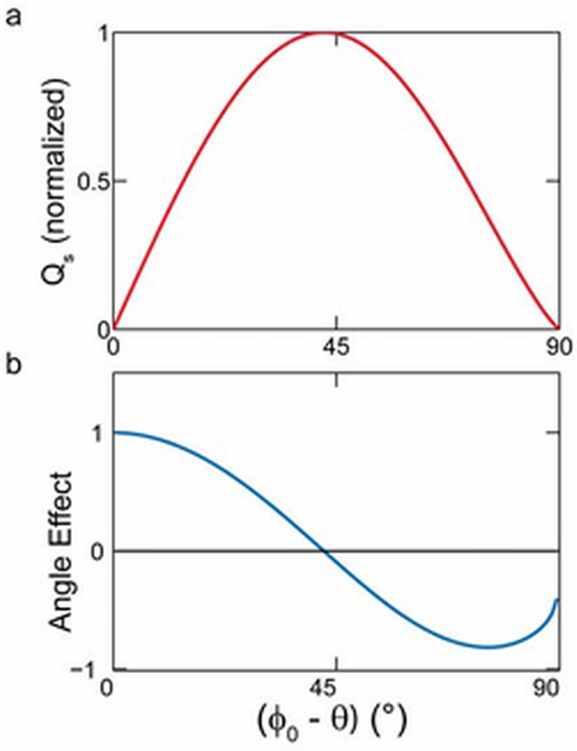

Figure 2.4: (a) Normalized alongshore sediment transport rate (Q_s) as a function of deep-water wave approach angle ($\phi_0 - \theta$), showing a maximum near 45°. (b) Corresponding 'angle effect' (the sensitivity of Q_s to shoreline orientation) indicating the transition from positive (stable, diffusive) to negative (unstable, anti-diffusive) diffusivity at the critical wave angle (from: Ashton et al. (2007)).

sandwaves (Ashton and Murray 2006a; Ashton and Murray 2006b; Falqués 2003; Falqués et al. 2017) (Fig. 2.5).

In all cases, the key driver of morphological change is not the absolute magnitude of transport but the gradients in transport rate alongshore. Where the transport into a given shoreline section exceeds the transport out, sediment accumulates, leading to local accretion. Conversely, where more sediment exits a section than enters, erosion occurs (Hunt et al. 2023; Robinet et al. 2018). These gradients emerge naturally from spatial heterogeneity in wave energy and direction, as well as from the shape of the coastline itself, leading to positive or negative feedback loops. Even small changes in orientation can lead to significant imbalances in transport when interacting with a consistent wave climate (Tran and Barthélemy 2020; Limber et al. 2017).



Figure 2.5: Examples of sandy shoreline features shaped by a wide set of morphodynamic processes: (a) Arabat Spit (Ukraine, Source: Google Earth); (b) cuspate shorelines at the eastern russian coast (from: Google Earth) (c) shoreline sand waves at the Gulf of Finland, Russia (source: Google Earth, image from TerraMetrics and GeoEye).

This framework has often been invoked to explain the emergence of rhythmic shoreline features as (Fig. 2.5):

- **Sand spits (panel a):** Elongated depositional features typically associated with asymmetric wave climates and strong littoral drift. HAWI can reinforce their development, but sediment availability and boundary conditions are equally important.
- **Cuspate forelands (panel b):** Triangular promontories that may form under persistent high-angle wave forcing, but whose growth is often modulated by sediment supply and local geological controls. variability also contribute.

- **Shoreline sand waves, evolving in toward flying sand spit (panel c):** Kilometre-scale undulations that can emerge from self-organization under high-angle wave incidence, though offshore bar dynamics and wave climate

Longshore drift is also highly susceptible to disruption by both natural and artificial features. Because the bulk of longshore transport is confined to the surf zone and adjacent nearshore, any feature that extends seaward to intersect this active transport zone can significantly reduce or even stop sediment movement (Roelvink et al. 2020; Masselink and Russell 2013).

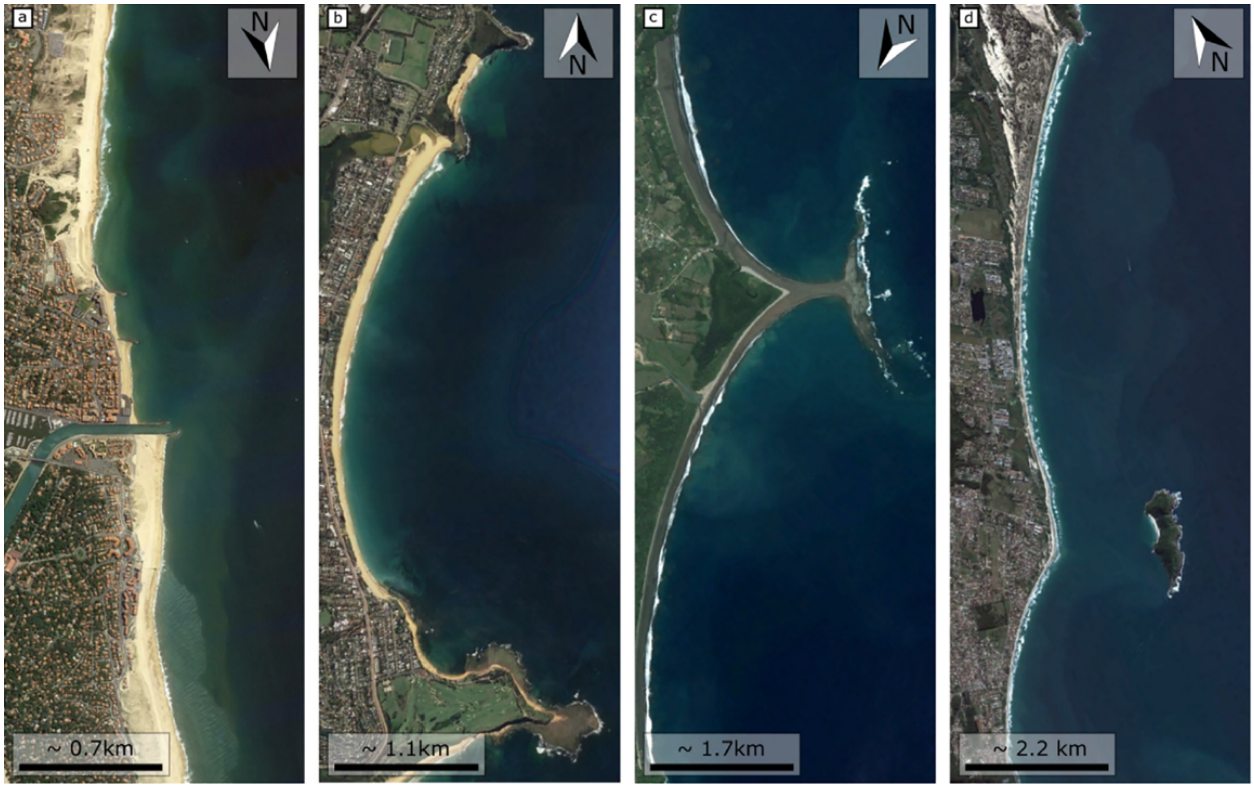

Figure 2.6: Examples of complex shoreline plan-view shapes influenced by inherited geology (e.g., headlands, offshore islands) or coastal hard structures. (a) Hossegor–Capbreton beaches, France; (b) Narrabeen Beach, Australia; (c) Punta Uvita, Costa Rica; (d) Campeche Beach, Brazil (from: Robinet et al. (2018)).

Natural disruptions occur where coastal morphology inherently modifies wave transformation and alongshore currents. Rocky headlands and outcrops refract and diffract incoming wave energy, producing persistent gradients in longshore transport (Masselink and Russell 2013; Xu et al. 2024; Álvarez-Cuesta et al. 2023). Tidal inlets act as partial physical barriers and sediment sinks, with ebb-tidal deltas storing substantial volumes of littoral material that would otherwise continue downdrift (Masselink and Russell 2013; Roelvink et al. 2020). Similarly, coral reefs and rocky shoals dissipate incident wave energy and alter nearshore current patterns, often redistributing sediment away from the alongshore pathway (Xu et al. 2024; Álvarez-Cuesta et al. 2023).

Anthropogenic structures replicate and intensify these effects. Groynes and jetties, aligned roughly perpendicular to the shoreline, intercept sediment moving alongshore, creating accretion zones on the updrift side and sediment deficits downdrift (Roelvink et al. 2020; Szmytkiewicz et al. 2000). Detached breakwaters, positioned offshore and parallel to the coast, reduce wave energy in

their lee, generating distinctive shoreline responses: salients, where the shoreline advances partway towards the structure, and tombolos, where complete attachment occurs (Masselink and Russell 2013; Durand et al. 2024). Seawalls, though primarily designed for shoreline protection, can act as unintended groynes when progressive shoreline retreat causes them to protrude into the surf zone (Dean 1987).

The degree to which a headland disrupts the alongshore sediment flux is primarily governed by its cross-shore extent relative to the surf-zone width. McCarroll et al. (2021b) expressed this control through the dimensionless ratio $B = X_h/X_s$, where $X_h = h_{\text{toe}}/\tan\beta$ represents the headland cross-shore extent and $X_s = h_b/\tan\beta$ the surf-zone width, with h_{toe} and h_b denoting the headland toe and breaking depths (Fig. 2.7). Their process-based simulations with XBeach identified three regimes: (i) full bypass for $B < 0.5$, where sediment flux remains similar to the open coast; (ii) partial bypass for $0.5 < B < 3$, where wave breaking occurs within the headland extent and transport is progressively reduced; and (iii) near-total blockage for $B > 3$, where longshore flux approaches zero. These thresholds provide a practical framework for linking headland geometry to sediment continuity at the regional scale.

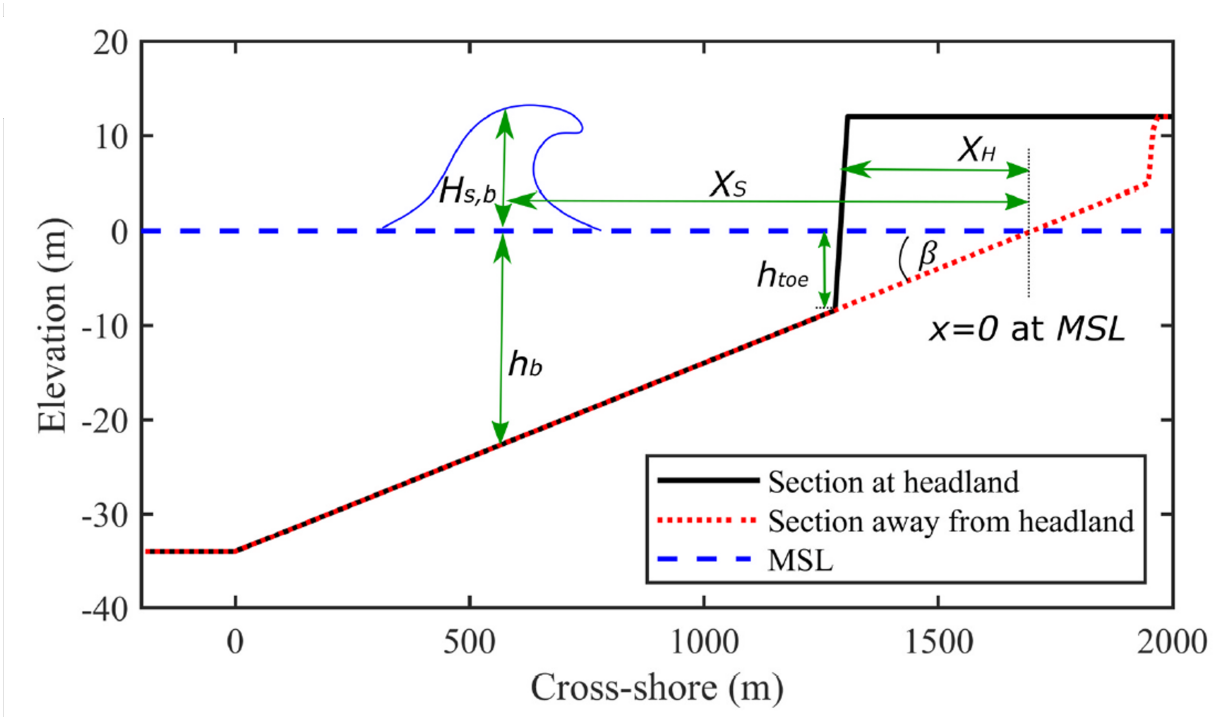

Figure 2.7: Cross-section indicating surf zone width (XS), depth at breaking (hb), significant wave height at breaking (Hs,b), slope angle (β) and mean sea level (from: McCarroll et al. (2021b)).

The morphodynamic consequences of such disruptions are substantial (see Fig. 2.6a). At Władysławowo harbor (Poland), shoreline progradation of more than 100 m occurred west of the breakwaters within decades, while the downdrift sector experienced comparable retreat (Szmytkiewicz et al. 2000). Similarly, field and modelling studies at Al-Gamil (Egypt) highlight that coastal structures can trigger shoreline adjustments exceeding hundreds of meters over relatively short timescales (Roelvink et al. 2020). In contrast, large-scale nourishment projects such as the Sand Engine (Netherlands) demonstrate how soft interventions can redistribute sediment over comparable distances through

natural alongshore transport processes, producing pronounced yet gradual shoreline realignments without fixed structures (Roelvink et al. 2020). These effects can persist for decades, fundamentally altering regional sediment budgets and modifying the long-term trajectory of shoreline change (Masselink and Russell 2013; Roelvink et al. 2020).

From an engineering perspective, control of longshore transport remains a central tool in coastal management. In harbour and navigation projects, jetties prevent inlet migration and maintain channel depth, while breakwaters create sheltered basins and influence sediment deposition patterns (Szmytkiewicz et al. 2000). In beach stabilisation, groyne fields compartmentalise sediment to maintain recreational or protective beach widths (Roelvink et al. 2020). In coastal protection schemes, detached breakwaters and artificial reefs attenuate wave energy while encouraging controlled accretion in targeted locations (Álvarez-Cuesta et al. 2023). The strategic placement of such structures is often combined with beach nourishment, maximising retention and extending the lifespan of placed sediments, as demonstrated in the Port Said intervention (Roelvink et al. 2020).

2.1.3 Sea-level rise effect

Sea-level change represents one of the most consequential long-term pressures acting on sandy shorelines. It arises from multiple interacting processes, including ocean thermal expansion, melting of polar ice sheets and mountain glaciers, and exchanges with terrestrial water storage (Fig. 2.8). Together, these mechanisms drive global and regional variations in mean sea level, altering the boundary conditions that govern coastal morphodynamics (Bozzeda et al. 2023). As mean sea level increases, waves and tides can propagate further inland, enhancing shoreline retreat and sediment redistribution over a wide range of temporal scales.

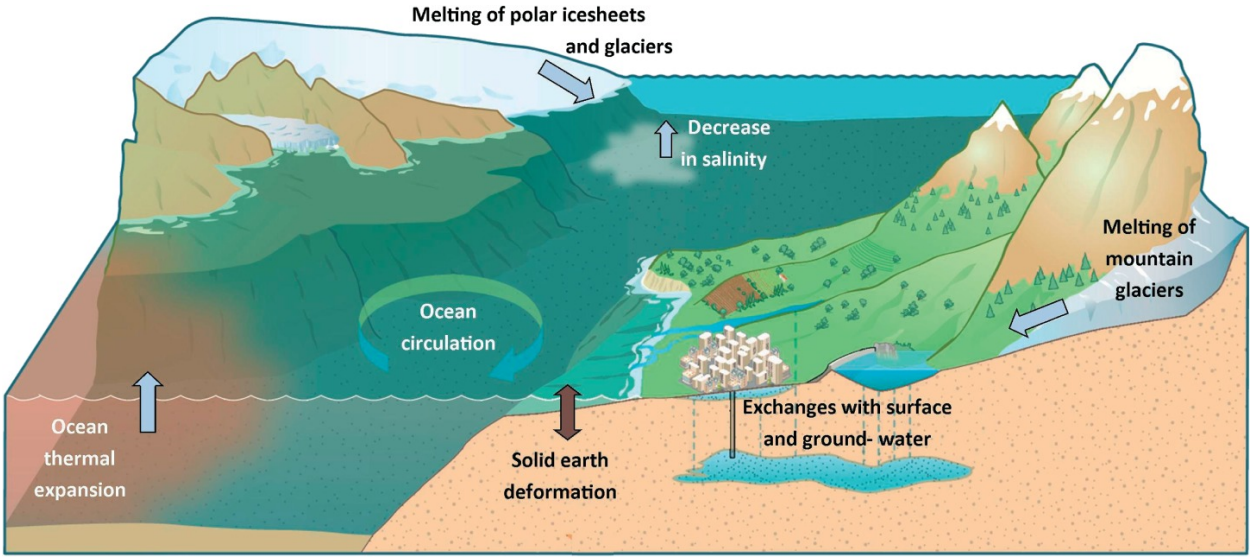

Figure 2.8: Main factors causing sea level changes (from: (Cazenave and Cozannet 2014)).

One of the first and most persistent consequences of rising sea level is the landward shift of the mean shoreline position. Even in the absence of storms, higher baseline water levels lead to more

frequent wave action on the upper parts of the beach, including dunes, berms, and other landforms previously shielded from regular inundation (Hunt et al. 2023; Masselink et al. 2023; Toimil et al. 2023b). These higher-frequency interactions result in greater sediment mobilization and export, ultimately driving gradual shoreline recession and profile adjustment through both cross-shore and longshore processes (Leach et al. 2021; Vitousek et al. 2017).

The impacts of extreme events are similarly amplified. Under elevated sea levels, storm surge and high-energy wave events exert their force further inland. The increased reach of wave runup and overtopping enhances dune erosion, facilitates barrier breaching, and promotes overwash deposition in low-lying coastal environments (Toimil et al. 2023b). While such events are episodic, their erosive potency is intensified by SLR, which acts not as a driver of extremes per se, but as a critical precondition that raises the baseline for damage potential (McCarroll et al. 2021a).

In many coastal zones, especially those subject to urban development or protected by hard infrastructure, the shoreline's ability to migrate naturally in response to SLR is obstructed. This results in "coastal squeeze", a narrowing of the active beach profile that limits sediment exchange and accelerates erosion in the constrained zone (McCarroll et al. 2021a; Vitousek et al. 2024). In such settings, erosion becomes not merely a function of hydrodynamic forcing, but of policy and planning decisions that fix the shoreline in space while the sea level is rising.

Over decadal to centennial timescales, the cumulative impact of SLR emerges as a dominant force in shoreline evolution. Model-based projections under high-emission scenarios indicate that many sandy coasts may retreat by tens of meters by 2100, including stretches historically characterized by accretion or relative stability (D'Anna et al. 2021b; Vitousek et al. 2024). Classical formulations such as the Bruun Rule have attempted to quantify this retreat by assuming a direct geometric relationship between SLR and horizontal shoreline displacement (Bruun 1962), yet such models have faced substantial criticism for oversimplifying the physical and sedimentary dynamics involved (Cooper et al. 2020).

Crucially, the signal of SLR-induced change does not immediately override natural variability. In the near term, fluctuations in storms, wave climate, and human interventions are expected to dominate observed shoreline changes. However, as the 21st century advances, SLR is projected to become a dominant driver of net shoreline retreat (D'Anna et al. 2021b; McCarroll et al. 2021a; Roelvink et al. 2020; Vousdoukas et al. 2017; D'Anna et al. 2022).

2.2 MODELLING LONG-TERM EVOLUTION OF SANDY COASTS

Projecting the evolution of sandy coasts under changing wave climates and sea-level rise requires models that can reconcile a wide range of spatial and temporal scales. Coastal morphodynamics span processes from turbulence and ripple formation occurring within seconds and centimeters, to shoreline migration and sea-level rise unfolding over centuries and kilometers. Capturing these

interactions has led to the development of multiple classes of models, from highly detailed process-based approaches (e.g., Delft3d, Xbeach) to reduced-complexity (e.g., LX-Shore and ShorelineS) and semi-empirical frameworks. Each class occupies a distinct place within the spatio-temporal modelling space, reflecting trade-offs between physical detail, computational cost, and predictive horizon (see Fig. 2.9).

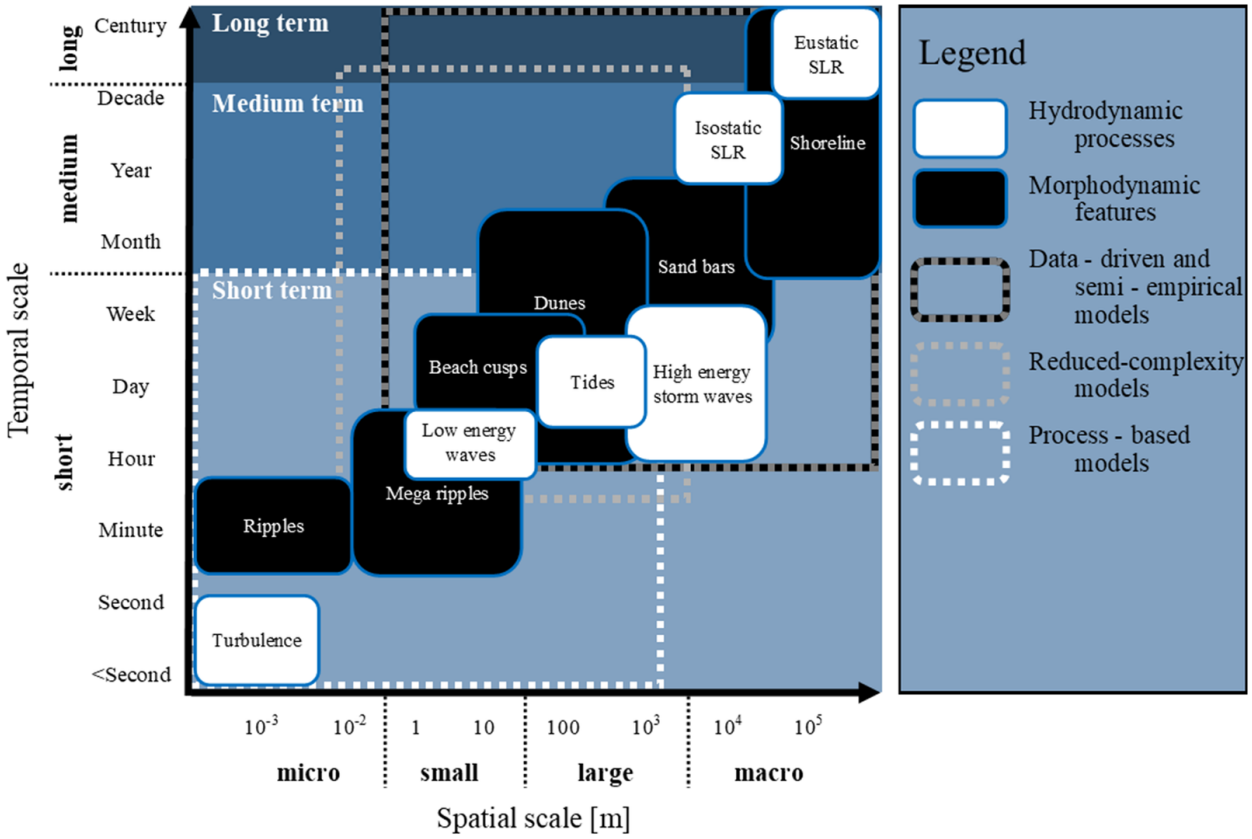

Figure 2.9: Schematic representation of the spatial and temporal scales associated with hydrodynamic processes (white), morphodynamic features (black), and their coverage by different modelling approaches (from: Hunt et al. (2023)).

2.2.1 The challenge of modelling long term coastal change

Shoreline evolution unfolds as a fundamentally three-dimensional process, shaped by the interaction of horizontal planform dynamics and profile morphodynamic responses operating across a wide range of spatial and temporal scales. At the decadal to centennial horizons relevant for coastal adaptation, this complexity is often simplified. Many traditional models reduce the shoreline to a single contour line, a one-line representation that marks the instantaneous land-sea boundary (Vitousek and Barnard 2015; Roelvink et al. 2009; Pelnard-Considère 1957). These models assume shore-parallel bathymetry and an invariant beach profile that translates landward or seaward without deformation. While this abstraction facilitates computational efficiency by collapsing vertical structure into a horizontal signal (Robinet et al. 2018), it inherently omits critical processes that govern shoreline change in both the planform and vertical dimensions.

In practice, coastal morphology adjusts through the coupled evolution of planform shape and beach profile. The shoreline does not merely retreat or advance; it rotates, curves, branches, and interacts with sedimentary features across the foreshore and shoreface. Planar changes, such as the development of spits, beach rotation, and embayment dynamics, reflect responses to longshore sediment gradients and spatial variability in wave direction and energy (Ashton and Murray 2006a; Ashton and Murray 2006b; Hunt et al. 2023). At the same time, profile changes manifest through processes like dune erosion, and shoreface steepening or flattening and longer-term adjustments in sediment accommodation driven by storms, seasonal cycles, and evolving boundary conditions (Blossier et al. 2017; Howd 1998; McCarroll et al. 2021a). These profile deformations can, in turn, modify wave transformation patterns and sediment transport pathways, feeding back into the horizontal dynamics (Davidson-Arnott 2005).

Thus, representing shoreline migration as a unidirectional, lateral shift along a static contour neglects part of morphological feedbacks, and structural disruptions that define coastal dynamics. The shoreline is not simply a line; it is a mobile interface embedded in a volumetric sediment budget, shaped by the convergence of longshore gradients, cross-shore processes, and evolving boundary conditions (Hunt et al. 2023; Vitousek et al. 2024). Capturing this complexity demands modelling frameworks that move beyond the one-line paradigm and engage with the three-dimensional nature of coastal evolution.

2.2.2 Shoreface response to sea-level rise

The notion that beaches tend toward a stable cross-shore shape dates back over a century. Fenneman (1902) recognized the development of a shore-parallel underwater terrace, essentially hinting at the equilibrium profile long before the term was coined. Johnson (1919) added to this early body of work by visualizing how sea-level rise (SLR) might result in an abrasion platform; a flattening of the profile as the sea transgresses inland. In the mid-20th century, more targeted studies began to explore the hydraulic scaling of profiles and seasonal variations (e.g., Johnson 1949), setting the groundwork for later modelling approaches.

The most influential development during this period came from Per Bruun, who worked across diverse environments, from Denmark to Florida, and introduced the concept of a statistical equilibrium profile (Bruun 1954). His work marked a shift toward seeing the beach profile as something that responds predictably to hydrodynamic forcing, especially over decadal timescales.

In 1962, Bruun proposed what would become one of the most cited—and debated—concepts in coastal morphodynamics: the Bruun Rule (Bruun 1962). The idea is straightforward in principle: if sea level rises, the beach profile shifts landward and upward, redistributing eroded material from the upper beach onto the nearshore, thereby preserving water depth across the profile. Early tests of this

theory, both in the lab and the field, gave partial support (e.g., Schwartz 1967). At the time, it offered a simple yet quantitative way to anticipate beach retreat, which helped it gain traction quickly.

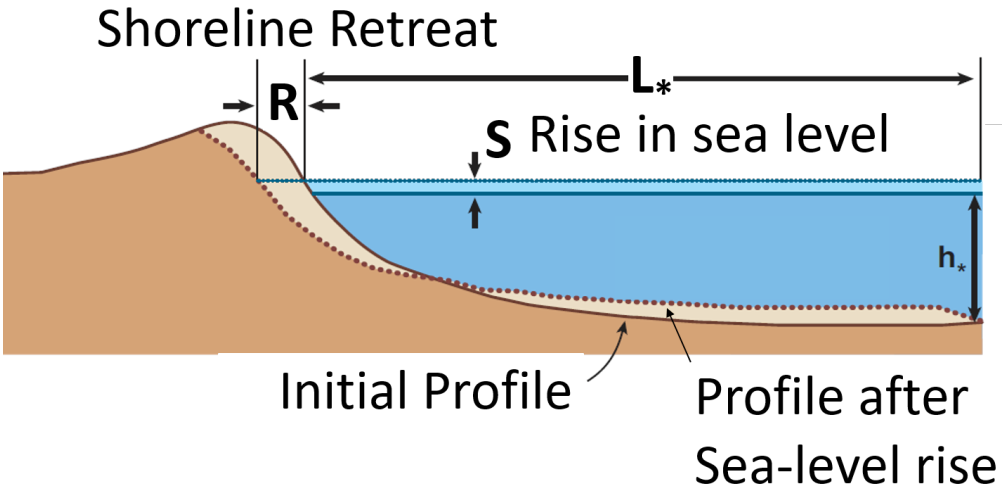

Figure 2.10: Conceptual diagram of the Bruun Rule illustrating coastal profile adjustment in response to SLR (adapted from Cooper and Pilkey (2004))

.

As illustrated in Fig. 2.10, according to the Bruun rule, a rise in sea level by an amount S leads to a corresponding retreat R of the shoreline, determined by the geometry of the profile up to the depth of closure (DoC). Assuming the active profile retains its form and all eroded material is conserved within the system, the retreat distance is given by:

$$R = \frac{S}{\tan \beta} \tag{2.2}$$

where β represents the average slope of the active profile (the section of the profile that adjusts rapidly to incident wave conditions). In this framework, sediment eroded from the upper beach is assumed to be redistributed offshore within the profile, such that total sediment volume remains constant.

The Bruun Rule became a central reference point in early shoreline response theory. Others built on or tested the theory in various settings. Dubois (1975) observed qualitative agreement with the Bruun model in Lake Michigan, documenting landward and upward shifts of profile elements. Hallermeier (1980) developed methods to calculate the closure depth, refining the definition of the active portion of the beach profile. Yet even early on, limitations were evident; adjustment timescales varied, and natural systems often deviated from the model's idealized assumptions.

From the late 1970s onward, field studies showed mixed results: Rosen (1978) found site-specific deviations, while Hands (1979) observed that beaches often responded only years later. This suggested that real-world systems adjust more slowly and through more complex processes than implied by the idealized equilibrium concept of the Bruun Rule.

These concerns led to a major symposium in 1980 to assess the model's assumptions and limitations, and by the end of that decade, alternatives were being tested. For example, Dean and

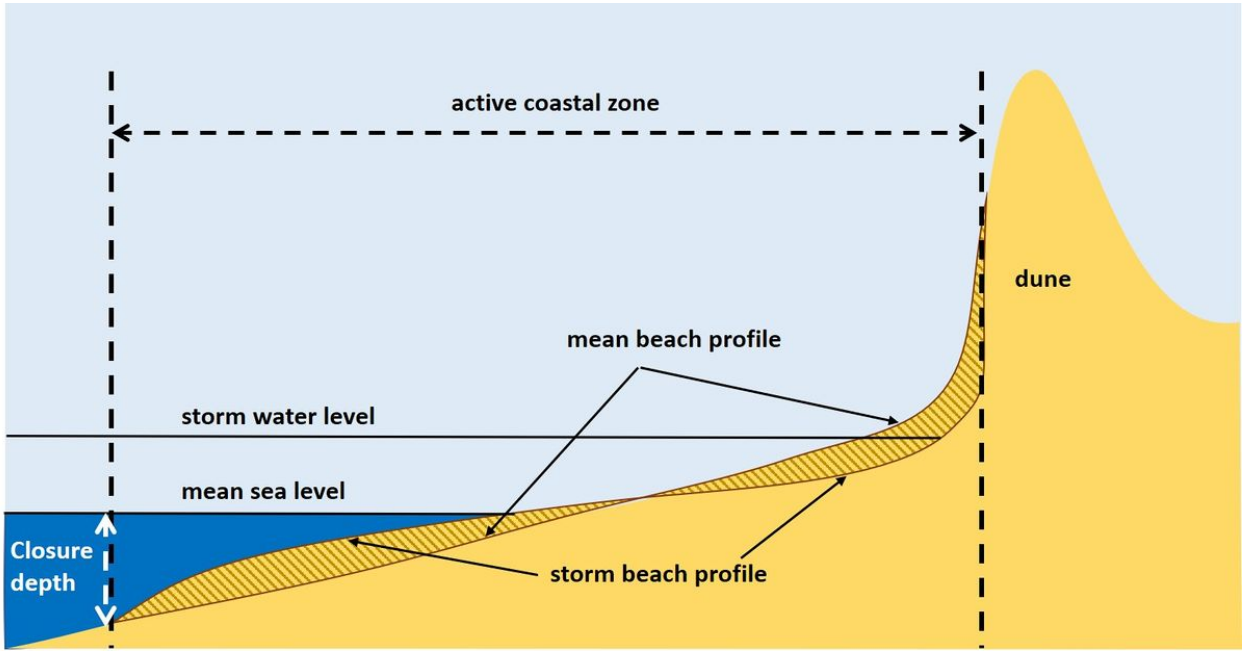

Figure 2.11: Conceptual cross-shore profile showing the active coastal zone bounded landward by the dune and seaward by the closure depth. Closure depth defines the seaward limit of significant sediment transport, while storm water levels drive erosion and profile change. Source: Coastal Wiki

Maurmeyer (1983) proposed models that looked beyond simple cross-shore slices, focusing instead on how entire barrier systems—beaches, dunes, inlets—might redistribute sediment in response to SLR. This marked a shift from thinking purely in terms of onshore translation to considering how sediment could move across broader spatial domains, including landward.

By the early 2000s, critiques intensified with Cooper and Pilkey (2004), who called for the abandonment of the Bruun Rule. They emphasized the model's reliance on assumptions—such as purely offshore transport and constant profile form; that failed to hold up empirically.

At the heart of their critique was the observation that the Bruun Rule rests on a set of assumptions that are not just simplified, but fundamentally false. It treats the coastal profile as a two-dimensional system, closed to sediment exchange in the alongshore or landward directions. In doing so, it assumes that all erosion from the upper beach is deposited offshore, with no net gain or loss of sand from the system. Yet real coastlines are dynamic, three-dimensional environments. Longshore drift, overwash during storms, and aeolian transport can remove or add sediment in directions the model simply does not account for. Cooper and Pilkey (2004) argued that such a closed-system response is "likely impossible to occur in nature". Moreover, the rule assumes that shoreline retreat is an inevitable response to SLR, ignoring the possibility of accretion in sediment-rich systems, a phenomenon that has been observed even under relatively rapid SLR Saintilan et al. (2020).

More recent approaches have tried to strike a balance. Davidson-Arnott (2005) proposed a conceptual model that explicitly includes landward sediment pathways like overwash and wind-driven transport. Building on this, Rosati et al. (2013) introduced a "modified Bruun Rule" that incorporates both offshore and onshore components of cross-shore flux. These efforts reflect a broader shift toward describing full-profile sediment exchange—not just maintaining volume but

considering where that volume actually goes. However, studies by Beuzen et al. (2018) and Atkinson et al. (2018) revealed that both original and modified Bruun formulations typically underestimated observed retreat, particularly when coastal structures were present.

Davidson-Arnott and Bauer (2021) further refined this framework by emphasizing that coastal response to rising water levels depends not only on geometric translation but on the balance between cross-shore accommodation and sediment supply within the active beach-dune system. Their model highlights the coupling between short-term storm processes and long-term sediment budgets: when sufficient sediment is available, the system may migrate landward through overwash and aeolian deposition, preserving dune volume; when sediment supply is limited or human interventions restrict landward migration, erosion and profile steepening dominate.

Recognizing the limitations of both geometric and parameterized approaches, McCarroll et al. (2021a) introduced ShoreTrans: a rules-based, profile-driven model designed to simulate coastal response to SLR over decadal to centennial timescales. Unlike the Bruun Rule and earlier models, ShoreTrans operates directly on observed 2D profiles. This allows capture of complex, site-specific features such as irregular dunes, cliffs, seawalls, and non-erodible substrates. Rather than assuming a uniform response, the model incorporates a detailed sediment budget that accounts for cross-shore fluxes, longshore gradients, back-barrier exchanges, and human interventions such as nourishment or dredging. Importantly, it can simulate both landward and seaward sediment transport, including barrier rollover and dune accretion, and can predict changes in beach width—an often overlooked but critical factor for coastal management.

However, ShoreTrans is inherently one-dimensional, operating along fixed, shore-normal transects. It does not resolve alongshore sediment transport internally (but can take into account Longhsore sediment transport (LST) as an input for each profile) and cannot simulate, alone, evolving shoreline orientation or planform features such as embayed beaches, cuspate forelands, or spit elongation. As such, its ability to capture morphodynamic feedbacks related to curvature, wave refraction, or sediment bypassing is limited. To tackle this issue, ShoreTrans has been integrated into hybrid modelling frameworks like IH-LANSloc (Álvarez-Cuesta et al. 2023), which combine planform shoreline evolution with shoreface profile adjustment, still, relying on fixed transects (an assumption that reaches its limit for sites showing large changes in shoreline orientation). Thus, although ShoreTrans represents a major step forward in shoreface modelling under SLR, especially in its handling of real profiles, structures, and non-erodible substrates, it remains best suited for scenarios where planform change is either minimal or can be resolved by coupling with separate shoreline evolution models.

2.2.3 *One-Line and planform evolution models*

Reduced complexity one-line shoreline models emerged as a necessary compromise between computational efficiency and physical realism. These models are computationally efficient and well-suited for long-term projections, unlike process-based models which are limited by high computational demands and error accumulation over decadal timescales (Zhang et al. 2012; Seenath 2022). They are particularly suited for decadal- to centennial-scale forecasting, where process detail is often outweighed by the need to capture emergent behaviors and large-scale trends.

The earliest and most foundational of these models is the Pelnard-Considère (1957) formulation. It describes shoreline change as a process governed by gradients in longshore sediment transport, under the assumption of shore-parallel depth contours and small shoreline undulations. The governing equation is

$$\frac{\partial y}{\partial t} = \frac{1}{D}\frac{\partial Q}{\partial x}, \tag{2.3}$$

where $y(x,t)$ is the shoreline position, t is time, x is the alongshore coordinate, Q is the longshore sediment transport rate, and D is the active profile height, typically the sum of the berm height and closure depths. This equation expresses that shoreline change is proportional to the gradient in longshore transport, normalized by the active profile height. Despite its simplifying assumptions, the model established the basis for subsequent shoreline evolution theories and remains a cornerstone of coastal morphodynamics (Falqués 2003; Karunarathna and Reeve 2013; Hurst et al. 2015). Its main limitations are well documented: it cannot represent complex two-dimensional shoreline geometries. It also does not resolve high-angle wave instabilities, neglects short-term variability such as storms or rip currents, and assumes homogeneous coastal morphology, without accounting for mixed sedimentary and structural settings such as alternating sandy stretches, hard substrates, or cliffs (Roelvink et al. 2020; Robinet et al. 2018).

Building on this conceptual foundation, the GENESIS model (Hanson 1989) introduced a more versatile numerical framework for simulating one-dimensional shoreline change. While still rooted in the Pelnard-Considère formulation, GENESIS extended its reach through the incorporation of features such as wave diffraction around structures, sediment transport influenced by groynes and jetties, and multi-segment coastlines with variable orientations. Widely adopted in engineering practice, GENESIS offered greater flexibility but required numerous site-specific input parameters, some of which are not easily obtained or validated. Moreover, it assumes a fixed nearshore bathymetry, with no feedback from shoreline evolution on wave transformation or sediment transport patterns (Ashton et al. 2001).

A distinct conceptual advance came with the Coastline Evolution Model (CEM) developed by Ashton et al. (2001). Unlike earlier one-line approaches, CEM emphasized the role of wave-climate asymmetry and high-angle wave incidence in driving planform instabilities. Using a grid-based approach, the model computes shoreline evolution through cell-to-cell gradients in longshore

sediment transport, enabling the spontaneous emergence of rhythmic features such as spits, cuspate forelands, and sand waves under persistent forcing. Its formulation, grounded in the CERC transport equation, allowed efficient exploration of mesoscale shoreline dynamics over centuries, though it remained limited to planform evolution without explicit cross-shore adjustment. Building on this foundation, the Coastline Evolution Model 2D (CEM2D) (Leach et al. 2021) extended the framework into two dimensions, incorporating sediment storage and redistribution across both the shoreline and the active shoreface. This development enabled the dynamic representation of beach and nearshore morphology, integration of variable water levels and SLR, and the capture of memory effects and more complex landform development. Positioned between reduced one-line models and computationally intensive process-based approaches, CEM2D broadened the applicability of reduced-complexity shoreline modelling to questions of long-term coastal change under evolving wave and water-level conditions.

More recently, the ShorelineS model (Roelvink et al. 2020) advanced planform modelling by adopting a free-form, vector-based representation of the coastline. Unlike one-line approaches tied to a fixed spatial discretisation (or mesh), ShorelineS allows is based on an adaptative discretisation of the shoreline, such that individual grid points (located on the shoreline) evolve independently, enabling the simulation of processes such as shoreline splitting, merging, and the development of complex features under variable wave climates. This flexibility makes it particularly suited to represent large-scale, nature-based interventions like the Sand Engine. However, in its initial form the model remained focused on long-term planform evolution, without explicitly resolving cross-shore seasonal adjustments or event-scale processes.

2.2.4 Hybrid and coupled approaches

As limitations of purely cross-shore or planform models became evident, later approaches sought to unify these dynamics more explicitly. CoastalMe (Payo et al. 2016), for instance, implemented a framework integrating component models to simulate morphological changes across complex coasts. Although capable of resolving nearshore processes, its reliance on simplified equilibrium profiles and weak coupling between morphology and wave propagation limited its ability to represent feedbacks with evolving bathymetry.

The Q2D-morfo model (Van Den Berg et al. 2012; Arriaga et al. 2017) represented an important step toward bridging one-line and process-based morphodynamic models. By solving the sediment mass conservation equation over a quasi-two-dimensional grid, it coupled alongshore transport with a heuristic parameterization of cross-shore sediment exchange driving the profile toward equilibrium. The inclusion of a shape-dependent diffusivity enabled the model to capture large-scale, wave-driven planform evolution while filtering out small-scale surf-zone dynamics. Subsequent developments, including the fuzzy shoreline algorithm, enhanced its ability to represent strong planform deviations such as those observed at the Zandmotor mega-nourishment. Beyond this,

Q2D-morfo has proven particularly valuable for exploring the emergence of kilometer-scale shoreline sand waves under oblique wave forcing, emphasizing the critical role of cross-shore coupling in the growth and migration of such features.

The CoSMoS-COAST model (Vitousek et al. 2017) represented another novel synthesis. Integrating four distinct components; including longshore transport, SLR-induced translation, residual shoreline trends, and cross-shore equilibrium change, offered a modular yet tractable model for climate-scale shoreline response. Its data assimilation via an extended Kalman filter allowed for improved parameter estimation and validation, making it applicable across a wide range of settings. Nevertheless, even if the (fixed) transect-based discretization is adapted for many environments, it constrained its ability to represent complex shoreline geometries, and by design such one-dimensional approaches are not well suited to capturing morphodynamic features, like the ones for instance associated with high-angle wave forcing, such as shoreline sand waves or flying spits.

LX-Shore, introduced by Robinet et al. (2018), advanced this paradigm by combining CEM-style planform dynamics with a disequilibrium-driven cross-shore transport component akin to ShoreFor (Davidson et al. 2013). Implemented in a 2D cellular grid and coupled with a spectral wave model, SWAN (Booij et al. 1999), LX-Shore allowed for the inclusion of hard structures and non-erodible boundaries. Its flexibility and low computational cost made it ideal for large-scale, long-term applications. However, its inability to simulate overwash, estuarine processes, or dynamic SLR presented clear areas for future development.

Parallel developments in hybrid modelling emerged through IH-LANS (Álvarez-Cuesta et al. 2021), which coupled simplified wave propagation with a one-line shoreline evolution model and introduced data assimilation for calibration. Its extension, IH-LANSloc, addressed a long-standing limitation by incorporating dynamic feedback between shoreline change and nearshore bathymetry using ShoreTrans and SWAN (Álvarez-Cuesta et al. 2023). IH-LANSloc improved representation of morphological feedback and supported complex coastal settings, including those with coral reefs, seagrasses, and engineered defenses. However, the model is still transect-based which limits its applicability in environments exhibiting large temporal changes in shoreline orientation.

Other models have been developed to predict medium to long-term shoreline evolution. Q2Dmorfo (Arriaga et al. 2017; Falqués et al. 2021) advanced the resolution of bathymetric change and two-way coupling with waves, at the expense of computational time. IH-MOOSE (Jaramillo et al. 2021) integrated cross-shore, planform, and rotation equilibrium for embayed beaches, offering a flexible and efficient solution for mid- to long-term predictions. COCOONED (Antolínez et al. 2019) and COAST-PROSIM (Scala et al. 2025) adopted multiscale and hybrid approaches, integrating SLR, dune erosion, and anthropogenic interventions while maintaining operational tractability.

2.2.5 Data-driven and machine learning approaches

Recent advances in coastal morphodynamic modelling have seen a growing integration of data-driven methods, particularly machine learning (ML), into the shoreline evolution toolbox. As the limitations of purely physics-based or reduced-complexity models become more evident, especially in representing nonlinear interactions, site-specific variability, and cumulative human interventions, ML offers an alternative pathway centered on pattern recognition and predictive skill (Mao et al. 2025).

A key advantage of ML models lies in their ability to represent strongly nonlinear systems with relatively modest calibration requirements (Simmons and Splinter 2025; Montaño et al. 2020). Their computational efficiency, often producing predictions in milliseconds compared to the hours required by process-based simulations, makes them especially attractive for operational forecasting or large-scale applications (Kumar and Leonardi 2025; Muroi et al. 2025). Moreover, some algorithms can quantify prediction uncertainty, providing useful decision-support tools for risk-based coastal management.

The application of ML and deep learning (DL) to shoreline prediction has gained momentum as a complement to traditional models. These approaches extract complex relationships directly from data, which allows them to reproduce shoreline dynamics without explicit representation of unresolved processes (Simmons and Splinter 2025; Montaño et al. 2020; Vitousek et al. 2017). Neural networks - particularly recurrent architectures such as NARX and LSTM - have demonstrated skill in capturing time-dependent shoreline behavior and often outperform classical statistical models (Boye et al. 2025; Calkoen et al. 2021). More recent developments include hybrid CNN–LSTM models, sequence-to-sequence architectures, and Transformer-based predictors, which improve temporal forecasting and reduce error propagation (Li et al. 2020; Kumar and Leonardi 2025; Yang et al. 2023).

Despite these advances, significant limitations remain. Model performance is highly data-dependent, and generalization across sites is difficult without site-specific calibration (Karunarathna and Reeve 2013; Kumar et al. 2020; Gomez-de La Peña et al. 2023). Furthermore, their black-box nature hampers interpretability, limiting physical insight into underlying processes. Importantly, while ML can reproduce anthropogenic signals that exist within the training data, it cannot reliably predict the effects of novel interventions—such as the introduction of a groin at a site where no such structure previously existed; since no analogue exists in the learning dataset (Mao et al. 2025; Montaño et al. 2020). In this respect, for the moment, ML approaches are probably best viewed as complementary to, rather than replacements for, physics-based or reduced-complexity models.

2.2.6 Comparative synthesis and applicability envelope

The comparative assessments of shoreline models reveal clear trade-offs between physical detail, computational tractability, and data dependence. Process-based models remain the reference for event-scale hazard analysis but are hardly practical for multi-decadal projections due to their high data requirements, computational cost, and limited ability to reproduce long-term beach evolution. Hybrid and reduced-complexity models (e.g., ShoreFor, CoSMoS-COAST, ShorelineS, LX-Shore) offer a pragmatic middle ground, embedding essential process representations within simplified frameworks. They have proven transferable across sites and time horizons, with skill often limited more by input data quality than by model formulation. Data-driven models, increasingly based on machine learning architectures, can match or exceed hybrid skill in data-rich settings, but their reliability diminishes when applied beyond the training domain (Montaño et al. 2020; Mao et al. 2025).

Taken together, this highlights that no single model class is universally optimal. Instead, each occupies an applicability envelope defined by timescale, data availability, and intended use: process-based for process studies, hybrid for climate-scale projections, and data-driven for large-scale monitoring where long records exist; an application area that has expanded considerably with the advent of high-frequency satellite imagery. This synthesis underlines the importance of matching model complexity to the decision context and provides the rationale for developing coupled or adaptive approaches that leverage the strengths of multiple frameworks.

2.3 UNCERTAINTY IN SHORELINE MODELLING

Shoreline change is inherently unpredictable, shaped by nonlinear interactions among waves, tides, sediment transport, and sea-level rise across a wide range of scales. This complexity, coupled with the limited predictability of future climate and wave conditions, makes shoreline projections intrinsically uncertain (Toimil et al. 2021; D'Anna et al. 2021b; D'Anna et al. 2022). Identifying the dominant drivers of uncertainty at different timescales is essential for prioritizing research efforts and focusing resources on reducing the most consequential uncertainties.

Uncertainties in shoreline projections arise from multiple, interacting sources, beginning with the boundary conditions prescribed to the models. Sea-level rise projections vary substantially among Shared Socioeconomic Pathways (SSPs) and ice-sheet feedbacks, leading to end-century ranges of approximately 0.4–1.0 m under intermediate to high scenarios (Toimil et al. 2020). Future wave climate projections remain regionally divergent: mean significant wave height changes are typically within ±10 %, while extreme events may increase by up to 30 % in some basins, and shifts in dominant wave direction can alter longshore transport patterns (Toimil et al. 2020). In addition, the stochastic sequencing and clustering of storms introduce intrinsic, irreducible variability that can drive shoreline deviations of several tens of metres over decadal timescales (Toimil et al. 2020).

Beyond external forcing, uncertainties also stem from model structure and parameterization. Reduced-complexity shoreline models depend on empirical coefficients and assumptions such as a fixed depth of closure, whose site-specific sensitivity limits model transferability and amplifies projection spread. Finally, upstream scenario uncertainty, originating from greenhouse gas emission pathways (or, recently SSPs) and propagated through global and regional climate models, further broadens the envelope of plausible shoreline trajectories (Toimil et al. 2020; Durkin et al. 2025; D'Anna et al. 2021b). Model structure itself introduces additional uncertainty. Widely used coastal

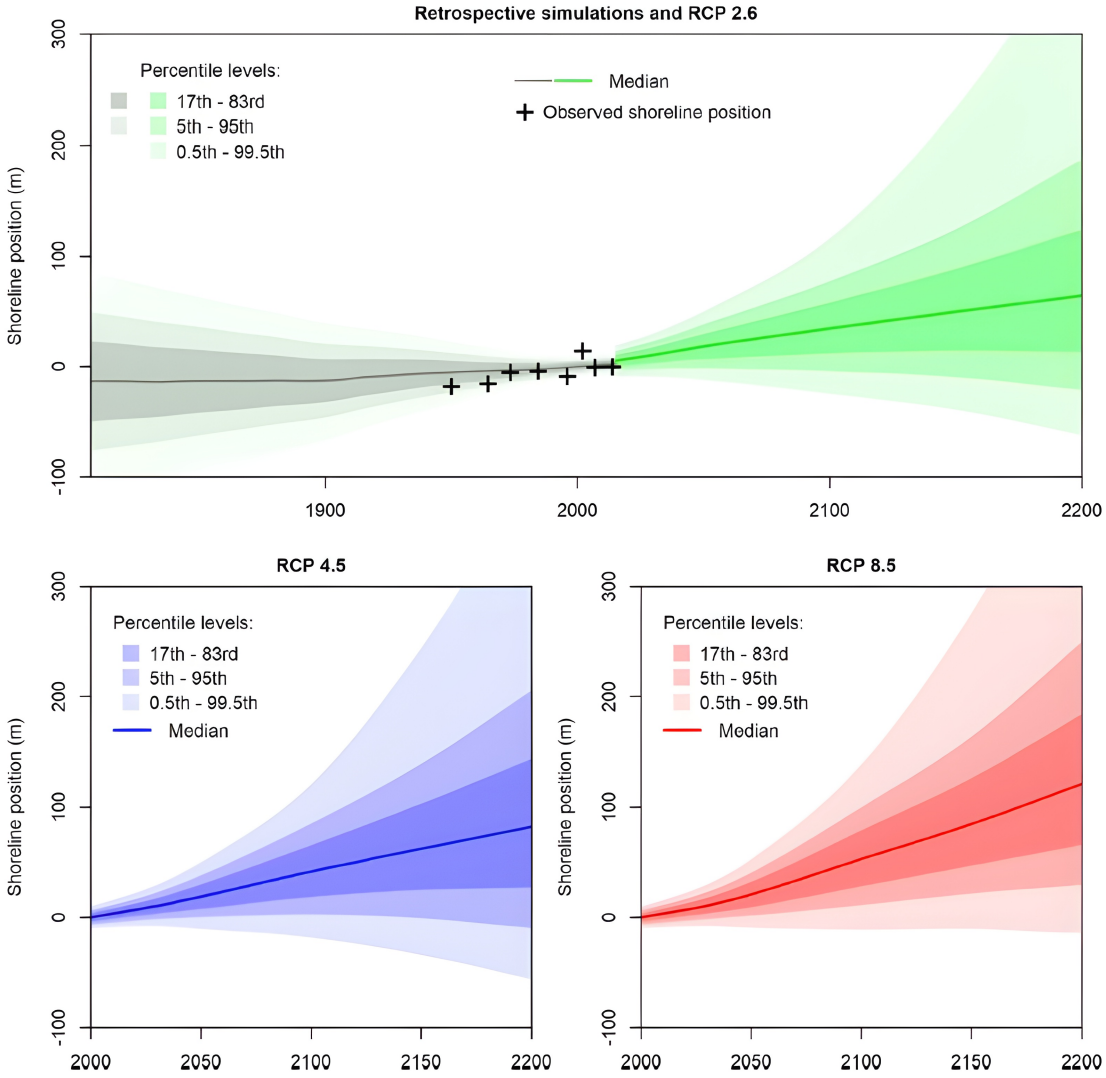

Figure 2.12: Example of shoreline change reconstructions and projections using the Bruun rule, expressed as median positions and percentile ranges over time. The figure illustrates the large uncertainty ranges associated with this approach, underscoring the structural uncertainty introduced by the choice of coastal impact model (from: Le Cozannet et al. (2019)).

impact models, such as the Bruun Rule or the Probabilistic Coastline Recession model (Ranasinghe et al. 2011), are based on fundamentally different assumptions, leading to divergent outcomes (see Fig. 2.12). For the sites analyzed by Le Cozannet et al. (2019), this structural uncertainty can contribute as much as 20–40 % of the variance in shoreline projections. Data availability compounds the problem: the reliability of Reduced Complexity Models is tightly linked to the length, resolution, and quality of shoreline records used for calibration and validation. Yet, in many complex coastal

settings, such datasets remain scarce (D'Anna et al. 2020; Álvarez-Cuesta et al. 2023). Finally, human interventions add another layer of difficulty. While models may account for nourishment or armoring by extrapolating past practices, such assumptions are tenuous in the face of uncertain socio-economic trajectories (Thiéblemont et al. 2021).

2.3.1 *Computational demands and model selection*

Rigorous uncertainty quantification in shoreline modelling requires ensembles large enough to capture the nonlinear interactions among forcing, sediment transport, and model parameters. Variance-based sensitivity methods such as Sobol analysis (Sobol 2001) require large ensembles of simulations to adequately sample the parameter space and obtain statistically stable estimates of sensitivity indices. Experience from recent shoreline studies suggests that robust convergence typically demands on the order of thousands of simulations (D'Anna et al. 2021b). This requirement creates a trade-off: only sufficiently fast models can support the ensemble runs necessary for meaningful uncertainty quantification.

This constraint has important implications for coastal modelling practice. Complex process-based models, while physically more complete, may prove computationally prohibitive for such large ensembles, forcing reliance on reduced-complexity approaches despite their acknowledged limitations. Another possible alternative is to emulate the computationally intensive model using statistical surrogates or metamodels which can approximate model outputs with negligible cost once trained, enabling full sensitivity or probabilistic analyses (Rohmer et al. 2022).

2.3.2 *Quantifying parameter influence through global sensitivity analysis*

Once uncertainty sources are identified, their relative importance must be quantified to guide model development and data collection priorities. GSA provides the systematic framework for this task, offering a rigorous approach to apportion output uncertainty among competing input sources. Unlike local sensitivity measures that examine parameter effects through small perturbations around nominal values, GSA explores the entire parameter space, providing a comprehensive assessment of parameter influence across all plausible conditions.

Variance-based approaches to GSA rely on Sobol indices (Soboĺ 1993), which decompose the total output variance into contributions from individual parameters and their interactions (Marrel et al. 2009; Chastaing et al. 2012). For a model output $Y = f(X_1, \ldots, X_p)$ with variance $\mathrm{Var}[Y]$, the first-order Sobol index for input X_i is defined as:

$$S_i = \frac{\mathrm{Var}_{X_i}\left(\mathbb{E}_{X_{\sim i}}[Y \mid X_i]\right)}{\mathrm{Var}[Y]}. \tag{2.4}$$

This measures the fraction of total output variance attributable solely to X_i, independent of its interactions.

Classical Sobol analysis assumes statistical independence of inputs. Under this condition, the full set of indices provides an exact variance decomposition. In coastal applications, however, inputs such as wave height and period are often correlated, requiring generalized approaches (Iooss and Prieur 2017; Gao et al. 2023) that incorporate covariance terms, though with added computational cost and reduced interpretability (Chastaing et al. 2012; D'Anna et al. 2021b).

2.3.3 Uncertainty propagation and temporal dynamics

Uncertainties propagate through models via cascade effects (Toimil et al. 2021), where uncertain inputs generate uncertain outputs with often amplified variance over time. GSA has proven valuable in quantifying how individual sources contribute to overall model spread in this context (D'Anna et al. 2021b; D'Anna et al. 2022).

The temporal evolution of uncertainty reveals distinct patterns. Short-to mid-term projections are often dominated by uncertainties in empirical parameters and storm chronology, with stochastic sequencing introducing variability that can mask or amplify longer-term trends. Beyond mid-century, sea-level rise (SLR) scenarios typically become the principal driver of projection spread (D'Anna et al. 2021b; D'Anna et al. 2022).

Interactions between uncertainty sources can further amplify effects in nonlinear ways. For example, correlations between uncertain wave sequences and empirical parameters may blend intrinsic and epistemic uncertainties, a phenomenon that remains insufficiently explored but may substantially affect projection reliability (Durkin et al. 2025; D'Anna et al. 2022).

Finally, deep uncertainty complicates shoreline forecasting. In many cases, the probability distributions of key inputs are themselves unknown, leading to ambiguity in ensemble-based projections. This ambiguity grows with projection timescale and becomes particularly evident when comparing probabilistic and extra-probabilistic frameworks. Thiéblemont et al. (2021) showed that high-end sea-level estimates derived from probabilistic models are systematically lower than those obtained using a possibilistic approach, indicating that probability-based methods may underestimate the full range of plausible outcomes in the presence of deep uncertainty. Variability in wave climate adds further complexity: different equilibrium-based models respond differently to shifts in intra-annual and interannual wave energy distributions, while deterministic wave projections can mask the true range of potential shoreline responses (D'Anna et al. 2021b; D'Anna et al. 2022).

2.4 SYNTHESIS AND RESEARCH GAP

This chapter has examined the principal physical drivers of medium to long-term shoreline change of wave-dominated sandy coasts, the evolution of shoreline modelling approaches, and the role of probabilistic frameworks in accounting for uncertainty. Three central insights emerge. First, longshore transport and sea-level rise constitute the dominant processes governing decadal–centennial shoreline evolution, with their interactions producing complex feedbacks that shape coastal planforms and profiles. Second, existing modelling approaches span a spectrum from highly simplified one-line models to process-based and hybrid frameworks. While reduced-complexity models capture emergent shoreline dynamics with efficiency, they often neglect critical cross-shore feedbacks; conversely, profile-based models resolve vertical responses but struggle to represent evolving shoreline orientation or longshore gradients. Third, probabilistic methods highlight that uncertainties stemming from forcing, structure, and parameters propagate strongly across timescales, underscoring the need for models that are not only physically credible but also computationally fast enough to allow uncertainty quantification.

Despite these advances, important gaps remain. Most shoreline models continue to rely on simplifying assumptions that artificially decouple cross-shore and longshore dynamics, treating them as isolated rather than integrated components of a single morphodynamic system. This fragmentation limits their capacity to represent the feedback loops through which sea-level rise, sediment transport, and shoreline geometry interact over planning-relevant timescales. Furthermore, most models either lack the capacity to handle real-world profile variability and human interventions, or cannot simulate complex planform adjustments such as rotation and bypassing around structures. Finally, probabilistic approaches, or at least, uncertainty quantifications, are increasingly recognized as essential, such that predictions should integrate this component.

The work presented in this thesis is motivated by these gaps. By coupling the planform-focused reduced-complexity model LX-Shore with the profile-based ShoreTrans model, I develop a new hybrid framework (LX-ST) capable of linking alongshore gradients with profile retreat under sea-level rise (SLR). This coupling explicitly acknowledges that shoreline migration is not a one-dimensional process but the emergent outcome of interactions between longshore and cross-shore sediment pathways. Through this integration, the model can resolve both the redistribution of sediment alongshore and the landward retreat of profiles across different settings, including those influenced by hard structures and sediment deficits. In doing so, this thesis advances beyond traditional one-line abstractions and purely profile-based rules, offering a computationally efficient yet physically grounded tool for scenario-based coastal risk assessment under climate change.

The focus is placed on medium- to long-term shoreline evolution driven by SLR and longshore sediment transport, while high-frequency wave-driven cross-shore exchanges are treated as short-term variability that averages out at longer timescales. Finally, the thesis explores to what extent LX-ST can also serve as a platform for uncertainty quantification, evaluating how variability in SLR,

erosion rates, and wave forcing propagates into shoreline projections and identifying the dominant sources of uncertainty across scales.

Chapter 3

Model Development

3.1 Introduction **38**

3.2 Models used for long-term modelling **38**

3.2.1 ShoreTrans 38

3.2.2 LX-Shore description 44

3.3 LX-ST development and tests on idealized and real cases **51**

3.1 INTRODUCTION

The work presented in this chapter contributes to the overall objectives of the thesis by addressing the challenge of simulating long-term shoreline change under sea-level rise through a modular coupling framework. The approach integrates the grid-based LX-Shore shoreline model with the ShoreTrans model, enabling a 3D representation of coastal evolution that captures interactions between alongshore sediment transport and shoreline orientation.

Within the broader structure of the thesis, this chapter provides the methodological core. It follows the general review of physical drivers and modelling approaches presented in earlier chapters, and it precedes the application of the framework to sensitivity analyses and probabilistic projections at Lacanau in Chapter 4.

This chapter is structured into two main components. First, detailed technical overviews of ShoreTrans and LX-Shore are provided. This first part aims at allowing readers to follow the assumptions, formulations, and numerical implementation of each model beyond the condensed accounts available in the published article. The ShoreTrans section gives a step-by-step account of the cross-shore translation algorithm and sediment budget terms, while the LX-Shore section outlines the sediment-fraction approach used to simulate coupled longshore and cross-shore processes.

Second, the chapter incorporates the peer-reviewed article that resulted from this work: "A coupling approach for long-term 3D morphological evolution of sandy coasts under sea-level rise" (Traboulsi et al. 2025). The article documents the integration of ShoreTrans and LX-Shore into the coupled LX-ST framework and provides some examples of test on idealised and real cases. It is included in its original journal format without modification.

3.2 MODELS USED FOR LONG-TERM MODELLING

3.2.1 ShoreTrans

▸ NOTE This section provides a detailed technical overview of the ShoreTrans model, drawing directly on the formulation and description presented by McCarroll et al. (2021a). The content has been paraphrased and reformulated for clarity and integration within the present thesis.

ShoreTrans is a rule-based shoreface translation and sediment budgeting tool designed to estimate profile and shoreline response at decadal to centennial timescales. Unlike parametric approaches that approximate cross-shore geometry, ShoreTrans operates directly on surveyed profiles, thereby accommodating irregularities such as perched dunes, seawalls, and non-erodible substrates.

Sediment budget framework

ShoreTrans applies sediment continuity to an observed cross-shore profile within a control volume that spans the *active profile* (Fig. 3.1). The upper bound is taken at the dune toe or barrier crest (X_C, Z_C), depending on the setting. The lower bound spans a range between a shallow limit Z_{D1} and a deeper limit Z_{D2}.

Following common practice, Z_{D1} and Z_{D2} can be tied to the annual and long-term depths of closure (DoC_1, DoC_2), which may be estimated using Hallermeier (1980) relations:

$$\mathrm{DoC}_1 = 2.28 H_{12,t} - 68.5 \left(\frac{H_{12,t}^2}{g T_t^2} \right), \tag{3.1}$$

$$\mathrm{DoC}_2 = (H_{s,t} - 0.3\sigma_{Hs}) T_{s,t} \left(\frac{g}{5000 D_{50}} \right)^{1/2}, \tag{3.2}$$

where $H_{12,t}$ is the significant wave height exceeded for 12 h in t years, T_t the associated peak period, $H_{s,t}$ an annual significant height, σ_{Hs} the wave-height standard deviation, $T_{s,t}$ a time-averaged period, and D_{50} the median grain size (McCarroll et al. 2021a).

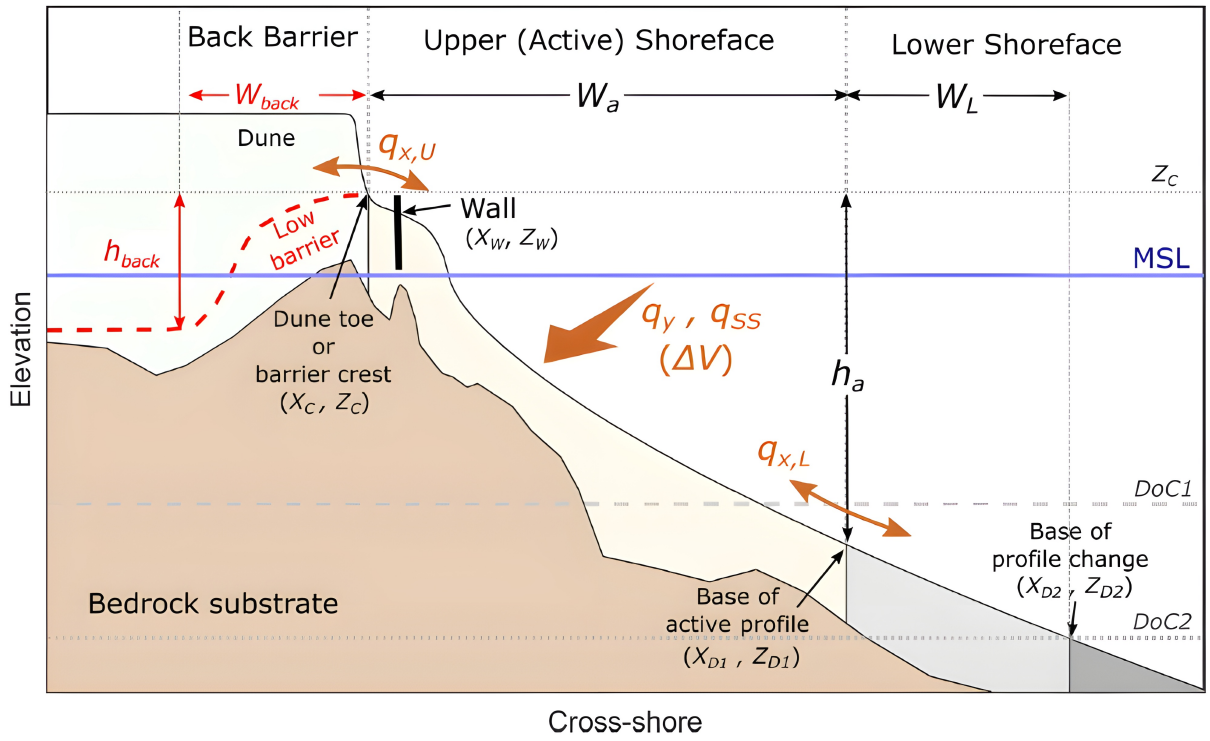

Figure 3.1: Conceptual diagram of the ShoreTrans model, showing the active profile bounded by Z_{D1} and Z_{D2} and the four main exchange terms: (i) SLR-induced translation, (ii) cross-shore exchange, (iii) longshore gradients, and (iv) external sources/sinks. (from: McCarroll et al. (2021a)).

For applications with rapid SLR, Z_{D1} tends to approach $-\mathrm{DoC}_1$, while $Z_{D2} \approx -\mathrm{DoC}_2$ (McCarroll et al. 2021a). The horizontal span of the active profile defines its width W_a; the characteristic vertical scale in the budget is the active height h_a.

Sediment continuity and the time-integrated equation

The fundamental principle underlying ShoreTrans is that shoreline change results from two competing processes: the geometric response to rising sea levels (which drives retreat) and sediment exchanges that can either accelerate or slow this retreat. Integrating Exner's equation across the active profile and adopting a positive-offshore sign convention yields this balance as a shoreline-rate equation:

$$\frac{dX}{dt} = -\frac{dS}{dt}\frac{W_a}{h_a} + \frac{1}{h_a}(q_{x,U} - q_{x,L} + \Delta q_y + q_{ss}), \tag{3.3}$$

where X is shoreline position, S sea level, $q_{x,U}$ the volumetric cross-shore input from the upper system (dunes/back-barrier), $q_{x,L}$ the exchange with the lower shoreface, Δq_y the net alongshore input to the control volume, and q_{ss} other sources/sinks (e.g., nourishment, dredging).

The first term represents the inevitable landward translation as higher water levels 'drown' the existing profile geometry - this is the classic Bruun effect. The remaining terms represent the 'fight back': sediment inputs from dunes, exchanges with deeper waters, and alongshore transport that can potentially offset sea-level-driven retreat. This framework makes clear that predicting coastal change requires understanding both the geometric constraints (through W_a/h_a) and the sediment budget components.

Over a finite step, ShoreTrans uses the time-integrated statement:

$$\Delta X = \Delta X_{\mathrm{SLR}} + \frac{\Delta V_{x,U} - \Delta V_{x,L}}{h_a} + \frac{\Delta V_y + \Delta V_{ss}}{h_a}, \tag{3.4}$$

where the ΔV are volumetric gains to the control volume per metre alongshore, consistent with Eq. (3.3).

Algorithmic profile translation under SLR

Rather than relying on simplified geometric assumptions, ShoreTrans evaluates ΔX_{SLR} through an algorithm that raises and translates the observed profile while conserving sediment volume within the active profile (Fig. 3.2). This approach preserves the complexity of real beach profiles, including irregular dune shapes and substrate variations.

The algorithm follows these steps:

1. raise the profile by ΔS to account for higher water levels;

2. translate onshore by a trial distance ΔX;

3. compute the volume error relative to the target change ΔV;

4. iterate on ΔX until the error is minimised.

Mathematically, this is expressed as:

$$z(x, t_1) = z(x - \Delta X, t_0) + \Delta S, \tag{3.5}$$

$$\Delta V_{\text{error}} = \int_a^b [z(x, t_1) - z(x, t_0)]\, dx - \Delta V. \tag{3.6}$$

The advantage of this approach is that it automatically accounts for profile irregularities that would confound simple geometric rules. To avoid unrealistic steps at the base of the active profile, ShoreTrans applies local smoothing over at least $\max(\Delta X, 0.1W_a)$ (Atkinson et al. 2018; McCarroll et al. 2021a).

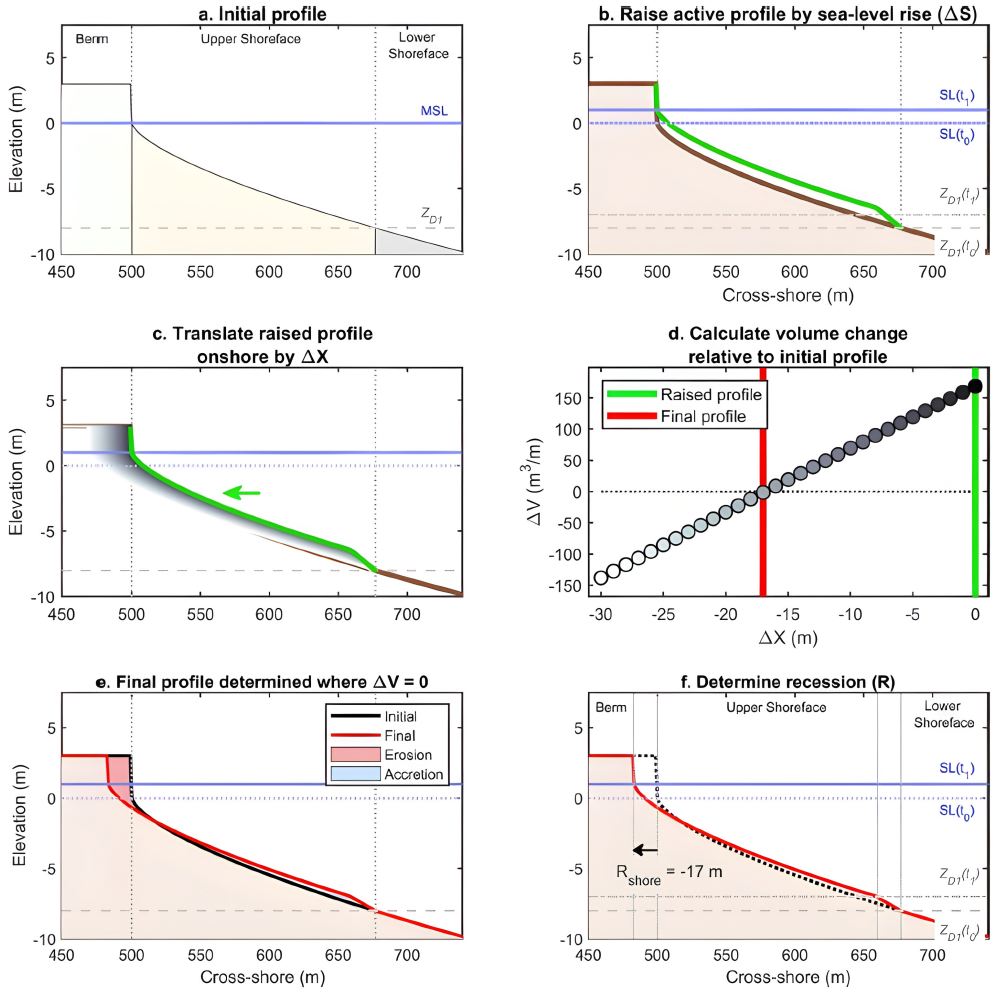

Figure 3.2: Schematic of the raise-translate-balance algorithm used to determine ΔX_{SLR}. The observed profile is first raised by ΔS, then shifted onshore; ΔX is selected by minimising a volume-error functional so that mass is conserved within the active profile (from: McCarroll et al. (2021a)).

Hard boundaries and non-erodible substrate

Real coastlines often encounter constraints that prevent simple landward translation. ShoreTrans addresses two critical cases: walls or cliffs that block retreat, and rocky outcrops that limit erosion.

For wall-backed profiles, the approach recognises that erosion demand cannot simply disappear; it must be accommodated elsewhere. Translation is first computed as if the wall were absent. The hypothetical erosion demand landward of the wall is then redistributed seaward as a triangular wedge (Fig. 3.3a), concentrating erosion in front of the structure. The wall-demand volume and wedge height are:

$$\Delta V_{\text{wall}} = \int_{X_w}^{a} [(Z_W + \Delta S) - z(x, t_1)]\, dx, \tag{3.7}$$

$$\Delta Z_{\text{WR}} = \frac{2\Delta V_{\text{wall}}}{\Delta X_{\text{WR}}}, \tag{3.8}$$

with ΔX_{WR} a user-set taper length (default $\approx W_a/3$ by analogy with Beuzen et al. (2018)). This 'wall effect' explains why beaches in front of seawalls often experience severe narrowing: the erosion that would naturally be spread across the profile becomes concentrated in the beach zone.

For non-erodible layers, ShoreTrans employs a clever workaround. A temporary rock-free surface is constructed by interpolating across outcrops, translation is performed on that surface, and the substrate is reinserted as a lower bound (Cowell et al. 2006; Kinsela et al. 2017):

$$z(x, t_1) = \max(z_{\text{RF}}(x, t_1), z_{\text{NE}}(x)). \tag{3.9}$$

This ensures that the final profile cannot erode below the rock surface while still allowing the sediment layers to respond to sea-level rise.

Barrier translation modes

Natural barriers respond to sea-level rise in markedly different ways depending on their height, width, and back-barrier configuration. ShoreTrans implements four translation modes that bracket the range of observed responses (Fig. 3.4): full barrier rollover, two intermediate dune-rollover variants, and pure encroachment (Cowell and Thom 1995; Rosati et al. 2013; Kinsela et al. 2017).

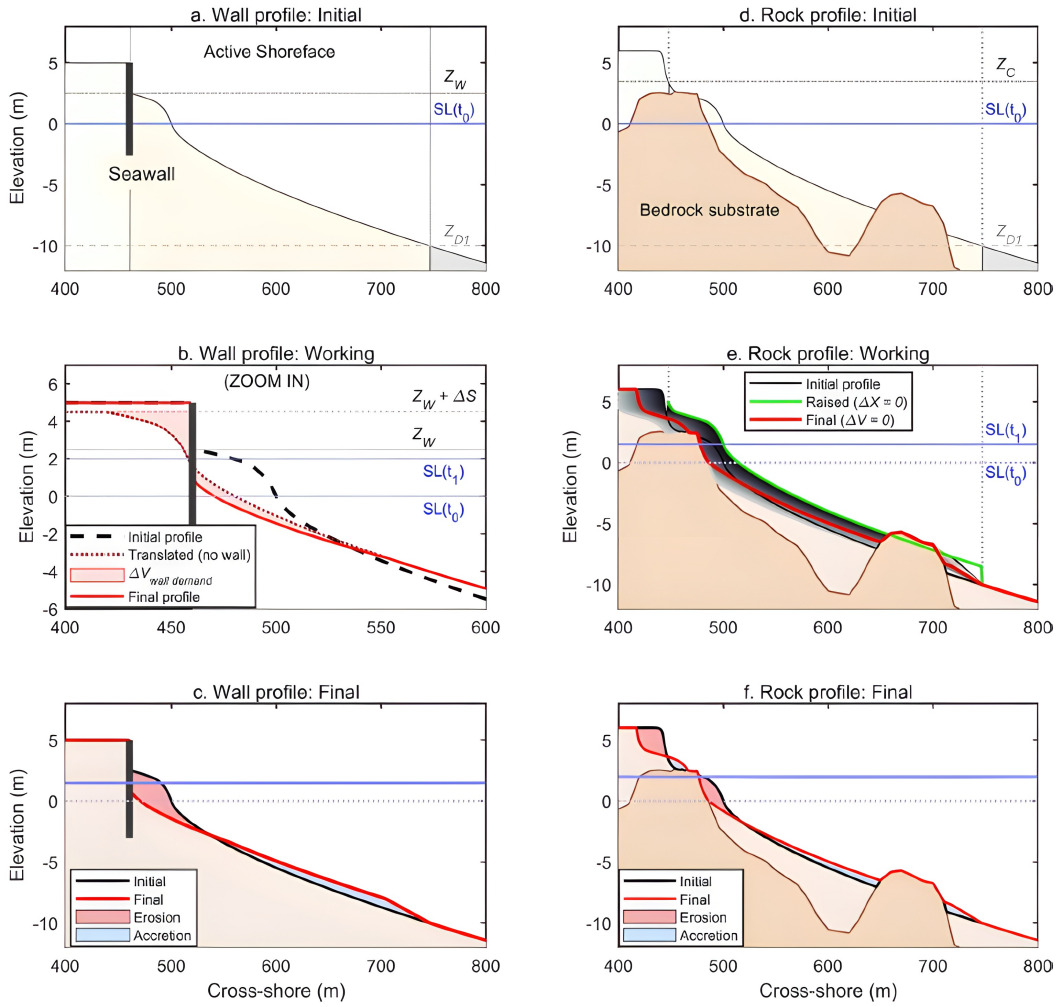

Figure 3.3: Treatment of hard boundaries and non-erodible layers. Left: wall-demand volume computed landward of the wall is redistributed seaward as a wedge. Right: translation with a non-erodible layer using a temporary rock-free surface and reinsertion as a lower bound (from McCarroll et al. (2021a)) .

These modes reflect fundamentally different sediment transport patterns:

$$\text{Type 1 (rollover):} \quad \text{Back-barrier and active profile raised and shifted.} \tag{3.10}$$

$$\text{Type 2 (dune rollover):} \quad z_i(x) = z_{i+1} - \tan\varphi, \quad a \leq x_i < X_C(t_1), \tag{3.11}$$

$$\text{Type 3 (capped crest):} \quad z_i(x) = Z_C, \quad a \leq x_i < X_C(t_1) \text{ where } z_i > Z_C(t_1), \tag{3.12}$$

$$\text{Type 4 (encroachment):} \quad \text{Active profile migrated inland without elevation gain} \tag{3.13}$$

Type 1 represents the extreme case where the entire barrier migrates landward through overwash processes, maximising retreat rates. Type 4 represents the opposite extreme where all eroded sediment moves offshore, minimising retreat. The intermediate modes (Types 2-3) allow for partial rollover of the dune face while maintaining different assumptions about crest evolution.

The choice between these modes has profound implications for recession rates: rollover scenarios can produce retreat rates 2-3 times larger than encroachment scenarios. Natural systems may exhibit

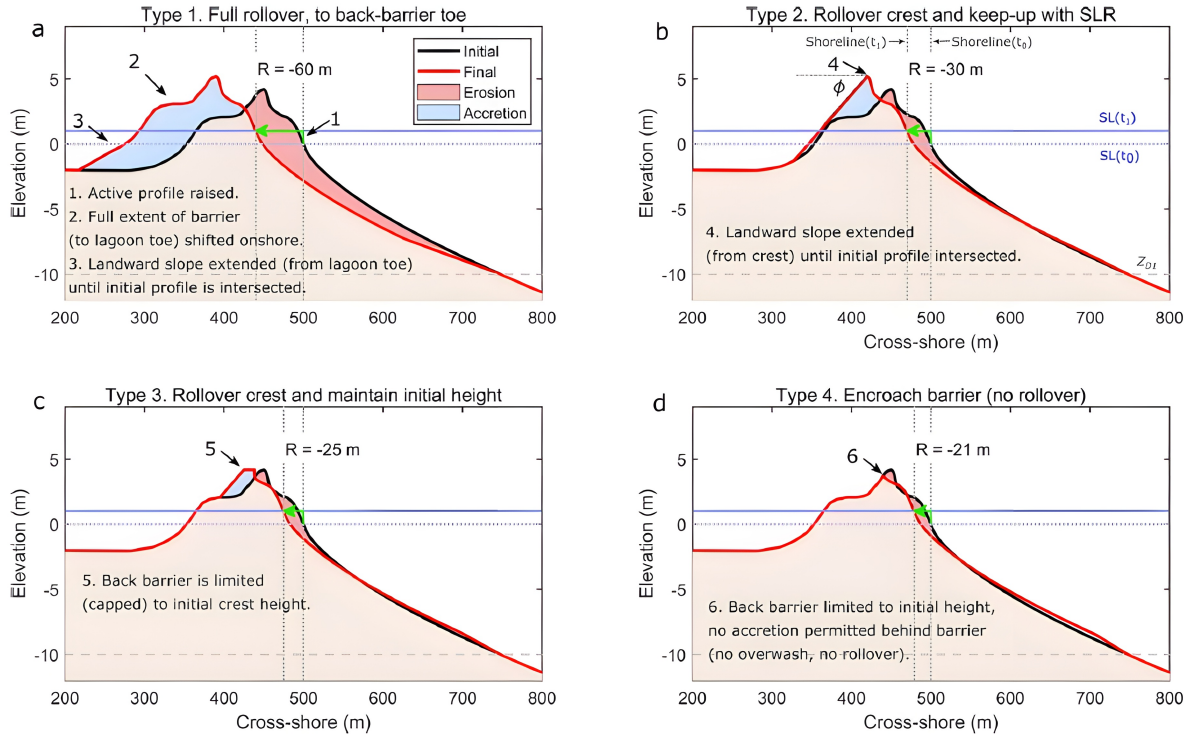

Figure 3.4: Four ShoreTrans translation modes: (a) full barrier rollover; (b) dune rollover with backslope control; (c) dune rollover with capped crest; (d) encroachment with no onshore transport beyond the crest (from McCarroll et al. (2021a)).

any of these behaviours depending on barrier height and substrate slope (Masselink et al. 2020; McCarroll et al. 2021a).

3.2.2 *LX-Shore description*

This subsection provides a technical overview of the LX-Shore model, drawing directly on the formulation and description presented by Robinet et al. (2018) and incorporating the subsequent developments for sea-level rise and real bathymetry merging described in Robinet et al. (2020) and Durand et al. (2024). The content is paraphrased and reorganised for clarity and consistency with the present thesis.

LX-Shore is designed for sandy coasts where overwash rarely occurs—typically beaches backed by high dunes or cliffs. This constraint allows the fundamental assumption that shoreline changes result from pure translation of beach profiles, dramatically reducing computational complexity while maintaining physical realism for a wide range of coastal environments.

LX-Shore represents the coastal domain as a two-dimensional field of sediment fraction $F \in [0, 1]$ defined on a Cartesian grid with spatial resolution d_{xy}. Values of $F = 1$ correspond to land cells, while $F = 0$ indicate water cells. The shoreline is identified as the ensemble of partially wet cells

($0 < F < 1$) that remain connected to at least one water cell, thus delineating the dynamic interface between land and sea (Robinet et al. 2018).

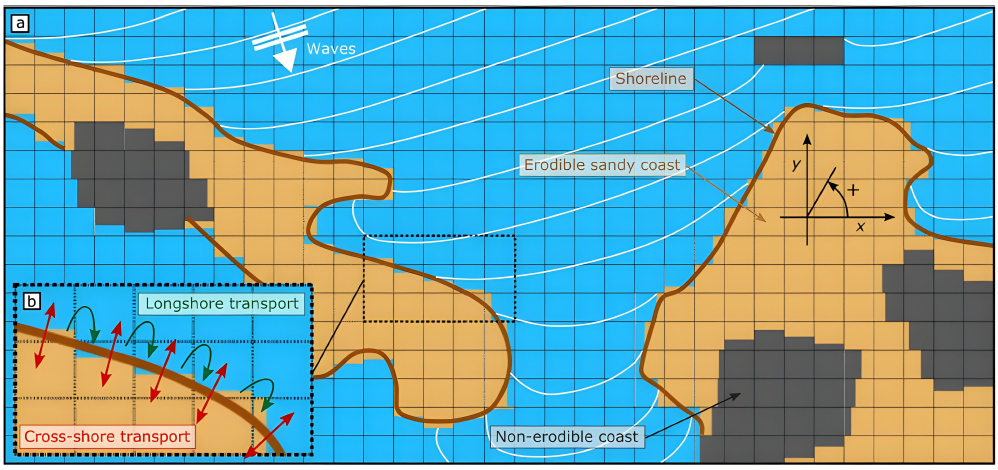

Figure 3.5: Overview of the features and processes integrated in the LX-Shore model. The model handles complex shoreline geometries including headlands and can simulate both longshore transport (along-shore sediment movement) and cross-shore transport (onshore-offshore sediment exchange)(from Robinet et al. (2018)).

Sediment fraction evolution and shoreline dynamics

The core innovation of LX-Shore lies in its treatment of sediment as a continuous fraction within each grid cell. The sediment fraction F is defined as the ratio between actual sediment volume and the maximum possible sediment volume that a cell can contain, where $F = V_s/V_{s,max}$ (Robinet et al. 2018).

This fraction evolves according to the fundamental balance equation:

$$F(t + \Delta t) = F(t) + \Delta F_l(t) + \Delta F_c(t), \tag{3.14}$$

where ΔF_l and ΔF_c represent sediment fraction changes due to longshore and cross-shore processes, respectively. Local redistribution laws are used on the adjacent cells where F gets below 0 or over 1.

The physical interpretation is straightforward: longshore processes redistribute sediment between adjacent cells along the coast, while cross-shore processes add or remove sediment from the nearshore system entirely. This dual mechanism highlights that both processes influence shoreline evolution, each operating through fundamentally different physical pathways.

For longshore processes, the sediment fraction change reflects the conservation principle that sediment leaving one cell must enter an adjacent cell:

$$\Delta F_l = \frac{(Q_{l,in} - Q_{l,out})\Delta t}{V_{s,max}}, \tag{3.15}$$

where $Q_{l,in}$ and $Q_{l,out}$ are the incoming and outgoing longshore sediment transport rates.

Cross-shore processes are included considering that the shoreline position fluctuates around a time-varying equilibrium position according to present and past wave conditions (Davidson et al. 2013). The beach profile is assumed to maintain its shape and to translate simultaneously with shoreline change caused by the cross-shore processes.This allows straightforward conversion of predicted cross-shore transport-driven shoreline change into variation in sediment fraction within the shoreline cells of the model. The sediment fraction variation resulting from cross-shore processes is given by:

$$\Delta F_c = \frac{\Delta S_c/\Delta t}{d_{xy}} \cdot \Delta t, \tag{3.16}$$

where $\Delta S_c/\Delta t$ is the average shoreline change rate caused by cross-shore processes during Δt. In LX-Shore, the cross-shore sediment transport is calculated using an adaptation of the empirical equilibrium-based ShoreFor model described in (Splinter et al. 2014).

Model architecture

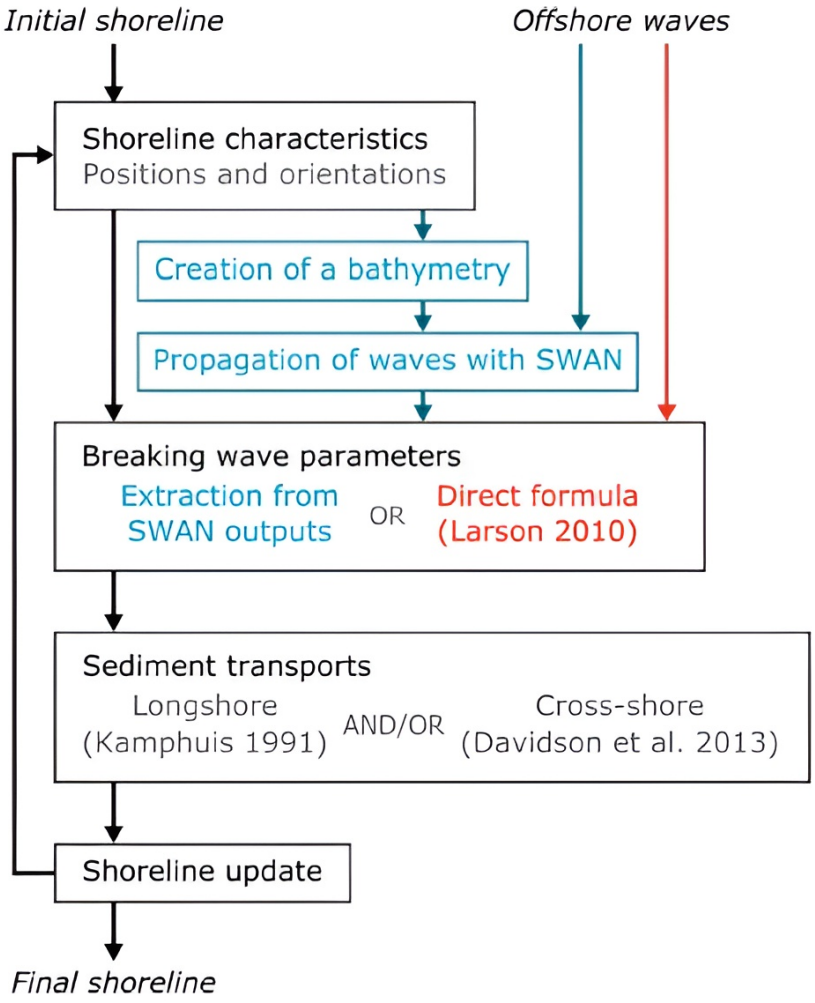

Figure 3.6: LX–Shore overview and architecture. At each step: (1) waves are propagated; (2) breaking conditions are extracted along shore normals; (3) longshore and cross-shore transports are computed; (4) F is updated and the shoreline is reconstructed (from Robinet et al. (2018)).

At each time step, offshore waves are transformed to the breaking line, longshore and cross-shore sediment transports are computed from local breaking conditions and shoreline geometry, and the sediment-fraction field is updated (Fig. 3.6). Two options exist for waves (Robinet et al. 2018): (i) a parameterised energy-flux/Snell option following Larson et al. (2010), with geometric shadowing (Ashton and Murray 2006a); or (ii) a dynamic coupling to the spectral wave model SWAN (Booij et al. 1999). In the coupled option, breaking is detected from the breaker index $\gamma_b = H_s/h$ and the breaking point is located by scanning along the local shore normal.

Within a shoreline cell (i, j), the local shoreline orientation is estimated from the row- and column-wise gradients of F over a 3×3 window, yielding a unit shore-normal vector. The shoreline position inside the cell is then placed along this normal at a distance

$$\ell_{ij} = \big(F_{ij} - 0.5\big) d_{xy}, \tag{3.17}$$

so that $\ell_{ij} = 0$ when $F_{ij} = 0.5$, and $\ell_{ij} = \pm d_{xy}/2$ when the interface reaches the cell faces. This construction provides a sub-cell shoreline suitable for extracting local breaking-wave properties and for computing sediment exchanges (Fig. 3.7).

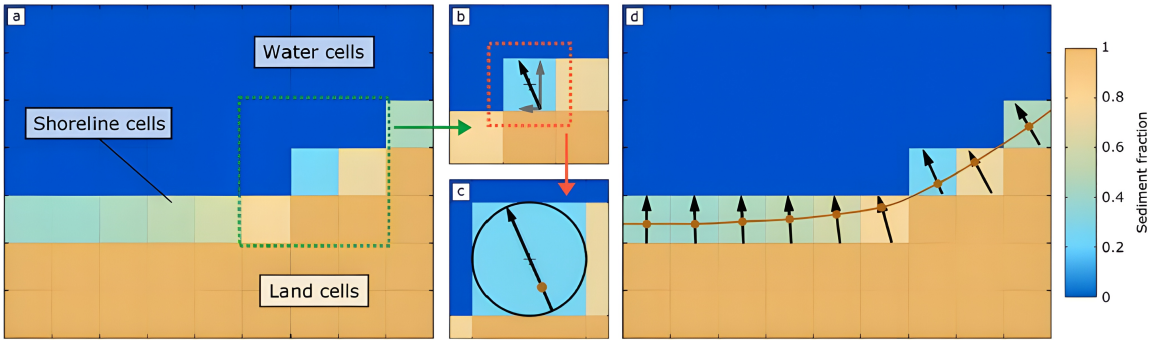

Figure 3.7: Shoreline detection from the sediment-fraction grid: (left) F field and 3×3 window; (middle) cell-based shore-normal from F-gradients; (right) sub-cell shoreline location using $\ell = (F - 0.5)d_{xy}$ (from Robinet et al. (2018)).

Longshore transport formulation

Longshore sediment transport is calculated using established empirical relationships, with LX-Shore implementing both the CERC (Coastal Engineering Research Center (U.S.) 1984) and Kamphuis (1991) formulations. The CERC formula represents the classical approach:

$$Q_l = \frac{\rho K}{(\rho_s - \rho)(1 - p)} \frac{\sqrt{g/\gamma_b} H_{s,b}^{2.5}}{16} \sin(2\theta_b), \tag{3.18}$$

while the Kamphuis formula incorporates additional beach characteristics:

$$Q_l = \frac{2.27 H_{s,b}^2 T_p^{1.5} m_b^{0.75} d_{50}^{-0.25}}{(\rho_s - \rho)(1 - p)} \sin^{0.6}(2\theta_b), \tag{3.19}$$

where $H_{s,b}$ is significant wave height at breaking, θ_b is the breaking wave angle, T_p is peak period, m_b is beach slope, and d_{50} is median grain size.

The choice between formulations reflects different modelling priorities. The CERC formula requires calibration of the coefficient K but offers compatibility with existing models like CEM. The Kamphuis formula incorporates more physical parameters and often provides better predictions without site-specific calibration (Smith et al. 2003), making it preferable for applications lacking extensive calibration datasets.

The added value in LX-Shore's longshore transport implementation lies in its handling of complex shoreline geometries. The model computes transport at boundaries between adjacent shoreline cells, requiring accurate determination of local shoreline orientation and wave incidence angles. This is achieved through a boundary-based coordinate system that automatically adjusts to shoreline curvature, enabling application to features like spits and embayments that challenge traditional approaches.

Durand et al. (2024) extended the parametrization of McCarroll et al. (2021b) to the LX-Shore model. In earlier versions of the model, bypassing occurred only when the shoreline intersected the tip of the obstacle, shoreline bypassing (SB), representing transport confined to the swash–surf zone, or headland bypassing swash–surfzone (HBS). The new implementation, full bypassing (FB), incorporates the subaqueous component of sediment transfer occurring within and seaward of the surf zone, up to the closure depth (headland bypassing nearshore, HBN), using the previous flux relation. This required developing a generic, dimensionless expression of Q_B/Q_0 with a single free parameter, ensuring smooth behaviour across varying Q_0 values and wave conditions. Through more than 800 simulations on synthetic embayments, Durand et al. (2024) demonstrated that accounting for FB markedly alters the predicted embayed-beach morphology. Compared with SB, FB reduces updrift accretion and beach rotation by roughly 30 %. Downdrift erosion is also overestimated by up to 20 % when only SB is considered. These results highlight that the inclusion of subaqueous bypassing redistributes sediment more evenly along the bay, yielding smoother and more realistic results. The FB formulation is therefore adopted in this work to represent seawall-controlled sediment continuity at Lacanau.

Cross-shore transport and equilibrium concepts

Cross-shore transport in LX-Shore builds on the equilibrium-based ShoreFor (Davidson et al. 2013) approach, which assumes that beaches tend toward equilibrium states determined by prevailing wave conditions. The fundamental concept is that shoreline position responds to disequilibrium between current and equilibrium wave energy conditions.

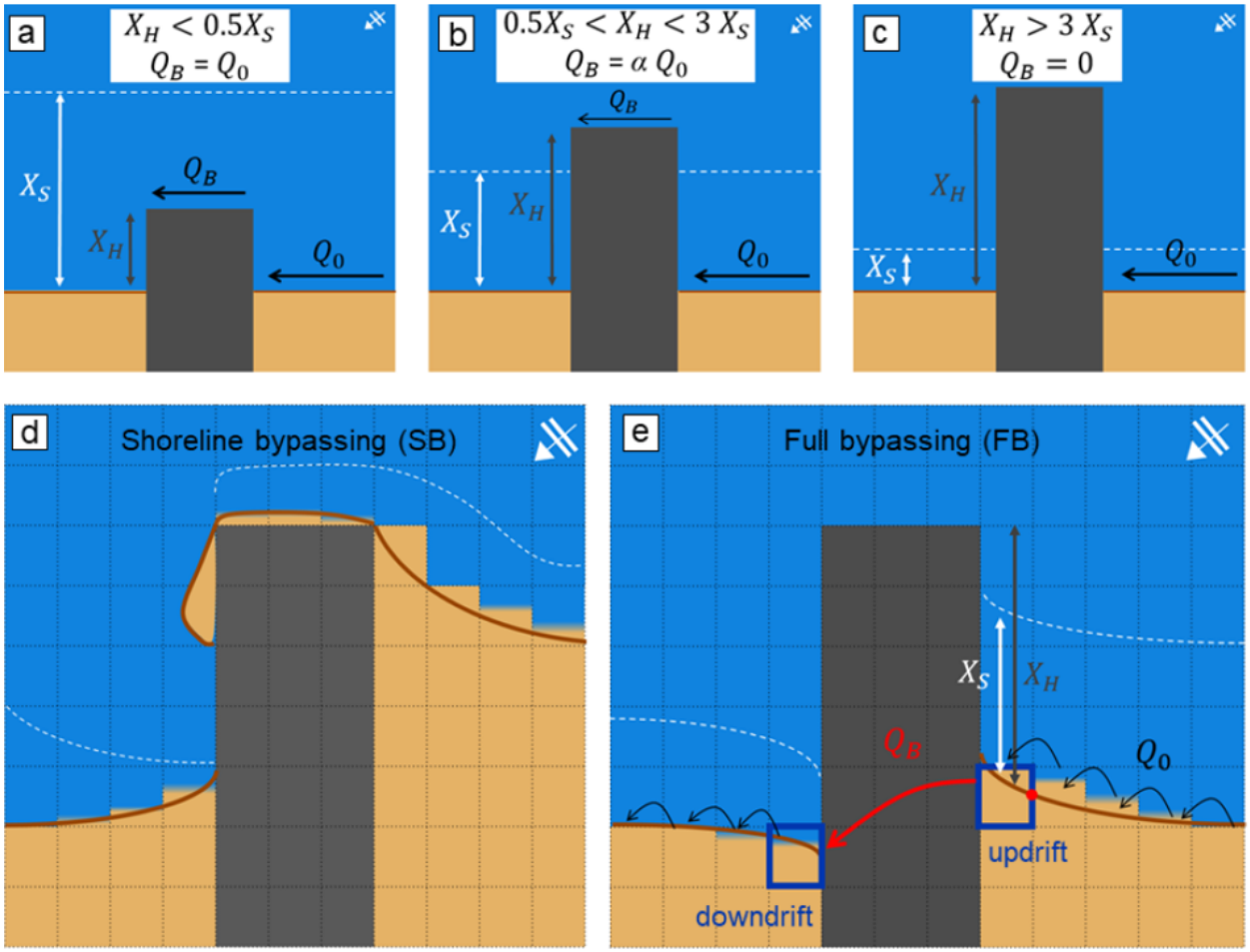

Figure 3.8: (a–c) Sediment bypassing regimes as a function of the ratio between headland extent (X_H) and surf-zone width (X_S). (d) Conceptual representation of shoreline bypassing in the initial version of LX-Shore. (e) Full bypassing scheme implemented in the present model. Sediment fluxes are exchanged between the shoreline cells adjacent to each side of the obstacle (blue-framed cells), with the bypassing transport Q_B evaluated at the updrift boundary of the updrift cell (red dot). The dotted white line indicates the offshore limit of the surf zone. From: Durand et al. (2024).

The model tracks the dimensionless fall velocity at breaking:

$$\Omega_b = \frac{H_{s,b}}{wT_p}, \tag{3.20}$$

where w is sediment settling velocity. The shoreline change rate depends on the disequilibrium $\Delta\Omega = \Omega_{eq} - \Omega_b$, where Ω_{eq} represents the equilibrium state based on wave history.

The cross-shore shoreline change rate is expressed as:

$$\frac{\Delta S_c}{\Delta t} = c_{\pm} P^{0.5} \frac{\Delta\Omega}{\sigma_{\Delta\Omega}} + b, \tag{3.21}$$

where P is wave energy flux at breaking, $c_{\pm}$ are rate coefficients for accretion and erosion, b captures long-term trends, and $\sigma_{\Delta\Omega}$ normalises the disequilibrium term.

This formulation captures the essential physics that beaches erode rapidly during storms (high wave energy, offshore transport) but recover slowly during calm conditions (low wave energy, onshore

transport). The model's strength lies in requiring only offshore wave data while producing realistic beach behaviour across timescales from storms to years.

Sea-level rise and Bruun rule

The sea-level rise module implements two complementary approaches. First, it allows investigation of how rising water levels modify wave transformation processes over existing bathymetry; an effect often overlooked but potentially significant for shoreline variability on intermediate timescales. Second, it incorporates the classical Bruun rule for long-term shoreline retreat:

$$dS = \frac{d\eta}{\tan \alpha} \tag{3.22}$$

where dS is the shoreline retreat, $d\eta$ is sea-level rise, and $\tan \alpha$ is the average beach profile slope.

Bathymetry reconstruction and non-erodible features

LX-Shore provides two approaches for wave computation, reflecting different priorities between computational efficiency and physical accuracy. Option 1 uses simplified wave refraction formulae suitable for relatively straight coastlines, while Option 2 couples with the SWAN spectral wave model for complex coastal geometries where wave focusing and shadowing effects become critical (Robinet et al. 2018).

A bathymetric reconstruction is needed when using Option 2. This reconstruction follows the principle that coastal profiles tend toward equilibrium shapes. The model propagates a power-law profile $h = \alpha d_{SL}^{\beta}$ offshore from each shoreline point, where d_{SL} is the distance from the shoreline and α, β are shape parameters (Robinet et al. 2018). For areas containing non-erodible features, a separate rocky profile is propagated and the two bathymetries are merged using weighted averaging to ensure smooth transitions. LX-Shore also allows merging an idealised bathymetry h_i with a reference bathymetry h_r using two depth thresholds: the closure depth D_c and a larger tuning depth $D_s > D_c$. The merged depth h_m is

$$h_m = h_i + (h_r - h_i), c_{ss} \tag{3.23}$$

$$c_{ss} = 3\mathrm{NDR}^2 - 2\mathrm{NDR}^3, \tag{3.24}$$

$$\mathrm{NDR} = \frac{h_i - D_c}{D_s - D_c} \tag{3.25}$$

where c_{ss} is a sigmoid-shaped coefficient. Non-erodible bottoms are enforced by limiting deepening below the measured rock where required (Robinet et al. 2020).

3.3 LX-ST DEVELOPMENT AND TESTS ON IDEALIZED AND REAL CASES

▸ NOTE This section consists of the peer-reviewed manuscript published as: *Traboulsi, M., Idier, D., Castelle, B., Robinet, A., Marieu, V., Durand, E., & McCarroll, R. J. (2025). A Coupling Approach for Long-Term 3D Morphological Evolution of Sandy Coasts under Sea-Level Rise. Environmental Modelling & Software.* (Accepted, July 13, 2025). It is presented in its original, published format to preserve the integrity of the peer-reviewed content.

▸ DISCLAIMER The results presented for the Lacanau site are part of a methodological and exploratory research framework. They should not be interpreted as operational projections nor used directly for applied studies or coastal management. Their value lies primarily in illustrating modelling approaches, sensitivities, and associated uncertainties, rather than providing predictions for local planning or decision-making.

Environmental Modelling and Software 193 (2025) 106624

Contents lists available at ScienceDirect

Environmental Modelling and Software

journal homepage: www.elsevier.com/locate/envsoft

A coupling approach for long-term 3D morphological evolution of sandy coasts under sea-level rise

Mohammad Traboulsi [a,b,*], Déborah Idier [a], Bruno Castelle [b], Arthur Robinet [c], Vincent Marieu [b], Elsa Durand [a,b,d], R. Jak McCarroll [e]

[a] BRGM, Orléans, F-45060, France
[b] Univ. Bordeaux, CNRS, Bordeaux INP, EPOC, UMR 5805, Allée Geoffroy Saint-Hilaire, Pessac, 33600, France
[c] BRGM, 24 Av. Léonard de Vinci, Pessac, F-33600, France
[d] Waeles Marine Consultants, 53 rue du Commandant Groix, Brest, 29200, France
[e] The University of Melbourne, Melbourne, Victoria, 3010, Australia

ARTICLE INFO

Keywords:
Shoreline change
Nearshore morphology
Modeling
Sea level rise
Artificial structures
Sandy coasts

ABSTRACT

This study presents a modular modeling framework for simulating medium- to long-term (decadal to centennial) coastal evolution, focusing on shoreface translation under the combined effects of sea-level rise (SLR) and waves. On these timescales, short-term storm-driven processes are treated as noise superimposed on longer-term trends. We couple the one-dimensional ShoreTrans model, which simulates SLR-driven profile adjustment, with the two-dimensional reduced-complexity model LX-Shore, which captures longshore sediment transport gradients. This coupling enables efficient simulation of three-dimensional morphological change across diverse sandy coastal settings, including environments with dunes, barriers, and hard structures. The framework is first applied to synthetic test cases to explore sensitivity to coupling strategies, then tested on a 5-km beach-dune system in southwest France fronted by a 1.2-km seawall. Results show reasonable agreement with observed shoreline evolution and demonstrate the value of the coupled approach in capturing morphodynamic feedbacks and trajectory shifts not reproduced when shoreline and shoreface processes are modeled independently.

1. Introduction

Coastal regions provide critical socioeconomic benefits and are home to approximately 40% of the world's population (Poumadère et al., 2015). Among these environments, sandy coastlines, which account for approximately one-third of the ice-free global shoreline (Luijendijk et al., 2018), are particularly attractive. In the context of climate change and rising sea levels, sandy coasts are expected to undergo significant long-term transformations (Ranasinghe, 2016). Even in regions where incident wave energy is projected to remain stable or decrease, such as along the Atlantic coast of Europe (Perez et al., 2015), sandy coasts remain vulnerable to significant long-term morphological change.

Incident wave energy is projected to remain stable or even decrease in certain regions, such as along the Atlantic coast of Europe (Perez et al., 2015). At the same time, shoreline fluctuations driven by cross-shore processes, ranging from storm-scale (hours) to seasonal or inter-annual timescales, are generally well captured by equilibrium-based models (e.g. Yates et al., 2009; Splinter et al., 2014; Jaramillo et al., 2021) and can be regarded as high-frequency noise superimposed on longer-term trends (Fenster et al., 2001). Accordingly, the dominant drivers of coastal change over the coming century are expected to be sea-level rise (SLR) (Vousdoukas et al., 2017; Cooper et al., 2020) and gradients in longshore sediment transport (LST) (Ashton and Murray, 2006a). For wave-dominated coasts, capturing the coupled influence of SLR and LST is therefore critical to predicting long-term shoreline evolution.

A wide range of reduced-complexity models have been developed to simulate long-term shoreline evolution (e.g. Vitousek et al., 2017; Antolínez et al., 2019; Robinet et al., 2018; Tran and Barthélemy, 2020; Chataigner et al., 2022), particularly in response to gradients in longshore sediment transport and sea-level rise. These models are computationally efficient and well-suited for long-term projections, unlike process-based models which are limited by high computational demands and error accumulation over decadal timescales (Zhang et al., 2012; Seenath, 2022b). Despite these advantages, several practical challenges remain. Some models depend on long-term observational datasets or require inverse calibration, limiting their use in data-scarce

* Corresponding author at: BRGM, Orléans, F-45060, France.
E-mail address: m.traboulsi@brgm.fr (M. Traboulsi).

https://doi.org/10.1016/j.envsoft.2025.106624
Received 24 February 2025; Received in revised form 10 July 2025; Accepted 13 July 2025
Available online 23 July 2025
1364-8152/© 2025 The Authors. Published by Elsevier Ltd. This is an open access article under the CC BY license (http://creativecommons.org/licenses/by/4.0/).

settings (Karunarathna and Reeve, 2013; Jaramillo et al., 2024; Azorakos et al., 2024). Cross-shore dynamics are often addressed using static profiles, which can limit the model's ability to represent long-term morphological responses such as barrier rollover or profile retreat under sea-level rise (Cooper et al., 2020; Lakku et al., 2024; Seenath, 2023, 2022a). Moreover, models that handle more complex shoreline geometries often rely on further simplifications (e.g., shore-parallel contours, fixed transects, fixed closure depth), limiting their application to real-world coastlines, especially where human interventions are, or will be, implemented (Seenath, 2022b; Jaramillo et al., 2024; Vitousek et al., 2017).

In response to these limitations, recent efforts have explored data-driven strategies (e.g. Montaño et al., 2020). These include integrating machine learning models trained on remote sensing or in-situ datasets. These approaches offer strong potential for site-specific forecasting and uncertainty quantification. While they often lack physical interpretability and can be constrained by data availability, they complement physics-based models by enabling rapid assessments and supporting probabilistic shoreline mapping in complex settings (e.g., Karunarathna and Reeve, 2013; Kumar et al., 2020; Gomez-de La Peña et al., 2023).

A notable example of over-simplification in many reduced-complexity models is the continued reliance on the Bruun rule (Bruun, 1962) to estimate shoreline retreat under sea-level rise. Despite its simplicity and minimal data requirements, which have contributed to its widespread use (Terres De Lima et al., 2021; D'Anna et al., 2021; Vousdoukas et al., 2020), the Bruun rule has been criticized for its underlying assumptions. In particular, the Bruun rule overlooks key factors such as shoreface morphology, sediment supply, accommodation space, and anthropogenic influences (Cooper et al., 2020). While efforts have been made to refine the Bruun rule by incorporating additional processes (e.g., dune dynamics, probabilistic frameworks), these adaptations still fail to capture the full complexity of coastal morphodynamics (Rosati et al., 2013; Davidson-Arnott, 2005; Ranasinghe et al., 2011).

The ShoreTrans model (McCarroll et al., 2021) represents a significant advance, providing a rules-based, sediment budget approach to simulate dynamic shoreface adjustments under SLR. Unlike previous attempts, ShoreTrans can incorporate a range of coastal features – including dunes, barriers, seawalls, and cliffs – but is inherently one-dimensional, operating along fixed, shore-normal transects. Crucially, ShoreTrans does not resolve alongshore sediment transport internally and cannot simulate evolving shoreline orientation or planform change. ShoreTrans has also been integrated into hybrid modeling frameworks such as IH-LANSloc (Álvarez-Cuesta et al., 2023), which combine shoreline evolution with shoreface profile adjustment. While such approaches improve, among other aspects, the representation of long-term cross-shore dynamics, they typically rely on fixed shore-normal transects, limiting their ability to simulate evolving shoreline planforms such as cuspate forelands, embayed beaches, or flying spits.

To address these limitations, we developed a modular coupling framework specifically designed for long-term morphological evolution (called LX-ST). LX-ST integrates the grid-based shoreline model LX-Shore (Robinet et al., 2018), which handles alongshore sediment transport and planform evolution, with the ShoreTrans model, which simulates cross-shore profile response to sea-level rise and sediment imbalances. LX-ST enables transects to evolve dynamically in both space and orientation, capturing two-way feedback between shoreline position and profile adjustment. This coupling does not aim to replace hybrid approaches such as IH-LANSloc, which are better-suited for storm-scale or short-term applications. Rather, LX-ST is designed for decadal to centennial applications, where wave-driven cross-shore fluctuations are assumed to act as stochastic variability superimposed on long-term trends. The framework supports a broader range of morphological behaviors – including dune rollover, shoreline reorientation, and the interaction with hard structures – without requiring site-specific reconfiguration.

This interactive coupling aims to enable the simulation of medium- to long-term coastal evolution in settings where neither model alone can fully represent the governing processes. The shoreline component supports complex morphologies, including non-erodible elements, headlands, spits, and embayments, while the shoreface component replaces static-profile assumptions with a dynamic, volume-conserving method capable of simulating diverse barrier responses — such as rollover, encroachment, and localized erosion in front of hard defenses. By allowing transects to remain orthogonal to the evolving shoreline, LX-ST captures the critical feedback between shoreline curvature, longshore sediment transport gradients, and long-term cross-shore profile evolution induced by sea-level rise. This approach enables a more consistent two-dimensional representation of long-term coastal change under sea-level rise.

The paper is organized as follows. Section 2 describes the coupling architecture and overall methodology. Section 3 applies the approach to three synthetic test cases, followed by a real-world application in Section 4, which presents long-term shoreline change projections for a 5-km beach-dune system near Lacanau, southwest France. Section 5 discusses model limitations and outlines future research directions. Finally, Section 6 summarizes the key findings.

2. Method

2.1. ShoreTrans

ShoreTrans is a shoreface translation and sediment budgeting model recognized for its simplicity and rules-based structure (McCarroll et al., 2021). Unlike traditional models (e.g. Bruun, 1962), which typically assume a consistent profile shape and focus solely on the translation of the shoreline, ShoreTrans estimates changes in the real profile shape. This capability enables accurate and realistic modeling of coastal dynamics. The model accounts for various factors, including armoring, hard rock cliffs, outcropping rocks, dune accretion, sediment fluxes (both longshore and cross-shore), and sediment sources and sinks. It effectively incorporates the effects of sea-level rise (SLR) and sediment supply, making it adaptable to diverse coastal environments including sandy, gravelly, rocky, and engineered coasts. ShoreTrans is suitable for modeling coastal changes over temporal scales ranging from 10 to 100 years.

ShoreTrans requires a 2D cross-shore profile. The model translates the active profile vertically and landward until the net sediment volume change equals zero. The active profile is the segment that responds to immediate changes caused by incident wave action, adapting at a pace that typically exceeds the rate of translation induced by SLR. Depending on the profile's shape, its upper boundary is defined as the dune toe or the barrier crest, while the lower boundary is considered the depth of closure DoC. The upper boundary also serves as the translation point — the reference location around which the active profile shifts in response to sea-level rise and sediment dynamics.

Once the basic translation parameters are established, ShoreTrans uses an algorithmic approach to optimize translation, ensuring volume conservation. This is achieved by minimizing the error in volume change (ΔV_{error}) using a fixed cross-shore resolution (1 m).

The ShoreTrans model identifies four distinct barrier response types (Fig. 1), each characterized by specific dynamics and responses to SLR and other environmental changes. Translation points are typically located at either the dune toe or crest, depending on the barrier response type described below. These types are as follows:

1. *Barrier Rollover*: The entire back-barrier and active profile are raised and shifted onshore. This response typically occurs in low-elevation barriers with a gentle hinterland gradient, where sediment is transported onshore, often through overwash processes.

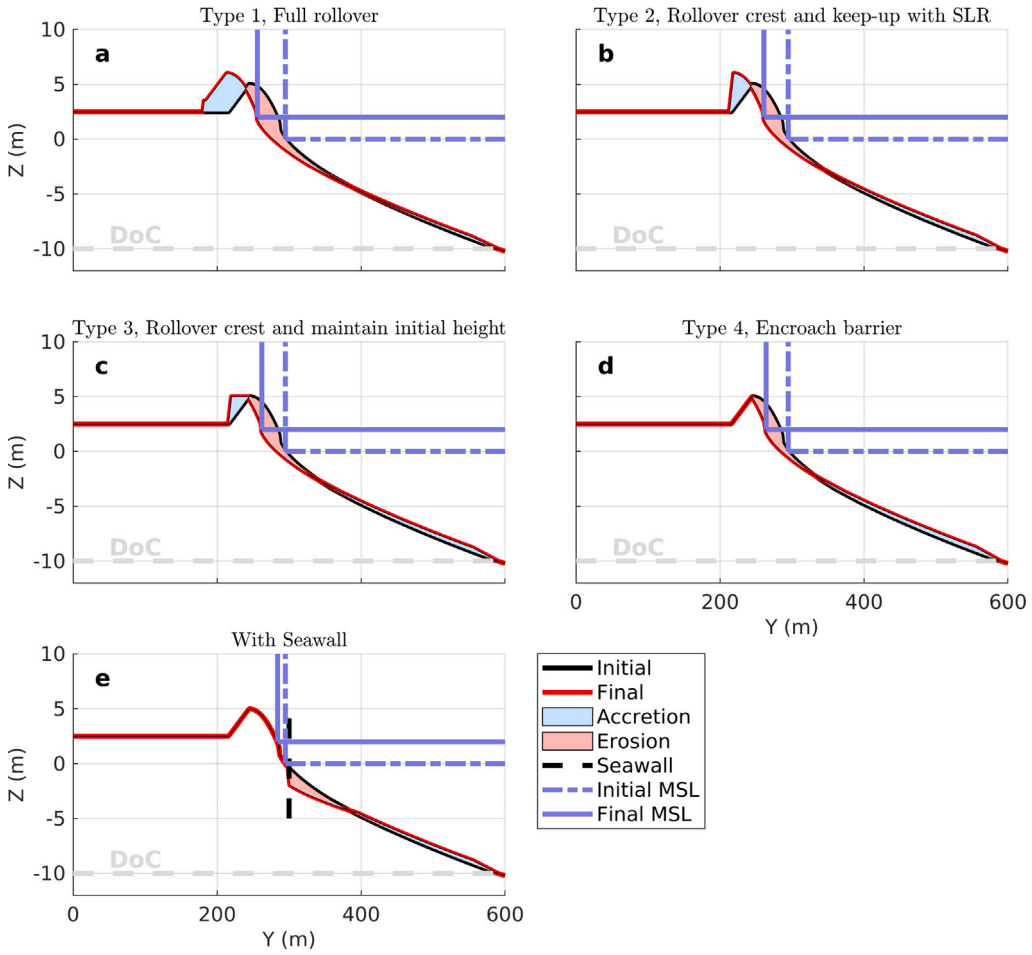

Fig. 1. Schematics of the ShoreTrans barrier response types with and without a seawall. Accretion (red), erosion (blue), initial/final mean sea levels (blue), and the seawall (dashed black) are indicated.

2. *Barrier Rollover (Keep up with SLR)*: The barrier crest is raised by the amount of sea level rise and translated onshore. A landward slope extends from the crest at an angle (Φ) until it intersects the initial profile. This response is seen in barriers where dunes or barrier crests dynamically respond to rising sea levels.
3. *Barrier Rollover (Maintain Initial Height)*: Similar to the previous type, but after translation, the barrier crest is capped at its initial level. This type of response occurs when the barrier or dune can roll over but is constrained in its vertical growth, possibly due to limitations in sediment supply or other geomorphological controls.
4. *Encroachment Barrier*: Here, the active profile is translated, but no increase in bed level is allowed onshore. This type of response is more common on bay barriers and mainland beaches characterized by steep topography.

In addition to these modes, the 'wall effect' is an important phenomenon to consider when a seawall is present. While not classified as a distinct mode, the wall effect describes how the presence of a seawall alters sediment dynamics (Fig. 1e), concentrating erosion directly in front of the structure. This occurs because the erosion that would typically occur landward of the seawall is redistributed offshore, producing a triangular erosion wedge, with its deepest point at the wall base. The extent of this wedge is often assumed to be one-third of the cross-shore width of the active profile.

Since LX-Shore is written in Fortran, the original ShoreTrans code (written in Matlab) has been rewritten in Fortran. Additionally, developments have been made to reduce computation time and allow the spatial resolution to be specified as a user-defined parameter.

2.2. LX-Shore

LX-Shore is a reduced-complexity shoreline model designed to simulate shoreline change along wave-dominated sandy coasts on large spatial, O(100–100000 m), and temporal, O(1-100 y), scales (Robinet et al., 2018). It is based on the concept of a grid-based one-line model approach (Fig. 2) first introduced in the CEM model by Ashton et al. (2001), Ashton and Murray (2006a,b).

A key strength of LX-Shore is its ability to model diverse shoreline morphologies, including sand spits, embayed beaches, salients, and non-erodible elements such as headlands and coastal defenses. This versatility is achieved by modeling changes in sediment volume contained within each grid cell instead of modeling explicitly cross-shore changes of the nodes composing the shoreline (Ashton et al., 2001; Ashton and Murray, 2006a,b). The sediment content of each cell is expressed as a fraction, determined by the ratio of the current sediment volume to the cell's maximum capacity, accounting for its size and any non-erodible regions. This sediment fraction ranges from 0 (water) to 1 (land). By applying simple interface reconstruction methods, complex shoreline geometries can be derived from any configuration of sediment fraction grid.

LX-Shore computes changes in sediment fraction driven by longshore and cross-shore transports (Fig. 2) (Robinet et al., 2018, 2020a). Longshore sediment transport is computed using either the CERC formula (USACE, 1984) or the formula of Kamphuis (1991). LX-Shore accounts for sediment bypassing around hard structures that obstruct longshore sediment transport (Durand et al., 2024). The short- to

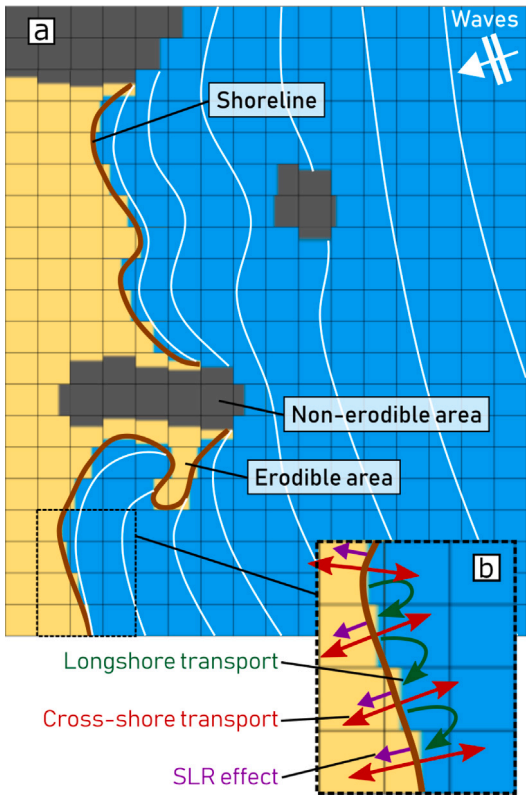

Fig. 2. Overview of LX-Shore: (a) Architecture and functionalities (b) Main processes (from Robinet et al., 2020c). Dark gray and yellow areas within the grid cells represent non-erodible and erodible regions, respectively.

medium-term cross-shore sediment transport is resolved using an adaptation of the equilibrium model ShoreFor (Davidson et al., 2013; Splinter et al., 2014), which is here switched off given the timescales addressed in this contribution. Wave conditions at breaking can be estimated either with the direct empirical formula of Larson et al. (2010) or the SWAN spectral wave model (Booij et al., 1999). The latter is particularly valuable for complex bathymetric settings, where wave refraction and energy focusing significantly influence breaking wave conditions and, consequently, shoreline evolution (Robinet et al., 2020b).

LX-Shore has been applied successfully to both synthetic scenarios (e.g., groynes, breakwaters, cuspates, flying sandspits) and real-world sites such as Truc Vert (France), Narrabeen (Australia), and Tairua (New Zealand) (Robinet et al., 2018, 2020a,b; Montaño et al., 2020).

By default, LX-Shore can internally account for SLR-driven shoreline retreat at each time step by activating the Bruun rule (see e.g., Robinet et al., 2020a). However, in the coupled LX-ST configuration used here, the Bruun rule is deactivated within LX-Shore, and cross-shore sediment transport is also switched off. Instead, all SLR-induced shoreline and profile adjustments are captured through explicit coupling with the ShoreTrans model (see Section 2.3).

For clarity, results shown in Section 3 include both the fully coupled LX-ST configuration (with Bruun OFF in LX-Shore), and, for comparison, simulations with stand-alone LX-Shore where the Bruun rule is activated. Longshore transport is computed using the Larson formula, which better suits morphologically active coasts with oblique wave incidence.

2.3. Coupling between LX-shore and ShoreTrans

Fig. 3 illustrates the coupling methodology between LX-Shore and ShoreTrans (LX-ST). This approach employs a time-splitting strategy, acknowledging the differing temporal scales of processes: wave-driven longshore sediment transport occurs at short timescales (hours to days) and is addressed by LX-Shore at frequent intervals (Δt_{LX}), whereas slower processes such as sea-level rise (SLR) and shoreface profile translation are managed by ShoreTrans at longer intervals (Δt_{ST}, typically annual to decadal).

At each coupling step, LX-Shore (2) independently computes the reference shoreline position $S_{ref}(t_{i-1})$ (2a), using its dedicated input set (1a). For the coupling, the reference shoreline is discretized into shore-normal transects spaced consistently according to the LX-Shore grid resolution (d_{xy}). These transects are subsequently used to extract cross-shore profiles from the provided topobathymetric grid (3), introduced explicitly to support ShoreTrans operations. The wave-driven sediment volume change per unit alongshore distance is computed (5) based on the difference between the coupling shoreline, $S_{cpl}(t_i)$ (4a), and the reference shoreline, $S_{ref}(t_{i-1})$ (2a):

$$\frac{dV}{ds} = -dR \times h_a \tag{1}$$

where dV/ds is the wave-driven volume change per unit alongshore distance s, dR is the shoreline change induced by wave-driven longshore transport, and h_a is the height of the active profile.

ShoreTrans (6) then updates the cross-shore profiles based on this sediment volume change and the projected sea-level rise (1c). As part of this update, the depth of Closure (DoC) is dynamically recalculated using the Hallermeier (1980) formula. The resulting time-varying DoC defines the lower boundary of the active coastal profile and is applied directly within ShoreTrans. The updated DoC is also passed back to LX-Shore.

From the updated profiles, a new shoreline, $S_{ST}(t_i)$ (7), is extracted, and the sediment fraction grid, $F_{ref}(t_i)$ (8), is recalculated accordingly. This updated sediment fraction grid is returned to LX-Shore, providing the updated reference shoreline $S_{ref}(t_i)$. Concurrently, the topobathymetric data is interpolated and adjusted (9) to reflect the newly calculated profiles and prepare for subsequent coupling cycles, depending on the chosen coupling mode.

At each subsequent ShoreTrans interval (Δt_{ST}), this coupling procedure – comprising shoreline extraction, volume calculation, profile updating, and sediment fraction grid recalculation – is repeated until the simulation concludes.

The interpolation of the topobathymetry (step 9 in Fig. 3) follows a novel interpolation-based method that we developed, which generates a dense, domain-wide point-cloud to ensure spatial consistency and accuracy in subsequent coupling iterations (Fig. 4).

This process begins with the identification and refinement of shoreline points (SPs) along the transects (Step 1). By default, SPs are defined at the Z-contour corresponding to the mean sea level, though users can modify this Z-value. A high-resolution shoreline is then generated from these points using the Akima interpolation method (Akima, 1970). Akima is preferred for handling sharp transitions without overshooting, unlike spline interpolation, which, while smooth, can be computationally intensive and less suited for abrupt changes.

Next, equidistant polylines (Step 2) are constructed within the interpolation domain, spaced uniformly at a distance dl from the shoreline. Each point on these polylines is assigned a Z-value interpolated from the topobathymetric grid, ensuring that the spacing is small enough to capture detailed profile variations, such as those caused by sea walls or other coastal structures. These newly interpolated points are then merged with the existing point cloud (Step 3) by masking the interpolation region and retaining points outside this region from the original dataset. This approach ensures that the shoreline evolution is properly captured over time.

LX-ST provides a flexible coupling framework that adapts to varying levels of coastal complexity and computational constraints. At its most advanced, the model dynamically updates both the position of cross-shore transects and their associated profiles as the shoreline evolves. This configuration – referred to as coupling level 3 – ensures that

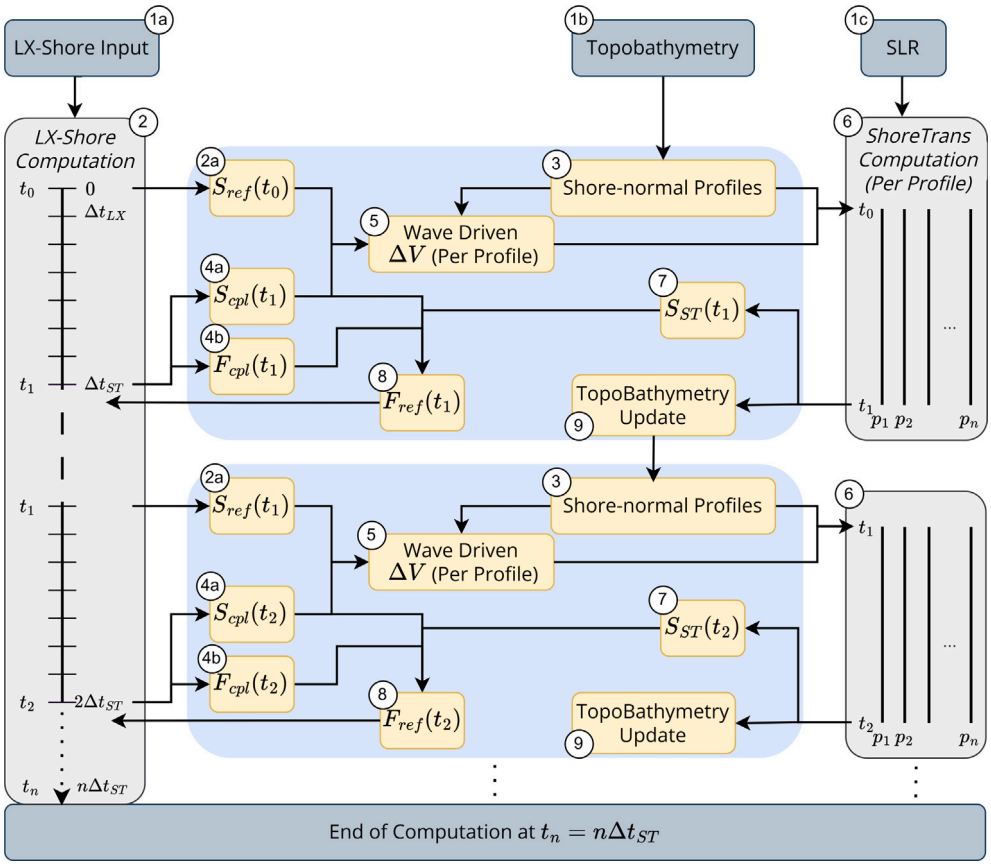

Fig. 3. Flowchart illustrating the coupling process between LX-Shore and ShoreTrans. The reference shoreline is denoted by $S_{\mathrm{ref}}(t_{i-1})$, while $S_{\mathrm{cpl}}(t_i)$ represents the coupling shoreline. The dashed line highlights periods of idle computation. Individual cross-shore profiles are indicated by p_k.

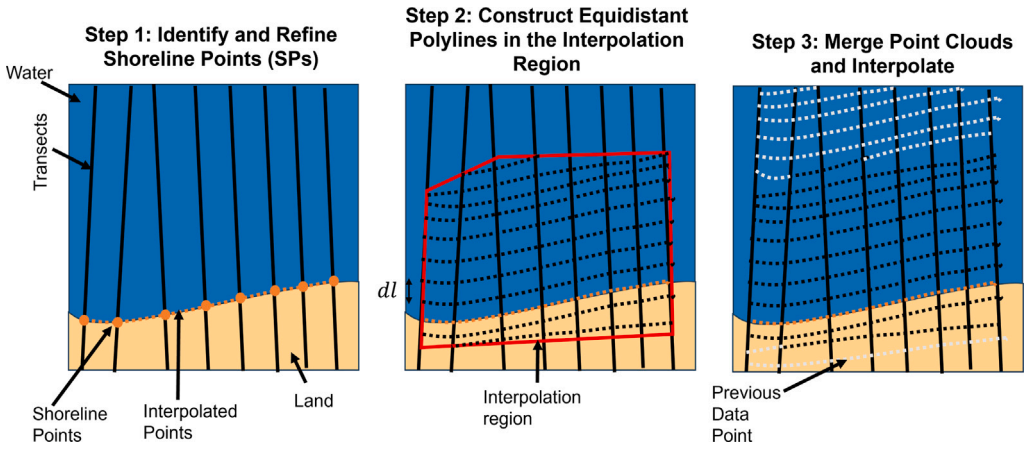

Fig. 4. Top-view image of the interpolation method used to create the point cloud.

morphological feedback are accurately captured in settings with strong curvature or rapidly changing shoreline geometry, making it ideal for simulating complex coastal systems. However, because this level involves higher computational costs, especially over long time periods or large domains, LX-ST also offers two streamlined alternatives.

Coupling level 2 maintains fixed transect positions while still incorporating shoreline feedback into profile updates. This intermediate configuration is conceptually similar to recent models such as IH-LANSloc, and strikes a balance between realism and efficiency, making it suitable for moderately complex coastlines. In Fig. 3, this corresponds to skipping step 9, meaning that ShoreTrans is applied to the original shore-normal profiles at each update, without adjusting their spatial position.

Finally, coupling level 1 excludes shoreline feedback entirely and assumes fixed transects, with profile changes driven solely by longshore sediment transport and sea-level rise. While this approach is less suited for dynamic coastlines, it offers significant gains in speed and is particularly useful for sensitivity analyses and comparison with other reduced-complexity models. In Fig. 3, this corresponds to skipping both step 8 (shoreline feedback update) and step 9 (topobathymetry interpolation), resulting in purely forward-driven updates.

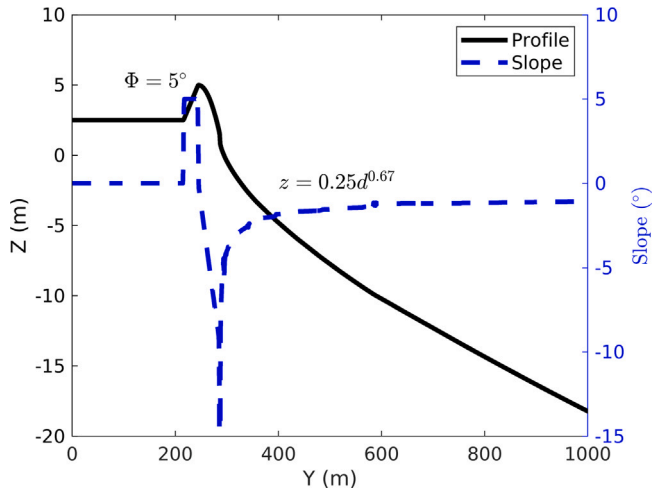

Fig. 5. The profile used to generate the topobathymetry for the synthetic test cases.

3. Synthetic test cases: Description and results

3.1. Test cases description

The main objective of these synthetic test cases is to illustrate the coupling capabilities and investigate the sensitivity of the results to the coupling procedure. To achieve this, we consider an idealized beach-dune profile (Fig. 5) and design three test cases (Fig. 6): (1) diffusion of a bulge under nearly shore-normal waves, (2) the effect of a longshore seawall under obliquely incident waves, and (3) the effect of a groyne under obliquely incident waves.

These test cases were selected to systematically assess the ability of the LX-ST coupling to handle varying degrees of shoreline planform evolution. Test case 1 (bulge) represents a scenario with strong temporal evolution of the shoreline planform, where significant added value from full coupling (level 3) is expected due to pronounced changes in shoreline orientation. Test case 2 (seawall) examines the effect of a seawall on an initially rectilinear shoreline, where levels 3 and 2 are anticipated to yield similar results, and level 1 is expected to deviate more significantly, highlighting the role of shoreline feedback in the presence of a fixed structure. Test case 3 (groyne) features a situation where only moderate changes in shoreline orientation occur and no seawall effect is present, so limited differences are expected among the three coupling levels. This selection enables a direct evaluation of the LX-ST coupling's performance across contrasting scenarios of planform change and management intervention. All cases use identical sediment properties and impose a linear 1 m SLR over their respective durations (5–100 y; see Table 1 for the key case parameters, and Supplementary Table S1 for the full configuration).

In all synthetic test cases, sediment bypassing around hard structures is represented using the shoreline-only bypassing (SB) scheme (Durand et al., 2024), wherein sediment is transported around an obstacle only when the shoreline itself extends beyond the tip of the structure. This choice is consistent with the simplified, idealized design of the test cases, and facilitates benchmarking against previous studies using comparable assumptions.

We run each case with both ShoreTrans modes (barrier rollover vs. encroachment) and LX-ST's three coupling levels (Section 2.3). Case 1 employs a realistic time series representative of a high-energy, wave-dominated coast (Castelle et al., 2017); Cases 2 and 3 use constant wave height and period with normally distributed incidence angles. By comparing coupling levels 1–3 across these management-relevant setups, we assess when and why dynamic transects (level 3) become essential to reproduce alongshore morphology.

To isolate decadal-scale trends, we run LX-ST with cross-shore transport turned off (ShoreFor deactivated, storm impact deactivated) and constant wave height and period, thereby removing all storm- and seasonal-scale fluctuations. Consequently, only longshore sediment transport and linear SLR drive shoreline change.

A comparison of the final shoreline positions for all test cases and a benchmark – LX-Shore (with Bruun rule activated) – is provided in Table 2. In the coupled LX-ST runs, the Bruun rule is deactivated in LX-Shore and SLR effects are instead handled by ShoreTrans (see Section 2.3).

3.2. Test case 1: Shoreline bulge

This test case explores how an initial shoreline bulge evolves under the combined influence of nearly shore-normal waves and an imposed sea-level rise of 1 meter over five years. The domain is 3 km long and 1.6 km wide, discretized with 100 m shoreline cells and a Topobathymetry resolution of 10 m (see Table 1). Wave forcing is prescribed using a realistic time series representative of a high-energy, wave-dominated coast (Castelle et al., 2017). To isolate the effects of longshore transport and sea-level rise, all simulations assume uniform sediment characteristics and cross-shore processes are deactivated.

As shown in Fig. 7a–b, the shoreline straightens as the bulge diffuses laterally, and the model captures this behavior with high spatial detail. The outcomes differ depending on the ShoreTrans translation mode. In the rollover mode, the dune system persists but exhibits strong alongshore variability: dunes narrow in the alignment of the former bulge due to localized sediment loss, while adjacent sectors widen from net sediment gain (see also supplementary Fig. S2). This results in a heterogeneous morphology shaped by the interaction of SLR and sediment redistribution. In contrast, the encroachment mode results in a more uniformly distributed coastal morphology. Here, shoreline diffusion and straightening dominate, and the central dune in the alignment of the initial shoreline bulge is completely eroded. This highlights the combined impact of SLR and diverging longshore sediment transport on the erosion and decay of the dune crest and the sensitivity to the rollover mode.

Using coupling level 2 (Fig. 7c–d), with fixed transect positions but retained shoreline feedback, the model still captures the overall trend toward straightening. However, it struggles to resolve finer details of erosion and accretion, particularly near the former bulge where shoreline curvature is greatest. This demonstrates the importance of allowing transects to move when simulating complex or rapidly changing coastlines.

In coupling level 1 (Fig. 7e–f), with both feedback and transect updates disabled, the model produces the greatest errors. Here, erosion in the bulge region is consistently overestimated, and the predicted shoreline is much less reliable.

3.3. Test case 2: Seawall

This test explores the coastal evolution of a straight shoreline with a localized 1-km-long seawall (Fig. 6b), subjected to obliquely-incident waves (30° from shore normal) and a linear SLR of 1 m over 100 years. The model domain is 5 km long and 1.4 km wide, discretized using 100 m shoreline cells and a topobathymetry resolution of 10 m (see Table 1). Wave height and period are held constant, while the angle of incidence follows a normal distribution.

In the absence of SLR, wave action is expected to induce minimal changes to the straight shoreline. However, with SLR, progressive erosion is anticipated along the entire coastline, while the presences of the seawall disrupts the alongshore sediment transport pathway. As shown in Table 2 and Fig. 8a–b, the shoreline evolves asymmetrically: updrift of the seawall, sediment accumulates due to wave-driven transport being blocked by the structure, partially offsetting erosion from sea-level rise. Downdrift, however, sediment supply is reduced, resulting

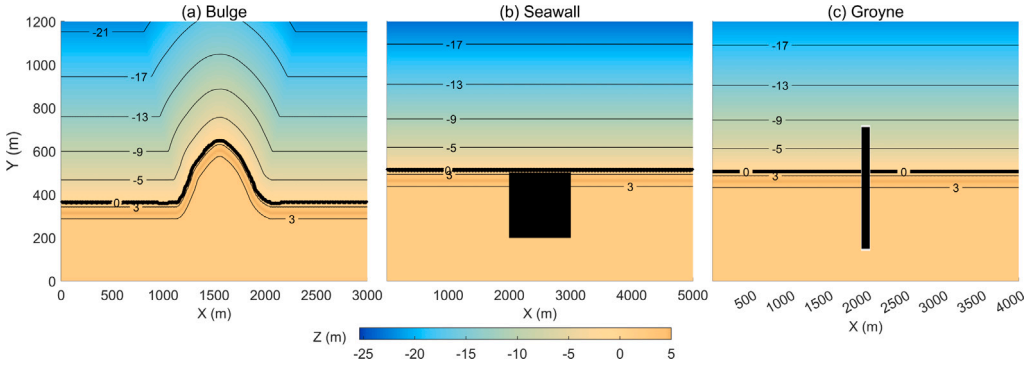

Fig. 6. Initial topobathymetry for test cases: (a) Bulge, (b) Seawall, and (c) Groyne.

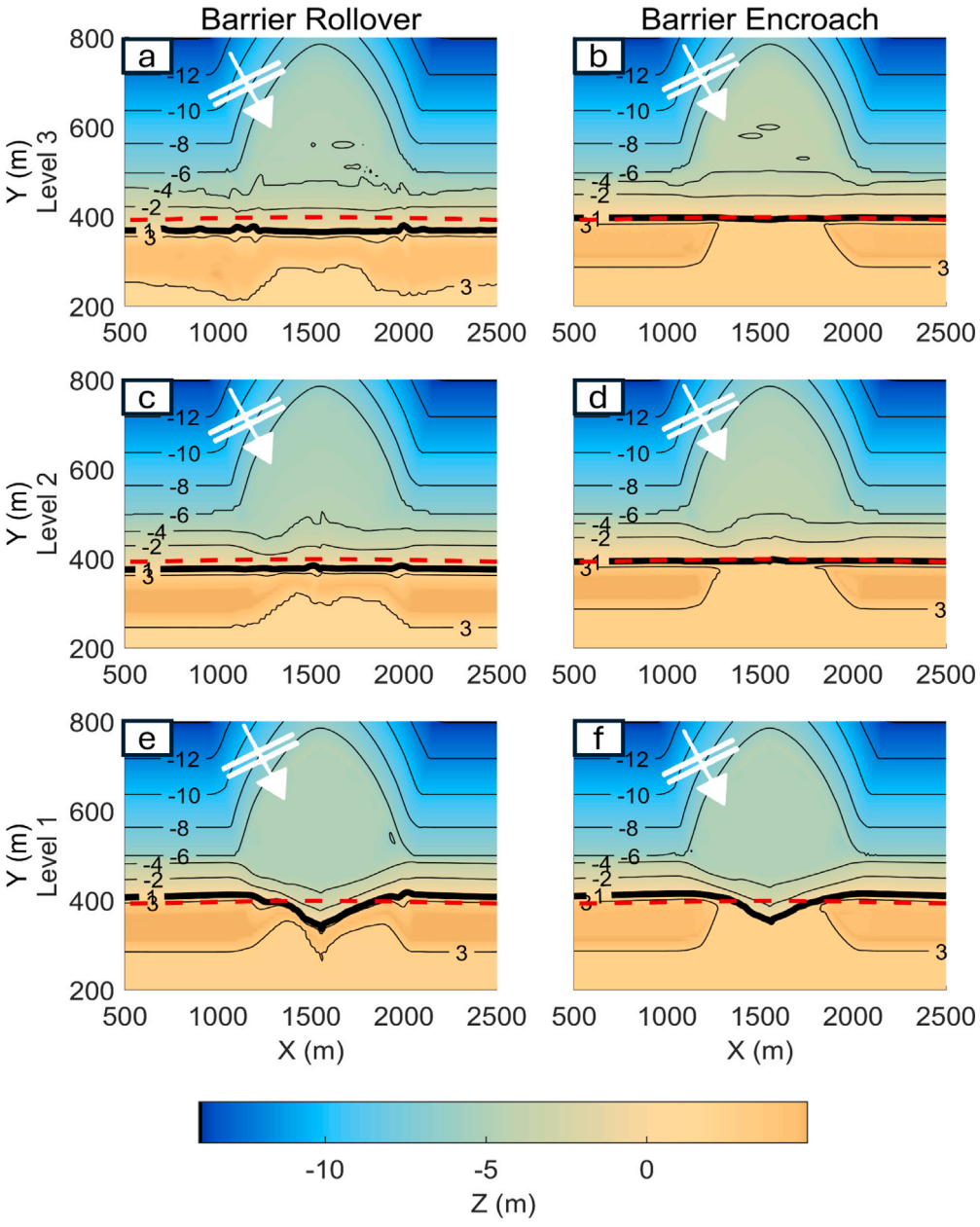

Fig. 7. Results for Case 1: Columns display two rollover modes – full rollover and encroachment– while the rows correspond to the three coupling levels offered by LX-ST (see Section 2.3). The thick black line indicates the shoreline at Z = MSL (Mean Sea level), and the dashed red line represents the shoreline derived from stand-alone LX-Shore with the Bruun rule activated (see Section 2.2).

Table 1
Summary of key parameters for the three synthetic test cases with ST: ShoreTrans Resolution, TB: Topobathymetry Resolution, LTF: Longshore Transport Formula, Dw: Depth at which waves are imposed, BC: Boundary Condition (H: Horizontal).

Test case	(1) Bulge	(2) Seawall	(3) Groyne
Computational grid			
Grid (km): $x \times y$	3×1.6	5×1.4	4×1.4
Cell size (m)	100	100	50
TB (m)	10	10	10
ST (m)	0.1	0.1	0.1
Simulation settings			
LTF	Kamphuis (1991)	Kamphuis (1991)	Kamphuis (1991)
Wave model	Larson et al. (2010)	Larson et al. (2010)	Larson et al. (2010)
Dw (m)	35	35	35
BC	Periodic H	Periodic H	Periodic H
SLR (m)	1 Linear	1 Linear	1 Linear
Hs (m)	$\mu = 1.14 \pm 0.3$	1	1.5
Tp (s)	$\mu = 11.13 \pm 2.19$	8	8 $\mathcal{N}(-5, 20)$[b]
θ (°)	$\mu = 12.5 \pm 0.36$[a]	$\mathcal{N}(30, 15)$[b]	10
Duration (y)	5	100	3
Δt_{LX} (h)	1	3	1
Δt_{ST} (y)	0.25	1	1
Δt_{TR}	0.25	20	

[a] Based on a realistic time series of a high-energy wave-dominated coast (see Figure S1).
[b] Normal distribution.

Table 2
Summary of maximum erosion (in meters) for each synthetic test case and coupling level, under two shoreline translation modes. Results from stand-alone LX-Shore (with Bruun rule activated) are shown for reference.

Test	Mode	LX-Shore + Bruun	Level 1	Level 2	Level 3
1- Bulge	Rollover	247 m	241 m	264 m	272 m
	Encroachment	247 m	240 m	248 m	245 m
2- Seawall	Rollover	18 m	15 m	37 m	40 m
	Encroachment	18 m	4 m	10 m	11 m
3- Groyne	Rollover	70 m	130 m	120 m	120 m
	Encroachment	70 m	110 m	100 m	70 m

in pronounced erosion that is amplified by the SLR. In the rollover mode, this leads to a maximum downdrift retreat of 37 m, while in the encroachment mode, erosion is more limited, reaching only 10 m. In front of the seawall, the absence of accommodation space causes a lowering of the upper profile, consistent with the 'wall effect' shown in Fig. 1e.

In coupling level 2 (Fig. 8c–d), which includes shoreline feedback but uses fixed transect positions, the model reproduces the same trends observed previously (see also the supplementary material, Fig. S3). The maximum deviations between levels 3 and 2 remain below 2.5 m, suggesting that coupling level 2 provides sufficient accuracy for relatively linear coasts with limited temporal changes in curvature. For such cases, the additional computational cost of implementing dynamic transects may not be necessary.

In contrast, for coupling level 1 (Fig. 8e–f), i.e disabling both shoreline feedback and transect updates. Both updrift sediment trapping and downdrift erosion are under-represented: the model does not account for the blocking and redistribution of sediment caused by the structure, leading to an overly simplified erosion pattern under sea-level rise.

3.4. Test case 3: Groyne

The test case investigates the evolution of a straight sandy shoreline disrupted by a single groyne, extending 20 m in width and 200 m offshore (Fig. 6c). The scenario involves obliquely-incident waves at a −5° angle and a linear SLR of 1 m over a decade (Table 1). The domain spans 4 km in length and 1.4 km in width, discretized with 50 m shoreline cells and a topobathymetry resolution of 10 m. Wave height and period are fixed while wave direction follows a normal distribution to account for natural variability. The primary objective is to examine how wave-driven sediment transport interacts with structures, such as groynes, in shaping beach-dune morphology under the combined influence of incident waves and SLR.

Initially, the groyne disrupts longshore sediment transport, causing sediment accumulation on the updrift side and erosion on the downdrift side. As sea level rises over time, these patterns of deposition and erosion become more pronounced. As shown in Fig. 9a–b, both ShoreTrans translation modes show similar shoreline behavior: accretion occurs updrift, while downdrift erosion increases. However there are two main differences. First, dune morphology diverges substantially: in the rollover mode, the dune migrates landward while maintaining volume; in contrast, the encroachment mode leads to rapid dune erosion due to limited accommodation space. Second, shoreline retreat is more pronounced in the rollover mode compared to encroachment (mean shoreline position: 490 m vs. 473 m from the offshore boundary).

This scenario exhibits low sensitivity to the coupling level. Level 1 uses fixed transects without shoreline feedback and already captures the main features of shoreline and dune evolution. Level 2 adds shoreline feedback while keeping transects fixed, slightly improving agreement with level 3. Level 3 dynamically updates both transects and profiles, but offers negligible benefit in this case due to minimal shoreline curvature change. Alongshore-averaged differences remain below 2 m across all levels (See Table 2).

A summary of final shoreline positions for all coupling levels and modes is provided in Table 2, including the LX-Shore + Bruun rule benchmark.

4. Real beach test case: Lacanau, southwest France

4.1. Test case description

Lacanau is a seaside resort located on the southwest coast of France along the Atlantic Ocean. The study site spans a 5-km meso- to macrotidal sandy shoreline exposed to high-energy waves predominantly coming from the west-northwest. Incident wave energy varies seasonally, with monthly mean significant wave height and peak wave period ranging from approximately 1.1 m and 8.5 s in July to 2.4 m and 13 s in January. Erosion rates range from 0.3 m/y to 3 m/y depending on the dataset and methodology used (Castelle et al., 2018; Nicolae Lerma et al., 2022; Castelle et al., 2022).

Lacanau was selected as a representative test case because it exemplifies common challenges faced by managed sandy coasts, including

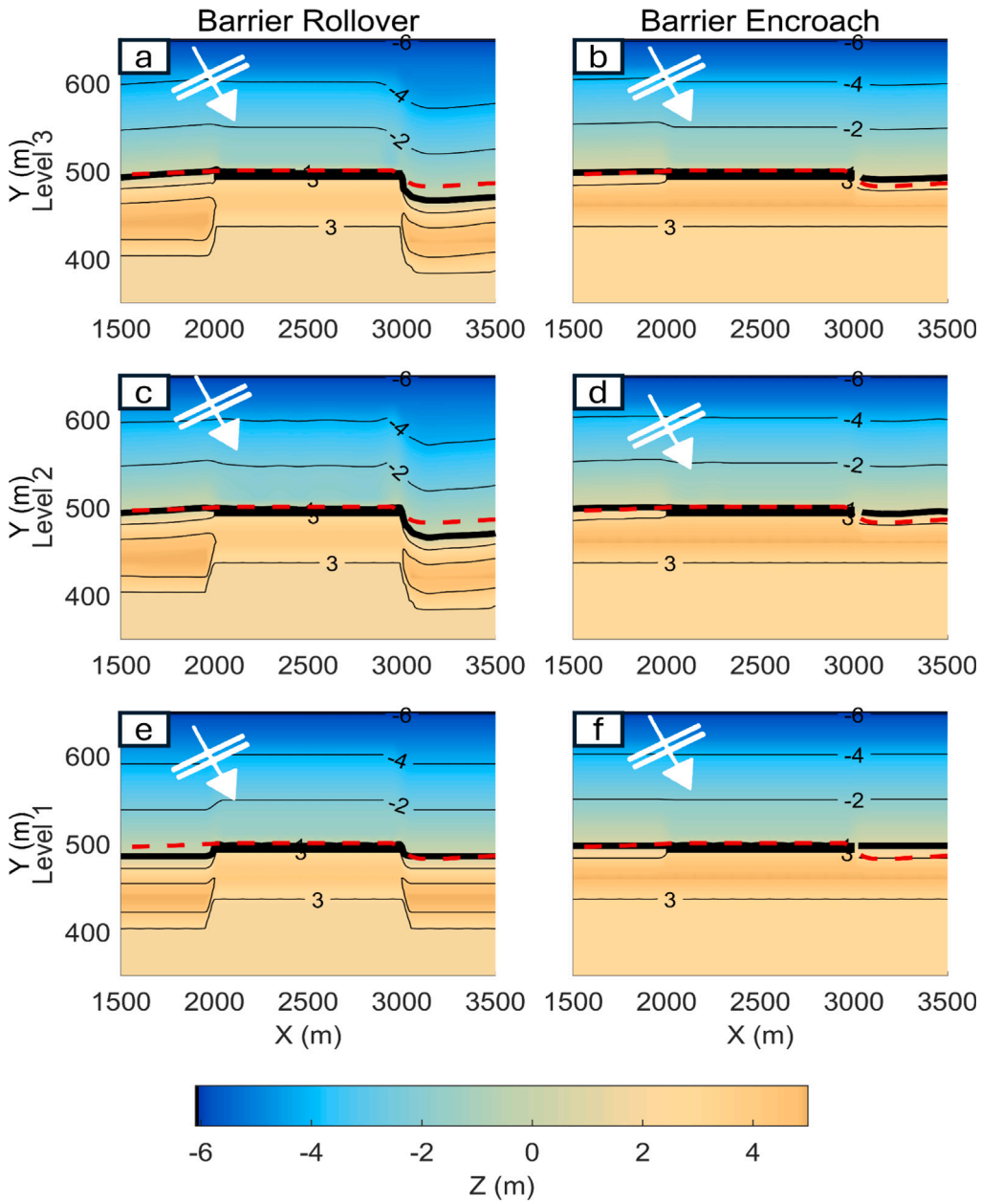

Fig. 8. Results for Case 2: Columns display two rollover modes – full rollover and encroachment – while the rows correspond to the three coupling levels offered by LX-ST (see Section 2.3). The thick black line indicates the shoreline, and the dashed red line represents the shoreline derived from stand-alone LX-Shore with the Bruun rule activated (see Section 2.2).

chronic erosion, sediment supply deficits, and the use of hard engineering structures that disrupt longshore transport. While the site is relatively straight, it offers a realistic setting for evaluating model coupling behavior under conditions of human intervention. The availability of high-resolution topographic and bathymetric data further supports its use as a benchmark case for assessing the LX-ST coupling approach, which simulates the interaction between alongshore, chronic erosion and sea level rise processes under coastal management constraints. This application is not intended as a predictive forecast of future shoreline change, but rather as a test of the coupling framework's ability to capture key morphodynamic feedback under realistic, data-informed conditions.

Initial topobathymetry was constructed using LiDAR topography collected in 2011 (Nicolae Lerma et al., 2019), complemented by bathymetric data from the Litto3D initiative – a collaboration between the French Hydrographic and Oceanographic Service (SHOM) and IGN – acquired over campaigns from Sep 2020 to Sep 2022. These datasets were interpolated onto a 10 (longshore) × 1 m (cross-shore) grid to generate a coherent topobathymetric surface. For modeling purposes, the shoreline was approximated by the 1.5 m elevation contour above mean sea level, serving as a proxy for the shoreline position and simplified as a straight line. Beyond this, the subaqueous profile was reconstructed using a longshore-averaged Dean profile calibrated with the observed topobathymetry surface mentioned earlier. For qualitative validation of coastal dune evolution, additional LiDAR data collected in autumn 2023 by OCNA were used.

Wave forcing data (1940–2024) were sourced from ERA5 (Hersbach et al., 2020), a global reanalysis product by the European Centre for Medium-Range Weather Forecasts (ECMWF). ERA5 provides hourly wave conditions at a 0.5° spatial resolution. For this study, data were extracted at a nearshore point offshore of Lacanau (approx. 50 m water depth; coordinates: −1.5°E, 44.5°N), covering the period from 2011 to

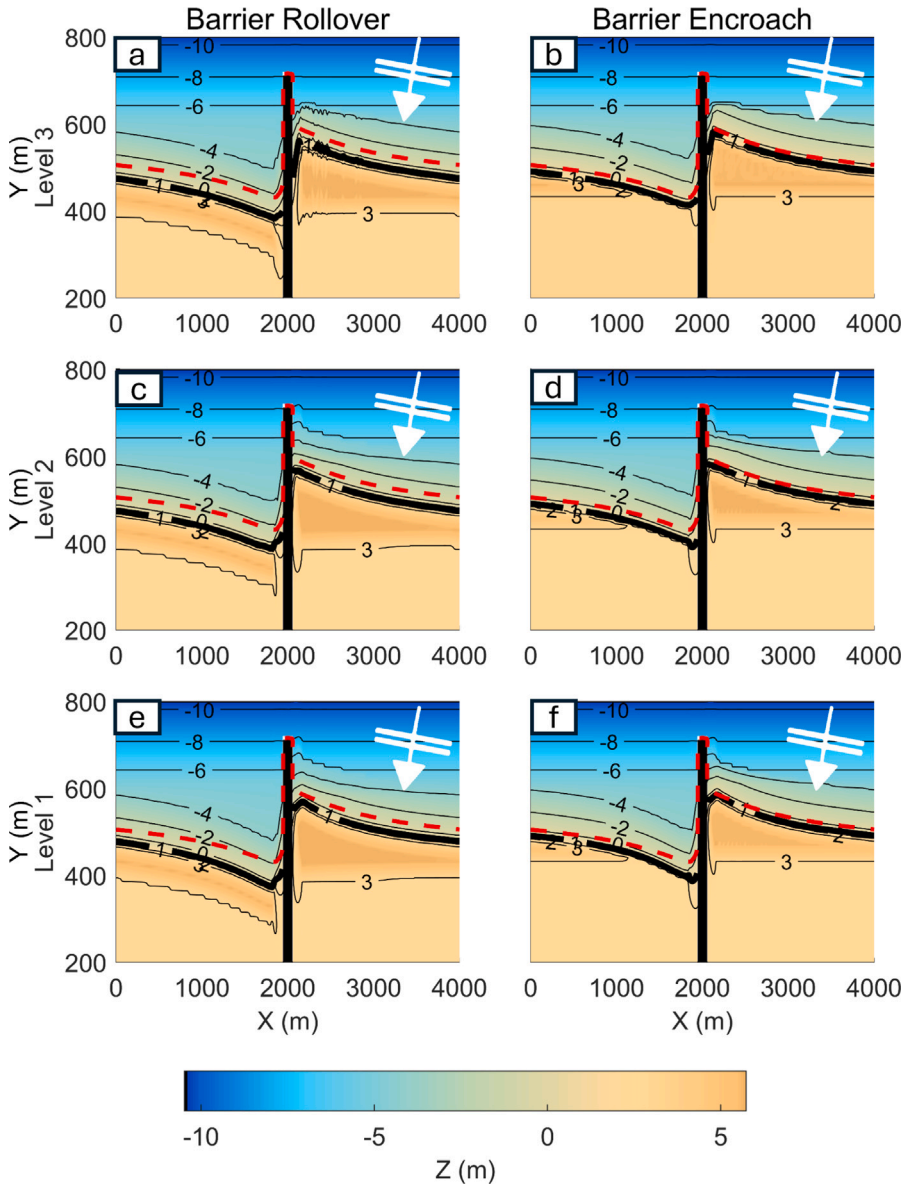

Fig. 9. Results for Case 3: Columns display two rollover modes – full rollover and encroachment – while the rows correspond to the three coupling levels offered by LX-ST (see Section 2.3). The thick black line indicates the shoreline, and the dashed red line represents the shoreline derived from stand-alone LX-Shore with the Bruun rule activated (see Section 2.2).

2024 (Fig. 10). To extend the dataset to 2100, the 1940–2024 time series was duplicated. A one-week moving average was applied at the duplication boundary to smooth the transition. This method preserves the statistical properties of the local wave climate while avoiding artificial discontinuities, enabling a controlled, stationary wave forcing input consistent with the illustrative scope of the Lacanau test case.

To simulate sediment transport around the seawall, we used the "full bypassing" (FB) method described in Durand et al. (2024). Unlike the "shoreline bypassing" (SB) approach used in idealized Test Case 2, the FB method accounts for subaqueous transport both inside and outside the surf zone. It allows sand to bypass coastal structures even when the shoreline does not reach the structure's tip.

The computational domain (Fig. 11a) spans 15 km (longshore) × 2.45 km (cross-shore), but analysis focuses on a 5 km central section (Supplementary table 2 summarizes the main parameters). The additional 10 km (not shown) is included to minimize the influence of open boundary conditions. The depth of closure is set to 13.5 m (estimated using the average depth of closure using the Hallermeier, 1980 formula), and the dune height is 17 m. The time step for longshore transport (Δt_{LX}) is 1 h. The shoreline is updated annually (Δt_{ST} = 1 y) using encroachment mode and LX-ST level 2 coupling. We use the median sea-level rise projection from the CMIP6 SSP5-8.5 scenario (Intergovernmental Panel On Climate Change (Ipcc), 2023; Garner et al., 2021; Kopp et al., 2023). Shared Socioeconomic Pathways (SSPs) are scenarios used in climate modeling to describe possible future developments in demographics, economics, technology, and policy. SSP5-8.5 corresponds to a high-end emission scenario characterized by rapid economic growth, continued fossil fuel use, and limited climate policy, leading to a radiative forcing of 8.5 W/m^2 by 2100. The median SLR trajectory is used as the baseline forcing in the simulations, while the 17th–83rd percentile envelope are used to illustrate the uncertainty range of the SLR input scenarios (Supplementary figure S5). This is combined with a steady erosion rate of 1.4 m/y, based on observed shoreline retreat over the period 1950–2023. This trend reflects the site's long-term sediment deficit and chronic erosion (Nicolae Lerma et al., 2022).

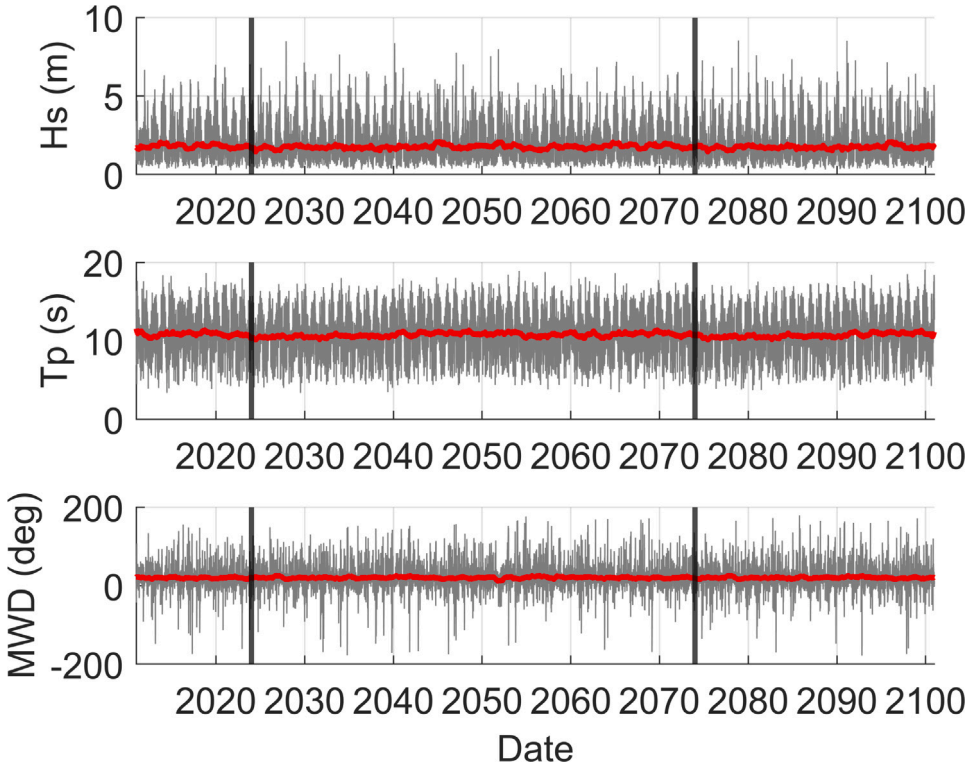

Fig. 10. Significant Wave Height (Hs), Peak Period (Tp), and Mean Wave Direction (MWD) from ERA5 wave data (1940–2024), extended to 2100 with duplication and one-week smoothing (vertical bands). MWD is in local coordinates, relative to the shore-normal.

4.2. Validation

To evaluate the performance of the LX-ST coupling, we performed a simulation covering the 2011–2023 period and compared the modeled results with annual dune front positions derived from LiDAR topographic surveys conducted between 2014 and 2023. Validation focused on the 10-m elevation contour, used here as a proxy for the dune front, and analyzed across 100 shore-normal transects. This proxy was selected to reduce the influence of short-term cross-shore fluctuations and better isolate decadal-scale morphodynamic trends, consistent with the model's intended scope. LiDAR data are available for each year within this period except 2015, allowing for nearly continuous year-by-year validation.

The box plots (Fig. 11b) show the distribution of these metrics across the domain. Overall, RMSE and MAE remain below 10 m, with median values around 8 m and 6 m, respectively, indicating robust performance for a reduced-complexity model. While most years exhibit stable errors, some outliers contribute to the upper whiskers – particularly 2014 and 2019 – coinciding with major storm events that caused abrupt morphological changes (Castelle et al., 2015, 2017; Laporte-Fauret et al., 2020). These short-term dynamics are not captured by the LX-ST coupling, which is designed to represent long-term trends. The moderate to high Nash–Sutcliffe Efficiency (NSE) values (median > 0.6) further suggest that the model performs well in simulating decadal shoreline evolution, despite omitting high-frequency processes.

We emphasize that no site-specific calibration was performed for this application. The reported metrics therefore reflect the model's ability to reproduce interannual shoreline evolution without tuning. Despite its reduced complexity and long-term focus, LX-ST shows good agreement with annual dune front positions derived from LiDAR data, suggesting its capability to capture observed trends across the 2014–2023 period.

In addition to assessing shoreline change, we qualitatively evaluated model performance in reproducing dune face evolution using 2023 LiDAR data (Fig. 11a). We focused on the upper dune face (elevation $Z > 5$ m), where the influence of cross-shore processes and short-term hydrodynamics is limited. Model predictions for 2023 were compared with observed topographic profiles along selected transects. Results show a reasonable agreement, with modeled (observed) landward shifts of 22 m (18 m) and 20 m (12 m) (Fig. 11c,e). Although high-resolution, multi-decadal LiDAR data are lacking to validate shoreface dynamics, the model's ability to capture upper dune face retreat provides confidence in its applicability for long-term morphodynamic simulations.

4.3. Results

Fig. 12a shows the final topobathymetry in 2100 from a simulation covering the 2011–2100 period, with the seawall initially aligned with the shoreline (see initial condition in Fig. 11a). Over time, the seawall evolves into a rigid feature protruding seaward within the profile due to chronic erosion, disrupting longshore sediment transport and effectively acting as a groyne. By 2100, three distinct zones emerge: (i) updrift of the seawall, sediment accumulation reduces shoreline retreat and preserves the dune system; (ii) in front of the seawall, the absence of accommodation space leads to intense scouring and complete beach erosion; and (iii) downdrift, limited sediment supply and ongoing erosion cause significant profile lowering and complete dune loss

Fig. 12b illustrates the projected shoreline position under the SSP5–8.5 scenario, showing the 50th percentile (median) and 17%–83% confidence interval. Downdrift of the seawall, maximum retreat exceeds 230 m, with an uncertainty band of 35 m — reflecting the compounded effects of sediment trapping, evolving topobathymetry, and nonlinear feedback captured by the model. Updrift of the seawall, erosion is partially mitigated by sediment accumulation, leading to a narrower envelope (~12 m) and moderate erosion (~110 m).

Cross-shore transects (Fig. 12c–e) provide detailed insights into profile evolution at representative positions downdrift, in front of, and updrift of the seawall. These panels compare the initial profile

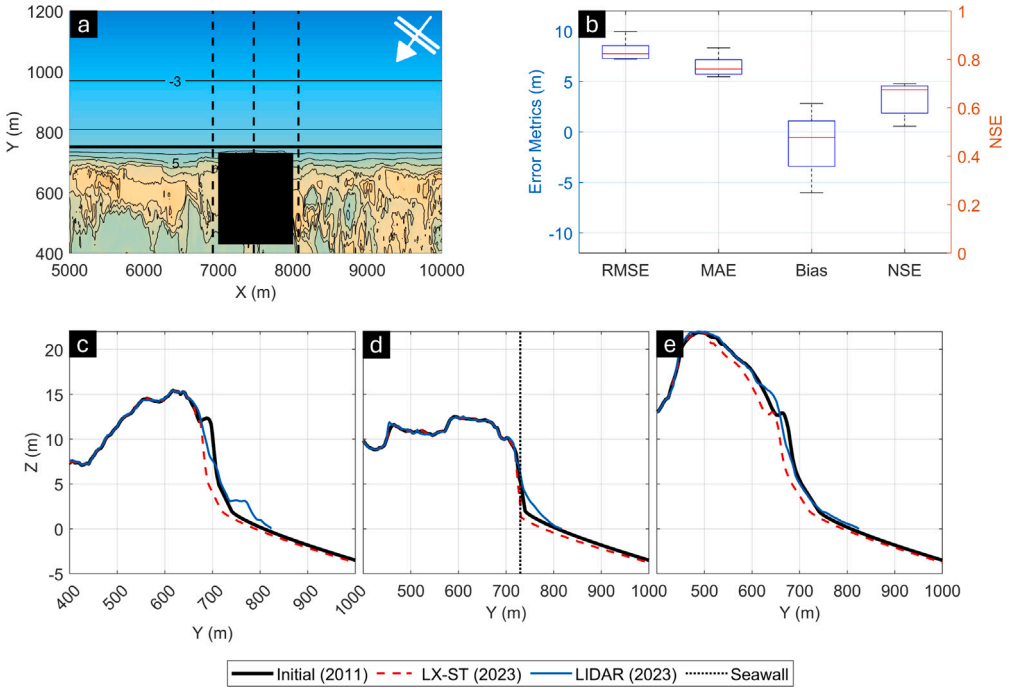

Fig. 11. (a) Initial topobathymetry with validation transects (dashed lines) and seawall location (solid black polygon); (b) Model performance from 2014–2023 based on 10-m contour, aggregated over the 5-km domain: RMSE, MAE, and Bias (left axis), NSE (right axis); (c–e) Cross-shore profiles at downdrift, seawall, and updrift transects showing the 2011 initial state, 2023 model output, and 2023 LiDAR.

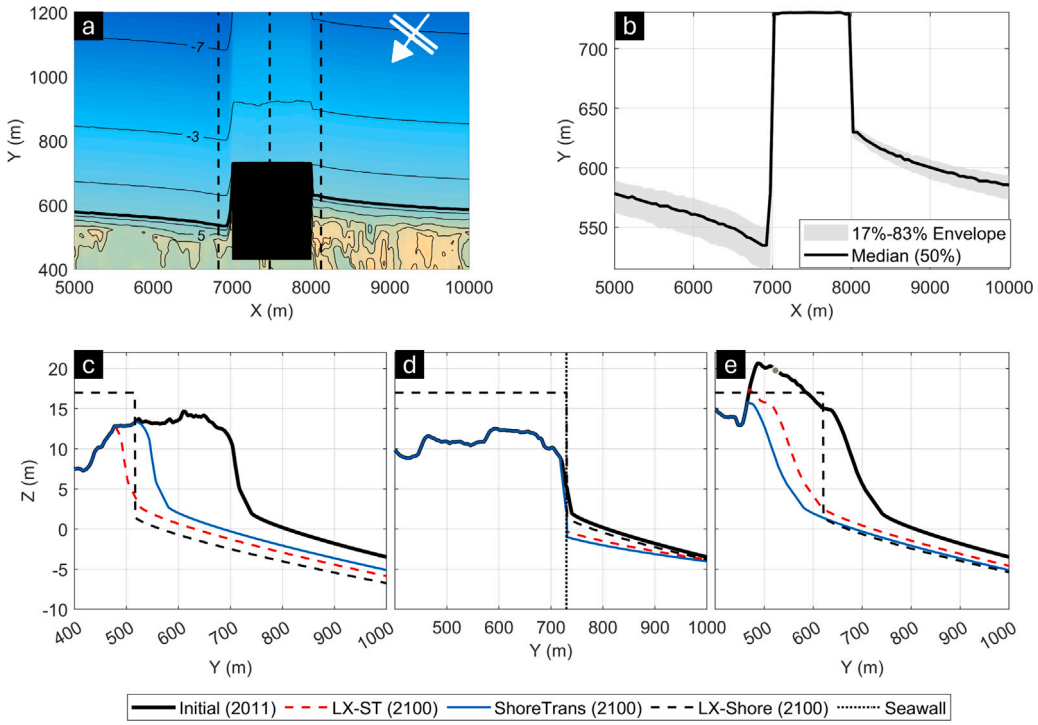

Fig. 12. (a) Final topobathymetry showing cross-shore transects and shoreline orientation; (b) Projected shoreline position in 2100 under SSP5-8.5, showing the median (black line) and 17%–83% confidence envelope (gray shading); (c–e) Cross-shore profile evolution from 2011 to 2100 at the downdrift, seawall, and updrift transects, respectively, comparing the initial topography (2011) with simulated profiles from LX-ST, ShoreTrans, and LX-Shore (with Bruun activated).

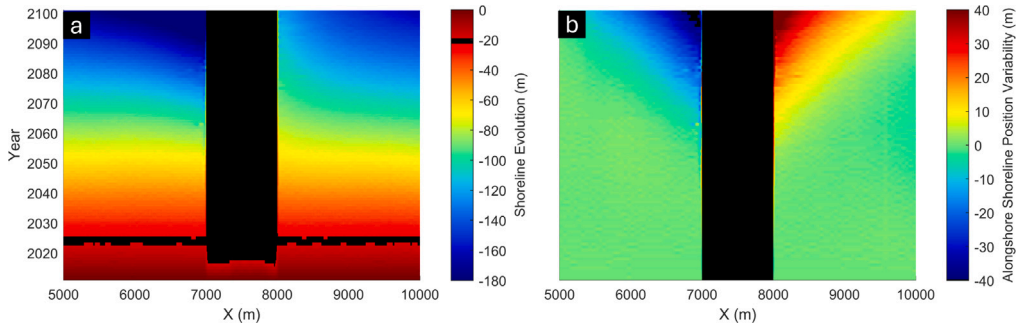

Fig. 13. (a) Shoreline evolution timestack with the -20 m value (seawall position) highlighted in black. (b) Alongshore shoreline position variability, calculated as the deviation of shoreline position from the longshore-averaged shoreline at each time step — the seawall section is masked for clarity.

(2011) with simulations from LX-ST (coupled), ShoreTrans (cross-shore only), and LX-Shore (Bruun). The comparison highlights the necessity of coupling both longshore, erosion and sea-level rise processes to resolve spatially complex morphodynamic responses.

At the updrift transect (Fig. 12e), shoreline retreat is more limited (110 m), and erosion of the upper profile is reduced due to sediment accumulation against the seawall. LX-ST captures both the retreat and the modified profile. Compared to LX-ST, ShoreTrans overestimates retreat as it lacks representation of longshore sediment inputs. LX-Shore underestimates retreat and does not reflect the internal redistribution of sediment across the profile.

At the seawall transect (Fig. 12d), LX-ST simulates localized scouring in front of the structure, leading to the development of a steep nearshore slope, consistent with the expected wall effect. ShoreTrans also reproduces this feature, which arises from the displacement of erosion seaward in the absence of accommodation space. LX-Shore does not resolve this process, as it lacks cross-shore adjustment capability.

At the downdrift transect (Fig. 12c), shoreline retreat exceeds 230 m, accompanied by a broad landward shift of the beach-dune system. LX-ST reproduces both the retreat magnitude and the evolving profile shape. ShoreTrans underpredicts retreat, as it does not account for the reduction in sediment supply due to longshore transport gradients. LX-Shore captures the retreat distance but fails to reflect the accompanying reshaping of the coastal profile.

Fig. 13 further illustrates a two-stage sequence with a clear trajectory shift around 2065 in the current scenario of SLR, chronic erosion, and steady wave climate. Before 2065, erosion remains quasi-uniform alongshore, primarily driven by SLR and sediment deficit, except near the seawall sector. After 2065, erosion progressively intensifies downdrift. This shift coincides with the point at which the updrift shoreline becomes sufficiently eroded that not all sediment bypasses the structure. As a result, less sediment reaches the downdrift area, leading to accelerated erosion in that region.

5. Discussion

5.1. Coupling strategy and benchmark

LX-ST is built around a fully dynamic coupling strategy which combines dynamic transect repositioning with feedback between shoreline evolution and shoreface profile translation. This approach is designed to simulate complex coastal geometries where both shoreline orientation and cross-shore morphology evolve over time. While the present study focuses on simplified configurations, the model structure remains applicable to more complex environments (e.g. rotating embayed beaches, migrating megacusps).

To balance realism and computational demand, LX-ST also includes level 2 and level 1 as simplified alternatives. Level 2 retains shoreline feedback but fixes transect positions, providing a compromise suited for moderately dynamic coastlines with limited curvature change. Level 1 omits both shoreline feedback and dynamic transects, making it computationally efficient but appropriate only for simple, linear coastlines.

Runtime performance reflects the increasing complexity of coupling. Normalizing the computation time of the Lacanau simulations to 100 years per kilometer of the longshore domain, levels 1, 2, and 3 require 0.74 min, 3 min, and 16–20 min, respectively. This flexibility allows users to match model configuration to site-specific morphological complexity and computational constraints. In comparison to other models, LX-ST performs competitively (see Table S1, with runtimes converted to computation time for 100 y/km). GENESIS (Hanson, 1989) is highly efficient but does not include profile coupling and lacks standardized runtime reporting. CoSMoS-COAST (Vitousek et al., 2017) enables rapid regional simulations (0.03–0.04 min per 100 y/km) but omits dynamic bathymetric updates and feedback between shoreline change and wave conditions. IH-LANSloc (Álvarez-Cuesta et al., 2023), which shares conceptual similarities with LX-ST level 2, is physically robust but more computationally demanding. It couples with SWAN for wave propagation, and to reduce runtime, long-term simulations are based on a single SWAN run per year, representing mean wave conditions. With this simplification, runtimes typically reach several hours for 10-year simulations over 1–10 km domains (i.e., up to 10–100 h per 100 y/km). In contrast, LX-ST level 2 uses the Larson formulation (Larson et al., 2010) for wave breaking and completes a 90-year simulation over 15 km in 30 min (3 min/100 y/km). Of course, running LX-ST with SWAN activated in the LX-Shore model would significantly increase the computation time of the LX-ST coupling, but would also allow better representing the wave dynamics (e.g. on rotating embayed beaches).

5.2. Trajectory shift

The future of sandy beaches under sea-level rise remains a subject of active debate. While there is broad consensus on their vulnerability, the literature offers contrasting perspectives on long-term outcomes. For example, Vousdoukas et al. (2020) project widespread shoreline retreat and the potential disappearance of many sandy coasts based on extrapolated trends and global-scale SLR scenarios. In contrast, Cooper et al. (2020) argue that beach survival depends not solely on retreat rates, but also on factors such as beach width and the availability of accommodation space. According to this view, beaches that are backed by dunes capable of rolling landward may persist, while those constrained by hard structures, such as seawalls or cliffs, are at a greater risk of extinction.

These perspectives frame the interpretation of our Lacanau test case, which explores a scenario driven by SLR and a chronic sediment deficit (encroachment mode). LX-ST's approach reveals that erosion patterns are not spatially uniform: the beach fronting the seawall is expected to completely disappear by 2050 due to the lack of accommodation space, consistent with the mechanisms described by Cooper et al. (2020). Meanwhile, the dune system downdrift, although initially resilient, is

already significantly impacted by 2050 and is projected to vanish by the end of the century.

Interestingly, the model captures a noticeable shift in coastal trajectory around 2065, driven by the combined effect of SLR and longshore sediment transport gradients. What starts as a relatively uniform retreat gradually transitions into an acceleration of erosion downdrift of the seawall. This highlights how long-term forcing can lead to nonlinear, location-specific responses. The results also show that dunes and roll-back systems, when unconstrained, remain relatively resilient, reinforcing the importance of available accommodation space in shaping shoreline evolution. While this scenario is not intended as a prediction for Lacanau, it illustrates how the LX-ST coupling can help identify key transitions and feedback in coastal morphology. Rather than aiming for global generalization, the model provides a complementary approach to large-scale assessments like Vousdoukas et al. (2020), offering more detailed insights at local to regional scales.

5.3. Limitations and model assumptions

Several simplifications (in the coupling strategy itself or inherited from ShoreTrans and LX-Shore) constrain the current implementation of LX-ST.

While ShoreTrans permits user-defined cross-shore sediment inputs – such as imposed dune growth rates – it does not internally simulate aeolian transport. As a result, wind-driven sand exchanges between the beach and dunes are not dynamically coupled to modeled beach morphology. This limits LX-ST's ability to capture feedback between beach width, fetch conditions, and dune accretion. In systems where aeolian processes contribute to dune maintenance and post-storm recovery, their exclusion may lead to an underestimation of the system's long-term buffering capacity (Elko et al., 2016). Incorporating a dynamic aeolian transport module that responds to evolving beach-dune geometry and wind forcing is a key direction for future development.

An important simplification of LX-Shore is the assumption of uniform sediment properties, such as grain size and sediment transport parameters. This is a common approach in reduced-complexity models (e.g Vitousek et al., 2017), but it may not hold in settings with significant sediment variability, where spatial changes in grain size could influence transport gradients and shoreline response. Incorporating variable sediment properties into LX-Shore would require substantial changes to the current framework. As a practical alternative, we recommend sensitivity testing where heterogeneity is suspected. For the Lacanau case, sediment characteristics are assumed to be relatively uniform, and targeted sensitivity tests confirm that grain size variations within plausible bounds have limited influence on model results (see Supplementary Material S6).

LX-ST is best suited for sandy, wave-dominated coasts and does not explicitly simulate key processes found in more dynamic environments such as deltaic systems, tidal inlets, or barrier islands affected by overwash and inlet migration. In these cases, more specialized models that resolve tidal flows, inlet morphodynamics, or storm-driven overwash are likely to be more appropriate (Hanson, 1989; Larson et al., 1989). Applying LX-ST to low-energy settings where longshore transport dominates, such as the Great Lakes, could increase its practical relevance. However, this presents challenges. Mean water levels in the Great Lakes can fluctuate by over 1 meter within a few decades, driven by variability in precipitation and evaporation (Gronewold et al., 2013). These relatively fast changes in water level fall outside the assumptions of gradual, long-term sea-level rise embedded in models like ShoreTrans. Addressing this limitation may require smoothing of water level input or adapting the SLR component to better reflect regional hydrological variability. Until then, use of LX-ST in such environments should be done cautiously and with a clear understanding of its constraints.

Currently, the LX-ST coupling uses a fixed time step for updating shoreline and profile positions. While simple and consistent, this approach ignores variations in forcing intensity. Implementing an adaptive time step – triggered by thresholds in shoreline change or sea-level rise – could improve computational efficiency and model stability, focusing resources on high-gradient periods.

Finally, while LX-ST has been applied to synthetic cases and a real beach-dune system (Lacanau), complete model validation remains limited. Without multi-decadal topobathymetric data isolating sea-level rise impacts, long-term validation remains challenging. LiDAR comparisons offer a partial check, but future applications should test the model across diverse settings and forcing scenarios using both planform and profile datasets.

Despite these limitations, LX-ST's modular design allows extension as needed — supporting the integration of dynamic dune modules, probabilistic forcings, or alternative sediment transport formulations. Rather than aiming to represent all processes, LX-ST serves as a flexible framework adaptable to evolving research and management needs. For practical applications requiring insight into both short- and long-term shoreline changes, a first approach could involve combining the LX-ST coupling with satellite or in situ data to estimate short-term statistical characteristics (e.g., daily, seasonal, interannual), which can then be integrated with the long-term projections from LX-ST.

6. Conclusion

This study introduced LX-ST, a modular and computationally efficient framework to simulate coastal evolution over decadal to centennial timescales. LX-ST bridges planform and profile-scale dynamics by coupling the two-dimensional shoreline model LX-Shore with the transect-based profile model ShoreTrans. Through this coupling, LX-ST enables dynamic feedback between longshore sediment transport, evolving shoreline curvature, and shoreface response to sea-level rise.

The framework provides three levels of coupling to accommodate different modeling requirements and computational resources. Level 3, the fully dynamic configuration, updates both shoreline position and transect orientation at each timestep, enabling the model to resolve feedback between evolving shoreline geometry and shoreface response. Level 2 retains shoreline feedback but employs fixed transect positions, representing a computationally efficient compromise for scenarios where changes in shoreline curvature are moderate. Level 1 is the most simplified option, omitting both shoreline feedback and transect updating; it is best suited for idealized or rectilinear shorelines where the effects of feedback are minimal and computational cost is a primary concern.

A suite of synthetic test cases demonstrates that model performance is strongly influenced by the choice of coupling level. In the bulge test case, designed to simulate a shoreline with significant planform variability, only the fully dynamic approach (level 3) accurately captures the feedback between evolving curvature and sediment redistribution. Lower coupling levels either misrepresent local erosion patterns (level 2) or fail to track shoreline realignment altogether (level 1). In contrast, for the seawall test case, where shoreline curvature evolves more modestly, level 2 provides a sufficiently accurate response while reducing computational cost. Finally, in the groyne test case, which primarily involves alongshore redistribution without substantial changes in shoreline geometry, level 1 yields results comparable to higher coupling levels. These findings underscore the importance of adapting the coupling strategy to site-specific morphodynamic complexity. Application to the Lacanau site, using level 2, further demonstrates the framework's capacity to resolve feedback and capture a trajectory shift driven by sea-level rise and sediment trapping updrift of the seawall.

A key next step is to run ensemble simulations with the LX-ST model to explore how uncertainty in sea-level rise and erosion rates affects long-term shoreline change. This will provide a more robust basis for scenario planning, without requiring changes to the existing model framework.

In summary, LX-ST provides a transparent and flexible methodology for coastal morphodynamic modeling, enabling the exploration of long-term shoreline trajectories, the identification of emergent feedback mechanisms, and the formulation of risk-based coastal management strategies in the context of climate change.

CRediT authorship contribution statement

Mohammad Traboulsi: Writing – review & editing, Writing – original draft, Visualization, Validation, Software, Methodology, Investigation, Formal analysis, Data curation, Conceptualization. **Déborah Idier:** Writing – review & editing, Writing – original draft, Validation, Supervision, Software, Resources, Project administration, Methodology, Funding acquisition, Conceptualization. **Bruno Castelle:** Writing – review & editing, Writing – original draft, Validation, Supervision, Software, Resources, Project administration, Methodology, Funding acquisition, Conceptualization. **Arthur Robinet:** Writing – review & editing, Validation, Software, Resources, Methodology, Investigation, Data curation, Conceptualization. **Vincent Marieu:** Writing – review & editing, Validation, Software, Resources, Methodology, Investigation, Data curation, Conceptualization. **Elsa Durand:** Writing – review & editing, Software. **R. Jak McCarroll:** Writing – review & editing, Software.

Code and data availability

The LX-ST code and its core component LX-Shore are not publicly available due to proprietary restrictions but may be shared upon reasonable request. Public release is planned within the next few years to support broader use and collaboration. The original ShoreTrans model is open-source and available at https://github.com/jakmccarroll/ShoreTrans. A Fortran implementation of ShoreTrans, adapted for use within LX-ST, is available at https://github.com/user689/ShoreTrans-fortran. The input data for all test cases, along with the MATLAB function used for shoreline-based topobathymetric interpolation, are publicly archived at https://doi.org/10.5281/zenodo.15586306. Topographic LiDAR data can be accessed through the Observatoire de la Côte de Nouvelle-Aquitaine (OCNA) at https://observatoire-cote-aquitaine.fr, and bathymetric data are available from the SHOM Litto3D database at https://diffusion.shom.fr.

Declaration of competing interest

The authors declare that they have no known competing financial interests or personal relationships that could have appeared to influence the work reported in this paper.

Acknowledgments

This work was carried out in the framework and was funded by Agence Nationale de la Recherche (ANR) grant number ANR-21-CE01-0015 and BRGM. Elsa Durand is funded by an ANRT/CIFRE contract (n° 2021/0579) between Waeles Marine Consultants, Bordeaux University, and BRGM. The authors thank Rémi Thiéblemont (BRGM) for providing the sea level rise projection datasets used for the SSP scenario simulations. ERA5 wave data is produced by the Copernicus Climate Change Service (C3S) at ECMWF. LiDAR topography data were provided by the Observatoire de la Côte de Nouvelle-Aquitaine (OCNA), while bathymetric data were sourced from the Litto3D initiative, a collaboration between the French Hydrographic and Oceanographic Service (Shom) and the French National Institute of Geographic and Forest Information (IGN). The authors gratefully acknowledge the constructive and thoughtful feedback provided by the four anonymous reviewers. Their comments significantly improved the clarity, rigor, and overall quality of this manuscript.

Appendix A. Supplementary data

Supplementary material related to this article can be found online at https://doi.org/10.1016/j.envsoft.2025.106624.

Data availability

I have included a section explaining what data is available and what data needs permission.

References

Akima, H., 1970. A New Method of Interpolation and Smooth Curve Fitting Based on Local Procedures. J. ACM 17 (4), 589–602. http://dx.doi.org/10.1145/321607.321609.

Álvarez-Cuesta, M., Losada, I., Toimil, A., 2023. A nearshore evolution model for Sandy Coasts: IH-LANSloc. Environ. Model. Softw. 169, 105827. http://dx.doi.org/10.1016/j.envsoft.2023.105827.

Antolínez, J.A.A., Méndez, F.J., Anderson, D., Ruggiero, P., Kaminsky, G.M., 2019. Predicting climate-Driven Coastlines with a simple and efficient multiscale model. J. Geophys. Res.: Earth Surf. 124 (6), 1596–1624. http://dx.doi.org/10.1029/2018JF004790.

Ashton, A.D., Murray, A.B., 2006a. High-angle wave instability and emergent shoreline shapes: 1. Modeling of sand waves, flying spits, and capes. J. Geophys. Res.: Earth Surf. 111 (F4), http://dx.doi.org/10.1029/2005JF000422.

Ashton, A.D., Murray, A.B., 2006b. High-angle wave instability and emergent shoreline shapes: 2. Wave climate analysis and comparisons to nature. J. Geophys. Res. 111 (F4), F04012. http://dx.doi.org/10.1029/2005JF000423.

Ashton, A., Murray, A.B., Arnoult, O., 2001. Formation of coastline features by large-scale instabilities induced by high-angle waves. Nature 414 (6861), 296–300. http://dx.doi.org/10.1038/35104541.

Azorakos, G., Castelle, B., Marieu, V., Idier, D., 2024. Satellite-derived equilibrium shoreline modelling at a high-energy meso-macrotidal beach. Coast. Eng. 191, 104536. http://dx.doi.org/10.1016/j.coastaleng.2024.104536.

Booij, N., Ris, R.C., Holthuijsen, L.H., 1999. A third-generation wave model for coastal regions: 1. Model description and validation. J. Geophys. Res.: Ocean. 104 (C4), 7649–7666. http://dx.doi.org/10.1029/98jc02622.

Bruun, P., 1962. Sea-Level Rise as a Cause of Shore Erosion. J. Waterw. Harb. Div. 88 (1), 117–130. http://dx.doi.org/10.1061/JWHEAU.0000252.

Castelle, B., Bujan, S., Ferreira, S., Dodet, G., 2017. Foredune morphological changes and beach recovery from the extreme 2013/2014 winter at a high-energy Sandy Coast. Mar. Geol. 385, 41–55. http://dx.doi.org/10.1016/j.margeo.2016.12.006.

Castelle, B., Dodet, G., Masselink, G., Scott, T., 2018. Increased winter-mean wave height, variability, and periodicity in the Northeast Atlantic over 1949–2017. Geophys. Res. Lett. 45 (8), 3586–3596. http://dx.doi.org/10.1002/2017GL076884.

Castelle, B., Marieu, V., Bujan, S., Splinter, K.D., Robinet, A., Sénéchal, N., Ferreira, S., 2015. Impact of the winter 2013–2014 series of severe Western Europe storms on a double-barred Sandy Coast: Beach and dune erosion and megacusp embayments. Geomorphology 238, 135–148. http://dx.doi.org/10.1016/j.geomorph.2015.03.006.

Castelle, B., Ritz, A., Marieu, V., Nicolae Lerma, A., Vandenhove, M., 2022. Primary drivers of multidecadal spatial and temporal patterns of shoreline change derived from optical satellite imagery. Geomorphology 413, http://dx.doi.org/10.1016/j.geomorph.2022.108360.

Chataigner, T., Yates, M., Le Dantec, N., Harley, M., Splinter, K., Goutal, N., 2022. Sensitivity of a one-line longshore shoreline change model to the mean wave direction. Coast. Eng. 172, 104025. http://dx.doi.org/10.1016/j.coastaleng.2021.104025.

Cooper, J.A.G., Masselink, G., Coco, G., Short, A.D., Castelle, B., Rogers, K., Anthony, E., Green, A.N., Kelley, J.T., Pilkey, O.H., Jackson, D.W.T., 2020. Sandy beaches can survive sea-level rise. Nat. Clim. Chang. 10 (11), 993–995. http://dx.doi.org/10.1038/s41558-020-00934-2.

D'Anna, M., Idier, D., Castelle, B., Vitousek, S., Le Cozannet, G., 2021. Reinterpreting the Bruun Rule in the Context of Equilibrium Shoreline Models. J. Mar. Sci. Eng. 9 (9), 974. http://dx.doi.org/10.3390/jmse9090974.

Davidson, M., Splinter, K., Turner, I., 2013. A simple equilibrium model for predicting shoreline change. Coast. Eng. 73, 191–202. http://dx.doi.org/10.1016/j.coastaleng.2012.11.002.

Davidson-Arnott, R.G.D., 2005. Conceptual model of the effects of sea level rise on Sandy Coasts. J. Coast. Res. 216, 1166–1172. http://dx.doi.org/10.2112/03-0051.1.

Durand, E., Castelle, B., Idier, D., Marieu, V., Robinet, A., Guérin, T., 2024. Influence of Rocky Obstacle Sand Bypassing on Embayed Beach Dynamics Using a Reduced-Complexity Shoreline Model. J. Mar. Sci. Eng. 12 (12), 2266. http://dx.doi.org/10.3390/jmse12122266.

Elko, N., Brodie, K., Stockdon, H., Nordstrom, K., Houser, C., McKenna, K., Moore, L., Rosati, J., Ruggiero, P., Thuman, R., et al., 2016. Dune management challenges on developed coasts. Shore Beach 84 (1), 15–28.

Fenster, M.S., Dolan, R., Morton, R.A., 2001. Coastal Storms and Shoreline Change: Signal or Noise? J. Coast. Res. 17 (3), 714–720, arXiv:4300222.

Garner, G.G., Hermans, T., Kopp, R.E., Slangen, A.B.A., Edwards, T.L., Levermann, A., Nowicki, S., Palmer, M.D., Smith, C., Fox-Kemper, B., Hewitt, H.T., Xiao, C., Aðalgeirsdóttir, G., Drijfhout, S.S., Golledge, N.R., Hemer, M., Krinner, G., Mix, A., Notz, D., Nurhati, I.S., Ruiz, L., Sallée, J.-B., Yu, Y., Hua, L., Palmer, T., Pearson, B., 2021. IPCC AR6 Sea Level Projections. http://dx.doi.org/10.5281/ZENODO.5914709.

Gomez-de La Peña, E., Coco, G., Whittaker, C., Montaño, J., 2023. On the use of convolutional deep learning to predict shoreline change. Earth Surf. Dyn. 11 (6), 1145–1160. http://dx.doi.org/10.5194/esurf-11-1145-2023.

Gronewold, A.D., Fortin, V., Lofgren, B., Clites, A., Stow, C.A., Quinn, F., 2013. Coasts, water levels, and climate change: A Great Lakes perspective. Clim. Change 120 (4), 697–711. http://dx.doi.org/10.1007/s10584-013-0840-2.

Hallermeier, R.J., 1980. A profile zonation for seasonal sand beaches from wave climate. Coast. Eng. 4, 253–277. http://dx.doi.org/10.1016/0378-3839(80)90022-8.

Hanson, H., 1989. GENESIS: A generalized shoreline change numerical model. J. Coast. Res. 1–27, arXiv:4297483.

Hersbach, H., Bell, B., Berrisford, P., Hirahara, S., Horányi, A., Muñoz-Sabater, J., Nicolas, J., Peubey, C., Radu, R., Schepers, D., Simmons, A., Soci, C., Abdalla, S., Abellan, X., Balsamo, G., Bechtold, P., Biavati, G., Bidlot, J., Bonavita, M., De Chiara, G., Dahlgren, P., Dee, D., Diamantakis, M., Dragani, R., Flemming, J., Forbes, R., Fuentes, M., Geer, A., Haimberger, L., Healy, S., Hogan, R.J., Hólm, E., Janisková, M., Keeley, S., Laloyaux, P., Lopez, P., Lupu, C., Radnoti, G., De Rosnay, P., Rozum, I., Vamborg, F., Villaume, S., Thépaut, J.-N., 2020. The ERA5 global reanalysis. Q. J. R. Meteorol. Soc. 146 (730), 1999–2049. http://dx.doi.org/10.1002/qj.3803.

Intergovernmental Panel On Climate Change (Ipcc), 2023. Climate Change 2021 – The Physical Science Basis: Working Group I Contribution to the Sixth Assessment Report of the Intergovernmental Panel on Climate Change, first ed. Cambridge University Press, http://dx.doi.org/10.1017/9781009157896.

Jaramillo, C., De Freitas, L., González, M., Medina, R., 2024. Equilibrium-Based Shoreline Evolution Models to Predict Coastal Response. J. Coast. Res. 116 (sp1), http://dx.doi.org/10.2112/JCR-SI116-128.1.

Jaramillo, C., Jara, M.S., González, M., Medina, R., 2021. A shoreline evolution model for embayed beaches based on cross-shore, planform and rotation equilibrium models. Coast. Eng. 169, 103983. http://dx.doi.org/10.1016/j.coastaleng.2021.103983.

Kamphuis, J.W., 1991. Alongshore sediment transport rate. J. Waterw. Port Coast. Ocean. Eng. 117 (6), 624–640. http://dx.doi.org/10.1061/(asce)0733-950x(1991)117:6(624).

Karunarathna, H., Reeve, D.E., 2013. A hybrid approach to model shoreline change at multiple timescales. Cont. Shelf Res. 66, 29–35. http://dx.doi.org/10.1016/j.csr.2013.06.019.

Kopp, R.E., Garner, G.G., Hermans, T.H.J., Jha, S., Kumar, P., Reedy, A., Slangen, A.B.A., Turilli, M., Edwards, T.L., Gregory, J.M., Koubbe, G., Levermann, A., Merzky, A., Nowicki, S., Palmer, M.D., Smith, C., 2023. The Framework for Assessing Changes To Sea-level (FACTS) v1.0: A platform for characterizing parametric and structural uncertainty in future global, relative, and extreme sea-level change. Geosci. Model. Dev. 16 (24), 7461–7489. http://dx.doi.org/10.5194/gmd-16-7461-2023.

Kumar, L., Afzal, M.S., Afzal, M.M., 2020. Mapping shoreline change using machine learning: A case study from the Eastern Indian coast. Acta Geophys. 68 (4), 1127–1143. http://dx.doi.org/10.1007/s11600-020-00454-9.

Lakku, N.K.G., Chowdhury, P., Behera, M.R., 2024. An improved hybrid model for shoreline change. Front. Mar. Sci. 11, 1459619. http://dx.doi.org/10.3389/fmars.2024.1459619.

Laporte-Fauret, Q., Castelle, B., Marieu, V., Bujan, S., Michalet, R., Rosebery, D., 2020. Coastal Dune Morphology Evolution Combining Lidar and UAV Surveys, Truc Vert beach 2011–2019. J. Coast. Res. 95 (sp1), 163. http://dx.doi.org/10.2112/SI95-032.1.

Larson, M., Byrnes, M.R., Kraus, N.C., Coastal Engineering Research Center (U.S.), Waterways Experiment Station (U.S.), United States, 1989. SBEACH : Numerical Model for Simulating Storm-Induced Beach Change. U.S. Army Engineer Waterways Experiment Station, Vicksburg, Miss, http://dx.doi.org/10.5962/bhl.title.47893.

Larson, M., Hoan, L.X., Hanson, H., 2010. Direct formula to compute wave height and angle at incipient breaking. J. Waterw. Port Coast. Ocean. Eng. 136 (2), 119–122. http://dx.doi.org/10.1061/(asce)ww.1943-5460.0000030.

Luijendijk, A., Hagenaars, G., Ranasinghe, R., Baart, F., Donchyts, G., Aarninkhof, S., 2018. The State of the World's Beaches. Sci. Rep. 8 (1), 6641. http://dx.doi.org/10.1038/s41598-018-24630-6.

McCarroll, R.J., Masselink, G., Valiente, N.G., Scott, T., Wiggins, M., Kirby, J.-A., Davidson, M., 2021. A rules-based shoreface translation and sediment budgeting tool for Estimating Coastal change: ShoreTrans. Mar. Geol. 435, 106466. http://dx.doi.org/10.1016/j.margeo.2021.106466.

Montaño, J., Coco, G., Antolínez, J.A.A., Beuzen, T., Bryan, K.R., Cagigal, L., Castelle, B., Davidson, M.A., Goldstein, E.B., Ibaceta, R., Idier, D., Ludka, B.C., Masoud-Ansari, S., Méndez, F.J., Murray, A.B., Plant, N.G., Ratliff, K.M., Robinet, A., Rueda, A., Sénéchal, N., Simmons, J.A., Splinter, K.D., Stephens, S., Townend, I., Vitousek, S., Vos, K., 2020. Blind testing of shoreline evolution models. Sci. Rep. 10 (1), http://dx.doi.org/10.1038/s41598-020-59018-y.

Nicolae Lerma, A., Ayache, B., Ulvoas, B., Paris, F., Bernon, N., Bulteau, T., Mallet, C., 2019. Pluriannual beach-dune evolutions at regional scale: Erosion and recovery sequences analysis along the Aquitaine Coast based on airborne LiDAR data. Cont. Shelf Res. 189, 103974. http://dx.doi.org/10.1016/j.csr.2019.103974.

Nicolae Lerma, A., Billy, J., Bulteau, T., Mallet, C., 2022. Multi-Decadal Seawall-Induced Topo-Bathymetric Perturbations along a Highly Energetic Coast. J. Mar. Sci. Eng. 10 (4), 503. http://dx.doi.org/10.3390/jmse10040503.

Perez, J., Menendez, M., Camus, P., Mendez, F.J., Losada, I.J., 2015. Statistical multi-model climate projections of surface ocean waves in Europe. Ocean. Model. 96, 161–170. http://dx.doi.org/10.1016/j.ocemod.2015.06.001.

Poumadère, M., Bertoldo, R., Idier, D., Mallet, C., Oliveros, C., Robin, M., 2015. Coastal vulnerabilities under the deliberation of stakeholders: The case of two French sandy beaches. Ocean & Coastal Management 105, 166–176. http://dx.doi.org/10.1016/j.ocecoaman.2014.12.024.

Ranasinghe, R., 2016. Assessing climate change impacts on open Sandy Coasts: A review. Earth-Sci. Rev. 160, 320–332. http://dx.doi.org/10.1016/j.earscirev.2016.07.011.

Ranasinghe, R., Callaghan, D., Stive, M.J.F., 2011. Estimating Coastal recession due to sea level rise: Beyond the Bruun rule. Clim. Change 110 (3–4), 561–574. http://dx.doi.org/10.1007/s10584-011-0107-8.

Robinet, A., Castelle, B., Idier, D., D'Anna, M., Le Cozannet, G., 2020a. Simulating the Impact of Sea-level Rise and Offshore Bathymetry on Embayment Shoreline Changes. J. Coast. Res. 95 (sp1), 1263. http://dx.doi.org/10.2112/SI95-244.1.

Robinet, A., Castelle, B., Idier, D., Harley, M., Splinter, K., 2020b. Controls of local geology and cross-shore/longshore processes on embayed beach shoreline variability. Mar. Geol. 422, 106118. http://dx.doi.org/10.1016/j.margeo.2020.106118.

Robinet, A., Idier, D., Castelle, B., D'Anna, M., Marieu, V., 2020c. LX-Shore user manual, code version 1.0, manual version 1.0.

Robinet, A., Idier, D., Castelle, B., Marieu, V., 2018. A reduced-complexity shoreline change model combining longshore and cross-shore processes: The LX-Shore model. Environ. Model. Softw. 109, 1–16. http://dx.doi.org/10.1016/j.envsoft.2018.08.010.

Rosati, J., Dean, R., Walton, T., 2013. The modified Bruun Rule extended for landward transport. Mar. Geol. 340, 71–81. http://dx.doi.org/10.1016/j.margeo.2013.04.018.

Seenath, A., 2022a. A new approach for incorporating sea-level rise in hybrid 2D/One-Line shoreline models. Sci. Rep. 12 (1), http://dx.doi.org/10.1038/s41598-022-23043-w.

Seenath, A., 2022b. On simulating shoreline evolution using a hybrid 2D/One-Line model. Coast. Eng. 178, 104216. http://dx.doi.org/10.1016/j.coastaleng.2022.104216.

Seenath, A., 2023. A new approach for handling complex morphologies in hybrid shoreline evolution models. Appl. Ocean Res. 141, 103754. http://dx.doi.org/10.1016/j.apor.2023.103754.

Splinter, K.D., Turner, I.L., Davidson, M.A., Barnard, P., Castelle, B., Oltman-Shay, J., 2014. A generalized equilibrium model for predicting daily to interannual shoreline response. J. Geophys. Res.: Earth Surf. 119 (9), 1936–1958. http://dx.doi.org/10.1002/2014jf003106.

Terres De Lima, L., Fernández-Fernández, S., Gonçalves, J.F., Magalhães Filho, L., Bernardes, C., 2021. Development of Tools for Coastal Management in Google Earth Engine: Uncertainty Bathtub Model and Bruun Rule. Remote. Sens. 13 (8), 1424. http://dx.doi.org/10.3390/rs13081424.

Tran, Y.H., Barthélemy, E., 2020. Combined longshore and cross-shore shoreline model for closed embayed beaches. Coast. Eng. 158, 103692. http://dx.doi.org/10.1016/j.coastaleng.2020.103692.

USACE, 1984. Shore Protection Manual. Vol. 1, Vicksburg, Miss, Dept. of the Army, Waterways Experiment Station, Corps of Engineers, Coastal Engineering Research Center, 1984, p. 652.

Vitousek, S., Barnard, P.L., Limber, P., Erikson, L., Cole, B., 2017. A model integrating longshore and cross-shore processes for predicting long-term shoreline response to climate change. J. Geophys. Res.: Earth Surf. 122 (4), 782–806. http://dx.doi.org/10.1002/2016jf004065.

Vousdoukas, M.I., Mentaschi, L., Voukouvalas, E., Verlaan, M., Feyen, L., 2017. Extreme sea levels on the rise along Europe's coasts. Earth' s Futur. 5 (3), 304–323. http://dx.doi.org/10.1002/2016ef000505.

Vousdoukas, M.I., Ranasinghe, R., Mentaschi, L., Plomaritis, T.A., Athanasiou, P., Luijendijk, A., Feyen, L., 2020. Sandy Coastlines under threat of erosion. Nat. Clim. Chang. 10 (3), 260–263. http://dx.doi.org/10.1038/s41558-020-0697-0.

Yates, M.L., Guza, R.T., O'Reilly, W.C., 2009. Equilibrium shoreline response: Observations and modeling. J. Geophys. Res.: Ocean. 114 (C9), http://dx.doi.org/10.1029/2009jc005359.

Zhang, W., Schneider, R., Harff, J., 2012. A multi-scale hybrid long-term morphodynamic model for wave-Dominated Coasts. Geomorphology 149–150, 49–61. http://dx.doi.org/10.1016/j.geomorph.2012.01.019.

Chapter 4

Lacanau Case & Projections

4.1 Preamble **69**

4.2 Introduction **69**

4.3 Study site, models, and methodology **71**

4.3.1 Study site 71

4.3.2 Numerical models 72

4.3.3 Model input 77

4.3.4 Global sensitivity analysis and design of numerical experiments 80

4.4 Results **82**

4.4.1 Coastal projections 82

4.4.2 Global Sensitivity Analysis 87

4.5 Discussion **91**

4.5.1 Added value of combined approaches and lessons learned 91

4.5.2 Limitations and residual uncertainties 92

4.5.3 Implications for coastal management 94

4.6 Conclusion **95**

4.1 PREAMBLE

The work presented in this chapter contributes to the overall objectives of the thesis by applying reduced-complexity shoreline modelling to quantify long-term coastal change under sea-level rise at Lacanau. Building on the LX-ST framework introduced previously, the focus here shifts from method description to application and uncertainty propagation. We combine large ensembles of LX-Shore with targeted LX-ST simulations to examine how uncertain sea-level trajectories to 2100, chronic erosion rates, and alternative barrier response modes interact to shape shoreline and nearshore evolution along a wave-dominated sandy coast with seawall protection.

▸ NOTE This chapter contains the paper currently in preparation: *Traboulsi, M., Idier, D., Castelle, B., Rohmer, J., Thieblemont, R., Nicolae Lerma, A, & D'anna M. (in preparation). Uncertainty quantification of shoreline and nearshore evolution at a wave-dominated sandy coast with seawall protection*. The paper has not yet been submitted or peer-reviewed and is included here in its pre-publication format.

▸ DISCLAIMER The results presented for the Lacanau site are part of a methodological and exploratory research framework. They should not be interpreted as operational projections or used directly for applied studies or coastal management. Their value lies in illustrating modelling approaches, sensitivities, and associated uncertainties, rather than providing precise predictions for local planning or decision-making.

4.2 INTRODUCTION

Sea-level rise (SLR) is accelerating under anthropogenic climate change, with projections ranging from several decimeters to over a meter by 2100 depending on greenhouse gas emissions and ice-sheet dynamics (Fox-Kemper et al. 2021; Kopp et al. 2023a). This acceleration, coupled with the deep uncertainties in future climate forcing, poses a profound challenge for coastal adaptation planning (Hinkel et al. 2019; Stammer et al. 2019). Anticipating future shoreline positions therefore requires not only central estimates, but also a careful accounting of the range of plausible trajectories. Without such an explicit treatment of uncertainty, coastal projections may underestimate the breadth of possible outcomes, potentially leading to maladaptation (Ranasinghe 2020; Cooper et al. 2020; Toimil et al. 2023a).

This issue is particularly relevant for sandy coasts. They represent roughly one-third of the world's ice-free shores and sustain critical socio-economic functions, from tourism and recreation to natural coastal protection (Luijendijk et al. 2018; Ghermandi and Nunes 2013). Yet these systems are increasingly threatened: between 24 % and 33 % of sandy beaches worldwide are already retreating, with large regional contrasts (Mentaschi et al. 2018; Vousdoukas et al. 2020). Under accelerating SLR, both the magnitude and spatial extent of erosion are expected to intensify (Athanasiou et al. 2020;

Thiéblemont et al. 2019). In this setting, quantitative risk assessments of shoreline change are needed to support long-term adaptation decisions. In many urbanized areas, however, artificial structures such as seawalls and groynes further complicate this picture. By disturbing natural sediment pathways on coastlines with strong longshore drift, they can create sharp spatial contrasts between updrift stability and downdrift erosion. In addition, seawalls can directly alter the beach immediately in front of them by limiting accommodation space, which, under a sediment-deficit, can lead to scouring at the structure's toe and eventual beach loss (McCarroll et al. 2021a). As a result, assessing future shoreline evolution requires not only quantifying overall retreat but also capturing these local effects around coastal defenses, since they drive localized hazards and management trade-offs.

Probabilistic shoreline modelling has become a promising way to address this challenge. Reduced-complexity approaches such as one-line models (e.g., Roelvink et al. 2020) and equilibrium cross-shore models (e.g., Splinter et al. 2014) combined with SLR impact model as the one of Bruun (Bruun 1962) provide computationally efficient means to propagate uncertain drivers such as SLR, wave climate, and sediment supply through large simulation ensembles (Ranasinghe et al. 2011; Vitousek et al. 2017). Their efficiency has made them the backbone of most existing probabilistic frameworks (D'Anna et al. 2020; Le Cozannet et al. 2019; Ding et al. 2018; Toimil et al. 2021). However, the same simplification that makes them attractive also defines their main limitation. By representing shoreline change as the displacement of a single contour, these models reduce a fundamentally two-dimensional system to one dimension and therefore do not, or at best only partially, capture the influence of profile shape, coastal structures, or rocky outcrops that often control the spatial variability of shoreline response (D'Anna et al. 2021a; Le Cozannet et al. 2019; Kopp et al. 2023b; Stripling et al. 2017; Xie et al. 2024).

Several approaches have sought to extend probabilistic shoreline modelling by explicitly accounting for shoreface evolution. The Bruun rule relates SLR-driven retreat to the active profile slope, but its accuracy is limited by assumptions on closure depth and uniform translation (Cooper et al. 2020; Cooper and Pilkey 2004). The Probabilistic Coastline Recession model (PCR) improves on this by simulating sediment losses at the dune toe during storms and inter-storm aeolian nourishment of dunes (Le Cozannet et al. 2019; Ranasinghe et al. 2011). More recently, the ShoreTrans model (McCarroll et al. 2021a) introduced a rules-based, volume-conserving framework to simulate cross-shore profile translation and barrier responses, including rollover, encroachment, and the wall effect associated with seawalls. Building on these advances, the coupled LX-ST framework (Traboulsi et al. 2025) integrates ShoreTrans with the alongshore model LX-Shore, enabling two-way feedback between shoreline orientation, cross-shore adjustment, and management constraints such as bypassing and hard structures .

In this study, we examine how uncertain SLR and multi-decadal erosion trends driven by sediment deficit, in the presence of coastal seawalls, shape the long-term evolution of sandy coastlines. To this end, we apply a probabilistic shoreline modelling framework to Lacanau beach, located on the

high-energy coast of southwest France, that has been documented over recent decades (Castelle et al. 2020).

The simulations represent physical baseline conditions, without accounting for future adaptive interventions such as nourishment or managed retreat. This approach isolates the intrinsic response of the coastline under unmanaged conditions, providing a reference against which adaptation strategies can later be evaluated.

Through a variance-based Global Sensitivity Analysis (GSA) (Saltelli et al. 2008), we track how the relative importance of SLR versus long-term sediment deficit shifts over time and space, revealing how uncertainty evolves across different temporal horizons and alongshore locations. Probabilistic projections from the LX-Shore model (Robinet et al. 2018) are compared with deterministic projections from the coupled LX-ST framework (Traboulsi et al. 2025). The results indicate that explicitly coupling shoreline and shoreface dynamics improves the representation of both the magnitude and sources of uncertainty in long-term shoreline change.

The paper is structured as follows: Section 4.3 introduces the study site, models, and methods. Section 4.4 presents the probabilistic shoreline projections and global sensitivity analysis. Section 4.5 discusses the implications for coastal risk assessment and adaptation planning, before drawing conclusions in Section 4.6.

4.3 STUDY SITE, MODELS, AND METHODOLOGY

4.3.1 Study site

Lacanau lies on the central Gironde coast of southwest France (Figure 4.1), along the meso–macrotidal Atlantic shoreline of Aquitaine. It is among the most energetic sandy coasts in Europe, with a tidal range exceeding 4 m during spring tides and persistent exposure to North Atlantic swells. The site combines high natural forcing (monthly mean wave heights range from 1.1 m in summer to 2.4 m in winter), with chronic erosion, a densely urbanized seafront (about 1,200 homes in the vulnerability area), and several coastal monitoring programs (Castelle et al. 2018b; Nicolae Lerma et al. 2019; Nicolae Lerma et al. 2022). The beach is characterized by a double sandbar system, while the dune crest reaches 15–20 m NGF, i.e. relative to the French national vertical datum (Nivellement Général de la France, IGN69). Since the late 19th century, vegetation planting and dune stabilization have progressively reduced dune mobility, constraining their natural role in buffering erosion (Nicolae Lerma et al. 2022). The central urbanized sector of Lacanau is fronted by a 1.2 km seawall, originally built in the 1970s and reinforced after the extreme 2013/2014 winter storms (Nicolae Lerma et al. 2022). The structure has been effective in protecting the seafront from landward erosion. However, it has also been associated with beach lowering and persistent narrowing in front of the wall, together with reduced seasonal variability of the beach profile (Nicolae Lerma et al. 2022).



Figure 4.1: (a) Location of the study site at Lacanau (red box) on the Aquitaine coast, situated between the Gironde Estuary and the Arcachon Lagoon, with the offshore Candhis wave buoy also indicated. (b) Top view of Lacanau beach and the seawall (photo by V. Marieu).

Previous studies indicate that Lacanau undergoes a persistent sediment deficit, which manifests as chronic shoreline retreat. Historical reconstructions show mean retreat rates of 0.3–0.5 m/y from 1875 to 1967, increasing to 0.5–1.5 m/y over 1 966–1 998 (Nicolae Lerma et al. 2022). These long-term trends, result from alternating phases of rapid erosion during severe winters and multi-annual recovery, reflecting the capacity of the beach–dune system to partially rebuild after high-energy events and maintain a degree of morphodynamic resilience. In the present work, we used the 1 964–2 014 shoreline (defined as the dune foot) dataset of Castelle et al. (2018b) derived from historical photograph along a 15 km strech of coast around Lacanau, but excluding the seawall section. Fig. 4.2 shows the alongshore median rates, with the grey band indicating the 95 % confidence intervals from the individual transect fits. To test for systematic alongshore variation, we performed a linear regression of shoreline retreat rate against alongshore distance over the 15 km domain. The resulting gradient (≈0.022 m/y/km) is negligible, indicating no significant alongshore trend. Consequently, the background erosion is treated as spatially uniform across the study area.

4.3.2 Numerical models

Predicting shoreline change over long time scales requires models that capture both the effect of SLR and gradients in longshore sediment transport. To this end, we apply two complementary approaches: LX-Shore (Robinet et al. 2018; Durand et al. 2024), a grid-based one-line shoreline model that resolves alongshore transport gradients and account for SLR using the Bruun model, and LX-ST (Traboulsi et al. 2025), which dynamically couples LX-Shore with the cross-shore shoreface model ShoreTrans (McCarroll et al. 2021a) to represent profile adjustment under SLR. The use of

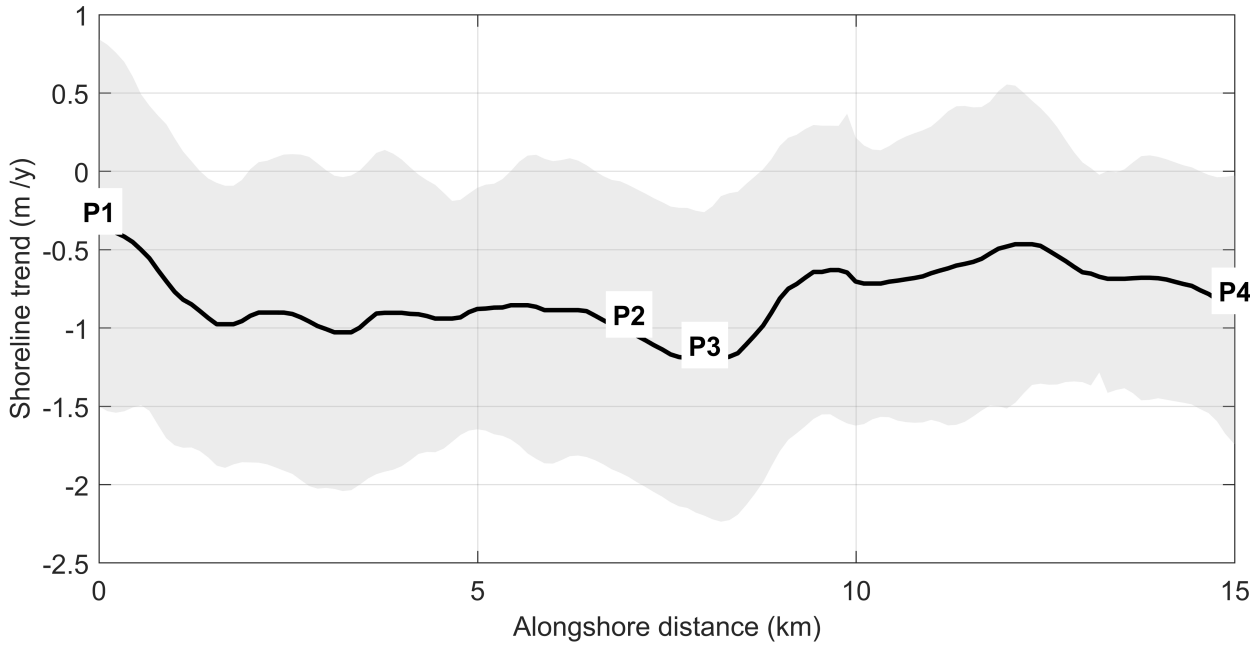

Figure 4.2: Alongshore retreat rates from robust linear fits of dune-foot position. The black line is the median; the shaded band shows the 95% confidence interval. Reference points P1 (0 km), P2–P3 (seawall), and P4 (15 km) match Fig. 4.1a

both models allows exploring coastal response to the concurrent action of alongshore redistribution and long-term cross-shore translation.

At the time scales considered here, short-term wave-driven cross-shore shoreline variability is not explicitly resolved and is instead assumed to average out relative to the cumulative effects of SLR-induced translation and alongshore sediment gradients. In the present study, we rely on the model setups developed by Traboulsi et al. (2025), which have been applied to Lacanau and shown to reproduce multi-decadal shoreline and nearshore changes with fair skill, supporting their suitability for the present uncertainty analysis.

The beach representative grain size is 220 µm, with a porosity of 0.4. Both models are run over a uniform 50 m grid extending 15 km longshore and 2.5 km cross-shore, and consider a fixed berm at 17 m. In the LX-ST setup, simulations use a yearly shoreline update and a morphological time step of 1 day, and the depth of closure is dynamically updated each year using the Hallermeier (1980) formula. The LX-Shore and LX-ST models and the respective setup are described in the following subsections.

LX-Shore

LX-Shore is a reduced-complexity shoreline model designed to simulate planform evolution of sandy coasts on scales of hundreds of meters to tens of kilometers, and timescales ranging from years to centuries (Robinet et al. 2018). It builds on the family of grid-based one-line models developed to represent longshore sediment transport gradients (e.g., Ashton et al. (2001)), enabling flexible representation of diverse shoreline morphologies, including spits, embayments, cuspate forelands,

and human-made structures. The shoreline is discretized into cells characterized by a sediment fraction, allowing the model to represent both erodible and non-erodible regions within the same grid.

In LX-Shore, wave-driven shoreline change from longshore sediment transport gradients is computed using empirical transport formulas such as Kamphuis (1991) and CERC (Coastal Engineering Research Center (U.S.) 1984). SLR-induced retreat can be incorporated and estimated as the cross-shore translation of the beach profile according to the Bruun (1962) model. Because of its computational efficiency, LX-Shore is particularly suited for large ensembles and probabilistic analyses of shoreline evolution (Robinet et al. 2018; D'Anna et al. 2020).

LX-Shore effectively simulates alongshore sediment redistribution and handles complex shoreline geometries. While developed in two dimensions, the one-line nature of the model imposes a simplified topo-bathymetric representation: inland cells are assumed to have a uniform elevation, which prevents the model from explicitly resolving the full extent of the shoreface. In this study, we switch off short-term cross-shore change to isolate multi-decadal trends (Fenster et al. 2001), which is a modelling choice, not an intrinsic limitation of LX-Shore. The model version used here includes the full bypassing (FB) formulation of Durand et al. (2024), which extends the original shoreline bypassing scheme by allowing sediment transport to occur within and seaward of the surf zone, up to the closure depth. This option is adopted to represent seawall-controlled sediment continuity at Lacanau. SLR is accounted for using a Bruun-type shoreline translation (Bruun 1962). This parameterization, together with the lack of an explicit shoreface, means that processes such as dune rollover and structure-induced scour are not reproduced within LX-Shore, which motivates the use of the coupled LX-ST configuration.

LX-ST

To overcome the limitations of LX-Shore in Shoreface modelling and translation, LX-ST was developed as a modular coupling framework linking LX-Shore with the ShoreTrans model (Traboulsi et al. 2025). ShoreTrans is a rules-based, one-dimensional profile model that simulates SLR-driven shoreline retreat and shoreface translation while conserving sediment volume (McCarroll et al. 2021a). It distinguishes between different dune response mechanisims to SLR such as rollover, encroachment, or wall effects in the presence of hard defenses (Fig. 4.4), providing a more realistic representation of long-term sediment balance than the Bruun rule. With respect to LX-Shore, LX-ST associates an increased computational time, limiting ensemble based modelling applications.

The coupled LX-Shore and ShoreTrans model (LX-ST) capture both alongshore and cross-shore long-term dynamics: LX-Shore models the evolving shoreline planform and provides longshore transport gradients, while ShoreTrans updates the cross-shore profiles based on these gradients and SLR. This results in a two-way feedback where shoreline curvature controls longshore transport patterns and sediment redistribution, while the evolving profiles in turn influence shoreline position

(Fig. 4.3). The coupling operates on three levels, from fixed transects with no feedback (level 1) to fully dynamic transects that continuously adjust to remain orthogonal to the changing shoreline (level 3) . Here we use a level 2 coupling in which cross-shore profiles evolve in response to sediment fluxes, while the transect positions remain fixed in time rather than being updated to follow changes in shoreline curvature. This assumption is appropriate for the relatively straight coastline of the study site and avoids introducing additional complexity associated with time-varying transect reorientation.

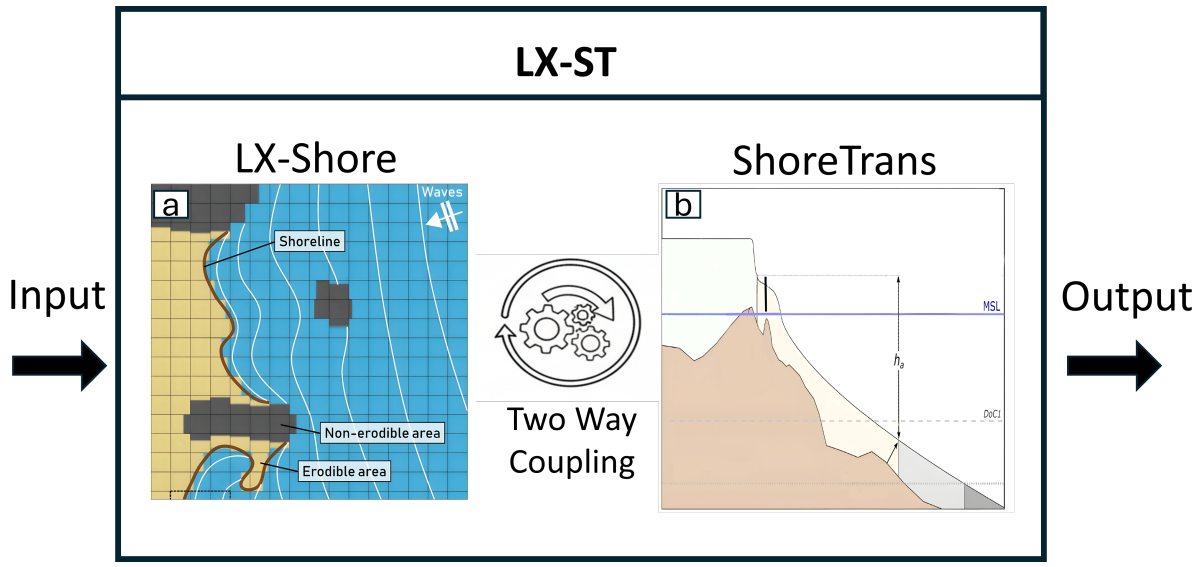

Figure 4.3: Conceptual diagram of the LX-ST framework, which couples the plan-view shoreline model LX-Shore (Robinet et al. 2018) with the cross-shore profile model ShoreTrans (McCarroll et al. 2021a). Inputs such as waves, SLR, and erosion rates drive the coupled simulations, while outputs include shoreline position, and topobathymetry.

Dune response modes in LX-ST

Beach–dune systems can exhibit fundamentally different responses to SLR, characterized by two contrasting modes of morphodynamic adjustment: rollover and encroachment (Cowell and Thom 1995; McCarroll et al. 2021a). These modes represent end-member behaviors that introduce significant structural uncertainty into long-term coastal evolution projections, with implications for dune preservation and coastal management strategies. Rollover tends to occur along low dune coasts with gentle hinterland slopes and ample accommodation space, where sediment can move freely landward. Encroachment, by contrast, dominates on steep or highly vegetated dunes, or where the hinterland is elevated or constrained by hard boundaries such as cliffs, seawalls, or urban areas.

In the rollover mode, sediment is transferred landward through overwash and/or aeolian transport during high-water events, allowing the entire beach–dune profile to migrate inland while broadly conserving its sediment volume (Rosati et al. 2013). Material eroded from the shoreface is redeposited behind the foredune, enabling the system to accommodate rising sea levels through coordinated onshore translation (Fig. 4.4).

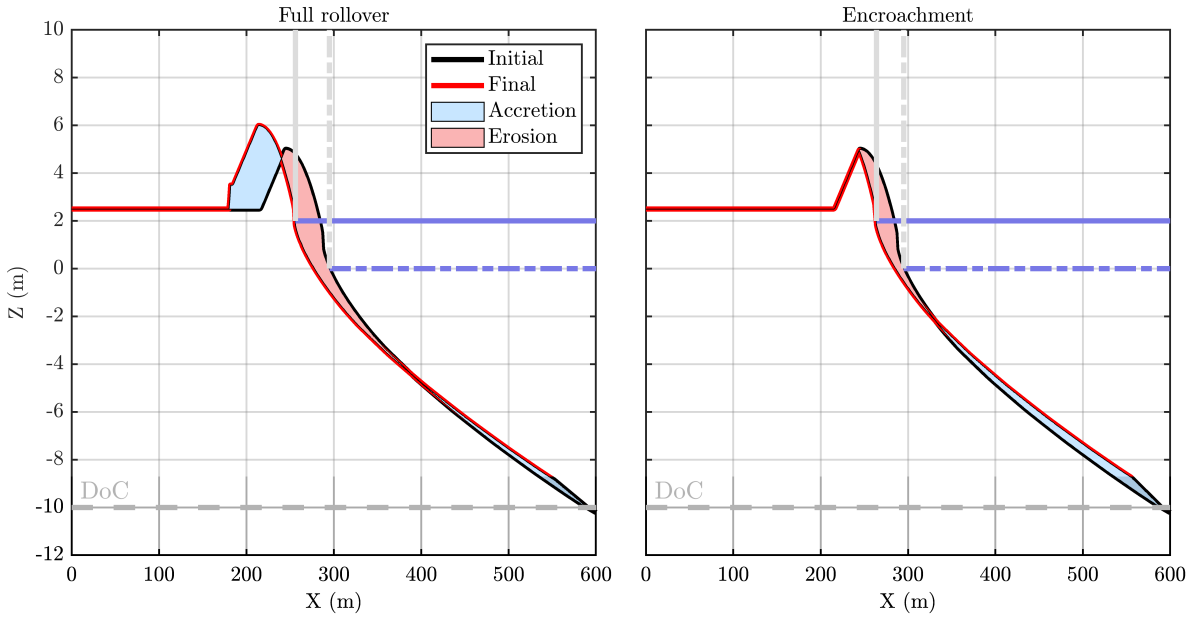

Figure 4.4: Schematics of two ShoreTrans dune response types for (a) full rollowver and (b) encroachment. Accretion (red), erosion (blue), initial/final mean sea levels (blue) are indicated, and Doc indicates the depth of closure.

Within the ShoreTrans framework (McCarroll et al. 2021a), this behavior encompasses several rollover modes. These include low-barrier overwash rollover, typically associated with low, frequently overtopped barriers, and dune–beach rollover, in which inland migration mainly occurs through aeolian processes on higher dunes with limited vegetation or fixation. The latter can therefore take place even for relatively high foredunes, provided sediment continuity is maintained and the hinterland offers sufficient accommodation space.

In the encroachment mode, the dune crest remains largely fixed while the shoreface continues to erode seaward. This occurs when the backshore is steep, elevated, physically constrained, or when dense vegetation stabilizes the dune and inhibits aeolian transport, preventing landward migration. Thus the shoreline retreats without equivalent dune translation, leading to progressive narrowing of the active beach and reduction in the system's capacity for adjustment.

These contrasting behaviors yield distinct morphodynamic outcomes. Rollover typically produces shoreline recession greater than predicted by the Bruun rule but maintains beach width through landward translation. Instead, encroachment results in retreat closer to Bruun-type estimates, with the shoreline effectively pinned against fixed topographic or artificial boundaries. Accurately representing both modes remains essential for reducing uncertainty in long-term shoreline evolution modelling.

4.3.3 Model input

Waves

For the present work, offshore wave conditions were extracted from ERA5 (Hersbach et al. 2020) at a grid point located offshore of Lacanau (approximately 50 m water depth, 44.5° N, −1.5° E, Fig. 4.1a). Waves come mostly from the west-northwest, with pronounced seasonal variability. Monthly mean significant wave height ranges from about 1.1 m in summer to 2.4 m in winter, with extremes exceeding 10 m during severe storms. Peak wave periods vary between 8.5 s in July and 13 s in January. This energetic wave climate drives intense longshore sediment transport rates (Idier et al. 2013), and the resulting large-scale alongshore gradients largely explain the chronic erosion observed along the coastal stretch around Lacanau (Castelle et al. 2022).

Hourly wave data (significant wave height, peak period, and mean direction) are extracted for the period 2 011–2 024 (replicated until 2100 as shown in Fig. 4.5). To construct future forcing, we assume wave-climate stationarity at centennial scales and replicate the ERA5 chronology to 2100. This choice reflects the working hypothesis that, for highly energetic coasts such as Aquitaine, long-term shoreline trajectories are primarily controlled by SLR and chronic erosion. Accordingly, the wave climate is assumed stationary, as projected changes in wave characteristics for this region remain moderate compared to the cumulative effects of SLR and sediment imbalance at multi-decadal time scales. While some studies suggest a small decrease in mean wave height over the twenty-first century (e.g. Charles et al. 2012c; Morim et al. 2019), recent analyses focusing on extreme wave conditions indicate no robust long-term trends for the Aquitaine coast (Lobeto et al. 2021), supporting the relevance of this simplifying assumption for the present analysis.

Sea-level rise

Sea-level rise projections were extracted from the NASA/IPCC AR6 Sea Level Projection Tool (NASA 2023) at the Lacanau nearest grid point, considering three representative scenarios: SSP2–4.5 (moderate), SSP5–8.5 (high), and a high-end case corresponding to the 83rd percentile of SSP5–8.5. The latter does not represent a distinct probabilistic scenario but the upper bound of the likely range, used to explore low-probability, high-impact outcomes linked to uncertain ice-sheet processes.

The projections were originally provided relative to a fixed geoid, without correction for land motion. To express sea-level change relative to the local coastline, a Glacial Isostatic Adjustment (GIA) correction was applied using the Bayesian model of Caron et al. (2018), which combines GPS and relative sea-level observations to infer present-day vertical land motion. At Lacanau, this correction indicates a slow subsidence of approximately 0.25 mm/y, which was added to the projections to obtain land-relative SLR.

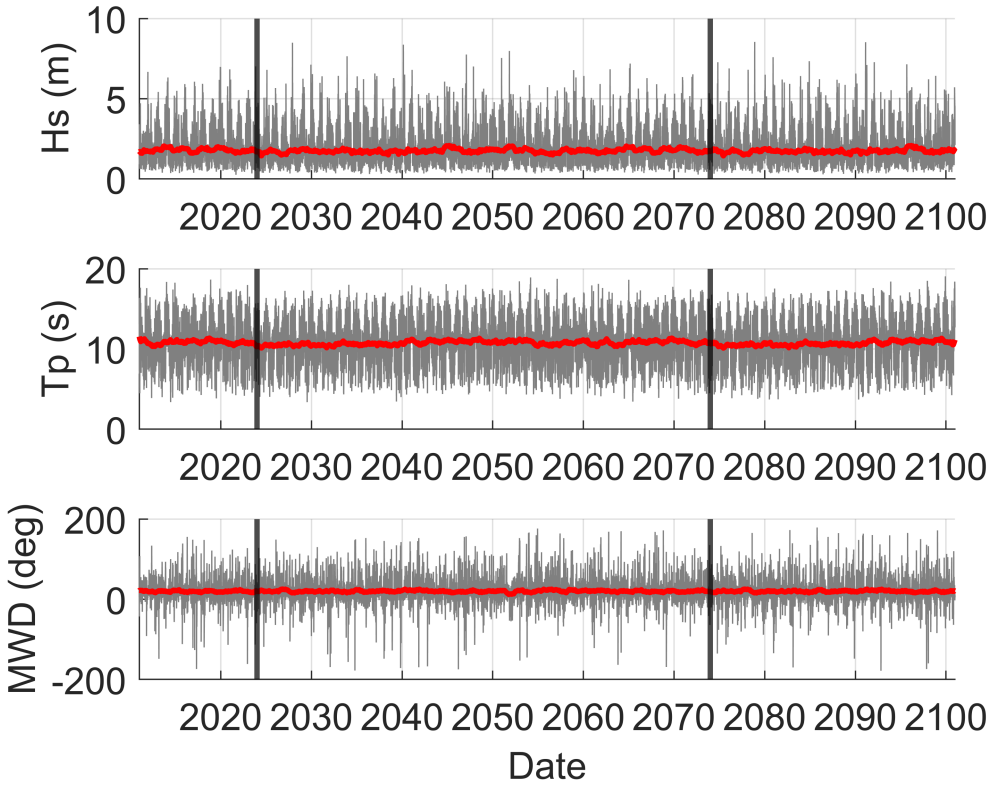

Figure 4.5: Time series of significant wave height (H_s), peak period (T_p), and mean wave direction (MWD) from ERA5 (1940–2024), extended to 2100 by duplication with a one-week smoothing window. The red line represents the moving mean. Vertical bands indicate duplication boundaries. MWD is expressed in local coordinates relative to the shore-normal.

The NASA/IPCC dataset provides annual probability distributions of sea-level change from 2010 to 2100, derived from quantile curves combining process-based model ensembles with expert assessment. These distributions include a well-constrained core, reflecting contributions from thermal expansion, glacier melt, and ice-sheet surface mass balance, and a high-end tail associated with low-confidence Antarctic instability scenarios. The discontinuity visible in the quantile structure (Fig. 4.6b) results from joining these two information sources, illustrating that extreme outcomes represent distinct, poorly constrained processes rather than a continuous extension of the central distribution. Consequently, the AR6 distributions cannot be approximated by a single Gaussian law (Kopp et al. 2023b; Kopp et al. 2023a). Annual series were reconstructed by interpolating the quantiles, ensuring monotonicity and preservation of the skewed, non-Gaussian behaviour of the projections.

Background shoreline retreat rate

As a prerequisite to defining model inputs, a dedicated shoreline analysis was conducted to quantify the long-term background retreat rate and derive its statistical distribution for the simulations. Beyond SLR, shoreline change at Lacanau reflects a persistent erosive signal driven by large-scale sediment deficit mostly due to alongshore gradients of longshore drift in the Lacanau area (Castelle

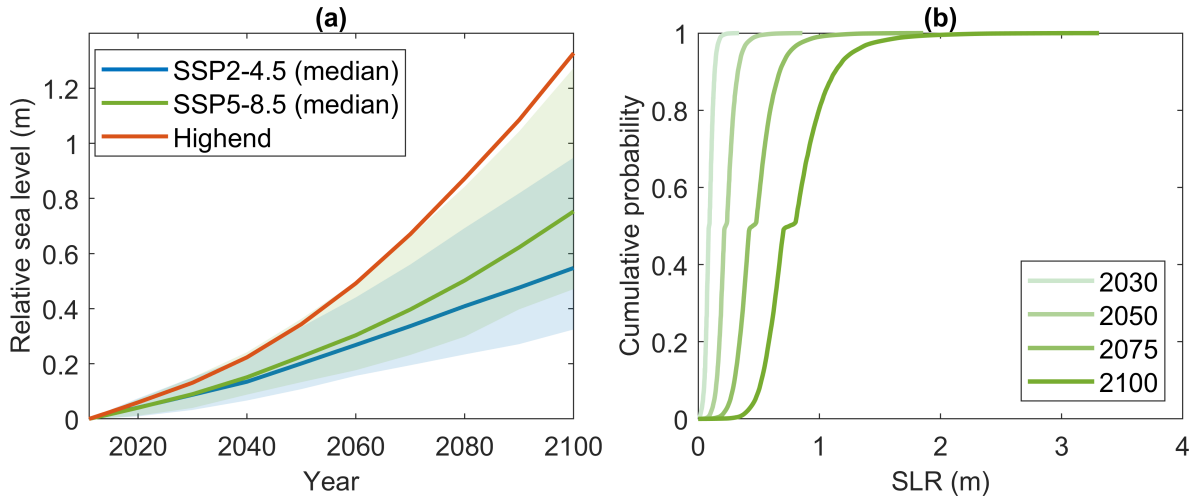

Figure 4.6: Sea-level rise scenarios at Lacanau. (a) Probabilistic trajectories for SSP2-4.5, SSP5-8.5, and the high-end scenario, showing 5–95% percentile ranges (shaded) and central estimates. (b) Example annual distributions for SSP5-8.5 in selected years, expressed as cumulative distribution functions (CDFs).

et al. 2022), which is not compensated by significant sediment supply. As a consequence, shoreline retreat persists even where the direct influence of SLR is limited, underlining the need to treat sediment budget constraints as an independent source of long-term uncertainty. To quantify this

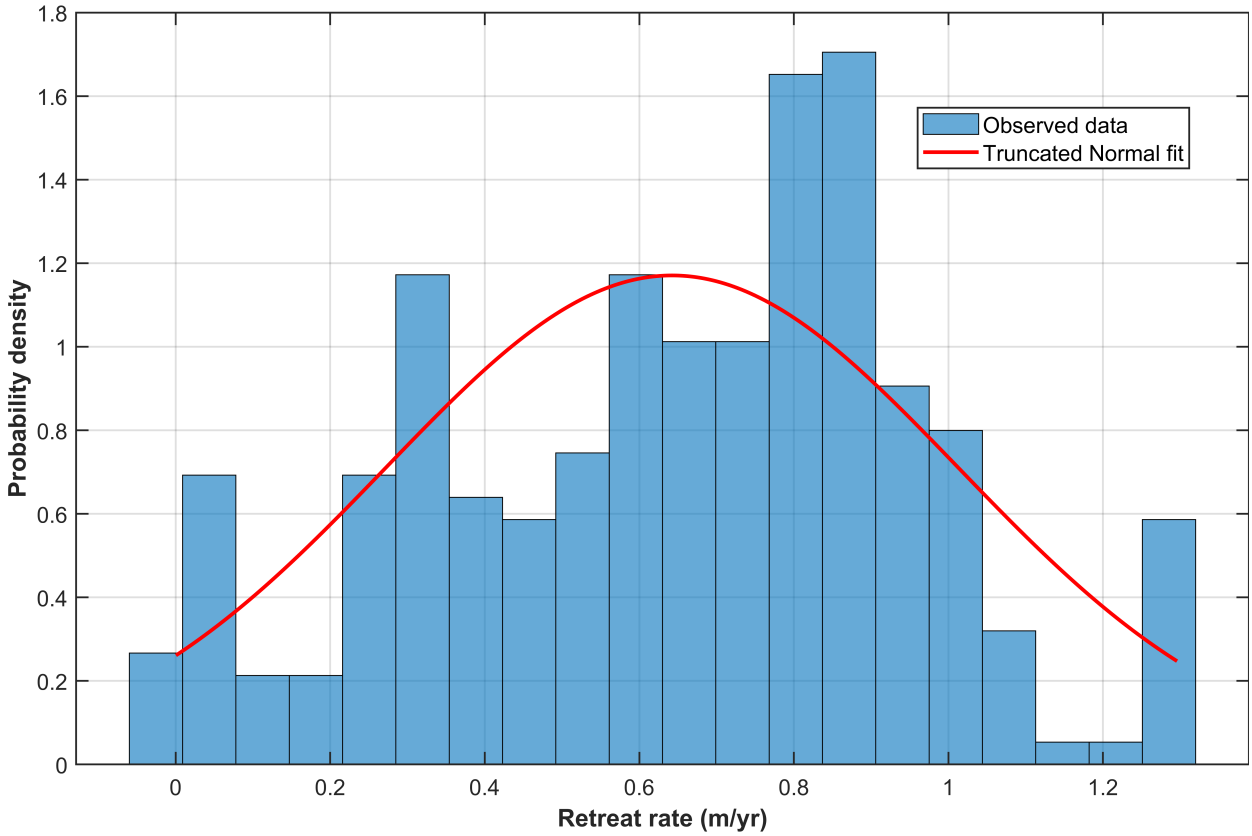

Figure 4.7: Distribution of background erosion rates at Lacanau derived from regression analysis of historical shoreline trends. Slopes were adjusted by subtracting the SLR contribution. The red curve shows the fitted truncated normal distribution.

chronic component, historical shoreline positions between 1950 and 2014 (Castelle et al. 2018b) were analyzed using linear regression, providing a robust measure of long-term retreat distinct from

short-term variability. The observed regression yielded an average erosion of ≈0.75 m/y (Fig. 4.2). The contribution of historical SLR over the same period was estimated using the Bruun-rule (1962), which indicated 0.11 ± 0.01 m/y of retreat attributable to SLR. This modest contribution confirms that the persistent shoreline recession at Lacanau cannot be explained by SLR alone, but rather reflects a dominant influence of regional sediment deficit and longshore transport imbalance.

This corrected distribution was modeled as a truncated normal distribution (Fig. 4.7), with bounds 0.00–1.30 m/y corresponding to the observed range of erosion. The fitted parameters are $\mu = 0.64\,\text{m/y} \pm 0.05\,\text{m/y}$ and $\sigma = 0.37\,\text{m/y} \pm 0.06\,\text{m/y}$. A Kolmogorov–Smirnov test (Feller 1948) confirmed the statistical consistency of this fit ($p = 0.071 > 0.05$). The truncated normal distribution therefore provides a simple yet adequate representation of the bulk observations while enforcing physically meaningful limits at the tails. This probabilistic characterization of chronic erosion was used as an input parameter in the GSA.

4.3.4 *Global sensitivity analysis and design of numerical experiments*

Global sensitivity analysis and Sobol' indices

Numerical simulations of shoreline change inherit uncertainties from input variables and their interactions. To quantify the relative importance of these uncertainties, a variance-based GSA was applied using first-order Sobol' indices (Sobol 2001; Saltelli et al. 2008). The principle of GSA is to propagate uncertain inputs through the model to obtain an ensemble of outputs and to decompose the results variance into partial contributions associated with each input and their interactions. This approach provides a systematic mean to identify which uncertain input variable contributes the most to model results, and has previously been applied to analyze uncertainties in long-term cross-shore evolution (D'Anna et al. 2020; D'Anna et al. 2021a; D'Anna et al. 2022) and longshore (**kroon_ranking_2020**) modelling studies.

For a given uncertain input variable X_i, the first-order Sobol' index S_i measures the share of output variance explained by X_i alone, assuming that the input variables are statistically independent, which is the case here:

$$S_i = \frac{\text{Var}\big(\mathbb{E}[Y \mid X_i]\big)}{\text{Var}(Y)}, \tag{4.1}$$

where Y is the simulated shoreline position, Var denotes variance, and $\mathbb{E}$ the conditional expectation. Intuitively, S_i expresses how much uncertainty would be reduced if X_i were fixed to its true value.

The First-order Sobol' indices were computed using the modularized sample-based method of Li and Mahadevan (2016), which estimates sensitivity measures directly from existing input–output populations without requiring additional model evaluations. The method separates the input sam-

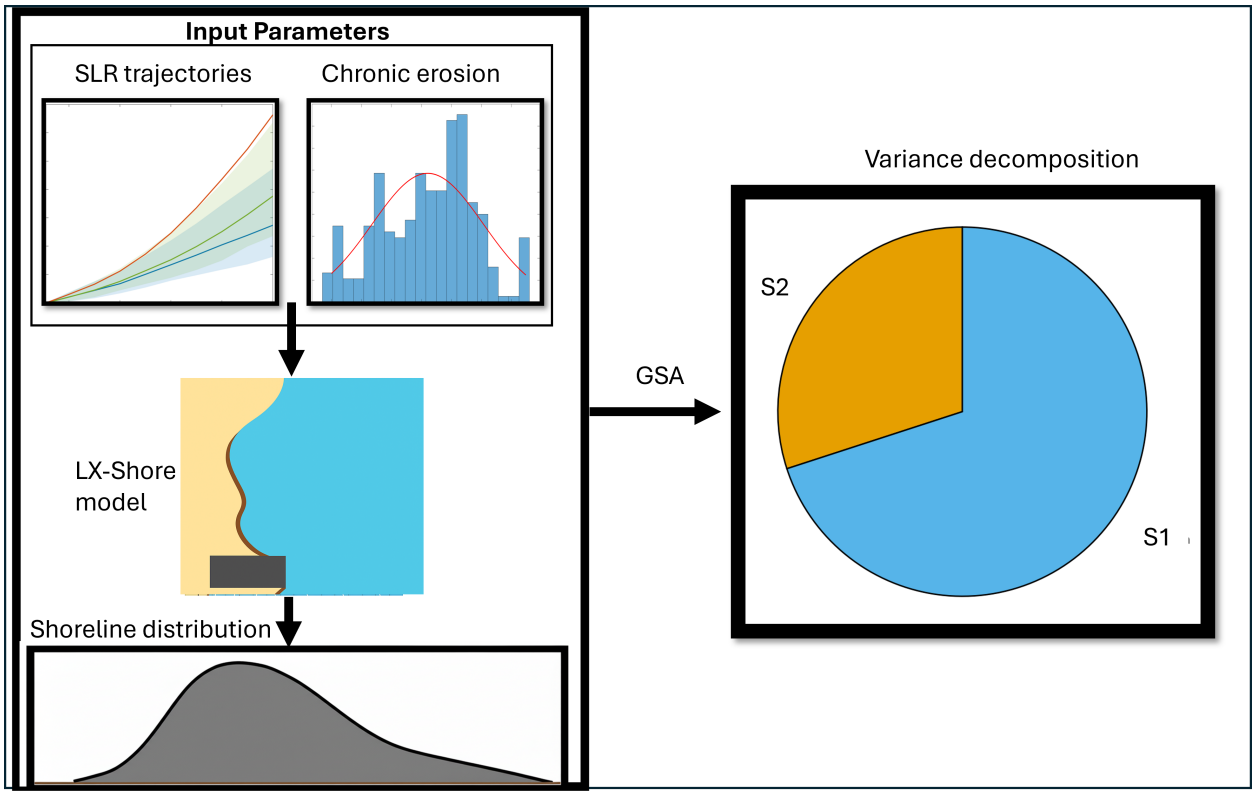

Figure 4.8: Illustration of the global sensitivity analysis (GSA) applied to Lacanau (LX-Shore simulations only). Variance decomposition of shoreline projections is performed for each simulation year based on uncertainties in SLR trajectories and background erosion rates.

pling, model evaluation, and index calculation steps, and remains valid even for correlated inputs, making it particularly suitable for post-processing structured quasi-random ensembles.

General objective

Three climate-forcing scenarios (SSP2-4.5, SSP5-8.5, and a high-end case) were analyzed independently. Within each scenario, two uncertain inputs were propagated through the model: (a) sea-level rise (SLR) trajectories derived from probabilistic NASA/IPCC AR6 distributions (Garner et al. 2023) and (ii) background shoreline retreat rates representing long-term sediment deficit, represented by a truncated normal distribution. All simulations covered the period 2011–2100 (89 years).

Sensitivity tests performed during the Lacanau model setup (Traboulsi et al. 2025) indicated that variations in sediment size within the observed range had negligible influence on century-scale shoreline retreat. Likewise, because wave climate is assumed stationary over the projection horizon, no significant change in the depth of closure is expected. For these reasons, the explicit uncertainty propagation and subsequent GSA were limited to SLR and background erosion rate. The Sobol-based analysis was thus applied separately within each SSP scenario rather than across them.

Design of numerical experiments

The design of numerical experiments distinguishes between two complementary modelling approaches. LX–Shore simulations provide a large probabilistic ensemble suitable for variance-based sensitivity analysis, while LX–ST simulations form a limited factorial set used to explore structural responses beyond the one-line representation.

▸ LX-Shore ensemble design In the LX-Shore simulations, input combinations of SLR and chronic erosion were sampled jointly using a Sobol' quasi-random sequence with Matousek–Affine–Owen scrambling (Hong and Hickernell 2003). Sobol sequences provide low-discrepancy coverage of the input space, reducing clustering and improving the efficiency of uncertainty propagation compared with purely random Monte Carlo draws. Scrambling further avoids deterministic alignment patterns that may bias variance estimates, enhancing robustness when ensemble sizes are finite (Sobol 2001; Sun et al. 2021). This design produced approximately 20,000 simulations (10,000 per SSP scenario), each yielding an annual shoreline trajectory over 2011–2100, and provided converged estimates of both probabilistic envelopes and Sobol sensitivity indices.

▸ LX-ST factorial design In contrast to the Sobol-based sampling used for LX-Shore, LX-ST simulations followed a factorial design to explicitly address structural uncertainties absent from the reduced-complexity framework. Three climate forcing scenarios (SSP2-4.5, SSP5-8.5, and a high-end case) were combined with two alternative dune response modes (rollover and encroachment). Within each scenario–mode combination, nine simulations were run using the 17th, 50th, and 83rd percentiles of both SLR and chronic erosion. The 17th and 83rd percentiles represent the "likely range" of outcomes in the IPCC framework, corresponding to an approximate 66 % probability interval (Fox-Kemper et al. 2021; Kopp et al. 2023b). This factorial design generated 38 simulations in total, producing a matrix of contrasting trajectories for shoreline position, dune crest elevation, and beach width under alternative assumptions about forcing conditions and coastal response.

Together, the two experimental designs are complementary: the LX-Shore simulation experiments aim at capturing a wide probabilistic range of parametric uncertainty, while LX-ST experiments aim at highlighting structural behaviours—such as rollover versus encroachment—that cannot be resolved within a one-line model alone.

4.4 RESULTS

4.4.1 Coastal projections

The response of the Lacanau shoreline to future SLR and sediment deficit scenarios are assessed through two complementary modelling approaches: probabilistic shoreline retreat from the LX-Shore ensemble, and morphodynamic trajectory analysis using LX-ST.

LX-Shore probabilistic projections

The probabilistic shoreline projections reveal relatively narrow envelopes by mid-century, and increasingly divergent pathways towards the end of the century (Fig. 4.9). By 2050, the median shoreline position relative to 2011 differs little between climate scenarios, with values near 43 m for SSP2-4.5 and SSP5-8.5, and 63 m for the high-end case. At this time horizon, ensemble spreads of roughly 20–63 m remain limited relative to late-century uncertainties, such that differences between scenarios are not yet distinguishable from intrinsic shoreline variability and model uncertainty.

By 2100, the envelopes widen considerably and scenario dependence becomes clear, consistent with the SLR projections. The median retreat roughly triples relative to mid-century, reaching 112 m for SSP2-4.5, 135 m for SSP5-8.5. Using the high-end case, retreat can exceed 225 m, reflecting highly adverse yet physically plausible conditions. The difference between the scenarios median shoreline position, which was negligible at mid-century, expands to nearly 23 m by 2100. This marks the point where the imprint of SLR overtakes natural fluctuations, in line with earlier probabilistic assessments (D'Anna et al. 2021a; Le Cozannet et al. 2019).

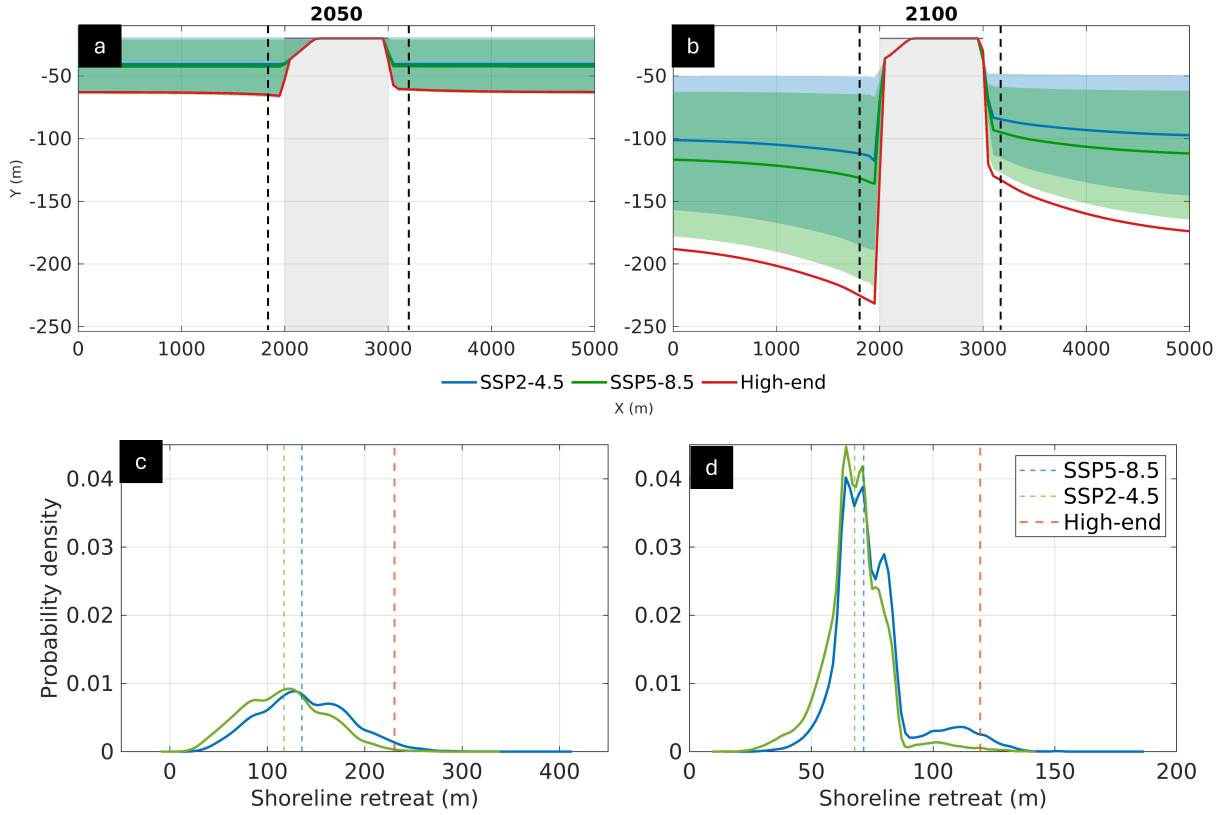

Figure 4.9: (a–b) Shoreline envelopes at 2050 and 2100 for SSP2-4.5 (blue), SSP5-8.5 (green), and the High-end (red) scenario. Shaded areas represent the 117th–83rd percentile ranges. The grey band indicates the zone of seawall presence, and the dotted lines denote the positions of the two transects. (c–d) Probability density functions of simulated shoreline retreat, for the year 2100, at two transects downdrift (c) and updrift (d) of the seawall.

The seawall induces a marked asymmetry between its updrift and downdrift sides. As anticipated, on the updrift side, the shoreline remains relatively stable, while the downdrift side experiences

stronger variability and accelerated erosion. During the first half of the century, retreat at the downdrift transects can still be approximated by a near-linear trend, explained by sediment entirely bypassing the structure (Durand et al. 2024). Beyond mid-century, however, the effect of the seawall becomes more pronounced as sediment is increasingly blocked updrift, leading to accumulation updrift and accelerated erosion downdrift (Fig. 4.10). In this way, the seawall gradually shifts from acting as a passive protection structure to behaving more like a groyne, notably affecting longshore sediment transport.

Figure 4.10 indicates the timing at which the seawall starts to generate accelerated erosion on the downdrift side for the considered climate scenarios. This is defined as the time when a shift in coastal behaviour occurs; what can be interpreted as a trajectory shift. The onset year is arbitrarily defined from the simulations as the first time the mean downdrift shoreline lies more than 10 m landward of the updrift section, providing a simple but robust indicator of this behaviour. Then, the onset years were analysed as a function of the imposed background erosion rate, which represents the long-term sediment deficit in the system. Three representative rates were considered: the median value (baseline) of the sampled distribution (0.64 m/y) and values 25 % higher and lower. A kernel-weighted estimation approach (Silverman 2018) was applied to compute smooth probability density functions of the onset year for each erosion rate, without rerunning the model for discrete cases.

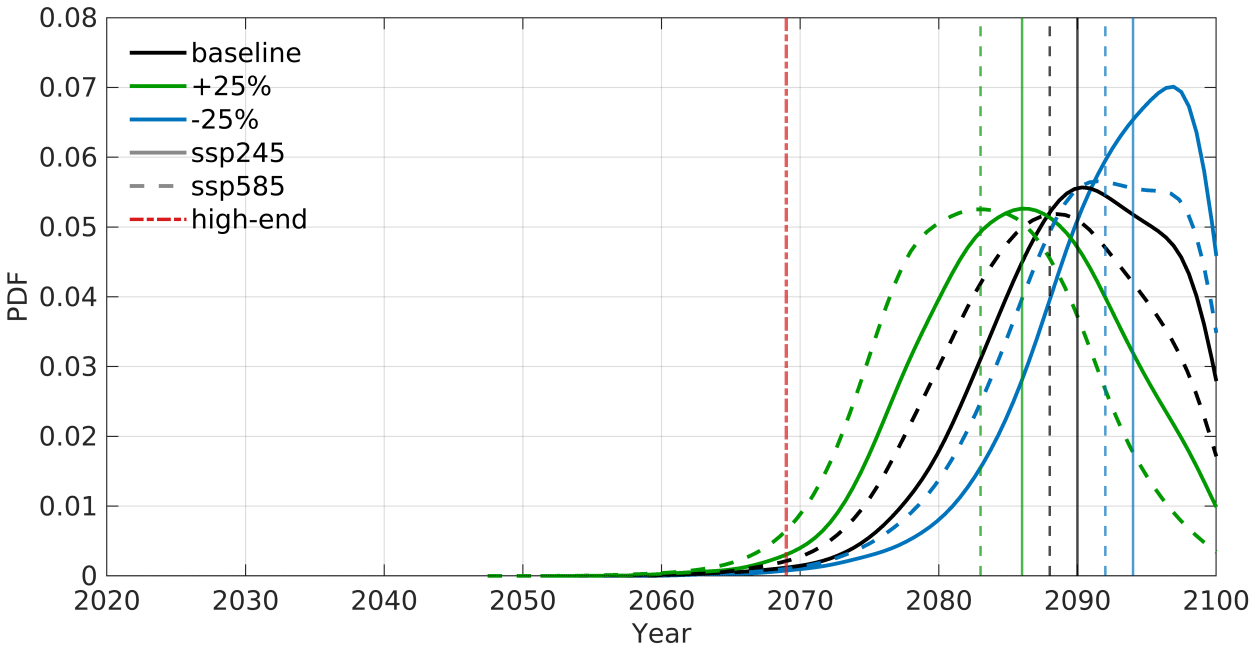

Figure 4.10: Probability density of the onset year of accelerated downdrift erosion under SSP2-4.5 and SSP5-8.5, the baseline (median sediment-deficit rate) and its ±25 % perturbations. The onset is defined as the first year when the mean shoreline position downdrift of the seawall exceeds the updrift retreat by more than 10 m. Solid and dashed lines correspond to SSP2-4.5 and SSP5-8.5, respectively. Vertical lines indicate median onset years, and the red line denotes the high-end scenario.

The distributions in Fig. 4.10 show that the onset of downdrift acceleration occurs within a relatively narrow window (2085–2090) for both SSP2–4.5 and SSP5–8.5 scenarios. Their median values are roughly 3 years apart, indicating that within this range of climatic forcing, the central timing of seawall-driven erosion is only weakly sensitive to mean sea-level differences. However, the

spread of onset years is noticeably broader under SSP5–8.5, reflecting the larger intrinsic variability of high-emission sea-level projections. This suggests that internal SLR uncertainty may still shift the onset of acceleration by several decades, even if the expected timing remains similar. In contrast, the high-end scenario yields an earlier transition (around 2069), due to the non-linear amplification of morphodynamic response under extreme forcing. The three sediment-deficit scenarios produce clearly separated probability distributions, confirming that variations in the chronic erosion rate have a stronger effect on the median onset year than the differences between moderate emission pathways. Increasing or decreasing the background erosion rate by 25 % shifts the median onset year by approximately four to five years across all SLR scenarios. The near-constant temporal offset indicates that sediment deficit and sea-level rise contribute additively, with limited interaction, and that the local sediment budget exerts the dominant control on the timing of downdrift erosion.

LX-ST morphodynamic trajectories

The LX-ST simulations highlight two distinct morphodynamic responses, depending on whether the dune system is allowed to roll over or remains fixed in place (Figure 4.11). Results are shown here for the SSP5-8.5 using the median SLR and the baseline background erosion rate conditions.

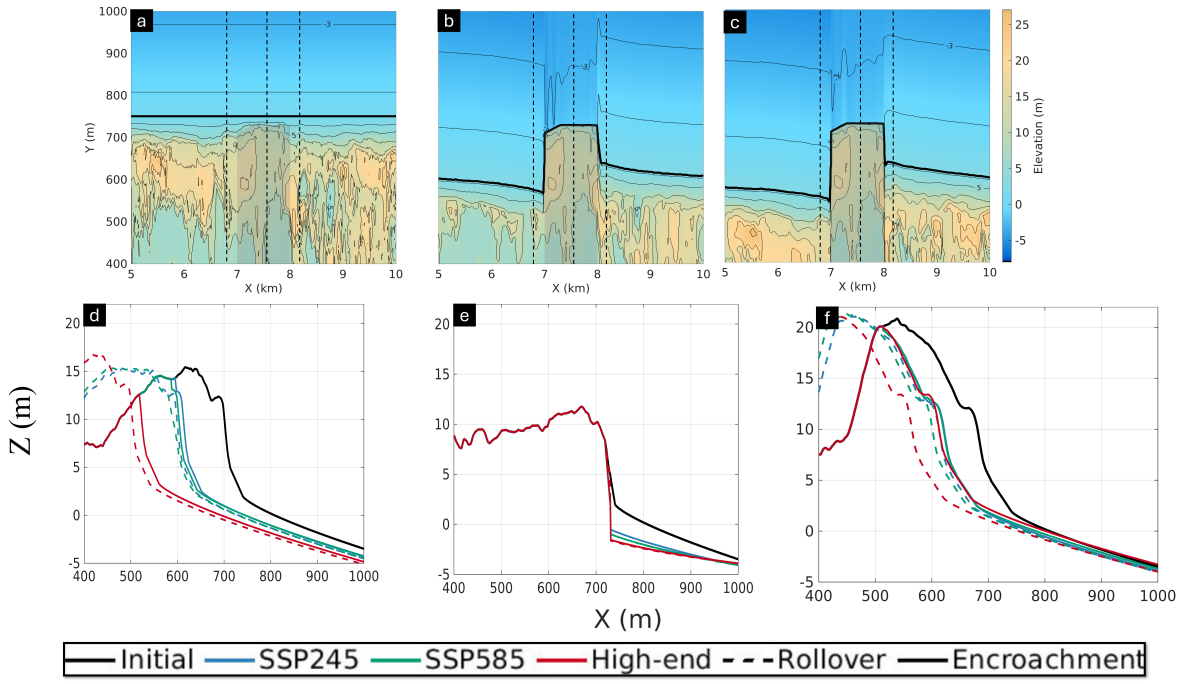

Figure 4.11: Shoreline–dune evolution simulated with LX–ST under sea-level rise forcing. (a) Initial condition in 2011, (b) 2100 topobathymetry with dune encroachment, and (c) 2100 topobathymetry with dune rollover, shown for SSP5–8.5 with median sea-level rise and baseline background erosion rate. Panels (d–f) present representative cross-shore transects at the downdrift (d), seawall (e), and updrift (f) locations, comparing initial conditions (black) with 2100 projections. Solid lines denote the encroachment case and dashed lines the rollover case.

The end-of-century simulations (Fig. 4.11b,c) underline the strong alongshore asymmetry generated by the seawall. In the encroachment case, the downdrift dune system is almost entirely eroded,

leaving only a narrow foreshore, whereas under rollover the dune ridge persists despite substantial retreat of the shoreline. Updrift of the structure, differences between the two dune adjustment modes yield comparable shoreline positions (≈15 m difference).

Transects provide further insight into these contrasting behaviours. The results discussed here correspond to the transect-elevation medians obtained from the nine simulations performed for each scenario. At the downdrift location (Fig. 4.11d), retreat is of similar magnitude for SSP2–4.5 and SSP5–8.5, regardless of the dune response mode, but clearly more pronounced under the high-end case. In encroachment mode, the 10 m contour migrates from 700 m initially to 616 m, 602 m, and 524 m by 2100, under SSP2-4.5, SSP5-8.5 and the high-end scenario respectively, corresponding to landward shifts of about 85–175 m. In rollover mode, the dune crest remains preserved and sediment is gradually redistributed landward, resulting in slightly greater retreat distances of 605 m, 590 m, and 504 m respectively, that is, between 95–195 m. This larger retreat is consistent with the expected landward translation of the entire active profile during rollover. However, in contrast to encroachment, the dune maintains its structure and continues to provide protection against marine flooding. Encroachment leads to a smaller apparent retreat but results in active dune erosion and higher risk of submersion.

At the seawall transect (Fig. 4.11e), the structure constrains the backshore dune crest and effectively fixes the shoreline position under all scenarios. In both rollover and encroachment modes, the active beach progressively narrows and eventually vanishes, leaving a steep, structure-controlled foreshore by 2100. To quantify this transition, the year of beach disappearance in front of the seawall was estimated from the LX-ST simulations, following the same probabilistic approach used for Fig. 4.10. We interpret the "disappearance year" as the year in which the 1.5 m shoreline contour retreats more than 20 m within the seawall sector. The resulting probability distributions (not shown) indicate that the loss of the active beach occurs early in the century for most realizations. Under SSP2-4.5 and SSP5-8.5, the median disappearance year is approximately 2040–2042, with interquartile ranges spanning 2024–2068 and 2024–2065, respectively. The high-end scenario shows immediate disappearance early on (2023) in both frameworks. Differences between the LX-ST standard and rollover configurations are negligible compared with the scenario spread, confirming that beach loss at the seawall is primarily governed by the persistent sediment deficit.

At the updrift location (Fig. 4.11f), retreat remains more moderate. In encroachment mode, the 10 m contour shifts from the initial 700 m position to 622 m for both SSP2–4.5 and SSP5–8.5, and to 604 m under the high-end scenario, corresponding to landward displacements of about 80–100 m. In rollover mode, the values are slightly larger, with the contour located at 611 m, 600 m, and 564 m, that is, retreat between 90 m and 135 m. These differences confirm that shoreline response remains relatively subdued on the updrift side, where the seawall limits local erosion and traps sediment. The greater retreat in rollover reflects the more uniform redistribution of sediment within the subaerial system, while encroachment involves limited translation but progressive dune scarping. Overall,

the updrift sector shows milder recession yet reduced capacity for alongshore sediment export, contributing to the downdrift deficit discussed in Section 4.4.1.

Overall, the seawall induces a marked reorganization of the alongshore sediment budget. Updrift, the observed relative stability and partial dune preservation, reflect the local trapping of sediment and the limited capacity for profile translation. At the structure itself, the active beach narrows progressively as wave reflection and sediment impoundment constrain cross-shore exchange. Downdrift, erosion is amplified as sediment supply reduces and the shoreline adjusts to the imposed deficit. These effects become more pronounced under increasingly pessimistic SSP scenarios, illustrating that coastal defenses can redistribute rather than mitigate coastal risk by shifting erosion pressures alongshore.

4.4.2 Global Sensitivity Analysis

The GSA based on the 2 10 000-member LX-Shore ensembles reveal a clear temporal evolution in the contribution of the uncertain inputs to the uncertainties in shoreline projections for the updrift (Fig. 4.12) and the downdrift (Fig. 4.13) sections. During the early decades, background erosion rate accounts for most of the variance across all scenarios. With time, however, the contribution of SLR uncertainties grow systematically. The shoreline trajectories (top panels) illustrate the expected divergence between scenarios, with retreat rates steepening under stronger forcing. Uncertainty envelopes also broaden markedly after mid-century, particularly under the high-end case, reflecting the rising contribution of SLR uncertainty to the spread in outcomes.

The Sobol indices for erosion rate (middle panels) display a gradual decline from initial values close to one, decreasing to 0.76-0.64 by 2100. In parallel, the Sobol indices for SLR (bottom panels) follow the inverse trajectory, rising from near-zero values around 2020 to 0.24–0.36 by 2100.

Patterns are similar at both the updrift and downdrift transects, with differences in Sobol indices of less than 0.02. This consistency indicates that the temporal shift from erosion-dominated to SLR-accelerating uncertainty is a robust feature of the system, regardless of the local position relative to the seawall.

The temporal evolution of the Sobol index for SLR, $S_2^{\mathrm{SLR}}(t)$, was examined using segmented regression (Fig. 4.14), which fits two linear segments to the sensitivity curve and identifies the year when the change in slope of S_2 is most pronounced. We refer to this year as the breakpoint. It indicates the onset of a phase in which sensitivity to SLR begins to increase relative to sensitivity to sediment deficit. In other words, the breakpoint marks a structural shift from a slow decrease in the fraction of variance explained by SLR to a sustained increase, during which uncertainties in future SLR become increasingly important contributors to uncertainty in shoreline projections. For both the SSP2-4.5 and SSP5-8.5, the breakpoints occur around $\tau \approx 2040$. Prior to this, the sensitivity

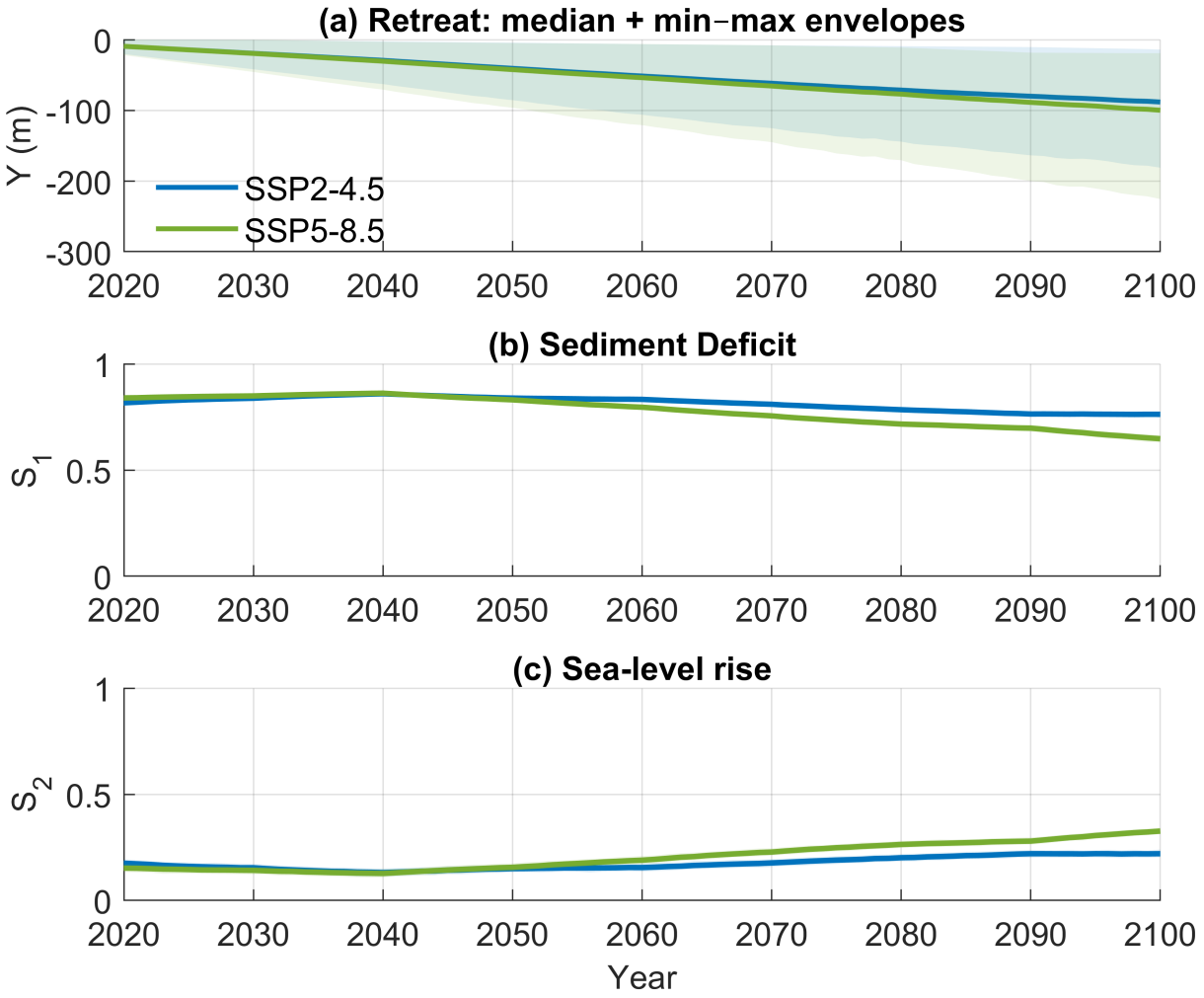

Figure 4.12: Shoreline evolution (updrift) and time-varying first-order Sobol' sensitivity indices (x = 8100 m) for SSP2-4.5, SSP5-8.5.

slope remains weakly negative, suggesting that SLR plays only a modest role in explaining variance. This change in behaviour is not a random fluctuation but a consistent feature across simulations, showing that the dynamics of sensitivity evolve in two distinct phases.

Taken together, these results highlight two robust effects. Stronger forcing (SSPs) not only shifts the breakpoint earlier in time but also amplifies the acceleration of SLR sensitivity once the breakpoint is passed. This indicates that under more extreme scenarios, the period during which erosion dominates the uncertainty budget is shortened, and the role of SLR uncertainties intensifies far sooner. The breakpoint analysis therefore provides a clear signal of when the system transitions into a regime of rapidly growing SLR sensitivity, which is a critical feature to consider in the interpretation of long-term coastal risk.

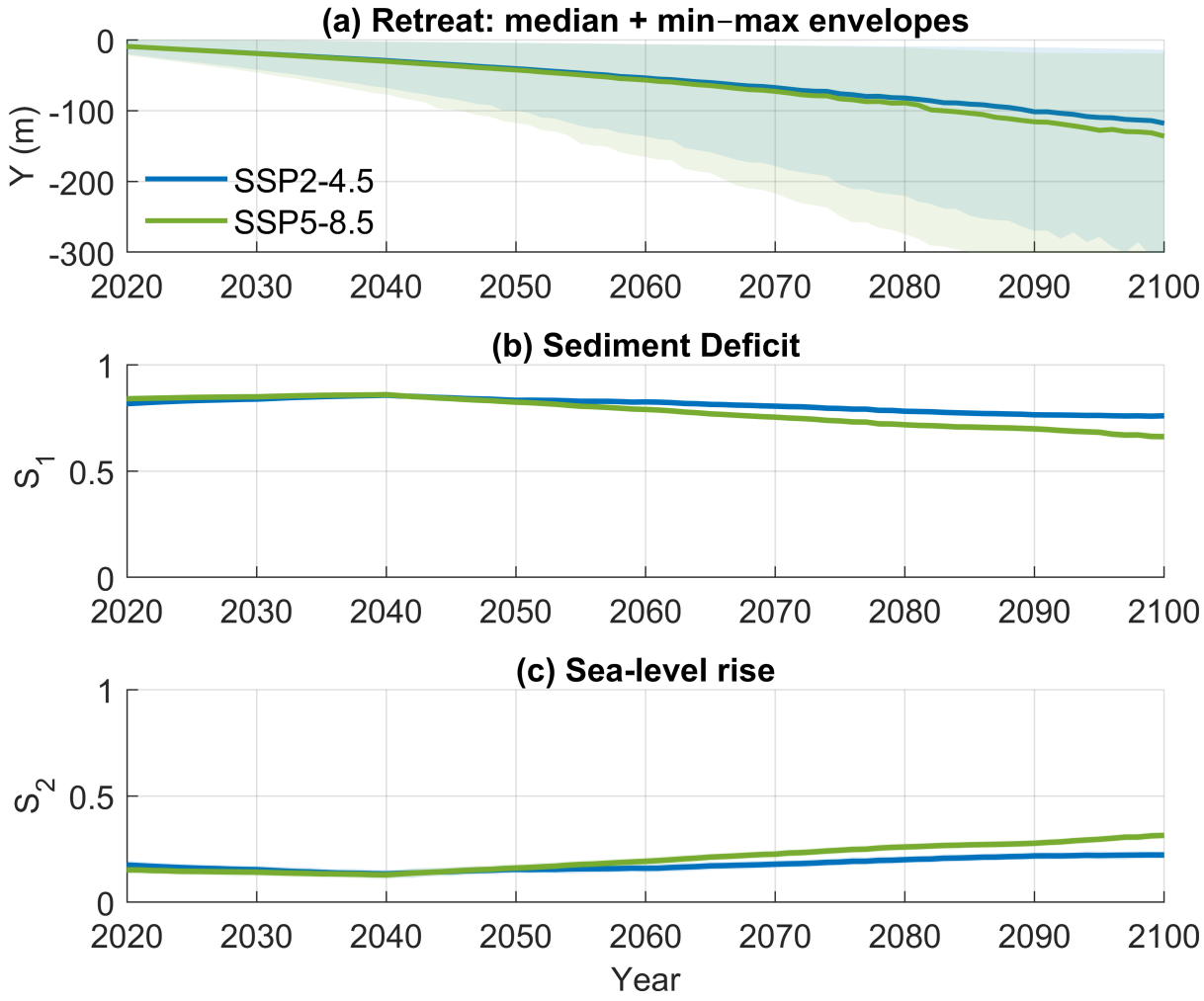

Figure 4.13: Shoreline evolution (downdrift) and time-varying first-order Sobol' sensitivity indices (x = 6900 m) for SSP2-4.5, SSP5-8.5.

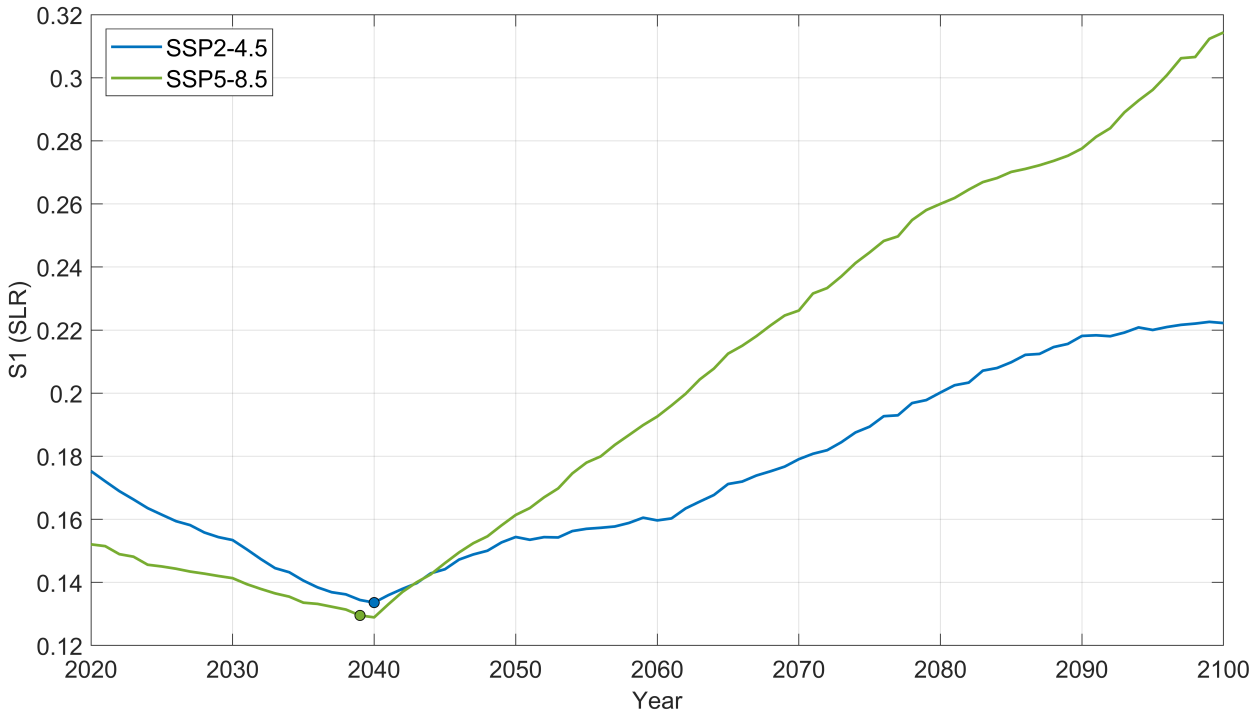

Figure 4.14: Breakpoint analysis of first-order Sobol indices for sea-level rise at the downdrift transect. The raw sensitivity curves are shown for SSP2-4.5 (blue), SSP5-8.5 (green), together with their statistically estimated breakpoints.

4.5 DISCUSSION

4.5.1 Added value of combined approaches and lessons learned

The ensemble results indicate that uncertainty in the background erosion rate dominates the shoreline projection uncertainties throughout most of the twenty-first century, whereas the relative contribution of sea-level rise uncertainty becomes significant only from mid- to late-century, depending on the forcing scenario (SSP or high-end case). This temporal sequence confirms earlier probabilistic analyses showing that SLR processes, are not as relevant in the near-term for high-energy wave-dominated beaches (D'Anna et al. 2021a; D'Anna et al. 2022). Therefore, the results underline the critical need to better understand, quantify, and attribute ambient erosion trends to their underlying causes, whether related to persistent sediment deficits, gradients in longshore transport, or human interventions that constrain sediment supply.

The results show that long-term sediment deficits, often maintained by gradients in littoral transport or anthropogenic constraints on sediment supply, dominate the trajectory of coastal change during the coming decades. Yet this background component remains largely unmonitored and poorly constrained, despite its decisive role in shaping near-term shoreline evolution (Vos et al. 2023). The scarcity of coordinated long-term observation programs and the lack of standardised methodologies for shoreline detection continue to limit our ability to identify persistent trends (Pollard et al. 2019; Alvarez-Cuesta et al. 2024). To reduce these uncertainties, robust multi-decadal datasets that combine satellite-derived shoreline mapping, historical imagery, and sediment budget assessments are required to distinguish natural variability from chronic deficit (Van Rijn 2011; Brunel et al. 2014). Developing regional monitoring and data-assimilation frameworks, linking repeated lidar surveys, bathymetric updates, and satellite observations within harmonised databases, would provide an operational foundation for detecting early signs of imbalance (Schmidt et al. 2013; Vitousek et al. 2024). Beyond improving model calibration, such systems are essential for building an evidence base that connects observed sediment losses to their drivers and supports adaptive sediment management in chronically eroding coasts.

The combined use of LX-Shore and LX-ST provides the means to interpret these erosion-dominated trajectories in both statistical and morphological terms. LX-Shore, through its large ensemble of realizations, quantifies the probabilistic range of shoreline retreat arising from uncertain erosion rates and sea-level rise, thereby isolating the relative contribution of each driver. LX-ST extends this probabilistic framework by introducing the cross-shore morphological responses associated with shoreline retreat, accounting for dune–beach coupling and volumetric adjustment through time. Together, the two models clarify how persistent sediment deficit drives distinct morphodynamic pathways, while sea-level rise gradually amplifies and reshapes these patterns. This dual perspective also points to a shift in monitoring priorities: from quantifying background erosion trends in the near term to detecting the onset of SLR-driven adjustments later in the century.

The morphodynamic simulations further illustrate that an equivalent amount of shoreline retreat can correspond to very different coastal states. Under rollover conditions, dunes migrate landward while maintaining their sediment volume and defense capacity, allowing the system to adjust gradually to ongoing erosion. In contrast, under encroachment, dune migration is inhibited and sediment losses lead to structural collapse, resulting in a rapid loss of protection despite a similar horizontal retreat distance. LX-ST makes this contrast explicit by resolving the internal sediment redistribution and volumetric changes that define these divergent trajectories.

These findings help reconcile contrasting perspectives in the literature. Global assessments such as Vousdoukas et al. (2020) highlight the near inevitability of shoreline retreat under rising sea levels, whereas morphodynamic studies of barrier adjustment emphasize the capacity of coastal systems to reorganize and maintain their protective function under adequate sediment supply (Cooper et al. 2020). Both views remain valid within their respective scales and assumptions. The probabilistic results from LX-Shore align with global projections by showing that the background retreat rate is statistically dominant across nearly all realizations, while the simulations of LX-ST demonstrate that the consequences of this retreat depend critically on the system's capacity to adjust through rollover rather than encroachment. For sediment-starved coasts such as Lacanau, this integrated view implies that monitoring and managing background erosion rate is as crucial as preparing for long-term sea-level rise, since the ability of dunes to migrate landward will largely determine whether retreat translates into continued resilience or irreversible loss of coastal function.

4.5.2 Limitations and residual uncertainties

Several important limitations constrain the generalization of our findings. A key simplification is the omission of wave climate uncertainty, despite its well-established influence on barrier dynamics through storm impacts and seasonal erosion–accretion cycles (D'Anna et al. 2021a; D'Anna et al. 2022). For the French Atlantic coast, wave projections provide some justification for this assumption (Laugel et al. 2014). Regional studies indicate that projected changes in mean significant wave height and dominant wave direction are generally modest relative to natural variability through mid-century, with no clear emergence of strong anthropogenic signals before then (Morim et al. 2019; Chaigneau et al. 2022). Toward the end of the century, high-resolution simulations for the Bay of Biscay indicate a general decrease of wave heights (up to −20 cm during summer), together with a clockwise shift of summer waves and winter swell, with potential implications for longshore transport along the Aquitanian coast (Charles et al. 2012b; Charles et al. 2012c). On the past period, while basin-scale hindcasts indicate upward trends in wave height over parts of the North Atlantic during the 20th century (Bertin et al. 2013; Castelle et al. 2018a), regional analyses for the Bay of Biscay reveal a more nuanced picture. In particular, buoy records offshore show an increase in summer significant wave height, alongside seasonal shifts in extreme wave direction, yet no significant trends are detected

closer to the Aquitanian coast (Charles et al. 2012a). Together, these findings indicate that, for the study site, it is reasonable to assume a constant wave climate throughout the 21st century.

Recent global projections indicate that mean and extreme wave trends may diverge, with 100-year return levels increasing by up to 2 m in some basins despite local mean decreases (Lobeto et al. 2021). However, for Lacanau, such high-energy events typically approach at low incidence angles and therefore exert limited influence on longshore transport in the present one-line configuration, where cross-shore processes are not explicitly represented. Consequently, their contribution to shoreline change is expected to be minor and was not analyzed further in this study.

A further limitation of this work concerns the treatment of internal climate variability and wave–energy fluctuations. In the Northeast Atlantic, winter-mean wave height and variability have increased over the past seven decades, producing more frequent energetic winters and episodic coastal impacts such as 2013–2014 (Castelle et al. 2018a). These decadal modes can dominate interannual shoreline variability and temporarily accelerate erosion, yet their influence is not represented here since cross-shore processes were intentionally switched off in LX-Shore to isolate long-term, sediment-supply-driven trends. This simplification is reasonable for assessing the multi-decadal response to sea-level rise at Lacanau, where extreme waves approach with low incidence angles and contribute little to longshore transport. Nonetheless, future extensions could account for wave-climate variability as an uncertain forcing parameter, allowing high-frequency fluctuations to be reflected in the projected shoreline envelopes.

In LX-ST, the rollover phenomenon is applied uniformly alongshore, providing a tractable way to represent the gradual landward translation of the dune–beach system under rising sea level. This simplification is consistent with the open-coast context of Lacanau, where barrier adjustment is primarily governed by marine processes and aeolian remobilisation rather than inlet migration or overwash. Field observations in the southern sector confirm that dunes can migrate landward through aeolian recycling of sand while maintaining their overall morphology (Bossard and Nicolae Lerma 2020; Lerma et al. 2025).

Nevertheless, this one-dimensional formulation neglects the spatial variability and feedback that arise when marine and aeolian processes interact dynamically. Recent studies have shown that coupling between subaerial and subaqueous sediment transport can significantly influence dune evolution and sediment connectivity at decadal scales (Van Westen et al. 2024b; Van Westen et al. 2024a). Capturing such interactions requires two- or three-dimensional, process-resolving morphodynamic models, but their computational cost remains prohibitive over centennial time horizons or multi-kilometre domains. LX-ST therefore offers a practical compromise: it enhances realism beyond purely geometric retreat models while retaining the simplicity required for long-term ensemble simulations.

The human dimension receives limited treatment in our analysis. Beyond seawalls, coastal communities employ diverse adaptation strategies that can significantly alter system behavior. Our

results should be interpreted as responses to "unmanaged" conditions with limited intervention, not as predictions of actual future conditions where adaptive management will likely play a larger role.

Finally, our analysis is geographically limited to a single site—Lacanau beach on the French Atlantic coast. While this location is reasonably representative of wave-dominated sandy coastlines, barrier systems worldwide exhibit enormous diversity in their geometry, sediment supply, wave climate, and human context. Broader application of our framework requires testing across multiple coastal types and geographic settings.

4.5.3 Implications for coastal management

The assessment of future coastal evolution under combined pressures: SLR, sediment imbalance, and human constraints, is essential for defining realistic adaptation needs (Nicholls et al. 2021). In the near term, shoreline change is mainly governed by processes such as sediment deficit, sediment continuity, and human confinement, whereas over longer horizons, rising mean sea level increasingly dictates the magnitude and persistence of coastal retreat. Effective adaptation therefore requires an understanding of how these controls interact and evolve across timescales. Because future SLR projections remain deeply uncertain, adaptation must be viewed as a continuous process in which decisions are periodically revisited as new knowledge emerges (IPCC 2022; Nicholls et al. 2021).

The rollover mode of the ShoreTrans code (and thus in the LX-ST simulations), corresponds to the natural landward translation of the coastal profile in response to sea-level rise, maintaining dune and beach functions while shifting inland (Pontee 2013). This migration enables the shoreline to preserve its relative position with respect to hydrodynamic forcing, provided that sufficient accommodation space and sediment connectivity exist. Similar behaviour has been observed in the southern sector of Lacanau, where field analyses have documented active dune remobilisation and landward migration through sand recycling and aeolian transport (Bossard and Nicolae Lerma 2020; Lerma et al. 2025). These observations support the plausibility of the rollover trajectories simulated with LX-ST.

However, this capacity for dune mobility is not universal. In many developed or stabilised coastal sectors, dense vegetation, engineered defences, and limited space for retreat restrict sand availability and inhibit landward migration (IPCC 2022). The potential for rollover therefore depends not only on external forcing and sediment supply but also on ecological and management conditions that govern sediment exchanges. In the short term, maintaining sediment continuity and providing room for this natural movement are essential for sustaining the resilience of beach–dune systems (Doody 2004).

In the near term, ensemble results show that the spread in shoreline retreat is driven mainly by uncertainty in the imposed background erosion rate rather than by differences in sea-level rise trajectories. Under identical forcing, higher sediment-deficit conditions lead to larger retreat

magnitudes and earlier onset of compound erosion. This outcome is consistent with field evidence that jetties, inlets, and storm-induced sediment trapping create longshore transport discontinuities and locally intensify erosion (Vitousek et al. 2024; Georgiou et al. 2024; Van Rijn 2011). Managing these gradients, and more broadly maintaining sediment connectivity through natural bypassing, dune mobility, or periodic nourishment, remains a practical priority for limiting chronic retreat while preserving coastal resilience.

Hard coastal defenses, such as seawalls, are widely adopted because they provide immediate and predictable protection levels in densely populated low-lying zones (IPCC 2022). However, these structures alter hydrodynamic and sedimentary processes and frequently transfer erosion or flooding problems to adjacent areas (Doody 2004). The LX-ST results clearly demonstrate this redistribution effect: while the seawall stabilizes the shoreline locally, it interrupts sediment bypassing, leading to enhanced downdrift erosion. Such outcomes exemplify the coastal squeeze mechanism described in numerous case studies (Pontee 2013).

The reliability of the LX-ST projections relies on sustained observation of coastal evolution. Regular shoreline and topographic surveys from satellites, UAVs, and LiDAR now capture the seasonal to interannual dynamics of beaches and dunes with increasing precision (Luijendijk et al. 2018; Schmidt et al. 2013; Bergsma et al. 2024). These observations are critical to detect shifts from rollover to encroachment and to recalibrate LX-ST as boundary conditions and sediment budgets evolve (Vitousek et al. 2024; Alvarez-Cuesta et al. 2024). Integrating such datasets into existing coastal monitoring programmes, including Litto3D and Copernicus, will strengthen the continuity of observations and provide the empirical basis needed to refine projections and guide adaptive management under deep uncertainty.

4.6 CONCLUSION

The simulations conducted in this study provide insights on how shoreline retreat evolves under the combined influence of sea-level rise, sediment deficit, and coastal structures. In all modeled scenarios, coastal recession persists throughout the century, with median retreat approximately tripling between mid- and end-century. By 2100, median shoreline displacement reaches about 112 m for SSP2-4.5 and 135 m for SSP5-8.5, while extreme but physically plausible realizations exceed 225 m. These outcomes indicate that even moderate sea-level rise trajectories would drive substantial shoreline retreat, exceeding thresholds commonly used in coastal management planning.

The probabilistic analysis reveals a gradual but distinct temporal shift in the relative sources of uncertainty. In the early decades, shoreline retreat uncertainty is mainly governed by variability in sediment deficits, whereas the influence of sea-level rise uncertainties strengthens progressively through time. Around 2040, a clear inflection occurs: sea-level rise starts contributing a noticeably larger fraction of the total variance, reflecting the growing sensitivity of shoreline projections to its range of possible trajectories. By 2100, uncertainties in sea-level rise explain roughly 30 % of the

total shoreline variance, marking a partial transition from locally driven to climate-driven sources of uncertainty. This pattern indicates that, even under high-end forcing, near-term evolution remains controlled by sediment imbalance, while long-term trajectories become increasingly shaped by uncertainty in future sea-level rise.

The simulations further show that coastal defenses introduce strong spatial contrasts in response. The seawall stabilizes the shoreline locally but disrupts sediment continuity, producing updrift accretion and pronounced downdrift erosion. Its role gradually evolves from passive protection to an active control on longshore transport. The disappearance of the active beach in front of the structure occurs around 2040–2042 across most realizations, well before the century's end, emphasizing that early morphological degradation may precede overt flooding hazards.

Beyond magnitudes, the mode of morphological adjustment emerges as a key indicator of coastal resilience. Under rollover behavior, the dune–beach system translates landward while maintaining its volumetric integrity and protective capacity. In contrast, assuming a dune encroachment leads to structural collapse of the foredune, reducing coastal buffering despite similar horizontal retreat distances. The same apparent shoreline displacement can therefore correspond to fundamentally different coastal states.

Finally, this work demonstrates the utility of coupling deterministic and probabilistic approaches to bridge the gap between physical realism and uncertainty quantification. The LX-Shore and LX-ST models jointly enable the analysis of both spatially integrated and profile-resolved translations, providing a scalable framework to explore future coastal trajectories in human-influenced settings.

While the results clarify several key controls, they also raise new questions. How transferable are these relationships across coasts with contrasting sediment budgets and wave regimes? To what extent can dynamic adaptation, such as managed retreat or sediment nourishment, delay the SLR-driven phase of sensitivity? And how can uncertainty in coupled morphodynamic projections be reduced without sacrificing computational efficiency? Addressing these questions will be essential to move from scenario-based assessments toward operational forecasting of long-term coastal change.

Chapter 5

Conclusion & Perspectives

5.1 Main Conclusion **98**

5.2 Key Findings **99**

5.3 Perspectives and future research direction **100**

5.3.1 Model development 100

5.3.2 Applications and scientific advancements 102

5.1 MAIN CONCLUSION

This thesis addressed a fundamental limitation in contemporary coastal science: the absence of modeling tools capable of simulating the coupled, three-dimensional evolution of wave-dominated sandy coasts under sea-level rise (SLR) at planning-relevant timescales.

The preceding chapters established that shoreline evolution emerges from interactions between planform-scale processes and profile-scale translations. Sediment gradients driven by oblique wave incidence modulate longshore transport and shape coastal geometry; simultaneously, SLR translates beach profiles landward, altering sediment storage and the depth available for transport. These coupled dynamics must be integrated to represent long-term coastal evolution accurately. Recognition of this coupling has motivated hybrid modeling approaches that link planform and shoreface dynamics.

Recent frameworks represent genuine progress toward integrating these components. IH-LANSloc couples wave propagation with shoreline evolution and dynamic feedback between shoreline change and nearshore bathymetry through integration with ShoreTrans and SWAN, enabling representation of complex coastal settings including coral reefs and engineered defenses. Q2Dmorfo advances the resolution of bathymetric change and two-way coupling with waves. CoSMoS-COAST integrates multiple shoreline response components within a data-assimilation framework. These models represent a substantial conceptual and operational advance over earlier one-line approaches that treated these processes in isolation.

Despite the advances in hybrid approaches, critical gaps persist. Planform-focused models simulate longshore sediment redistribution efficiently but lack explicit representation of SLR-driven profile translation; conversely, profile-based models accurately capture retreat under SLR and real-world complexity such as seawalls, but cannot resolve alongshore transport or planform evolution. Most existing hybrids attempt coupling but at computational costs prohibitive for rigorous uncertainty quantification. These tensions—between planform and profile representation remain fundamentally unresolved in existing frameworks.

The main objectives of this work were therefore twofold. The first was to improve predictions of sandy-coast evolution under SLR by explicitly accounting for shoreface response within a planform model. The second was to use the developed framework to explore how uncertainties in external forcing and model structure influence long-term shoreline and nearshore evolution. This was achieved through a hybrid framework of sensitivity analysis and deterministic applications designed to isolate the relative contributions of SLR trajectories, sediment budget constraints, and profile responses. These goals were guided by the central hypothesis that a coupled, reduced-complexity approach could reproduce the essential three-dimensional behaviour of coastal systems and that, by doing so, it can improve our understanding of such systems.

Rather than extending conventional one-line models that assume a fixed active profile, this research establishes an explicit coupling between the dynamics of the shoreline planform and the evolution of the shoreface profile. This formulation enables exploration of how different dune response modes control nearshore evolution under rising sea levels.

5.2 KEY FINDINGS

The LX-ST framework has been developed to better account for the dynamic interactions between alongshore sediment transport, sea-level rise (SLR), and local boundary conditions, in the shoreline and shoreface modeling on long-term time scales (decades).

LX-ST addresses the long-standing separation between alongshore and shoreface processes through the development of a coupling method linking LX-Shore, which computes planform evolution and sediment-transport gradients, with ShoreTrans, which governs the volumetric response of the shoreface to rising sea level. This modular architecture enables three-dimensional simulations of coastal evolution at decadal to centennial scales while preserving the computational efficiency required for ensemble analyses. The three coupling levels implemented in LX-ST offer a practical balance between process representation and computation time. Synthetic tests showed that stronger coupling is necessary to reproduce realistic erosion–accretion patterns, particularly along curved coastlines and near coastal structures, while intermediate coupling remains sufficient for general assessments of nearly rectilinear coasts. In practice, normalized runtimes range from less than one minute per 100 years and kilometer for the simplest configuration to about three minutes for the intermediate level and roughly twenty minutes for the fully dynamic mode, allowing long-term, kilometer-scale simulations to be completed within minutes to hours on standard CPUs.

Applications of LX-ST demonstrate that assessing coastal risk cannot rely solely on projected shoreline retreat distances. The coastal response is inherently three-dimensional, as shoreline change depends not only on the landward translation of the profile but also on how dunes and barriers adjust to rising sea level. Whether the system undergoes rollover, maintaining sediment continuity, or encroachment, where dune mobility is restricted, leads to markedly different long-term outcomes. In addition, spatial variability in shoreline orientation and longshore sediment flux drives complex feedbacks between beach and dune morphology that further modulate local retreat patterns. In the Lacanau case study, while similar shoreline retreat were predicted, two contrasting behaviours were identified. In rollover trajectories, sufficient accommodation space allows the beach–dune system to migrate landward while preserving its overall sediment continuity and protective capacity. In contrast, encroachment occurs when the upper beach and dune are constrained by steep or stabilized backshore topography, such as high vegetated dunes or hard boundaries, which limit landward translation. Under these conditions, the active profile continues to erode seaward, leading to progressive beach narrowing and dune crest lowering. These findings highlight that identical retreat magnitudes may correspond to either system persistence or complete functional loss.

Simulations at Lacanau illustrate how coastal defences modify sediment pathways and spatial response. The seawall prevents landward retreat, producing local scour at its base and enhanced downdrift erosion. Indeed, the first years (or decades depending on the scenarios), there is sediment bypass from the alongshore updrift to downdrift side of seawall, while, as the shoreline retreats due to sediment deficit chronic erosion and SLR, sediment bypass decreases until a state where there is not bypass anymore . In fact, the seawall acts progressively like a groyne. While the structure stabilizes the protected site in the short term (first years/decades), it interrupts sediment continuity and increases erosion downdrift, highlighting the trade-offs inherent in fixed defences.

Beyond these local effects, LX-ST highlights that shoreline evolution does not follow a continuous or linear pathway but may undergo trajectory shifts as feedbacks between sea-level rise, sediment transport, and coastal morphology evolve. These shifts mark transitions between distinct response regimes, for instance from near-uniform retreat to spatially differentiated erosion once sediment bypass is reduced or morphological thresholds are crossed. They reflect the emergence of self-reinforcing feedbacks that alter both the rate and spatial pattern of change. Detecting such transitions is essential for anticipating abrupt adjustments in coastal behavior and for identifying periods when small external changes can trigger accelerated or localized retreat. From a management perspective, recognizing these shifts helps define when adaptation strategies should move from incremental maintenance toward broader, system-scale interventions.

Probabilistic shoreline projections at Lacanau were obtained using LX-Shore within a GSA framework, which allows quantifying how different sources of variability shape long-term shoreline evolution. Results show that in the first decades, variability is largely controlled by background retreat rates linked to sediment deficit. As SLR accelerates, its contribution to the total variability progressively increases and becomes dominant by mid-century under high-end scenarios. The identification of transition periods, when SLR effects begin to outweigh sediment-driven retreat, provides valuable insight into the timing of critical morphodynamic shifts relevant for coastal planning. While LX-Shore captures these probabilistic shoreline trajectories, LX-ST complements this approach by explicitly resolving profile translations and dune evolution under selected deterministic scenarios, thereby linking probabilistic shoreline evolution with physically consistent representations of dune response.

5.3 PERSPECTIVES AND FUTURE RESEARCH DIRECTION

5.3.1 Model development

Future developments of LX-ST should first target practical improvements to its computational and structural framework before expanding its physical scope.

A priority lies in the implementation of adaptive time stepping, enabling the coupling frequency to vary according to the magnitude of shoreline or profile change. Such an approach would allocate shorter time steps during periods of rapid sea-level rise or high morphodynamic activity and longer intervals otherwise. This would optimize computational resources, particularly for century-scale simulations at coupling Levels 2–3, where current fixed time steps may lead to unnecessary computation.

A second priority concerns a more explicit representation of beach–dune interactions and management practices. In its current form, LX-ST assumes a static dune crest when using the encroachment mode and does not simulate the role of vegetation, wind transport, or anthropogenic modifications such as mechanical reshaping and nourishments. Extending the coupling with simplified parameterizations of dune recovery or sediment supply would improve the model's ability to represent the long-term effects of soft interventions. Integration with eco-morphodynamic models such as AeoLiS (Van Westen et al. 2024a), which can handle aeolian feedbacks and vegetation growth, could further enhance this component while remaining computationally efficient.

The inclusion of aggregated cross-shore processes constitutes another avenue for improvement. Although LX-ST intentionally filters short-term fluctuations, representing the net morphological imprint of storm clusters or seasonal erosion–accretion cycles would bridge the gap between episodic and long-term dynamics. Such formulations could rely on empirical envelopes or probabilistic corrections that preserve the model's reduced-complexity philosophy while capturing cumulative morphodynamic tendencies.

The representation of geological and structural constraints could also be further refined. ShoreTrans already incorporates non-erodible layers and hard boundaries, yet this capability is not fully exploited within the coupled framework. While LX-ST already handles hard structures such as seawalls and groynes through ShoreTrans and the bypassing schemes in LX-Shore, its current implementation assumes homogeneous substrate conditions. Extending the framework to include spatially variable erodibility and bedrock elevation would allow the model to account for geological controls on sediment continuity and onshore accommodation. Such developments would improve the capacity of LX-ST to simulate coasts where sandy stretches alternate with partially confined or rocky sectors.

Finally, computational optimization and scalability remain essential to enable probabilistic and ensemble applications. Most of the computational cost is currently concentrated in the interpolation routines and ShoreTrans updates. Streamlining these steps, parallelizing the coupling procedure, and improving data exchange between modules would substantially reduce runtime, facilitating uncertainty quantification within the coupled environment.

5.3.2 Applications and scientific advancements

The next step for LX-ST is to extend its application across a broader range of coastal settings and management contexts. Applying the model to contrasting environments such as embayed beaches, barrier–lagoon systems, or coasts strongly influenced by geological or anthropogenic constraints will help evaluate its transferability and the role of boundary conditions in shaping long-term adjustment. Through these tests, LX-ST could help distinguish how morphodynamic regimes diverge between rollover and encroachment responses and how such differences lead to distinct trajectory shifts under progressive sea-level rise.

A second research direction involves exploring beach-loss trajectories under climate forcing. Ensemble simulations using varying sea-level and sediment-supply scenarios would allow quantification of when and where dominant processes shift through time. Identifying these transition periods would provide a practical means of linking model results to the timing of adaptation needs and to the detection of nonlinear or threshold behaviors in coastal response.

LX-ST also provides a framework for the assessment of coastal-management strategies in a consistent and process-based manner. By integrating soft interventions such as beach nourishment or dune management alongside hard structures like seawalls and setbacks, the model can be used to evaluate their combined long-term effectiveness and their implications for sediment continuity. Such applications would contribute to assessing the coherence between local and regional sediment-sharing strategies, particularly along managed or compartmentalized coasts.

Finally, a key challenge remains the communication of probabilistic results to stakeholders. Translating ensemble outputs into accessible indicators of coastal risk or adaptation thresholds will be essential for practical implementation. Close collaboration with coastal managers would facilitate the interpretation of model ensembles in terms of exposure timelines, residual risk, and adaptation pathways, fostering the use of LX-ST as a decision-support tool for long-term coastal planning.

Appendix A

SUPPLEMENTARY MATERIAL for: A Coupling Approach for Long-Term 3D Morphological Evolution of Sandy Coasts under Sea-Level Rise

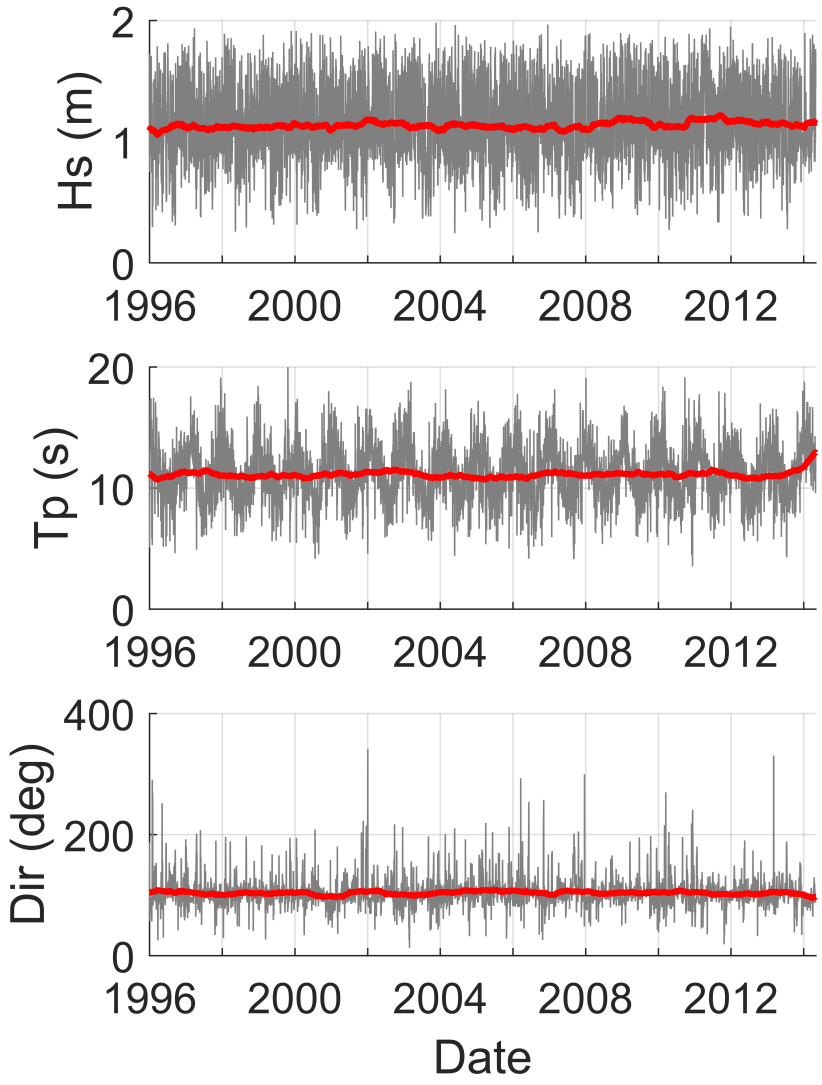

Figure S1: Time series, adapted from wave data ata high-energetic beach in France, showing: (a) offshore wave height, (b) peak period, and (c) incidence angle used in Test Case 1 (shoreline bump) as summarized in Table 1. The thick red line represents the 90-day moving average.

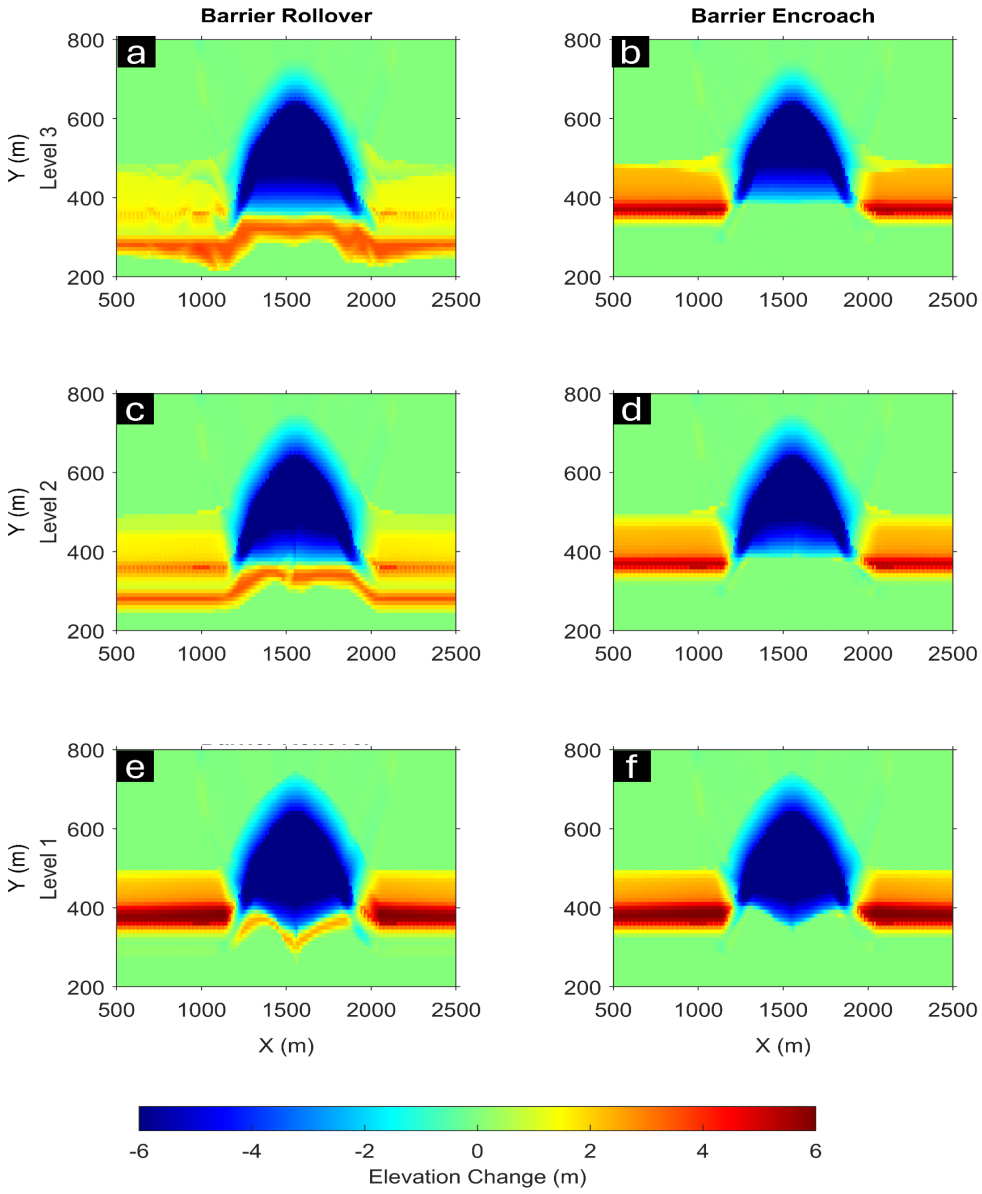

Figure S2: Difference Between Initial and Final Topobathymetry for Case 1: Columns represent two rollover modes—full rollover and encroachment—while rows depict the three coupling levels.

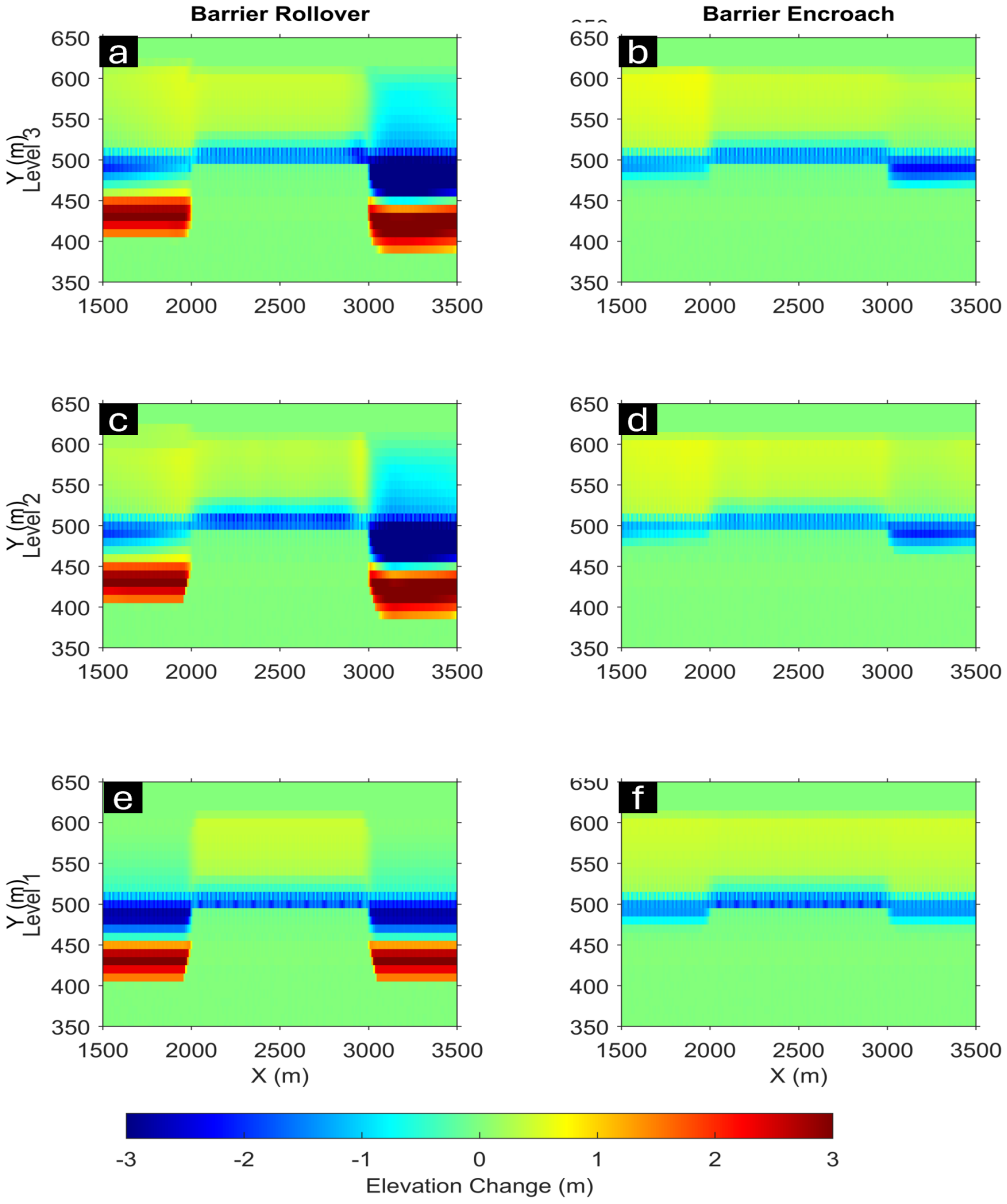

Figure S3: Difference Between Initial and Final Topobathymetry for Case 2: Columns represent two rollover modes—full rollover and encroachment—while rows depict the three coupling levels.

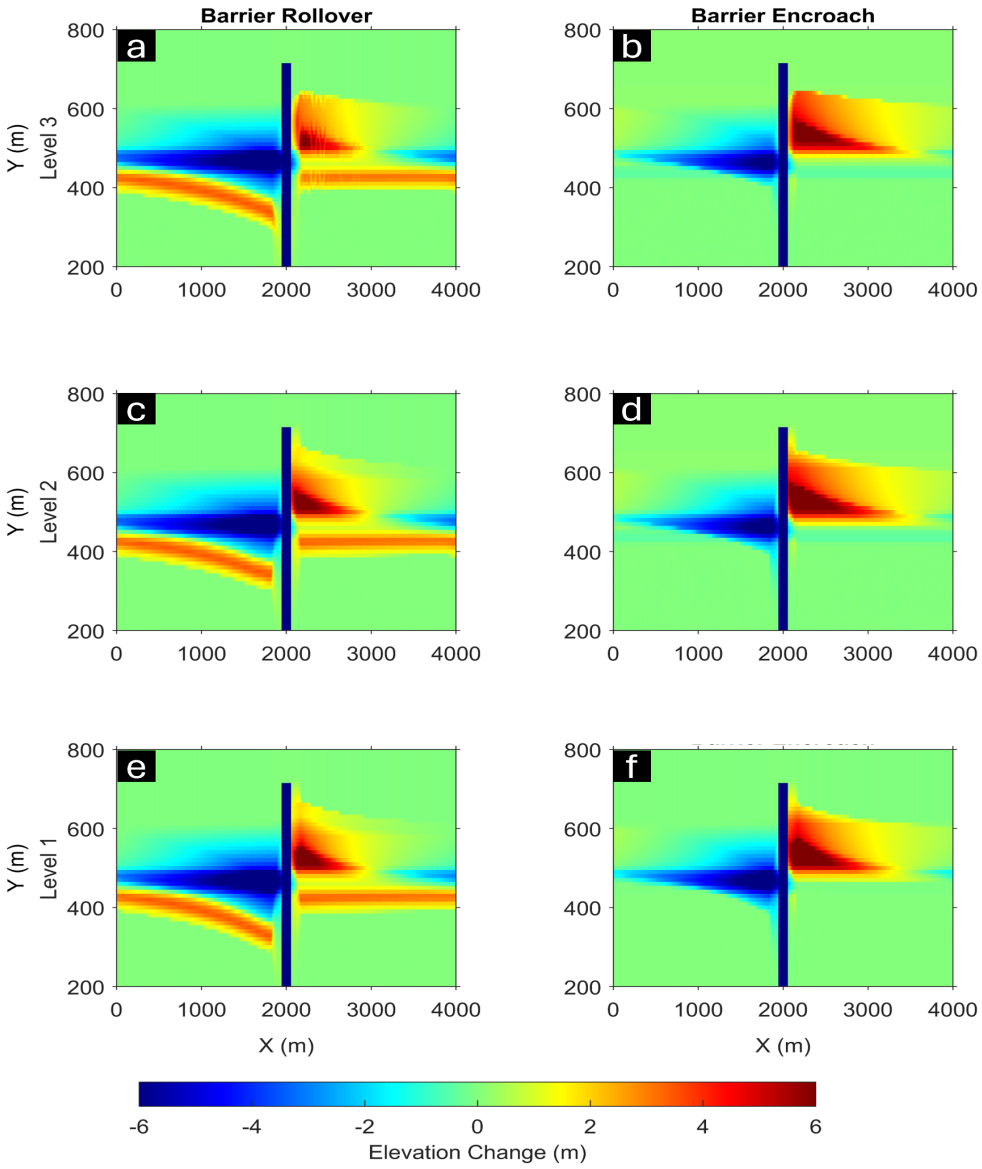

Figure S4: Difference Between Initial and Final Topobathymetry for Case 3: Columns represent two rollover modes—full rollover and encroachment—while rows depict the three coupling levels.

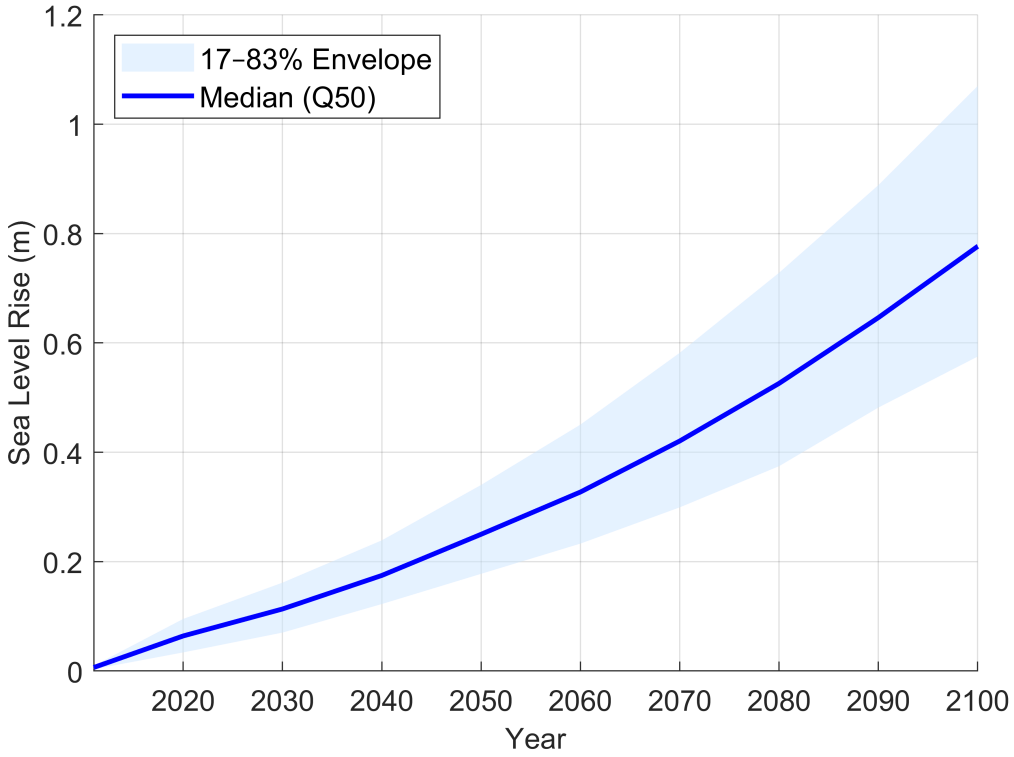

Figure S5: Projected sea-level rise at Lacanau under the SSP5-8.5 scenario from 2010 to 2150. The shaded area represents the uncertainty envelope between the 17th and 83rd percentiles, while the solid line shows the median (50th percentile).

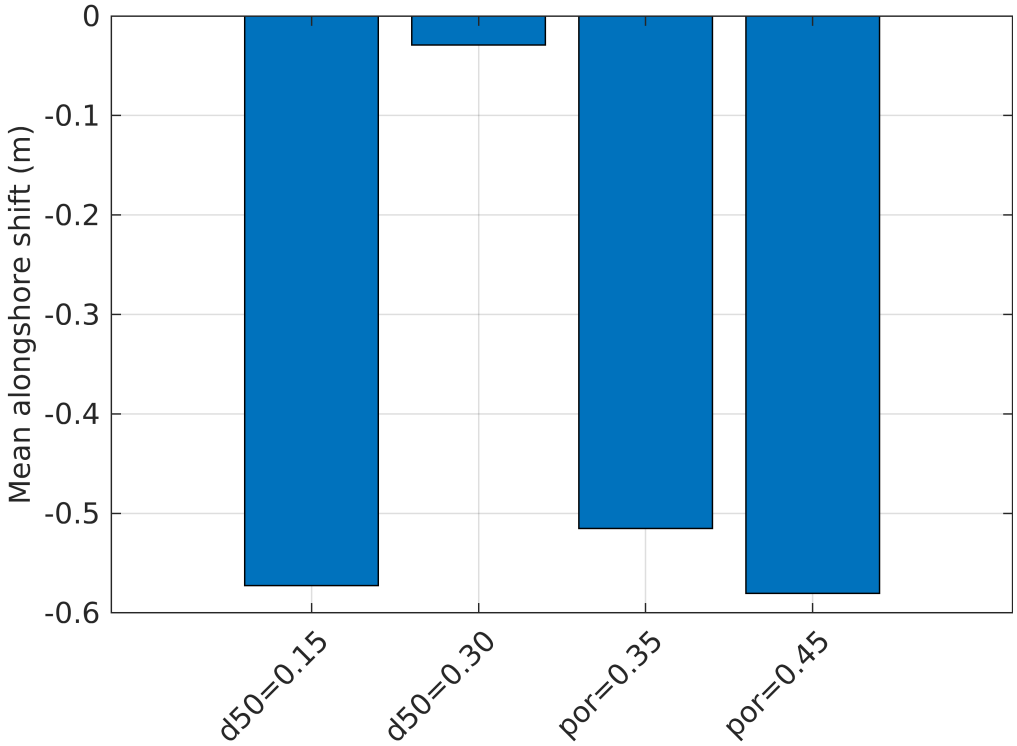

Figure S6: Mean alongshore shift in shoreline position under varying sediment properties in the Lacanau simulation. Each bar represents the difference in longshore-averaged shoreline position at year 2100 (in meters) relative to the baseline case (d_{50} = 0.22 mm, porosity = 0.4).

Table S1: Estimated computational cost of LX-ST and selected coastal evolution models. All runtimes are normalized per 100 simulated years per kilometer of coastline. LX-ST runtimes obtained on a laptop with Intel Core i5-12500H (2.50 GHz), 32 GB RAM.

Model	**Type**	**Simulation Scale**	**Runtime Estimate (/100 y/km)**
LX-ST [This paper]	Reduced-complexity/hybrid	15 km / 90 y (10×1 m grid)	Level 1: 0.74 min Level 2: 3 min Level 3: 16–20 min
GENESIS [1]	One-line (empirical)	1–100+ km / decades	Est. 1–5 min
CoSMoS-COAST [2]	Hybrid + data assimilation	500 km / 100 y	0.03–0.04 min
IH-LANSloc [3]	Semi-process-based	1–10 km / 10 y	Est. 20–36 h*
CoastalME [4]	Behavior-oriented raster–vector	0.5–1 km / 1 y	Est. 50-150 h

*Includes numerical wave model to compute breaking conditions; runtimes are not strictly comparable.

Table S2: Summary of the model setup for the three synthetic test cases and the real test case, with ST: ShoreTrans Resolution, TB: Topobathymetry Resolution, LTF: Longshore Transport Formula, Dw: Depth at which waves are imposed, BC: Boundary Condition (H: Horizontal).[1] Based on a realistic time series from a high-energy beach. [2] Normal distribution.

Test Case	(1) Bulge	(2) Seawall	(3) Groyne	(4) Lacanau
Computational Grid				
Grid (km x km):	3×1.6	5×1.4	4×1.4	15×2.5
Cell Size (m)	100	100	50	50
TB (m)	10	10	10	10
ST (m)	0.1	0.1	0.1	1
Profile Settings				
DoC (m)	5	5	5	15
Berm Height (m)	2.5	2.5	2.5	6
Sediment Properties				
d50 (mm)	0.22	0.22	0.22	0.22
Porosity	0.4	0.4	0.4	0.4
ρ_{sand} (kg/m^3)	2650	2650	2650	2650
ρ_{water} (kg/m^3)	1025	1025	1025	1025
Simulation Settings				
LTF	Kamphuis	Kamphuis	Kamphuis	Kamphuis
Wave Model	Larson	Larson	Larson	Larson
Dw (m)	35	35	35	50
BC	Periodic H	Periodic H	Periodic H	Open
SLR (m)	1 Linear	1 Linear	1 Linear	SSP 5-8.5 (Q50)
Hs (m)	$\mu = 1.14 \pm 0.3$	1	1.5	$\mu = 1.81 \pm 7$
Tp (s)	$\mu = 11.13 \pm 2.19$	8	8	$\mu = 10.85 \pm 7$
θ (°)	$\mu = 12.5 \pm 0.36$[1]	$\mathcal{N}(30, 15)^2$	$\mathcal{N}(-5, 20)^2$	$\mu = 20 \pm 0.4$
Duration (y)	5	100	10	91
Δt_{LX} (h)	1	3	3	24
Δt_{ST} (y)	0.25	1	1	1
Δt_{TR} (y)	0.25	20	1	91

References

[1] H. Hanson, Genesis: a generalized shoreline change numerical model, Journal of Coastal research (1989) 1–27.

[2] S. Vitousek, P. L. Barnard, P. Limber, L. Erikson, B. Cole, A model integrating longshore and cross-shore processes for predicting long-term shoreline response to climate change, Journal of Geophysical Research: Earth Surface 122 (4) (2017) 782–806.

[3] M. Álvarez-Cuesta, I. J. Losada, A. Toimil, A nearshore evolution model for sandy coasts: Ih-lansloc, Environmental Modelling & Software 169 (2023) 105827.

[4] A. Payo, D. Favis-Mortlock, M. Dickson, J. W. Hall, M. Hurst, M. J. Walkden, I. Townend, M. C. Ives, R. J. Nicholls, M. A. Ellis, Coastalme version 1.0: A coastal modelling environment for simulating decadal to centennial morphological changes, Geosci. Model Dev. Discuss 2016 (2016) 1–45.

References

Alvarez-Cuesta, M, A Toimil, and I J Losada (Apr. 2024). "Which data assimilation method to use and when: unlocking the potential of observations in shoreline modelling". In: *Environmental Research Letters* 19.4, p. 044023. DOI: 10.1088/1748-9326/ad3143 (cit. on pp. 91, 95).

Álvarez-Cuesta, M., I.J. Losada, and A. Toimil (Nov. 2023). "A nearshore evolution model for sandy coasts: IH-LANSloc". In: *Environmental Modelling & Software* 169. Publisher: Elsevier BV, p. 105827. DOI: 10.1016/j.envsoft.2023.105827 (cit. on pp. 5, 7, 18, 20, 26, 29, 33).

Álvarez-Cuesta, M., A. Toimil, and I.J. Losada (Oct. 2021). "Modelling long-term shoreline evolution in highly anthropized coastal areas. Part 1: Model description and validation". In: *Coastal Engineering* 169. Publisher: Elsevier, p. 103960. DOI: 10.1016/j.coastaleng.2021.103960 (cit. on p. 29).

Antolínez, José A. A. et al. (June 2019). "Predicting Climate-Driven Coastlines With a Simple and Efficient Multiscale Model". en. In: *Journal of Geophysical Research: Earth Surface* 124.6. tex.ids= antolinez_predicting_2019-1 publisher: American Geophysical Union (AGU), pp. 1596–1624. DOI: 10.1029/2018jf004790 (cit. on pp. 5, 29).

Arriaga, Jaime et al. (Mar. 2017). "Modeling the long-term diffusion and feeding capability of a mega-nourishment". en. In: *Coastal Engineering* 121, pp. 1–13. DOI: 10.1016/j.coastaleng.2016.11.011 (cit. on pp. 28, 29).

Ashton, Andrew, A. Brad Murray, and Olivier Arnoult (Nov. 2001). "Formation of coastline features by large-scale instabilities induced by high-angle waves". In: *Nature* 414.6861. Publisher: Nature Publishing Group, pp. 296–300. DOI: 10.1038/35104541 (cit. on pp. 27, 73).

Ashton, Andrew D. and A. Brad Murray (2006a). "High-angle wave instability and emergent shoreline shapes: 1. Modeling of sand waves, flying spits, and capes". In: *Journal of Geophysical Research: Earth Surface* 111.F4. DOI: 10.1029/2005JF000422 (cit. on pp. 17, 23, 47).

— (Dec. 2006b). "High-angle wave instability and emergent shoreline shapes: 2. Wave climate analysis and comparisons to nature". In: *Journal of Geophysical Research* 111.F4, F04012. DOI: 10.1029/2005JF000423 (cit. on pp. 17, 23).

Ashton, Andrew D., A. Brad Murray, and Ryan Littlewood (May 2007). "The Response of Spit Shapes to Wave-Angle Climates". en. In: *Coastal Sediments '07*. New Orleans, Louisiana, United States: American Society of Civil Engineers, pp. 351–363. DOI: 10.1061/40926(239)27 (cit. on p. 16).

Athanasiou, Panagiotis et al. (July 2020). "Uncertainties in projections of sandy beach erosion due to sea level rise: an analysis at the European scale". en. In: *Scientific Reports* 10.1, p. 11895. DOI: 10.1038/s41598-020-68576-0 (cit. on p. 69).

Atkinson, Alexander L. et al. (June 2018). "Laboratory investigation of the Bruun Rule and beach response to sea level rise". en. In: *Coastal Engineering* 136. tex.ids= atkinson_laboratory_2018-1 publisher: Elsevier BV, pp. 183–202. DOI: 10.1016/j.coastaleng.2018.03.003 (cit. on pp. 26, 41).

Bailard, James A. and Douglas L. Inman (Mar. 1981). "An energetics bedload model for a plane sloping beach: Local transport". en. In: *Journal of Geophysical Research: Oceans* 86.C3, pp. 2035–2043. DOI: 10.1029/JC086iC03p02035 (cit. on p. 14).

Bergsma, Erwin W. J. et al. (July 2024). "Shoreliner: A Sub-Pixel Coastal Waterline Extraction Pipeline for Multi-Spectral Satellite Optical Imagery". en. In: *Remote Sensing* 16.15, p. 2795. DOI: 10.3390/rs16152795 (cit. on p. 95).

Berman, Greg (Apr. 2011). *Longshore Sediment Transport*. Technical Report. Barnstable, Massachusetts: Woods Hole Sea Grant Program & Cape Cod Cooperative Extension (cit. on p. 15).

Bertin, Xavier, Elizabeth Prouteau, and Camille Letetrel (July 2013). "A significant increase in wave height in the North Atlantic Ocean over the 20th century". en. In: *Global and Planetary Change* 106, pp. 77–83. DOI: 10.1016/j.gloplacha.2013.03.009 (cit. on p. 92).

Beuzen, T. et al. (June 2018). "Physical model study of beach profile evolution by sea level rise in the presence of seawalls". en. In: *Coastal Engineering* 136. Publisher: Elsevier BV, pp. 172–182. DOI: 10.1016/j.coastaleng.2017.12.002 (cit. on pp. 26, 42).

Blossier, B. et al. (Oct. 2017). "Shore and bar cross-shore migration, rotation, and breathing processes at an embayed beach". en. In: *Journal of Geophysical Research: Earth Surface* 122.10. Publisher: American Geophysical Union (AGU), pp. 1745–1770. DOI: 10.1002/2017jf004227 (cit. on p. 23).

Booij, N., R. C. Ris, and L. H. Holthuijsen (Apr. 1999). "A third-generation wave model for coastal regions: 1. Model description and validation". In: *Journal of Geophysical Research: Oceans* 104.C4. Publisher: American Geophysical Union (AGU), pp. 7649–7666. DOI: 10.1029/98jc02622 (cit. on pp. 29, 47).

Bossard, Victor and Alexandre Nicolae Lerma (Oct. 2020). "Geomorphologic characteristics and evolution of managed dunes on the South West Coast of France". en. In: *Geomorphology* 367, p. 107312. DOI: 10.1016/j.geomorph.2020.107312 (cit. on pp. 93, 94).

Boye, Cynthia Borkai, Peter Ekow Baffoe, and Paul Boye (Mar. 2025). "Shoreline predictive model using artificial intelligence for the homogeneous beach of the Western Coast of Ghana". In: *Nova Geodesia* 5.1. Publisher: Society of Land Measurements and Cadastre from Transylvania, p. 303. DOI: 10.55779/ng51303 (cit. on p. 30).

Bozzeda, Fabio et al. (Oct. 2023). "Global patterns in sandy beach erosion: Unraveling the roles of anthropogenic, climatic and morphodynamic factors". In: *Frontiers in Marine Science* 10. tex.ids= bozzeda_global_2023-1 publisher: Frontiers Media SA. DOI: 10.3389/fmars.2023.1270490 (cit. on pp. 11, 20).

Brunel, C. et al. (Jan. 2014). "20th century sediment budget trends on the Western Gulf of Lions shoreface (France): An application of an integrated method for the study of sediment coastal reservoirs". en. In: *Geomorphology* 204, pp. 625–637. DOI: 10.1016/j.geomorph.2013.09.009 (cit. on p. 91).

Bruun, Per (1954). *Coast erosion and the development of beach profiles*. Vol. 44. US Beach Erosion Board (cit. on p. 23).

— (Feb. 1962). "Sea-Level Rise as a Cause of Shore Erosion". In: *Journal of the Waterways and Harbors Division* 88.1. Publisher: American Society of Civil Engineers, pp. 117–130. DOI: 10.1061/JWHEAU.0000252 (cit. on pp. 21, 23, 70, 74, 80).

Calkoen, Floris et al. (Mar. 2021). "Traditional vs. Machine-Learning Methods for Forecasting Sandy Shoreline Evolution Using Historic Satellite-Derived Shorelines". en. In: *Remote Sensing* 13.5. Publisher: MDPI AG, p. 934. DOI: 10.3390/rs13050934 (cit. on p. 30).

Caron, L. et al. (Mar. 2018). "GIA Model Statistics for GRACE Hydrology, Cryosphere, and Ocean Science". en. In: *Geophysical Research Letters* 45.5. tex.ids= caron_gia_2018-1, pp. 2203–2212. DOI: 10.1002/2017GL076644 (cit. on p. 77).

Castelle, Bruno and Gerd Masselink (2023). "Morphodynamics of wave-dominated beaches". In: *Cambridge Prisms: Coastal Futures* 1. tex.ids= castelle_morphodynamics_2023 publisher: Cambridge University Press, e1. DOI: 10.1017/cft.2022.2 (cit. on pp. 2, 12, 14).

Castelle, Bruno et al. (2018a). "Increased winter-mean wave height, variability, and periodicity in the northeast atlantic over 1949–2017". In: *Geophysical Research Letters* 45.8. tex.ids= castelle_increased_2018, pp. 3586–3596. DOI: 10.1002/2017GL076884 (cit. on pp. 92, 93).

Castelle, Bruno et al. (Jan. 2018b). "Spatial and temporal patterns of shoreline change of a 280-km high-energy disrupted sandy coast from 1950 to 2014: SW France". en. In: *Estuarine, Coastal and Shelf Science* 200, pp. 212–223. DOI: 10.1016/j.ecss.2017.11.005 (cit. on pp. 71, 72, 79).

Castelle, Bruno et al. (Nov. 2020). "16 years of topographic surveys of rip-channelled high-energy meso-macrotidal sandy beach". In: *Scientific Data* 7.1. Publisher: Nature Publishing Group UK London, p. 410. DOI: 10.1038/s41597-020-00750-5 (cit. on p. 71).

Castelle, Bruno et al. (2022). "Primary drivers of multidecadal spatial and temporal patterns of shoreline change derived from optical satellite imagery". In: *Geomorphology* 413. DOI: 10.1016/j.geomorph.2022.108360 (cit. on pp. 77, 78).

Cazenave, Anny and Gonéri Le Cozannet (Feb. 2014). "Sea level rise and its coastal impacts". en. In: *Earth's Future* 2.2, pp. 15–34. DOI: 10.1002/2013EF000188 (cit. on p. 20).

Chaigneau, Alisée A et al. (2022). "Impact of wave-water level non-linear interactions for the projections of mean and extreme wave conditions along the coasts of western Europe". In: *EGUsphere* 2022. Publisher: Copernicus Publications Göttingen, Germany, pp. 1–40 (cit. on p. 92).

Charles, E et al. (2012a). "Wave climate variability and trends in the Bay of Biscay from 1958 to 2001". In: *Journal of Climate* 25.6, pp. 2020–2039 (cit. on p. 93).

Charles, Elodie et al. (2012b). "Climate change impact on waves and longshore sediment flux of the Aquitanian coast". In: *HOUILLE BLANCHE-REVUE INTERNATIONALE DE L EAU* 6. Publisher: EDP SCIENCES SA 17, AVE DU HOGGAR, PA COURTABOEUF, BP 112, F-91944 LES ULIS …, pp. 26–33. DOI: 10.1051/lhb/2012036 (cit. on p. 92).

Charles, Elodie et al. (2012c). "Climate change impact on waves in the bay of biscay, france". In: *Ocean Dynamics* 62.6. tex.ids= charles_climate_2012 publisher: Springer, pp. 831–848 (cit. on pp. 77, 92).

Chastaing, Gaelle, Fabrice Gamboa, and Clémentine Prieur (Jan. 2012). "Generalized Hoeffding-Sobol decomposition for dependent variables - application to sensitivity analysis". In: *Electronic Journal of Statistics* 6.none. DOI: 10.1214/12-EJS749 (cit. on pp. 33, 34).

Chataigner, T. et al. (2022). "Sensitivity of a one-line longshore shoreline change model to the mean wave direction". In: *Coastal Engineering* 172, p. 104025. DOI: 10.1016/j.coastaleng.2021.104025 (cit. on p. 5).

Coastal Engineering Research Center (U.S.) (1984). *Shore protection manual*. tex.ids= USACE, coastal_engineering_research_center_us_shore_1984-1. Vicksburg, MS: U.S. Army Corps of Engineers, Waterways Experiment Station. DOI: 10.5962/bhl.title.47829 (cit. on pp. 15, 47, 74).

Cooper, J. A. G. et al. (Oct. 2020). "Sandy beaches can survive sea-level rise". In: *Nature Climate Change* 10.11. Publisher: Springer Science and Business Media LLC, pp. 993–995. DOI: 10.1038/s41558-020-00934-2 (cit. on pp. 3, 4, 21, 69, 70, 92).

Cooper, J. Andrew G. and Orrin H. Pilkey (Nov. 2004). "Sea-level rise and shoreline retreat: time to abandon the Bruun Rule". en. In: *Global and Planetary Change* 43.3-4. Publisher: Elsevier BV, pp. 157–171. DOI: 10.1016/j.gloplacha.2004.07.001 (cit. on pp. 4, 24, 25, 70).

Cooper, J.A.G. and J. Pile (June 2014). "The adaptation-resistance spectrum: A classification of contemporary adaptation approaches to climate-related coastal change". en. In: *Ocean & Coastal Management* 94. Publisher: Elsevier BV, pp. 90–98. DOI: 10.1016/j.ocecoaman.2013.09.006 (cit. on p. 2).

Cowell, P.J. and B. G. Thom (Jan. 1995). "Morphodynamics of coastal evolution". In: *Coastal Evolution*. Ed. by R.W.G Carter and B. G. Thom. 1st ed. Cambridge University Press, pp. 33–86. DOI: 10.1017/cbo9780511564420.004 (cit. on pp. 2, 42, 75).

Cowell, Peter J. et al. (Jan. 2006). "Management of Uncertainty in Predicting Climate-Change Impacts on Beaches". en. In: *Journal of Coastal Research* 221, pp. 232–245. DOI: 10.2112/05A-0018.1 (cit. on p. 42).

D'Anna, M. et al. (Aug. 2021a). "Uncertainties in Shoreline Projections to 2100 at Truc Vert Beach (France): Role of Sea□Level Rise and Equilibrium Model Assumptions". en. In: *Journal of Geophysical Research: Earth Surface* 126.8, e2021JF006160. DOI: 10.1029/2021JF006160 (cit. on pp. 70, 80, 83, 91, 92).

D'Anna, M. et al. (Aug. 2022). "Effects of stochastic wave forcing on probabilistic equilibrium shoreline response across the 21st century including sea-level rise". en. In: *Coastal Engineering*

175, p. 104149. DOI: 10.1016/j.coastaleng.2022.104149 (cit. on pp. 21, 31, 34, 80, 91, 92).

D'Anna, Maurizio et al. (June 2020). "Impact of model free parameters and sea⊠level rise uncertainties on 20⊠years shoreline hindcast: the case of Truc Vert beach (SW France)". en. In: *Earth Surface Processes and Landforms* 45.8, pp. 1895–1907. DOI: 10.1002/esp.4854 (cit. on pp. 33, 70, 74, 80).

D'Anna, Maurizio et al. (Sept. 2021b). "Reinterpreting the Bruun Rule in the Context of Equilibrium Shoreline Models". In: *Journal of Marine Science and Engineering* 9.9. Publisher: Multidisciplinary Digital Publishing Institute tex.ids: maurizio2021, p. 974. DOI: 10.3390/jmse9090974 (cit. on pp. 5, 14, 21, 31–34).

Davidson, M.A., K.D. Splinter, and I.L. Turner (Mar. 2013). "A simple equilibrium model for predicting shoreline change". In: *Coastal Engineering* 73. tex.ids= davidson_simple_2013 publisher: Elsevier BV, pp. 191–202. DOI: 10.1016/j.coastaleng.2012.11.002 (cit. on pp. 12, 29, 46, 48).

Davidson-Arnott, Robin G. D. (Nov. 2005). "Conceptual model of the effects of sea level rise on sandy coasts". In: *Journal of Coastal Research* 216. Publisher: Coastal Education and Research Foundation, pp. 1166–1172. DOI: 10.2112/03-0051.1 (cit. on pp. 23, 25).

Davidson-Arnott, Robin G.D. and Bernard O. Bauer (Dec. 2021). "Controls on the geomorphic response of beach-dune systems to water level rise". en. In: *Journal of Great Lakes Research* 47.6, pp. 1594–1612. DOI: 10.1016/j.jglr.2021.05.006 (cit. on p. 26).

De Bakker, A. T. M. et al. (Oct. 2016). "Cross-shore sand transport by infragravity waves as a function of beach steepness: SAND TRANSPORT BY INFRAGRAVITY WAVES". en. In: *Journal of Geophysical Research: Earth Surface* 121.10, pp. 1786–1799. DOI: 10.1002/2016JF003878 (cit. on p. 13).

Dean, R. G. (Nov. 1987). "Coastal Armoring: Effects, Principles and Mitigation". en. In: *Coastal Engineering 1986*. Taipei, Taiwan: American Society of Civil Engineers, pp. 1843–1857. DOI: 10.1061/9780872626003.135 (cit. on p. 19).

Dean, R.G. and E.M. Maurmeyer (1983). "Models for beach profile response". In: *Handbook of Coastal Processes and Erosion*. Boca Raton, Florida: C.R.C. Press, pp. 151–166 (cit. on p. 24).

Dean, Robert G. (Feb. 1995). "CROSS-SHORE SEDIMENT TRANSPORT PROCESSES". In: *Advances in Coastal and Ocean Engineering*. tex.ids= liu_cross-shore_1995 ISSN: 1793-0731, pp. 159–220. DOI: 10.1142/9789812797582_0004 (cit. on p. 12).

Dennis, Karen Clemens, Isabelle Niang-Diop, and Robert James Nicholls (1995a). "Sea-level rise and Senegal: Potential impacts and consequences". In: *Journal of Coastal Research*. Publisher: JSTOR, pp. 243–261 (cit. on p. 4).

Dennis, Karen Clemens et al. (1995b). "Sea-Level Rise and Argentina: Potential Impacts and Consequences". en. In: *Journal of Coastal Research* 14 (cit. on p. 4).

Ding, Yan et al. (2018). "Probabilistic shoreline change modeling and risk estimation of erosion". In: *Coastal Engineering Proceedings* 36, pp. 1–1 (cit. on p. 70).

Doody, J. Pat (2004). "'Coastal squeeze' – an historical perspective". en. In: *Journal of Coastal Conservation* 10.1, p. 129. DOI: 10.1652/1400-0350(2004)010[0129:CSAHP]2.0.CO;2 (cit. on pp. 94, 95).

Dubarbier, Benjamin et al. (Jan. 2015). "Process-based modeling of cross-shore sandbar behavior". en. In: *Coastal Engineering* 95, pp. 35–50. DOI: 10.1016/j.coastaleng.2014.09.004 (cit. on p. 14).

Dubois, R.N. (1975). "Shoreline erosion and the Bruun Rule: an evaluation for Lake Michigan". In: *Journal of Geology* 83.4, pp. 427–439 (cit. on p. 24).

Durand, Elsa et al. (Dec. 2024). "Influence of Rocky Obstacle Sand Bypassing on Embayed Beach Dynamics Using a Reduced-Complexity Shoreline Model". In: *Journal of Marine Science and Engineering* 12.12. Publisher: MDPI, p. 2266. DOI: 10.3390/jmse12122266 (cit. on pp. 19, 44, 48, 49, 72, 74, 84).

Durkin, Connor J., Avidesh Seenath, and Michiel A.F. Knaapen (Aug. 2025). "A critical review of closure depth theories and uncertainties: implications for shoreline modelling and coastal management". en. In: *Ocean & Coastal Management* 267, p. 107732. DOI: 10.1016/j.ocecoaman.2025.107732 (cit. on pp. 32, 34).

Falqués, A. (Nov. 2003). "On the diffusivity in coastline dynamics". en. In: *Geophysical Research Letters* 30.21. Publisher: American Geophysical Union (AGU). DOI: 10.1029/2003gl017760 (cit. on pp. 17, 27).

Falqués, A. et al. (July 2021). "A New Morphodynamic Instability Associated With Cross-Shore Transport in the Nearshore". en. In: *Geophysical Research Letters* 48.13. Publisher: American Geophysical Union (AGU). DOI: 10.1029/2020gl091722 (cit. on p. 29).

Falqués, Albert et al. (May 2017). "Formation mechanisms for self‐organized kilometer‐scale shoreline sand waves". en. In: *Journal of Geophysical Research: Earth Surface* 122.5, pp. 1121–1138. DOI: 10.1002/2016JF003964 (cit. on p. 17).

Feller, W. (June 1948). "On the Kolmogorov-Smirnov Limit Theorems for Empirical Distributions". en. In: *The Annals of Mathematical Statistics* 19.2, pp. 177–189. DOI: 10.1214/aoms/1177730243 (cit. on p. 80).

Fenneman, N. M. (Jan. 1902). "Development of the Profile of Equilibrium of the Subaqueous Shore Terrace". en. In: *The Journal of Geology* 10.1. Publisher: University of Chicago Press, pp. 1–32. DOI: 10.1086/620977 (cit. on p. 23).

Fenster, Michael S., Robert Dolan, and Robert A. Morton (2001). "Coastal Storms and Shoreline Change: Signal or Noise?" In: *Journal of Coastal Research* 17.3. JSTOR: 4300222 Publisher: Coastal Education & Research Foundation, Inc., pp. 714–720 (cit. on pp. 14, 74).

Fox-Kemper, B. et al. (2021). "Ocean, cryosphere and sea level change". In: *Climate change 2021: The physical science basis. Working group I contribution to the sixth assessment report of the IPCC*. Ed. by V. Masson-Delmotte, P. Zhai, A. Pirani, et al. Cambridge, UK and New York, NY, USA: Cambridge University Press, pp. 1211–1362. DOI: 10.1017/9781009157896.011 (cit. on pp. 2, 69, 82).

Gallagher, Edith L, Steve Elgar, and RT Guza (1998). "Observations of sand bar evolution on a natural beach". In: *Journal of Geophysical Research: Oceans* 103.C2. Publisher: Wiley Online Library, pp. 3203–3215 (cit. on p. 13).

Gao, Yifu, Abdullah Sahin, and Jasper A. Vrugt (Apr. 2023). "Probabilistic Sensitivity Analysis With Dependent Variables: Covariance□Based Decomposition of Hydrologic Models". en. In: *Water Resources Research* 59.4, e2022WR032834. DOI: 10.1029/2022WR032834 (cit. on p. 34).

Garner, G. G. et al. (Aug. 2021). *IPCC AR6 Sea Level Projections*. tex.copyright: Creative Commons Attribution 4.0 International. DOI: 10.5281/ZENODO.5914709 (cit. on p. 2).

Garner, Gregory et al. (2023). *IPCC AR6 WGI Sea Level Projections*. en. Artwork Size: 11701334484 Bytes Pages: 11701334484 Bytes. DOI: 10.26050/WDCC/AR6.IPCC-DDC_AR6_SUP_SLPR (cit. on p. 81).

Georgiou, Ioannis Y, Duncan M FitzGerald, and Kevin C Hanegan (Feb. 2024). "Storm and tidal interactions control sediment exchange in mixed-energy coastal systems". en. In: *PNAS Nexus* 3.2. Ed. by Jiahua Zhang, pgae042. DOI: 10.1093/pnasnexus/pgae042 (cit. on p. 95).

Ghermandi, Andrea and Paulo A.L.D. Nunes (Feb. 2013). "A global map of coastal recreation values: Results from a spatially explicit meta-analysis". en. In: *Ecological Economics* 86, pp. 1–15. DOI: 10.1016/j.ecolecon.2012.11.006 (cit. on p. 69).

Gomez-de La Peña, Eduardo et al. (Nov. 2023). "On the use of convolutional deep learning to predict shoreline change". In: *Earth Surface Dynamics* 11.6, pp. 1145–1160. DOI: 10.5194/esurf-11-1145-2023 (cit. on p. 30).

Hallermeier, Robert J. (Jan. 1980). "A profile zonation for seasonal sand beaches from wave climate". In: *Coastal Engineering* 4, pp. 253–277. DOI: 10.1016/0378-3839(80)90022-8 (cit. on pp. 24, 39, 73).

Hallin, Caroline (2019). "Long-term beach and dune evolution Development and application of the CS-model". en. In: Publisher: Unpublished. DOI: 10.13140/RG.2.2.36390.37447 (cit. on p. 13).

Hally-Rosendahl, Kai, Falk Feddersen, and R. T. Guza (July 2014). "Cross□shore tracer exchange between the surfzone and inner□shelf". en. In: *Journal of Geophysical Research: Oceans* 119.7. tex.ids= HallyRosendahl2014, pp. 4367–4388. DOI: 10.1002/2013JC009722 (cit. on p. 14).

Hands, Edward B (1979). "Changes in rates of shore retreat: Lake Michigan, 1967-76". In: *Journal of Great Lakes Research* 5(3–4), pp. 172–177 (cit. on p. 24).

Hanson, Hans (1989). "GENESIS: a generalized shoreline change numerical model". In: *Journal of Coastal research*. JSTOR: 4297483 Publisher: JSTOR, pp. 1–27 (cit. on p. 27).

Harley, Mitchell D. et al. (May 2022). "Single extreme storm sequence can offset decades of shoreline retreat projected to result from sea-level rise". In: *Communications Earth & Environment* 3.1. tex.ids= harley_single_2022, p. 112. DOI: 10.1038/s43247-022-00437-2 (cit. on p. 11).

Hersbach, Hans et al. (July 2020). "The ERA5 global reanalysis". In: *Quarterly Journal of the Royal Meteorological Society* 146.730, pp. 1999–2049. DOI: 10.1002/qj.3803 (cit. on p. 77).

Hinkel, Jochen et al. (Mar. 2019). "Meeting User Needs for Sea Level Rise Information: A Decision Analysis Perspective". en. In: *Earth's Future* 7.3, pp. 320–337. DOI: 10.1029/2018EF001071 (cit. on p. 69).

Hoagland, Steven W.H. et al. (Sept. 2023). "Advances in Morphodynamic Modeling of Coastal Barriers: A Review". en. In: *Journal of Waterway, Port, Coastal, and Ocean Engineering* 149.5, p. 03123001. DOI: 10.1061/JWPED5.WWENG-1825 (cit. on p. 6).

Hoefel, Fernanda and Steve Elgar (2003). "Wave-induced sediment transport and sandbar migration". In: *Science* 299.5614. Publisher: American Association for the Advancement of Science, pp. 1885–1887 (cit. on p. 13).

Hong, Hee Sun and Fred J. Hickernell (June 2003). "Algorithm 823: Implementing scrambled digital sequences". en. In: *ACM Transactions on Mathematical Software* 29.2, pp. 95–109. DOI: 10.1145/779359.779360 (cit. on p. 82).

Howd, Peter (May 1998). "Beach Processes and Sedimentation, Second Edition". en. In: *Eos, Transactions American Geophysical Union* 79.19. tex.ids= howd_beach_1998-1 publisher: American Geophysical Union (AGU), pp. 231–231. DOI: 10.1029/98eo00170 (cit. on p. 23).

Hunt, Emily et al. (2023). "Shoreline modelling on timescales of days to decades". en. In: *Cambridge Prisms: Coastal Futures* 1. Publisher: Cambridge University Press (CUP). DOI: 10.1017/cft.2023.5 (cit. on pp. 5, 6, 11, 14, 17, 21–23).

Hurst, Martin D. et al. (Dec. 2015). "Exploring the sensitivities of crenulate bay shorelines to wave climates using a new vector-based one-line model: SENSITIVITY OF CRENULATE BAYS". en. In: *Journal of Geophysical Research: Earth Surface* 120.12. Publisher: American Geophysical Union (AGU), pp. 2586–2608. DOI: 10.1002/2015jf003704 (cit. on p. 27).

Idier, Déborah et al. (Jan. 2013). "Longshore sediment flux hindcast: spatio-temporal variability along the SW Atlantic coast of France". en. In: *Journal of Coastal Research* 165, pp. 1785–1790. DOI: 10.2112/SI65-302.1 (cit. on p. 77).

Iooss, Bertrand and Clémentine Prieur (2017). *Shapley effects for sensitivity analysis with correlated inputs: comparisons with Sobol' indices, numerical estimation and applications*. Version Number: 7. DOI: 10.48550/ARXIV.1707.01334 (cit. on p. 34).

IPCC (May 2022). *The Ocean and Cryosphere in a Changing Climate: Special Report of the Intergovernmental Panel on Climate Change*. 1st ed. Cambridge University Press. DOI: 10.1017/9781009157964 (cit. on pp. 94, 95).

Jaramillo, Camilo et al. (Oct. 2021). "A shoreline evolution model for embayed beaches based on cross-shore, planform and rotation equilibrium models". In: *Coastal Engineering* 169, p. 103983. DOI: 10.1016/j.coastaleng.2021.103983 (cit. on pp. 14, 29).

Johnson, Douglas Wilson (1919). *Shore Processes and Shoreline Development*. jhonson_shore_1919. New York: John Wiley & Sons (cit. on p. 23).

Johnson, J.W. (Aug. 1949). "Scale effects in hydraulic models involving wave motion". en. In: *Eos, Transactions American Geophysical Union* 30.4. Publisher: American Geophysical Union (AGU), pp. 517–525. DOI: 10.1029/tr030i004p00517 (cit. on p. 23).

Kamphuis, J. William (Nov. 1991). "Alongshore sediment transport rate". In: *Journal of Waterway, Port, Coastal, and Ocean Engineering* 117.6. Publisher: American Society of Civil Engineers (ASCE), pp. 624–640. DOI: 10.1061/(asce)0733-950x(1991)117:6(624) (cit. on pp. 15, 47, 74).

Karunarathna, Harshinie and Dominic E. Reeve (Sept. 2013). "A hybrid approach to model shoreline change at multiple timescales". In: *Continental Shelf Research* 66, pp. 29–35. DOI: 10.1016/j.csr.2013.06.019 (cit. on pp. 27, 30).

Kinsela, M. A. et al. (June 2022). "Mapping the Shoreface of Coastal Sediment Compartments to Improve Shoreline Change Forecasts in New South Wales, Australia". en. In: *Estuaries and Coasts* 45.4, pp. 1143–1169. DOI: 10.1007/s12237-020-00756-7 (cit. on p. 11).

Kinsela, Michael et al. (Dec. 2017). "Second-Pass Assessment of Potential Exposure to Shoreline Change in New South Wales, Australia, Using a Sediment Compartments Framework". en. In: *Journal of Marine Science and Engineering* 5.4, p. 61. DOI: 10.3390/jmse5040061 (cit. on p. 42).

Komar, Paul (1977). *Beach Processes and Sedimentation*. English. Englewood Cliffs: Prentice Hall (cit. on p. 11).

Kopp, Robert E. et al. (July 2023a). "Communicating future sea-level rise uncertainty and ambiguity to assessment users". en. In: *Nature Climate Change* 13.7, pp. 648–660. DOI: 10.1038/s41558-023-01691-8 (cit. on pp. 69, 78).

Kopp, Robert E. et al. (Dec. 2023b). "The Framework for Assessing Changes To Sea-level (FACTS) v1.0: a platform for characterizing parametric and structural uncertainty in future global, relative, and extreme sea-level change". In: *Geoscientific Model Development* 16.24, pp. 7461–7489. DOI: 10.5194/gmd-16-7461-2023 (cit. on pp. 70, 78, 82).

Kumar, Lalit, Mohammad Saud Afzal, and Mohammad Mashhood Afzal (Aug. 2020). "Mapping shoreline change using machine learning: a case study from the eastern Indian coast". In: *Acta Geophysica* 68.4, pp. 1127–1143. DOI: 10.1007/s11600-020-00454-9 (cit. on p. 30).

Kumar, Pavitra and Nicoletta Leonardi (Apr. 2025). "Predicting Morphological Changes Along a Macrotidal Coastline Using a Two⊠Stage Machine Learning Model". en. In: *Water Resources Research* 61.4. Publisher: American Geophysical Union (AGU). DOI: 10.1029/2024wr037523 (cit. on p. 30).

Larson, Magnus, Le Xuan Hoan, and Hans Hanson (Mar. 2010). "Direct formula to compute wave height and angle at incipient breaking". In: *Journal of Waterway, Port, Coastal, and Ocean Engineering* 136.2. Publisher: American Society of Civil Engineers (ASCE), pp. 119–122. DOI: 10.1061/(asce)ww.1943-5460.0000030 (cit. on p. 47).

Laugel, Amélie et al. (Dec. 2014). "Wave climate projections along the French coastline: Dynamical versus statistical downscaling methods". en. In: *Ocean Modelling* 84, pp. 35–50. DOI: 10.1016/j.ocemod.2014.09.002 (cit. on p. 92).

Le Cozannet, Gonéri et al. (Jan. 2019). "Quantifying uncertainties of sandy shoreline change projections as sea level rises". en. In: *Scientific Reports* 9.1, p. 42. DOI: 10.1038/s41598-018-37017-4 (cit. on pp. 32, 70, 83).

Leach, Chloe et al. (Sept. 2021). "The Coastline Evolution Model 2D (CEM2D) V1.1". In: *Geoscientific Model Development* 14.9. Publisher: Copernicus Publications Göttingen, Germany, pp. 5507–5523. DOI: 10.5194/gmd-14-5507-2021 (cit. on pp. 21, 28).

Lerma, Alexandre Nicolae et al. (2025). "From fixed to transgressive coastal dunes, the conditions and timing of the transition along the Aquitaine coast, France". In: *Coastal dynamics* (cit. on pp. 93, 94).

Li, Chenzhao and Sankaran Mahadevan (Sept. 2016). "An efficient modularized sample-based method to estimate the first-order Sobol' index". en. In: *Reliability Engineering & System Safety* 153, pp. 110–121. DOI: 10.1016/j.ress.2016.04.012 (cit. on p. 80).

Li, Yong et al. (2020). "A CNN–LSTM Method for the Morphology Evolution Prediction of Beach Mega-Nourishment". In: *IEEE Access* 8. Publisher: Institute of Electrical and Electronics Engineers (IEEE), pp. 184512–184523. DOI: 10.1109/access.2020.3030119 (cit. on p. 30).

Limber, Patrick W., Peter N. Adams, and A. Brad Murray (Jan. 2017). "Modeling large-scale shoreline change caused by complex bathymetry in low-angle wave climates". en. In: *Marine Geology* 383. Publisher: Elsevier BV, pp. 55–64. DOI: 10.1016/j.margeo.2016.11.006 (cit. on p. 17).

Lobeto, Hector, Melisa Menendez, and Iñigo J. Losada (Apr. 2021). "Future behavior of wind wave extremes due to climate change". en. In: *Scientific Reports* 11.1, p. 7869. DOI: 10.1038/s41598-021-86524-4 (cit. on pp. 77, 93).

Luijendijk, Arjen et al. (Apr. 2018). "The State of the World's Beaches". In: *Scientific Reports* 8.1. Publisher: Nature Publishing Group, p. 6641. DOI: 10.1038/s41598-018-24630-6 (cit. on pp. 2, 3, 69, 95).

Mao, Yongjing et al. (July 2025). "Benchmarking shoreline prediction models over multi-decadal timescales". en. In: *Communications Earth & Environment* 6.1, p. 581. DOI: 10.1038/s43247-025-02550-4 (cit. on pp. 30, 31).

Marrel, Amandine et al. (Mar. 2009). "Calculations of Sobol indices for the Gaussian process metamodel". en. In: *Reliability Engineering & System Safety* 94.3, pp. 742–751. DOI: 10.1016/j.ress.2008.07.008 (cit. on p. 33).

Masselink, G et al. (2020). "Impacts of climate change on coastal geomorphology and coastal erosion relevant to the coastal and marine environment around the UK". In: *MCCIP Science Review* 2020, pp. 158–189 (cit. on p. 44).

Masselink, Gerd and Paul Russell (2013). "Impacts of climate change on coastal erosion". en. In: *MCCIP Science Review 2013*. Artwork Size: 16 pages Medium: pdf Publisher: Marine Climate Change Impacts Partnership (MCCIP), Lowestoft, UK, 16 pages. DOI: 10.14465/2013.ARC09.071-086 (cit. on pp. 18–20).

Masselink, Gerd et al. (Nov. 2023). "Role of Atmospheric Indices in Describing Shoreline Variability Along the Atlantic Coast of Europe". en. In: *Geophysical Research Letters* 50.22. Publisher: American Geophysical Union (AGU). DOI: 10.1029/2023gl106019 (cit. on p. 21).

Masson-Delmotte, V. et al., eds. (2021). *Climate change 2021: The physical science basis. Working group I contribution to the sixth assessment report of the intergovernmental panel on climate*

change. Cambridge, UK and New York, NY, USA: Cambridge University Press. DOI: 10.1017/9781009157896 (cit. on p. 2).

McCarroll, R. Jak et al. (May 2021a). "A rules-based shoreface translation and sediment budgeting tool for estimating coastal change: ShoreTrans". In: *Marine Geology* 435. Publisher: Elsevier BV, p. 106466. DOI: 10.1016/j.margeo.2021.106466 (cit. on pp. 6, 7, 14, 21, 23, 26, 38–41, 43, 44, 70, 72, 74–76).

McCarroll, R. Jak et al. (Apr. 2021b). "An XBeach derived parametric expression for headland bypassing". In: *Coastal Engineering* 165, p. 103860. DOI: 10.1016/j.coastaleng.2021.103860 (cit. on pp. 19, 48).

Mentaschi, Lorenzo et al. (Aug. 2018). "Global long-term observations of coastal erosion and accretion". en. In: *Scientific Reports* 8.1, p. 12876. DOI: 10.1038/s41598-018-30904-w (cit. on p. 69).

Midun, Zamali and Say-Chong Lee (1995). "Implications of a Greenhouse-Induced Sea-Level Rise: A National Assessment for Malaysia". en. In: *Journal of Coastal Research* 14 (cit. on p. 4).

Montaño, Jennifer et al. (Feb. 2020). "Blind testing of shoreline evolution models". In: *Scientific Reports* 10.1. Publisher: Springer Science and Business Media LLC. DOI: 10.1038/s41598-020-59018-y (cit. on pp. 5, 30, 31).

Morim, Joao et al. (Sept. 2019). "Robustness and uncertainties in global multivariate wind-wave climate projections". en. In: *Nature Climate Change* 9.9, pp. 711–718. DOI: 10.1038/s41558-019-0542-5 (cit. on pp. 77, 92).

Muroi, Subaru Ken et al. (July 2025). "Machine learning methods for predicting shoreline change from submerged breakwater simulations". en. In: *Engineering Applications of Artificial Intelligence* 152. Publisher: Elsevier BV, p. 110726. DOI: 10.1016/j.engappai.2025.110726 (cit. on p. 30).

NASA (2023). *IPCC AR6 sea level projection tool*. URL: https://sealevel.nasa.gov/ipcc-ar6-sea-level-projection-tool (cit. on p. 77).

Nicholls, Robert J. et al. (May 2021). "Integrating new sea□level scenarios into coastal risk and adaptation assessments: An ongoing process". en. In: *WIREs Climate Change* 12.3, e706. DOI: 10.1002/wcc.706 (cit. on p. 94).

Nicolae Lerma, Alexandre et al. (2019). "Pluriannual beach-dune evolutions at regional scale: Erosion and recovery sequences analysis along the aquitaine coast based on airborne LiDAR data". In: *Continental Shelf Research* 189, p. 103974. DOI: 10.1016/j.csr.2019.103974 (cit. on p. 71).

Nicolae Lerma, Alexandre et al. (Apr. 2022). "Multi-Decadal Seawall-Induced Topo-Bathymetric Perturbations along a Highly Energetic Coast". In: *Journal of Marine Science and Engineering* 10.4, p. 503. DOI: 10.3390/jmse10040503 (cit. on pp. 71, 72).

Osborne, Philip D. and Brian Greenwood (Apr. 1992). "Frequency dependent cross-shore suspended sediment transport. 2. A barred shoreface". en. In: *Marine Geology* 106.1-2, pp. 25–51. DOI: 10.1016/0025-3227(92)90053-K (cit. on p. 13).

Payo, Andrés et al. (Nov. 2016). *CoastalME version 1.0: a Coastal Modelling Environment for simulating decadal to centennial morphological changes*. DOI: 10.5194/gmd-2016-264 (cit. on p. 28).

Pelnard-Considère, Roger (1957). "Essai de théorie de l'évolution des formes de rivage en plages de sable et de galets". fre. In: Publisher: Persée-Portail des revues scientifiques en SHS tex.copyright: free (cit. on pp. 22, 27).

Pollard, James A., Susan M. Brooks, and Tom Spencer (Apr. 2019). "Harmonising topographic & remotely sensed datasets, a reference dataset for shoreline and beach change analysis". en. In: *Scientific Data* 6.1, p. 42. DOI: 10.1038/s41597-019-0044-3 (cit. on p. 91).

Pontee, Nigel (Nov. 2013). "Defining coastal squeeze: A discussion". en. In: *Ocean & Coastal Management* 84, pp. 204–207. DOI: 10.1016/j.ocecoaman.2013.07.010 (cit. on pp. 94, 95).

Poumadère, Marc et al. (2015). "Coastal vulnerabilities under the deliberation of stakeholders: The case of two French sandy beaches". In: *Ocean & Coastal Management* 105, pp. 166–176. DOI: 10.1016/j.ocecoaman.2014.12.024 (cit. on p. 2).

El-Raey, M (1995). "Potential Impacts of Accelerated Sea-Level Rise on Alexandria Governorate, Egypt". en. In: *Journal of Coastal Research* 14 (cit. on p. 4).

Ranasinghe, Roshanka (Feb. 2020). "On the need for a new generation of coastal change models for the 21st century". en. In: *Scientific Reports* 10.1, p. 2010. DOI: 10.1038/s41598-020-58376-x (cit. on p. 69).

Ranasinghe, Roshanka, David Callaghan, and Marcel J. F. Stive (June 2011). "Estimating coastal recession due to sea level rise: Beyond the Bruun rule". In: *Climatic Change* 110.3–4. Publisher: Springer Science and Business Media LLC, pp. 561–574. DOI: 10.1007/s10584-011-0107-8 (cit. on pp. 32, 70).

Revision World (2025). *Longshore drift*. Authority: Revision World Networks Ltd. URL: https://revisionworld.com/gcse-revision/geography/coastal-landscapes/coastal-processes/longshore-drift (cit. on p. 16).

Robinet, Arthur et al. (Nov. 2018). "A reduced-complexity shoreline change model combining longshore and cross-shore processes: The LX-Shore model". In: *Environmental Modelling & Software* 109. Publisher: Elsevier BV, pp. 1–16. DOI: 10.1016/j.envsoft.2018.08.010 (cit. on pp. 5–7, 11, 17, 18, 22, 27, 29, 44–47, 50, 71–75).

Robinet, Arthur et al. (May 2020). "Simulating the Impact of Sea-level Rise and Offshore Bathymetry on Embayment Shoreline Changes". In: *Journal of Coastal Research* 95.sp1. tex.ids: robinet_simulating_2020, p. 1263. DOI: 10.2112/SI95-244.1 (cit. on pp. 14, 44, 50).

Roelvink, Dano et al. (Nov. 2009). "Modelling storm impacts on beaches, dunes and barrier islands". In: *Coastal Engineering* 56.11–12. Publisher: Elsevier BV, pp. 1133–1152. DOI: 10.1016/j.coastaleng.2009.08.006 (cit. on p. 22).

Roelvink, Dano et al. (July 2020). "Efficient Modeling of Complex Sandy Coastal Evolution at Monthly to Century Time Scales". In: *Frontiers in Marine Science* 7. Publisher: Frontiers Media SA, p. 535. DOI: 10.3389/fmars.2020.00535 (cit. on pp. 7, 18–21, 27, 28, 70).

Roelvink, J. A. and M. J. F. Stive (Apr. 1989). "Bar□generating cross□shore flow mechanisms on a beach". en. In: *Journal of Geophysical Research: Oceans* 94.C4, pp. 4785–4800. DOI: 10.1029/JC094iC04p04785 (cit. on p. 13).

Rohmer, Jeremy et al. (Oct. 2022). "Partitioning the contributions of dependent offshore forcing conditions in the probabilistic assessment of future coastal flooding". en. In: *Natural Hazards and Earth System Sciences* 22.10, pp. 3167–3182. DOI: 10.5194/nhess-22-3167-2022 (cit. on p. 33).

Rosati, J.D., R.G. Dean, and T.L. Walton (June 2013). "The modified Bruun Rule extended for landward transport". In: *Marine Geology* 340. Publisher: Elsevier BV, pp. 71–81. DOI: 10.1016/j.margeo.2013.04.018 (cit. on pp. 25, 42, 75).

Rosen, Peter S. (Jan. 1978). "A regional test of the Bruun Rule on shoreline erosion". en. In: *Marine Geology* 26.1-2. Publisher: Elsevier BV, pp. M7–M16. DOI: 10.1016/0025-3227(78)90052-x (cit. on p. 24).

Ruessink, B.G. (May 1998). "The temporal and spatial variability of infragravity energy in a barred nearshore zone". en. In: *Continental Shelf Research* 18.6, pp. 585–605. DOI: 10.1016/S0278-4343(97)00055-1 (cit. on p. 13).

Saintilan, N. et al. (June 2020). "Thresholds of mangrove survival under rapid sea level rise". en. In: *Science* 368.6495, pp. 1118–1121. DOI: 10.1126/science.aba2656 (cit. on p. 25).

Sallenger Jr, Asbury H, Robert A Holman, and William A Birkemeier (1985). "Storm-induced response of a nearshore-bar system". In: *Marine Geology* 64.3-4. Publisher: Elsevier, pp. 237–257 (cit. on p. 13).

Saltelli, Andrea et al. (2008). *Global sensitivity analysis: the primer*. John Wiley & Sons (cit. on pp. 71, 80).

Scala, Pietro et al. (Jan. 2025). "COAST-PROSIM: A Model for Predicting Shoreline Evolution and Assessing the Impacts of Coastal Defence Structures". en. In: *Water* 17.2. Publisher: MDPI AG, p. 269. DOI: 10.3390/w17020269 (cit. on p. 29).

Schmidt, A., F. Rottensteiner, and U. Soergel (May 2013). "MONITORING CONCEPTS FOR COASTAL AREAS USING LIDAR DATA". en. In: *The International Archives of the Photogrammetry, Remote Sensing and Spatial Information Sciences* XL-1/W1, pp. 311–316. DOI: 10.5194/isprsarchives-XL-1-W1-311-2013 (cit. on pp. 91, 95).

Schwartz, Maurice L. (Jan. 1967). "The Bruun Theory of Sea-Level Rise as a Cause of Shore Erosion". en. In: *The Journal of Geology* 75.1. Publisher: University of Chicago Press, pp. 76–92. DOI: 10.1086/627232 (cit. on p. 24).

Seenath, Avidesh (Dec. 2022). "On simulating shoreline evolution using a hybrid 2D/one-line model". In: *Coastal Engineering* 178. tex.ids: seenath_simulating_2022-1, p. 104216. DOI: 10.1016/j.coastaleng.2022.104216 (cit. on pp. 5, 27).

Silverman, Bernard W (2018). *Density estimation for statistics and data analysis*. Routledge (cit. on p. 84).

Simmons, Joshua A. and Kristen D. Splinter (Apr. 2025). "Data-driven shoreline modelling at timescales of days to years". en. In: *Coastal Engineering* 197. Publisher: Elsevier BV, p. 104685. DOI: 10.1016/j.coastaleng.2024.104685 (cit. on p. 30).

Smith, Ernest R, Ping Wang, and Jun Zhang (2003). "Evaluation of the CERC formula using large-scale model data". In: *Proceedings of coastal sediments*. Vol. 3 (cit. on p. 48).

Smith, G.G. and G.P. Mocke (July 2002). "Interaction between breaking/broken waves and infragravity-scale phenomena to control sediment suspension transport in the surf zone". en. In: *Marine Geology* 187.3-4, pp. 329–345. DOI: 10.1016/S0025-3227(02)00385-7 (cit. on p. 13).

Sobol, I.M (Feb. 2001). "Global sensitivity indices for nonlinear mathematical models and their Monte Carlo estimates". en. In: *Mathematics and Computers in Simulation* 55.1-3, pp. 271–280. DOI: 10.1016/S0378-4754(00)00270-6 (cit. on pp. 33, 80, 82).

Soboĺ, Ilya Meyerovich (1993). "Sensitivity estimates for nonlinear mathematical models". In: 1, p. 407 (cit. on p. 33).

Splinter, Kristen D. et al. (Sept. 2014). "A generalized equilibrium model for predicting daily to interannual shoreline response". In: *Journal of Geophysical Research: Earth Surface* 119.9. Publisher: American Geophysical Union (AGU), pp. 1936–1958. DOI: 10.1002/2014jf003106 (cit. on pp. 14, 46, 70).

Stammer, D. et al. (Aug. 2019). "Framework for High□End Estimates of Sea Level Rise for Stakeholder Applications". en. In: *Earth's Future* 7.8, pp. 923–938. DOI: 10.1029/2019EF001163 (cit. on p. 69).

Stripling, Stuart et al. (Mar. 2017). "Regional-scale probabilistic shoreline evolution modelling for flood-risk assessment". en. In: *Coastal Engineering* 121, pp. 129–144. DOI: 10.1016/j.coastaleng.2016.12.002 (cit. on p. 70).

Sun, Xifu et al. (June 2021). "Comparing methods of randomizing Sobol' sequences for improving uncertainty of metrics in variance-based global sensitivity estimation". en. In: *Reliability Engineering & System Safety* 210, p. 107499. DOI: 10.1016/j.ress.2021.107499 (cit. on p. 82).

Svendsen, Ib A (1987). "Analysis of surf zone turbulence". In: *Journal of Geophysical Research: Oceans* 92.C5. Publisher: Wiley Online Library, pp. 5115–5124 (cit. on p. 14).

Szmytkiewicz, Marek et al. (May 2000). "Coastline changes nearby harbour structures: comparative analysis of one-line models versus field data". en. In: *Coastal Engineering* 40.2, pp. 119–139. DOI: 10.1016/S0378-3839(00)00008-9 (cit. on pp. 18–20).

Thiéblemont, Rémi et al. (Dec. 2019). "Likely and High-End Impacts of Regional Sea-Level Rise on the Shoreline Change of European Sandy Coasts Under a High Greenhouse Gas Emissions Scenario". en. In: *Water* 11.12, p. 2607. DOI: 10.3390/w11122607 (cit. on p. 70).

Thiéblemont, Rémi et al. (July 2021). "Deep uncertainties in shoreline change projections: an extra-probabilistic approach applied to sandy beaches". en. In: *Natural Hazards and Earth System Sciences* 21.7, pp. 2257–2276. DOI: 10.5194/nhess-21-2257-2021 (cit. on pp. 33, 34).

Thornton, EB, RT Humiston, and W Birkemeier (1996). "Bar/trough generation on a natural beach". In: *Journal of Geophysical Research: Oceans* 101.C5. Publisher: Wiley Online Library, pp. 12097–12110 (cit. on p. 13).

Toimil, A., M. Álvarez-Cuesta, and I.J. Losada (Jan. 2023a). "Neglecting the effect of long- and short-term erosion can lead to spurious coastal flood risk projections and maladaptation". en. In: *Coastal Engineering* 179, p. 104248. DOI: 10.1016/j.coastaleng.2022.104248 (cit. on pp. 6, 69).

Toimil, A. et al. (Mar. 2020). "Climate change-driven coastal erosion modelling in temperate sandy beaches: Methods and uncertainty treatment". en. In: *Earth-Science Reviews* 202. tex.ids= toimil_climate_2020-1, p. 103110. DOI: 10.1016/j.earscirev.2020.103110 (cit. on pp. 31, 32).

Toimil, Alexandra et al. (June 2021). "Visualising the Uncertainty Cascade in Multi-Ensemble Probabilistic Coastal Erosion Projections". In: *Frontiers in Marine Science* 8. tex.ids= toimil_visualising_2021-1, p. 683535. DOI: 10.3389/fmars.2021.683535 (cit. on pp. 5, 31, 34, 70).

Toimil, Alexandra et al. (June 2023b). "Demonstrating the value of beaches for adaptation to future coastal flood risk". In: *Nature Communications* 14.1. Publisher: Springer Science and Business Media LLC. DOI: 10.1038/s41467-023-39168-z (cit. on pp. 6, 21).

Traboulsi, Mohammad et al. (Sept. 2025). "A coupling approach for long-term 3D morphological evolution of sandy coasts under sea-level rise". en. In: *Environmental Modelling & Software* 193, p. 106624. DOI: 10.1016/j.envsoft.2025.106624 (cit. on pp. 38, 70–74, 81).

Tran, Yen Hai and Eric Barthélemy (June 2020). "Combined longshore and cross-shore shoreline model for closed embayed beaches". In: *Coastal Engineering* 158. Publisher: Elsevier, p. 103692. DOI: 10.1016/j.coastaleng.2020.103692 (cit. on pp. 5, 17).

Trowbridge, John and Donald Young (1989). "Sand transport by unbroken water waves under sheet flow conditions". In: *Journal of Geophysical Research: Oceans* 94.C8. Publisher: Wiley Online Library, pp. 10971–10991 (cit. on p. 13).

Van De Wal, Roderik et al. (Oct. 2024). "Sea Level Rise in Europe: Impacts and consequences". en. In: *State of the Planet* 3-slre1. Publisher: Copernicus GmbH, pp. 1–33. DOI: 10.5194/sp-3-slre1-5-2024 (cit. on p. 2).

Van Den Berg, N., A. Falqués, and F. Ribas (Sept. 2012). "Modeling large scale shoreline sand waves under oblique wave incidence". en. In: *Journal of Geophysical Research: Earth Surface* 117.F3, 2011JF002177. DOI: 10.1029/2011JF002177 (cit. on p. 28).

Van Rijn, L.C. (Dec. 2011). "Coastal erosion and control". en. In: *Ocean & Coastal Management* 54.12, pp. 867–887. DOI: 10.1016/j.ocecoaman.2011.05.004 (cit. on pp. 91, 95).

Van Westen, Bart et al. (Aug. 2024a). "AeoLiS: Numerical modelling of coastal dunes and aeolian landform development for real-world applications". en. In: *Environmental Modelling & Software* 179, p. 106093. DOI: 10.1016/j.envsoft.2024.106093 (cit. on pp. 93, 101).

Van Westen, Bart et al. (Mar. 2024b). "Predicting marine and aeolian contributions to the Sand Engine's evolution using coupled modelling". en. In: *Coastal Engineering* 188. tex.ids= van_westen_predicting_2024-1, p. 104444. DOI: 10.1016/j.coastaleng.2023.104444 (cit. on p. 93).

Vitousek, Sean and Patrick L. Barnard (July 2015). "A NONLINEAR, IMPLICIT ONE-LINE MODEL TO PREDICT LONG-TERM SHORELINE CHANGE". In: *The Proceedings of the Coastal Sediments 2015*. San Diego, USA: WORLD SCIENTIFIC. DOI: 10.1142/9789814689977_0215 (cit. on p. 22).

Vitousek, Sean et al. (Apr. 2017). "A model integrating longshore and cross-shore processes for predicting long-term shoreline response to climate change". In: *Journal of Geophysical Research: Earth Surface* 122.4. Publisher: American Geophysical Union (AGU), pp. 782–806. DOI: 10.1002/2016jf004065 (cit. on pp. 5, 21, 29, 30, 70).

Vitousek, Sean et al. (Nov. 2024). "Scalable, data-assimilated models predict large-scale shoreline response to waves and sea-level rise". en. In: *Scientific Reports* 14.1. tex.ids= vitousek_scalable_2024-1 publisher: Springer Science and Business Media LLC. DOI: 10.1038/s41598-024-77030-4 (cit. on pp. 21, 23, 91, 95).

Voller, Vaughan R., John B. Swenson, and Chris Paola (Jan. 2020). "The thin blue line: A review of shoreline dynamics across time scales and environments". In: *Earth Surface Processes and Landforms* 45.1. Publisher: Wiley, pp. 96–108. DOI: 10.1002/esp.4705 (cit. on p. 11).

Volonte, Claudio R and Robert J Nicholls (1995). "Uruguay and Sea-Level Rise: Potential Impacts and Responses". en. In: tex.ids= volonte1995uruguay publisher: JSTOR (cit. on p. 4).

Vos, K. et al. (Sept. 2023). "Benchmarking satellite-derived shoreline mapping algorithms". en. In: *Communications Earth & Environment* 4.1, p. 345. DOI: 10.1038/s43247-023-01001-2 (cit. on p. 91).

Vousdoukas, Michalis I. et al. (Mar. 2017). "Extreme sea levels on the rise along Europe's coasts". In: *Earth's Future* 5.3. Publisher: American Geophysical Union (AGU), pp. 304–323. DOI: 10.1002/2016ef000505 (cit. on pp. 5, 21).

Vousdoukas, Michalis I. et al. (Mar. 2020). "Sandy coastlines under threat of erosion". In: *Nature Climate Change* 10.3. Publisher: Springer Science and Business Media LLC, pp. 260–263. DOI: 10.1038/s41558-020-0697-0 (cit. on pp. 3, 69, 92).

Xie, Danghan et al. (Feb. 2024). "Impacts of Climate Change on Coastal Hydrodynamics Around a Headland and Potential Headland Sediment Bypassing". en. In: *Geophysical Research Letters* 51.4, e2023GL105323. DOI: 10.1029/2023GL105323 (cit. on p. 70).

Xu, Wei et al. (Oct. 2024). "Dynamics of Sandy Shorelines and Their Response to Wave Climate Change in the East of Hainan Island, China". en. In: *Journal of Marine Science and Engineering* 12.11, p. 1921. DOI: 10.3390/jmse12111921 (cit. on p. 18).

Yang, Zhihai et al. (Sept. 2023). "A Transformer Model for Coastline Prediction in Weitou Bay, China". en. In: *Remote Sensing* 15.19. Publisher: MDPI AG, p. 4771. DOI: 10.3390/rs15194771 (cit. on p. 30).

Yates, M. L., R. T. Guza, and W. C. O'Reilly (Sept. 2009). "Equilibrium shoreline response: Observations and modeling". In: *Journal of Geophysical Research: Oceans* 114.C9. Publisher: American Geophysical Union (AGU). DOI: 10.1029/2009jc005359 (cit. on pp. 12, 14).

Zhang, Wenyan, Ralf Schneider, and Jan Harff (May 2012). "A multi-scale hybrid long-term morphodynamic model for wave-dominated coasts". In: *Geomorphology* 149–150. Publisher: Elsevier BV tex.ids: zhang_multi-scale_2012, pp. 49–61. DOI: 10.1016/j.geomorph.2012.01.019 (cit. on pp. 5, 27).